



## PHD

### **Design of a single cylinder research engine and development of a computer model for lean burn combustion studies**

Moore, David Stephen

*Award date:*  
1987

*Awarding institution:*  
University of Bath

[Link to publication](#)

## **Alternative formats**

If you require this document in an alternative format, please contact:  
[openaccess@bath.ac.uk](mailto:openaccess@bath.ac.uk)

Copyright of this thesis rests with the author. Access is subject to the above licence, if given. If no licence is specified above, original content in this thesis is licensed under the terms of the Creative Commons Attribution-NonCommercial 4.0 International (CC BY-NC-ND 4.0) Licence (<https://creativecommons.org/licenses/by-nc-nd/4.0/>). Any third-party copyright material present remains the property of its respective owner(s) and is licensed under its existing terms.

### **Take down policy**

If you consider content within Bath's Research Portal to be in breach of UK law, please contact: [openaccess@bath.ac.uk](mailto:openaccess@bath.ac.uk) with the details. Your claim will be investigated and, where appropriate, the item will be removed from public view as soon as possible.

**Design of a Single Cylinder Research  
Engine and Development of a Computer  
Model for Lean Burn Combustion Studies**

submitted by David Stephen Moore  
for the degree of Ph.D. of the  
University of Bath 1987

**Copyright**

Attention is drawn to the fact that copyright of the thesis rests with its author. The copy of the thesis has been supplied on condition that anyone who consults it is understood to recognise that its copyright rests with its author and that no quotation from the thesis and no information derived from it may be published without the prior consent of the author.

This thesis may be made available for consultation within the University and Library and may be photocopied or lent to other libraries for the purposes of consultation.

*DS Moore*

UMI Number: U006943

All rights reserved

INFORMATION TO ALL USERS

The quality of this reproduction is dependent upon the quality of the copy submitted.

In the unlikely event that the author did not send a complete manuscript and there are missing pages, these will be noted. Also, if material had to be removed, a note will indicate the deletion.



UMI U006943

Published by ProQuest LLC 2013. Copyright in the Dissertation held by the Author.  
Microform Edition © ProQuest LLC.

All rights reserved. This work is protected against  
unauthorized copying under Title 17, United States Code.



ProQuest LLC  
789 East Eisenhower Parkway  
P.O. Box 1346  
Ann Arbor, MI 48106-1346

UNIVERSITY OF BATH LIBRARY		
31	- 7 JUL 1983	
PHD		

5023058



*To Natalie and*

*my family*

## Summary

The work described here was undertaken as part of a collaborative (CASE) award with Dorman Diesels Ltd., Stafford between October 1984 and September 1987. The major part of the project has been the design of the 1SE single cylinder research engine based on the company's 6SE turbocharged six cylinder in-line engine. Particular emphasis has been placed on the balancing requirements and the method of simulating turbocharged conditions on the engine. The designs for the major components, including the primary and secondary balancers employed, are discussed in detail. Designed as a versatile research tool, which can be converted for diesel or spark-ignited natural gas operation, two engines (diesel and gas) have been built.

Emission legislation, particularly in the USA, has resulted in a drastic reduction in permitted  $\text{NO}_x$  levels. Dorman, seeing a need to protect their market share for gas engines, have embarked on the development of a lean burn natural gas engine. The engine features a divided chamber design: a small fraction of the charge (pilot supply) at a mixture ratio close to stoichiometric is ignited in a small pre-chamber (15cc). The high energy "torch" produced is used to initiate combustion of the lean mixture in the main chamber.

To lend understanding to the mixing process within the pre-chamber and to guide the experimental work at the University, on the gas version of the new 1SE engine, a theoretical study using the proprietary CFD code PHOENICS has been undertaken. The study considered the factors which determine mixture formation: pilot supply pressure relative to boost pressure, pilot mixture and pre-chamber volume. To date the PHOENICS model predictions remain unsubstantiated by any experimental work.

The two versions of the new engine have both run successfully, though considerable commissioning work is required before they can be used alongside their multi-cylinder counterparts for development work.

### **Acknowledgements**

The author wishes to express his thanks to the many people at the University and Dorman Diesels Ltd. who have been involved with the project.

In particular the author wishes to thank:

Dr. S.J. Charlton, project supervisor, for his guidance and help throughout.

The employees in the design and development departments at Dorman; especially Mr. W.J. Pugh, Mr. B. Veitch and Mr. R. Dawes for their advice and enthusiasm during the design of the single cylinder engine.

The author is also indebted to Dr. M. Wilson for his invaluable assistance in the running of the PHOENICS program.

Many thanks are extended to Mr. L. Duddridge for his thorough work on the engine installation.

The financial support of the Science and Engineering Research Council and Dorman Diesels Ltd. is also acknowledged.

## List of Contents

	Page
Title	1
Summary	111
Acknowledgements	1v
Contents	v
Nomenclature	1x
<b>PART I</b>	
1. Introduction	1
2. Literature Survey	6
2.1 Single Cylinder Engines	6
2.1.1 Single - Multi-Cylinder Matching Criteria	6
2.1.2 Single Cylinder Engine Balancing	8
2.2 Lean-burn Combustion	11
2.2.1 NO <sub>x</sub> Formation	14
2.2.2 Methods of NO <sub>x</sub> Reduction in Existing Engines	15
2.2.3 The Divided Chamber Stratified Charge Engine	17
2.2.4 Commercial Lean Burn Natural Gas Engines	18
2.3 Multi-dimensional Modelling	20
2.3.1 Finite Difference Methods	20
2.3.2 Model Applications	22
Figures	
<b>PART II</b>	
3. Preliminary Design	27
3.1 Design Outline	27
3.1.1 Background	28
3.1.2 Design Constraints	30
3.1.3 Engine Services	31
3.1.4 Experimentation	34
3.1.5 Preliminary Design of Major Components	35
3.2 Balancing of a Reciprocating Engine	39

3.2.1 Rotational Balance	40
3.2.2 Reciprocating Balance	40
3.3 Reciprocating Balance of a Single Cylinder Engine	41
3.3.1 Primary Balance	42
3.3.2 Secondary Balance	44
3.4 Balancing of the 1SE Engine	45
3.4.1 Excitation Induced by Reciprocating Forces	45
3.4.2 Reciprocating Balance Solution for the 1SE	46
3.5 Summary of the Preliminary Design	48

#### Tables and Figures

4. Detailed Design	51
4.1 Design Methodology	51
4.2 Engine Component Design	53
4.2.1 Primary and Secondary Balancers	53
4.2.2 Crankshaft and Balance Weight Assembly	55
4.2.3 Balancer Box	57
4.2.4 Crankcase	58
4.2.5 Flywheel	60
4.2.6 Gearcase	61
4.2.7 Sump	61
4.2.8 Suspension Plates	62
4.3 Engine Ancillaries	62
4.3.1 Oil Pump	62
4.3.2 Water Pump	63
4.3.3 Starter	63
4.3.4 Governor-Actuator	64
4.3.5 Fuel Lift Pump (diesel) and Magneto (gas)	65
4.4 Parametric Simulation Study of Exhaust Conditions	65
4.4.1 Single Cylinder Pressurised Exhaust Installation	65
4.4.2 Simulation Models using SPICE	67
4.4.3 Simulation Results	69

#### Tables and Figures

### **PART III**

<b>5. Description of the PHOENICS Fluid Dynamics Program</b>	<b>73</b>
5.1 The PHOENICS Fluid Dynamics Program	74
5.1.1 Solution Method	75
5.1.2 Solution Procedure	76
5.1.3 Program Structure	77
5.2 Initial In-cylinder Air Motion Model	84
5.2.1 Construction of the Piston In-cylinder Model	85
5.2.2 Assessment and Validation of Results	86

#### **Figures**

<b>6. Computational Study of Pre-chamber Mixture Formation</b>	<b>91</b>
6.1 In-cylinder Model with Pre-chamber	91
6.2 Separate 3D Pre-chamber Model	93
6.2.1 Pre-chamber Geometry	94
6.2.2 Setting of Pre-chamber Boundary Conditions	95
6.2.3 Assumptions Made in the Model	98
6.3 Parametric Study	102
6.3.1 Input and Output Files	103
6.3.2 The Pre-chamber Mixing Process	105
6.3.3 Presentation and Discussion of Simulation Results	106

#### **Tables and Figures**

### **PART IV**

<b>7. Installation and Instrumentation of Rig</b>	<b>114</b>
7.1 Rig Description	114
7.1.1 Induction System	115
7.1.2 Exhaust System	116
7.1.3 Natural Gas System	118
7.1.4 Engine Coolant System	119
7.1.5 Engine Oil System	119
7.2 Instrumentation	120

#### **Figures**

<b>8. Early Running Experiences of the 1SE Engine</b>	<b>123</b>
8.1 Starting the Engine	123
8.2 Operation of the Mixers	124
8.3 Engine Load	125
8.4 Engine Shut-down	126
8.5 Acquisition System	127
Figures	

<b>9. Discussion and Conclusions</b>	<b>128</b>
9.1 Discussion	128
9.1.1 CASE Project	128
9.1.2 MEDUSA CAD System	130
9.1.3 The PHOENICS CFD Code	132
9.2 Recommendations for Future Work	133
9.3 Conclusions	135

<b>References</b>	<b>136</b>
-------------------	------------

## **Appendices**

1: Connecting Rod Small and Big End Masses	146
2: Rotating Forces of a Single Cylinder Engine	147
3: Derivation of Engine Reciprocating Forces	149
4: Vibration due to Unbalanced Forces	151
5: Skeleton PHOENICS Satellite	155
6: Skeleton PHOENICS Ground-station	162
7: Pre-chamber Satellite	169
8: Pre-chamber Ground-station	178
9: Analysis of the Pre-chamber Mixing Process	188

Figures

## Nomenclature

### Abbreviations

AFR	air-fuel ratio
AIVO	after inlet valve opening
BDC	bottom dead centre
BMEP	brake mean effective pressure
BTDC	before top dead centre
EVC	exhaust valve closing
EVO	exhaust valve opening
IMEP	indicated mean effective pressure
IVC	inlet valve closing
IVO	inlet valve opening
TDC	top dead centre

### General Notation

Symbol	Description	Units
a	distance of centroid of conrod from big end	m
A	a constant	N
b	distance of centroid of conrod from small end	m
B	a constant	N
c	spring stiffness	N/m
c <sub>1</sub>	concentration of natural gas	-
c <sub>2</sub>	concentration of residuals	-
C	a constant	N
C <sub>m</sub>	coefficient of mass	-
C <sub>p</sub>	specific heat at constant volume	KJ/kgK
CR	compression ratio	-
C <sub>v</sub>	specific heat at constant volume	KJ/kgK
C <sub>+</sub>	coefficient of dependent variable	-
D	a constant	N
f	fuel-air ratio	-
F	force	N
f <sub>p</sub>	fuel-air ratio in pre-chamber	-
f <sub>m1x</sub>	fuel-air ratio in cylinder	-
H	enthalpy	KJ
k	damping constant	kg/s
K	turbulence kinetic energy	KJ
L	connecting rod centre distance	m
m	mass	kg
M	mass of engine installation	kg
m <sub>c</sub>	mass of gas and air in cylinder	kg
m <sub>T</sub>	mass transferred	kg
p	pressure	N/m <sup>2</sup>
q <sub>m</sub>	total mass flow of air	kg/s
r	radius	m
R	crank radius	m
R	specific gas constant	KJ/kgK
R <sub>0</sub>	universal gas constant	KJ/kmolK
S	source term of dependent variable	-
t	time	s



T	temperature	K
u	velocity component in x-direction	m/s
v	velocity component in y-direction	m/s
V	a constant	N
V <sub>1</sub>	total cylinder volume	m <sup>3</sup>
V <sub>c</sub>	cylinder clearance volume	m <sup>3</sup>
V <sub>m</sub>	value of mass	kg
V <sub>p</sub>	pre-chamber volume	m <sup>3</sup>
V <sub>s</sub>	swept volume	m <sup>3</sup>
V <sub>+</sub>	value of dependent variable	-
w	velocity component in z-direction	m/s
W	a constant	N
x	amplitude of vibration	m
y	displacement of piston from TDC	m

#### Greek Notation

$\gamma$	ratio of specific heats	-
$\Gamma$	diffusion coefficient	-
$\delta$	damping factor	1/s
$\epsilon$	turbulence dissipation rate	1/s
$\eta$	frequency ratio	-
$\theta$	crank angle	rad
$\nu$	damping coefficient	-
$\rho$	density	kg/m <sup>3</sup>
$\phi$	equivalence ratio	-
$\phi$	dependent variable	-
$\phi$	connecting rod obliquity	rad
$\psi$	phase angle	rad
$\omega$	angular velocity	rad/s
$\omega_0$	natural frequency	rad/s
$\Omega$	forcing frequency	rad/s

#### Subscripts

AIR	air
B	balance
BE	big end
C	connecting rod
E	east cell face
GAS	natural gas
H	high cell face
L	low cell face
max	maximum
MIX	mixture
N	north cell face
P	typical point
PIN	crankpin
RECIP	reciprocating
RES	residuals
S	south cell face
SE	small end
T	previous time-step value
W	west cell face
WEBS	crankwebs

# PART I

# CHAPTER 1

## 1. Introduction

In any manufacturing industry there is a continuous need for development of existing products to ensure that they not only remain competitive within the market place, but also continue to conform to the ever increasing pressures of legislation. Often this work is done simply by taking the product and placing it under test conditions similar to its operating environment. As the product becomes more complicated however, there is then a requirement to alter particular parameters and to observe their effects on the many performance criteria.

Dorman Diesels Limited of Stafford and Lincoln, which was formerly part of the GEC Diesels Group, manufacture high-speed diesel engines from under 10 litres to 50 litres displacement. Their engines are used primarily as marine propulsion units or as the prime mover in electrical generating sets. In February 1984 Dorman launched the "SE" diesel range. Initially this consisted of the 6SE, a turbocharged six cylinder in-line engine, featuring unit injectors and having a displacement of 23 litres. The overall engine range concept includes six and eight in-line, and twelve and sixteen cylinder vee engines, using identical line components, such as connecting rod, piston, cylinder liner and cylinder head with valve gear. In addition, many of the auxiliary items - water pump, oil pump components, oil cooler and camshaft drive gears - are common. Under reciprocal licensing agreements the V12 version of the engine (12SE) is currently manufactured by Paxman Diesels Limited, Colchester: a management company of GEC. Future production of the 12SE will be at Stafford. Development of the in-line eight (8SE) is far advanced, for launch in the autumn of 1987. The V16 is under development at Paxman.

As part of the broad development strategy Dorman commissioned the design of a single cylinder research engine to be based as closely as possible on the the existing 6SE engine. Not only would the engine be an invaluable tool for undertaking basic research, but it would

also provide important development support to the "SE" range, and thus help to ensure its competitiveness and its ability to meet new legislation in the future. The design for the single cylinder research engine has formed the major part of the work undertaken by the author at the University between October 1984 and September 1987, under a collaborative CASE award with the company and the Science and Engineering Research Council.

The main advantages of a single cylinder research engine in comparison with its multi-cylinder counterpart are well known and may be summarised as follows:

- (a) only one set of prototype components need be produced
- (b) assembly/dismantling times are greatly reduced
- (c) access for instruments is generally superior
- (d) running costs are reduced.

Possible disadvantages include:

- (e) additional means required to balance engine
- (f) in-cylinder conditions may not be identical to the multi-cylinder engine because of differing interference effects on the manifolds
- (g) the single cylinder will have unduly large frictional overheads.

In spite of these disadvantages, its greater flexibility means that the role of the single cylinder engine is gaining in importance. Today, thanks to advanced engine simulation packages, tied in with many thousands of running hours on a single cylinder engine, manufacturers are able not only to reduce development costs, but also feel confident that the engine will perform as expected before investing heavily in the commercialisation of the multi-cylinder engine.

Increasing environmental awareness, particularly in the USA, has led to the imposition of stringent exhaust emission regulations. These regulations, as well as applying to automotive engines, now apply to industrial engines in both urban and rural areas. At present federal legislation states that emissions should not exceed 250 tons/acre per annum of total emissions ( $\text{NO}_x + \text{CO} + \text{HC}$ ) irrespective of the number of engines in a particular installation.

Conventional spark-ignition engines generally operate with an air-fuel mixture close to the stoichiometric ratio, thereby ensuring stable combustion with good efficiency. Unfortunately under this mode of operation there is the tendency to produce excessive exhaust emissions, in particular carbon monoxide ( $\text{CO}$ ) and oxides of nitrogen ( $\text{NO}_x$ ).  $\text{CO}$  is formed during combustion by dissociation reactions, and due to the relative lack of oxygen at these air-fuel ratios persists into the exhaust stream.  $\text{NO}_x$  is formed in the high temperature regions of the combustion chamber and in general the longer that high temperatures prevail in the chamber the higher the  $\text{NO}_x$  emissions.

Many different routes are available to the development engineer for the reduction of these emissions including: retarded ignition, catalytic converters, exhaust gas recirculation and the adoption of lean combustion - known as "lean burn". In the lean burn concept the mixture ratio is significantly above stoichiometric, the excess air being used to limit combustion temperatures and to supply oxygen for complete combustion. For small saloon car petrol engines (<1.6 litres) lean burn is proving to be an effective means of limiting emissions without the need to resort to expensive palliatives.

For many years Dorman have converted a proportion of their diesel production for operation as spark-ignited natural gas engines. Generally this has involved reducing the compression ratio to about 8:1 and replacing the fuel injection equipment with a spark ignition system and a gas carburettor. This type of engine is used throughout the world but is especially popular in the USA as a source of power for natural gas pumping applications. Typically, the engine would be

used to extract natural gas from a disused oil well, the engine itself being fuelled by the natural gas.

With current Dorman gas engines operating with a mixture close to stoichiometric,  $\text{NO}_x$  emissions are in the range 20-27 g/kWh (15-20 g/bhph) and are thus becoming unacceptable in their main market. To be able to first maintain, then increase, its market penetration in the USA, Dorman have embarked on the development of a lean burn 6SE gas engine which can meet the low ( $\text{NO}_x$ ) emissions. The target for the engine is  $\text{NO}_x$  emissions of less than 2.0 g/kWh. (Caterpillar and Waukesha already have engines to meet the new standards). The engine features a very small pre-chamber in which a combustible mixture is ignited by a conventional spark-plug. The high energy flame or "torch" produced then initiates combustion of the lean mixture in the main chamber. In order to develop the correct mixture in the pre-chamber both fuel and air may be supplied to each chamber. The main chamber is supplied in the normal way, via a carburettor, from the intake manifold. The pre-chamber is fed directly through a check valve, and indirectly from the cylinder during the compression stroke.

To aid Dorman in their 6SE gas engine development work, the single cylinder engine, which has been designed for either natural gas or diesel operation (depending on build), has been set up at the University as a lean burn natural gas engine. A second single cylinder engine has been set up for diesel work at Stafford.

In order to lend understanding to the problem of mixture formation in the pre-chamber and to guide the experimental work a theoretical study has been undertaken. The basis of the computational model is the proprietary CFD (computational fluid dynamics) code PHOENICS. The areas of investigation relate only to events in the pre-chamber up to the point of ignition. In particular, the requirements for pilot supply pressure and mixture strength and pre-chamber volume have been studied.

To date, the findings from the theoretical work remain unsubstantiated by any experimental investigation. In the initial phase of the project there has been insufficient time to allow this, though it is intended that this will be carried out during the second stage, which will also include full commissioning of the rig.

The layout of the thesis embraces the activities described above, and may be considered as being divided into four parts:

- Part I      Introduction and background, including a review of the literature relevant to the project - Chapters 1 and 2.
  
- Part II     The design of the 1SE single cylinder research engine. An overview of the "parent" 6SE six cylinder engine; the constraints imposed on the design of the single cylinder engine and the design methodology are described in Chapter 3. In Chapter 4 the detailed design of the key components is presented.
  
- Part III    Description of the PHOENICS code (Chapter 5); and development of a mathematical model leading to a parametric study of the pre-chamber mixing process (Chapter 6).
  
- Part IV    Rig installation and initial instrumentation at the University (Chapter 7). Early running experiences of the gas version of the engine are given in chapter 8. General discussion of the project, recommendations for future work and conclusions are presented in chapter 9.



## CHAPTER 2

## **2. Literature Survey**

This chapter contains a review of the literature pertaining to single cylinder engines, lean burn combustion and multi-dimensional modelling. For single cylinder engines particular attention was paid to the methods used to compensate for the inherent out-of-balance of such engines, and the techniques employed to ensure that results obtained from them would be compatible with their multi-cylinder counterparts. The review of lean burn combustion provides an overview of the topic which is inevitably dominated by its application to the automotive industry. The same section also summarises the application of natural gas as a fuel. These two areas are brought together to discuss the reasons for lean burn combustion of natural gas. Details are also given of some commercial lean burn natural gas engines. The final section, multi-dimensional modelling, reviews the use of finite difference methods, particularly their application to in-cylinder mixing and combustion processes.

### **2.1 Single Cylinder Engines**

The literature available on single cylinder engines is wide-ranging. They are a versatile tool and are widely used in research and development for all types of engine. To ensure that results obtained from them are to be of value it is important to take account of the experimentation to be undertaken and understand how this affects the overall engine design and installation.

#### **2.1.1 Single - Multi-cylinder Matching Criteria**

The Dorman 1SE single cylinder engine (bore 160 mm) is to be used to provide support for the existing multi-cylinder development engines. It is clear that whatever line of research is pursued that the main criterion in the design of the single cylinder is to ensure compatibility between its results and those of the multi-cylinder engines. Thus the specification of the inlet and exhaust systems and

the methods of simulating a turbocharged engine are of vital importance (1). In the open literature, however, there is little information available which rigorously addresses this problem.

McKenzie and Dexter (2) introduce five conditions which a single cylinder engine should fulfil when simulating a multi-cylinder engine.

- (i) The in-cylinder components of both engines should be identical;
- (ii) The single should operate at the same IMEP as the multi-cylinder engine;
- (iii) Coolant and lubricant flow rates per cylinder and temperatures should be identical to those on the multi-cylinder engine;
- (iv) Conditions before the intake ports in the cylinder head should be identical to those on the multi-cylinder engine;
- (v) Conditions after the exhaust ports on the cylinder head when the valves are open should be identical to those on the multi-cylinder engine.

In practice it is not possible to fully satisfy all these conditions. And, of course, a single cylinder cannot provide information on the interaction between cylinders. Points (i) and (iii) cause least difficulty. It is normal to construct the single with the same cylinder components as on the multi-cylinder engine. (Assessment of new in-cylinder geometries should only take place after results from the single have been carefully correlated - "base-lined" - with the multi-cylinder engine). If, as on the 6SE, the engine features unit heads the third criterion can be met by thermostatic control of the oil and coolant temperatures.

Conditions (iv) and (v) are more easily satisfied when the single is to operate as a naturally aspirated rather than a turbocharged engine. Manifolding on the single, identical to the inlet and exhaust portions at each cylinder on the multi-cylinder engine, will correctly reproduce the variations in pressure due to one cylinder breathing and exhausting, but will obviously not simulate the

pulsations due to other cylinders. Where the single cylinder is to represent a pressure charged engine the inlet and exhaust systems must be designed to mimic the performance of the turbocharger turbine and compressor. On the inlet side this is achieved by positioning a plenum chamber at the same distance from the cylinder as the compressor or charge air cooler would be situated on the multi-cylinder engine. Identical pressure and temperature conditions are reached by passing the pressurised air, supplied from an external compressor, through an air cooler or heater. Simulation of the turbocharger for a compact manifold - as on the 6SE - is best achieved by incorporating an orifice plate, plenum and gate valve, capable of operating at high exhaust temperatures, in the exhaust system. The orifice size is chosen to correctly shape the exhaust pulse, whilst the mean exhaust pressure is adjusted by the setting of the gate valve. The large plenum is used to damp out pulsations before the gate valve. Assuming the pressure relationship over the load and speed range is known, or can be predicted, the exhaust back pressure can then be regulated to give the same levels as on the multi-cylinder engine. Figures 2.1 and 2.2 show the air intake and exhaust systems of a Ricardo 'Atlas' engine (2).

The remaining condition - to match IMEP rather than BMEP - is necessary since the frictional losses of a single cylinder engine are very different from those of a multi-cylinder version. This ensures that the in-cylinder conditions, which determine the work done by the gas on the piston, are identical to the multi-cylinder engine and are not distorted by the different parasitic losses of the single. The losses are not identical due to one cylinder supplying all the power for the geartrain and the need to drive balancer shafts.

### 2.1.2 Single Cylinder Engine Balancing

The need for balancer shafts arises because a single cylinder engine is inherently unbalanced. Early engines ran slowly and were sufficiently heavy that the transmission of inertia forces outside the engine could be neglected. As speeds increased and engines

became lighter these forces tended to shake the whole engine structure. The first widely used method, one that is still used on small single cylinder engines today, involves counterbalanced flywheels at each end of the crankshaft (3). A small amount of extra weight was added to the rim of each flywheel on the side opposite the crankpin. Keeping the balancing forces symmetrical required the use of two flywheels, and as engines became more compact this method became less practical; so the weights were shifted to the crankshaft. Other means of balancing were tried. Harkness (3) describes the use of oscillating counter balancers, which proved successful in the reduction of the inertia forces on a small 7 hp single cylinder engine, but were unacceptable from the point of power absorption and noise.

For large, high speed, single cylinder research engines the disturbing forces due to the inertia of the piston assembly and connecting rod may be large. To reduce the engine vibration to acceptable levels primary and, quite often, secondary balancers are employed. Each balancer set consists of two shafts arranged symmetrically, which rotate in opposite directions to one another. The primary balancers revolve at engine speed, whilst those of the secondary run at twice engine speed.

McKenzie and Dexter (2) state unequivocally that for research engines both primary and secondary balancers are required, though without giving any indication of the size of the disturbing forces. French et al (4) in the design of the 'Atlas' engine (bore 216 mm) for high BMEP operation adopted both primary and secondary balancers, which are gear driven from the crankshaft. The search for very high outputs also forced them to use a disc web type crankshaft; the crank webs are circular and run directly in two main bearings. Full rotating balance of the crankshaft and the big end of the connecting rod was obtained by bolting balance weights immediately outside the circular webs.

When designing a single cylinder engine (bore 130 mm) for lubricant, emissions and fuel research Griffin and Wittek (5) also concluded

that the engine would require both primary and secondary balancers as it was intended to run to speeds of 3600 rev/min. They considered upgrading an existing engine used for similar work, but rejected this as being uneconomic. This engine had only been designed to operate at speeds up to 850 rev/min. and had been bolted to a concrete block weighing over 9000 kg to bring the vibration down to an acceptable level.

French (6) in a paper discussing the design of the 'Hydra' universal test engine (bore 80-94 mm) points out that provision was made for primary and secondary balancers. This arose because, by using an appropriate short stroke, it was intended to run the engine to 10 000 rev/min. In the event, running experience on the first engine showed them to be unnecessary. Chen and Flynn (7) in the development of a single cylinder compression ignition engine (bore 105 mm) adopted a chain drive for primary balancers mounted in a bedplate below the engine, instead of the more usual gear drive. The reasons cited for this approach were to enable changes in the piston mass to be easily accommodated, whilst keeping modifications to an existing crankcase to a minimum. Secondary balancers were not used.

Roca et al (8), having decided that both primary and secondary balancers were required for their large bore (360 mm) research engine because it would be bolted directly to the floor and not on elastic elements, proposed various balancer layouts to determine the best solution for their particular installation. For each scheme the extent of balance achieved was calculated. The solution chosen followed very much the standard practice; the balancers located symmetrically below the crankshaft and driven by an intermediate idler gear (figure 2.3). Positioning the balancers above the crankshaft was considered in that it offered a more compact design. Normally the lack of space precludes this option, but in this case it was rejected as it would result in the engine's centre of gravity being raised.

The importance of reducing vibration levels to an acceptable point is not to be underestimated. If left unchecked the large disturbing

forces will not only limit the life of the engine, but can have serious effects on the accuracy of results. Griffin (5) highlights problems associated with injection characteristics caused by unpredictable vibrations in the pump drive, governor linkage and valve mechanism, much of which is initiated by engine vibration.

## 2.2 Lean Burn Combustion

Lean combustion in spark ignited engines has long been recognised as a means of both improving engine efficiency and lowering emissions. Research work on lean burn is dominated by its application to automotive engines, where there is a pressing need for fuel savings, as conventional fuel reserves become depleted, and for lowering of emissions under growing environmental awareness and legislative pressure. To date, the demand for smooth performance and good acceleration has made it difficult to utilize the benefits of lean mixtures.

The success of any lean burn engine design is influenced by two key factors: the mixture distribution and the in-cylinder turbulence, because as the air-fuel ratio is increased flame speeds are reduced and mixtures become difficult to ignite. Uniformity of mixture is important not only between cylinders but also within the charge entering a given cylinder (9). The "quantity" distribution - the difference between the leanest and richest cylinder - determines which cylinder is likely to suffer from the onset of erratic combustion and misfire, whilst the "quality" of the charge entering a cylinder plays an important part in the flame initiation and propagation (9,10). Quader (10) suggested that flame initiation is helped by, amongst other factors, decreased turbulence, but that the rate of propagation of the flame is increased by higher levels of turbulence. Thus the promotion of the "correct" level of turbulence within an engine is very important.

The in-cylinder turbulence level is determined by the interaction of inlet swirl with the compression-induced squish flow, and is thus

directly related to the combustion chamber geometry and induction system. Many researchers (11-14) have experimented with different combustion chamber and piston designs to improve lean burn operation. The use of higher compression ratios in an engine has benefits in both thermal efficiency and in promoting increased squish action for bowl in piston designs, though this latter advantage is somewhat negated by the increased piston weight. The "May Fireball" combustion chamber (11) overcomes this with the "bowl" being located in the cylinder head: the piston is flat. A smaller bump clearance, because of a higher compression ratio, means that the volume of the endgas, which dictates the onset of knock, is correspondingly reduced. This and the higher burning rates, due to increased squish action, allows the use of leaner mixtures. Lean operation in a Honda engine was achieved by Yagi et al (14) by using a dual chamber design. Combustion of the "rich" mixture in the small auxiliary chamber is initiated by a conventional spark-plug. The hot gas, expelled through narrow connecting conduits, provides the ignition source for the leaner mixture in the main chamber. This stratified charge design was found to have better anti-knock qualities than a conventional engine and was therefore able to tolerate both a higher compression ratio, leading to improved fuel economy, and leaner mixtures, resulting in reduced emissions.

The flow fields produced by the induction system play a key role in the performance of an engine. The effect on swirl formation of non-conventional valves - shrouded, vortex - or by including vanes or guides in the inlet tracts has been studied by many researchers (15-18). In petrol engines intensified swirl-induced mixing extends the lean limit of operation - by improving the homogeneity of the fuel-air charge and increasing combustion rates - and thus offers benefits in lowered emissions and better consumption. These advantages are offset by reduced volumetric efficiency and an increase in combustion noise (15). However, intense swirl is not the same as intense mixing. Too strong a swirl may centrifuge and coalesce fuel droplets leading to undesirable stratification of the charge. This may result in lean zones being present in the ignition area at the time of firing, which may either prevent combustion from taking place or lead



to quenching before combustion is completed (16). Conversely, a controlled degree of stratification may offer further improvements in economy and emissions, where a rich mixture under the spark-plug ignites surrounding leaner mixture (17).

Vafadis and Whitelaw (18) concluded that the coupling between the induction process and the field flow at TDC is governed by the relative size, strength and orientation of the intake-generated vortices, which determine the fluid flow at IVC, and by the combustion chamber geometry, which dictates its transformation during compression. They found that large-scale tumbling and swirl motion generated by the induction process could be enhanced by compression and/or piston geometry, whilst small-scale vortices have negligible effect on the TDC flow field.

All these effects have either been observed directly using techniques such as LDA (laser doppler anemometry) or hot wire anemometry, or by careful measurement of gross performance parameters; for example, emissions, specific fuel consumption. The findings of some of these papers, plus the works of a large number of other researchers investigating the fundamentals of lean burn, are presented by Germane et al (19) in a review of lean burn combustion in spark ignited engines.

Study of natural gas combustion has revolved around its use as an alternative fuel, or as a supplement to an existing expensive or diminishing fuel source. In Britain interest in the use of natural gas in all types of engine (diesel conversion, spark ignition and gas turbines) was renewed by the arrival of North Sea oil and gas (20,21). Others (22,23), in the early 1970s, saw it as a means of reducing emissions - through dual-fuelling - in view of imminent legislation around the world, though particularly in the USA. More recently interest has been re-awakened on grounds of cost (24) and the possibility of further reductions in emissions (25).

In New Zealand, where natural gas is an indigenous fuel source, much work has recently been undertaken on dual-fuelling as a means of reducing the high cost of imported diesel (26-28). In stationary engines dual-fuelling has long been used, but little work has been done on its suitability, as is intended in New Zealand, for transportation.

In the following sub-sections the parameters which affect emissions, particularly nitrogen oxides ( $\text{NO}_x$ ), are considered.  $\text{NO}_x$  receives the most attention in spark ignited natural gas engines as it is normally the highest level emittant. From the methods available to reduce emissions the advantages of a lean burn engine with pre-chamber are described. The section is concluded with details of some commercial lean burn natural gas engines.

### 2.2.1 $\text{NO}_x$ Formation

The formation of nitrogen oxide during combustion is a result of the reactions involving nitrogen and oxygen molecules present in the combustion chamber. It is formed in the bulk combustion gases rather than in the region near the combustion chamber surfaces. The most likely chain reaction, known as the Zeldovich mechanism sets forth the primary NO formation as:



The reaction rates are temperature sensitive; with NO formation being significant at high temperatures. As a result NO formation occurs only between ignition and the point of rapid cooling caused by the expansion of the combustion gases. Peak concentrations are dependent, therefore, on maximum cycle temperatures and the time available for the reaction.

The primary engine operating parameter affecting the emissions of nitrogen oxides ( $\text{NO}_x$ ) is air-fuel ratio. Figure 2.4 compares the

variation of  $\text{NO}_x$  emissions from a naturally aspirated single cylinder research engine operating on gasoline with operation on natural gas (29). This shows the characteristic rapid reduction in  $\text{NO}_x$  as the mixture is moved away from stoichiometric. Leaner mixtures have a cooling effect and richer mixtures inhibit  $\text{NO}_x$  formation due to the low concentration of the reactants  $\text{N}_2$  and  $\text{O}_2$ .

### 2.2.2 Methods of $\text{NO}_x$ Reduction in Existing Engines

To a certain extent exhaust emission levels can be reduced through adjustment of some of the external operating parameters. In the USA, under the acronym BACT - Best Available Control Technology - four techniques are recognised as a means of achieving emission reductions on existing engines.

- (i) Altered Air-Fuel Ratio
- (ii) Retarded Ignition Timing
- (iii) Charge Air Cooling
- (iv) Power Deration

#### (i) Air-Fuel Ratio

As stated previously air-fuel ratio is a dominant factor that affects emissions. Figure 2.5 illustrates the effect for both naturally aspirated and turbocharged engines (30). The terminology, rich and lean, means that the engine operates to the left or right of the peak  $\text{NO}_x$  curve as well as indicating mixture strength relative to stoichiometric. If the engine can be made to run leaner substantial reductions in  $\text{NO}_x$  can be achieved. Servé (30) showed that for a turbocharged natural gas engine, in standard configuration, the  $\text{NO}_x$  reduction amounts to about 5% for a 1% increase in charge air density. This is illustrated in figure 2.6. The optimum operating point is denoted on the plot. The fuel consumption penalty is significant (about 3%) but manageable for the first 50% reduction in  $\text{NO}_x$ , but tends to increase exponentially if additional reduction is attempted. Introducing excess air has two effects. The additional

air provides a cooling effect on the charge and the lean ratio will reduce the peak cylinder pressures by slowing combustion rates (figure 2.7). The net effect is a lower peak cycle temperature with a corresponding lower  $\text{NO}_x$  formation rate.

There is obviously a limit to the extent to which an engine can be operated in the lean direction. At very lean air-fuel ratios combustion becomes too unstable to permit continuous engine operation and the bsfc increases rapidly. Cyclic stability, a measure of the maximum firing pressure variation, cycle to cycle, deteriorates and damage to major engine components becomes a possibility. This is defined as the lean limit. (In the paper no formal definition is given as to what level of instability determines the knock limit: merely that at this point the quality of speed control is unacceptable). With this mixture the spark plug alone is inadequate to initiate and sustain a strong flame front. Misfire and quenching result and HC emissions increase (30).

#### (ii) Retarded Ignition Timing

The effect of retarded ignition timing from the optimum point is shown in figure 2.6. The  $\text{NO}_x$  reduction is due to the lower peak firing pressures (and therefore cycle temperatures). The penalty in bsfc, however, is severe.

#### (iii) Charge Air Cooling

Gains in  $\text{NO}_x$  reduction by the use of charge air cooling are evident in figure 2.8. An average 25% reduction is realised for a 22°C drop in air manifold temperature. A practical limit is imposed here; an inter-cooler cannot bring the manifold temperature closer than about 5°C to ambient (30).

#### (iv) Engine Deration

Deration does bring about a reduction in emission levels due to lower combustion pressures. However, the method is generally unacceptable to engine manufacturers and users in that capital costs per kW of power output are inversely proportional to unloading.

#### 2.2.3 The Divided Chamber Stratified Charge Engine

There are several advantages in modifying the combustion process to allow a turbocharged engine to operate at leaner mixtures. A conventional natural gas engine will not run satisfactorily at air-fuel ratios in excess of about 21:1 ( $\phi=0.85$ ) because of low flame propagation rates, which cause loss of power and efficiency (figure 2.9) and a tendency to misfire due to marginal kernel formation at the spark plug. (Note: here the equivalence ratio  $\phi$  is defined equal to the fuel-air ratio divided by the stoichiometric fuel-air ratio). The longer ignition delay and the slower burning characteristics of natural gas mean that more advanced spark timing is required as mixtures become leaner (31) - see figure 2.10. The advance in spark timing is limited by the onset of knock, which is attributed to small quantities of less knock resistant higher paraffins (such as butane) in natural gas, which is largely composed of highly knock resistant methane (32). Further evidence for this is provided by Karim and Ali (33) who determined the ignition and knock limits at various compression ratios and spark timings for a conventional naturally aspirated gas engine. Figure 2.11, taken from their findings, shows typical results obtained at a fixed compression ratio and intake temperature. Advancing the spark timing widens the knock limits but not necessarily the ignition limits which remain virtually unaltered by changes in spark timing.

Thus it becomes evident that if  $\text{NO}_x$  levels are to be reduced further by operating at mixtures leaner than possible with a conventional engine, a means must be found to improve combustion stability. One solution is a more "powerful ignition" system, such as a pre-chamber.

Properly designed, the inadequacies of a single spark plug are overcome as the burning gases that are expelled from a pre-chamber have sufficient energy to penetrate and ignite an extremely lean mixture.

Extending the lean limit of operation using a pre-chamber can result in both reduced  $\text{NO}_x$  and better fuel consumption. Efficiency, based on the Otto cycle, is given by:

$$\text{eff.} = 1 - 1/\text{CR}^{\gamma-1} \quad \text{CR is the compression ratio}$$

As the mixture becomes leaner the ratio of the specific heats of the gases,  $\gamma = C_p/C_v$ , approaches that of air, increasing the theoretical thermal efficiency of the lean burn engines compared with engines which operate with more nearly stoichiometric mixtures. Other considerations such as turbocharger efficiency and other losses resulting from the increased air flow (pumping losses into the pre-chamber) may somewhat diminish the fuel consumption improvement.

#### 2.2.4 Commercial Lean Burn Natural Gas Engines

In the USA amendments made in 1976 and 1977 to the Clean Air Act of 1970 have resulted in exhaust emissions from stationary sources coming under government legislation. Stationary sources include steel mills and boilers as well as internal combustion engines used to generate power. The legislation limits total emissions ( $\text{NO}_x + \text{HC} + \text{CO}$ ) to 250 tons/acre per year, which translates roughly to 5.8 g/kWh (4.3 g/bhph) for a 6000 hp installation or 3.5 g/kWh (2.6 g/bhph) for 10000 hp (34). In addition various state boards impose far more restrictive measures. Southern California Air Quality District, for example, limit  $\text{NO}_x$  to 1.0 g/kWh (0.75 g/bhph).

This legislative pressure has lead a number of gas engine manufactures in the USA - the intended market for the Dorman 6SE gas engine - to launch new engines over the past few years designed specifically to meet the stringent requirements for lower  $\text{NO}_x$

emissions. In the Caterpillar gas engine design (35), based on an existing diesel engine, the diesel fuel injector is replaced by a coil and spark-plug assembly. Lean burn operation (equivalence ratio equal to 1.5) is achieved by a so-called "fast burn combustion chamber" with a cupped piston to provide a high squish effect. The resulting engine (bore and stroke 170 x 190 mm) has good economy, whilst meeting the  $\text{NO}_x$  emission levels of 2.7 g/kWh. Waukesha (36) and Delaval (37) both adopted the pre-combustion chamber concept for their lean burn engines. A section through the cylinder head of the Delaval engine is shown in figure 2.12.

The GL Series Waukesha engine (bore and stroke 216 x 191 mm) operates at a lean air-fuel ratio of 29:1. Ninety-five percent of the lean mixture is fed through the carburettor, intake manifolds and intake valves in the conventional manner. The remaining 5% is fed to the small pre-combustion chamber, through a pair of check valves, at a near stoichiometric ratio. This mixture is ignited by a high energy, long duration spark ignition system. The "torch" produced ignites the charge in the main chamber. With air flow requirements for lean burn combustion more than 75% higher than for the standard or "rich burn" gas engine for equivalent power, the engine is equipped with high capacity turbochargers, low restriction manifolds and a large carburettor. The consistency of the air-fuel ratio is an important element in the performance of a lean burn engine. To reduce fluctuations in air density caused by environmental changes the charge air temperature is thermostatically controlled to maintain a consistent air-fuel ratio.

The PRECOM Delaval engine (356 x 381 mm) though larger in size than the Waukesha engine employs very much the same combustion technology. Again, during the scavenging and induction periods, a pilot gas supply fills the pre-chamber to produce a near stoichiometric mixture, which is then ignited to provide a high energy ignition source for the leaner, main cylinder charge. The advantage of this dual chamber design is the highly stable "cycle-to-cycle" combustion, allowing the engine to satisfy the stringent emission requirements without any fuel penalty or exhaust gas aftertreatment.

## 2.3 Multi-dimensional Modelling

Over the past decade there has been a growth in the development and availability of fluid flow programs aimed at solving a diverse range of fluid dynamic problems. Applications include internal combustion engines, nuclear power, turbomachinery, aerospace and process engineering (38). Most of the growth can be attributed to the introduction of improved computing power at lower cost, along with the continually rising cost of prototype development. Whilst finite element methods have been used for some of this work (39) this review concentrates on finite difference methods: they are predominant in flow analysis; and the PHOENICS program used for the investigation of pre-chamber mixture formation employs finite difference techniques.

### 2.3.1 Finite Difference Methods

In the UK the majority of programs have originated from one or other of the two major centres for computational fluid dynamics: Imperial College, London and UMIST, Manchester. For simplicity these programs, in contrast with most finite element packages, tend to be tailored for particular applications and their names are usually acronyms formed from the problem and numerical solution type. Thus LAST-STEP (Laminar Steady and Time-dependent Simulations with the TEACH Elliptic Program) (40) has been written for the solution of laminar flows which are either steady or time-dependent. Its origins can be traced back to the TEACH program, an early finite difference solution scheme developed for teaching purposes at Imperial, which has formed the basis for a family of similar programs. PASSABLE (Parabolic Solution Scheme Appplied to Boundary Layer Equations) (41) is limited to parabolic, steady-state flows, i.e. where there is a predominant flow direction. It does however include a turbulence model. Some of the university programs are available commercially (42), though it is still the case that many establishments outside the university environment rely upon "in-house" specialised application programs (43,44). Outside the UK, a great deal of work has been done recently in Japan, using powerful computers that allow



modelling of complex geometries coupled with fine grid resolutions. In the USA many of the fluid flow programs have been developed under defence contracts.

Significantly, much of the modelling work concerns the application of finite difference numerical solution schemes to the prediction of fluid flows within internal combustion engines. The ability to realistically model fluid motion and fuel burning has obvious advantages in terms of hastening and simplifying engine design and development. The most sophisticated "in-cylinder" computer software is probably the "RPM" (Reciprocating Piston Motion) code developed at Imperial College, under Gosman and various co-workers (45-47), for the "realistic" modelling of engine conditions.

The program employs finite difference techniques for the solution of partial differential equations for conservation of mass, momentum and energy in time and space. Solution of these governing equations, in discretized form, is carried out on a finite difference grid (see figure 2.13). At each "cell" or "sub-domain", formed by the curvilinear grid frame, values of the three velocity components (axial, radial and circumferential), pressure, enthalpy, mixture fraction, turbulence energy and its dissipation rate are evaluated. To account for valve and piston movement a moving grid is constructed. Thus the grid between the piston crown and cylinder head expands and contracts with the piston motion: the grid in the piston bowl is fixed but able to translate with the moving grid (figure 2.13). Representation of curved boundaries, in rectangular cartesian coordinates, is approximated by artificially castellated boundaries by appropriate "blocking" of cells in the finite difference grid (42). In order to accurately represent finer details, for example a complex bowl shape or flow near a valve, and to reduce numerical errors, a fine grid resolution is required. Higher numbers of cells avoid the problem of "smoothing" (the phenomenon of over-estimation of diffusion due to the solution method - known as numerical diffusion), but at the expense of computation time. Fields of values for all the dependent variables must be specified as initial conditions for the solution procedure (pressure, temperature and velocity, as well as turbulence

intensity for each cell). These initial values are either inferred from experimental data or from previous numerical calculations. (Chapter 5 gives a more detailed account of the finite difference technique in the description of the PHOENICS code).

### 2.3.2. Model Applications

The need for better efficiency and lower emissions in both diesel and spark ignited engines has provided the main impetus for multi-dimensional modelling. It is increasingly being recognised that engine design must be more firmly based on a fundamental understanding of in-cylinder processes. To this end work is progressing on two fronts: the study of in-cylinder air motion, generally motored compression and expansion; and modelling of various combustion processes. Current knowledge of the flow processes within engines, determined from theoretical and experimental techniques, is reviewed by Arcoumanis and Whitelaw (48).

The flow fields in a cylinder exhibit complex three dimensional structures. To model the full three dimensional geometry incurs considerable computer run-times and so it is common to make use of geometric symmetry. On the compression and expansion strokes axial symmetry may exist where the combustion chamber geometry is symmetric or where any three-dimensional structures produced by the induction system are short lived (49). Unfortunately real engines seldom satisfy these criteria. Nevertheless much useful work has been done. Matsuoka et al (50) compared measured swirl velocities in the combustion bowl of a DI (direct injection) diesel engine, obtained by laser doppler anemometry, with predictions of a two-dimensional laminar model at various swirl intensities and engine speeds. The model employed a 24 (radial direction) by 20 (axial) grid with the calculations taking place every 1/4 or 1/6 of a crank angle degree.

In the investigation of flows in a deep-bowl combustion chamber Ikegami et al (51) made similar simplifications; the piston bowl being assumed to be axi-symmetric and having a rectangular cross-

section. The computation starts at inlet valve closing and in common with other researchers (45,50) the air is assumed to exhibit solid body rotation. The work investigated the effect on the air motion of different swirl ratios, engine speed and clearance heights.

Gosman et al (47) compared predictions using the "RPM" multi-dimensional model, in conjunction with three versions of the K- $\epsilon$  turbulence model, with experimental data. The predictions of mean flow and turbulence intensity did not differ with the various turbulence models. They also found that whilst predictions of the mean flow were in good agreement at TDC, agreement during compression was poor: the predicted intake-generated vortices persisted longer. Modifications to the inlet conditions on the mean flow and turbulence intensity were shown to have a significant influence during early compression, but gradually diminished to a small level by TDC. During the study problems were encountered with the numerical accuracy of the predictions: results were dependent on mesh density and the computational time step-size. The errors could not be completely eliminated because the fine mesh with the one degree step-size, which was felt to be adequate, incurred substantial computing times. Instead the penalty of a three degree step-size had to be accepted. Brandstätter et al (52) in a combined experimental-theoretical investigation into the inlet flow produced by a helical port, as commonly used in DI diesel and petrol engines, employed a mesh of 16,320 active cells. Even so, there were regions, where a higher mesh density would have been desirable.

Although it was not intended to model combustion in this work an overview is included for completeness. Much work has been done on modelling the combustion process: primarily that associated with the diesel engine. These models fall into two types: firstly zero-dimensional or phenomenological models, in which burning rates are modelled by empirical relationships, and secondly those which involve the solution of the basic conservation equations of mass, momentum, energy, chemical species, and mixing and reaction rates throughout the combustion chamber.

Shahed et al (53,54) proposed a development of the zero-dimensional model in which the diesel fuel jet is considered as fully vaporised and made up of multiple zones. Each zone has its unique species and properties. Combustion takes place when the mixture consistency in a particular zone falls within the burning limits. The model tracks the mass and composition of each zone but has no knowledge of the combustion chamber geometry. Different geometries are accounted for in the setting of the initial conditions and in the empirical characteristics of the spray. Perfect gas law relationships are used to determine the instantaneous cylinder pressure, based on the total combustion chamber volume at the time, and to evaluate the thermodynamic properties within each zone. Whilst these models are computationally more efficient than the multi-dimensional models, the fact that they are largely empirical means they cannot be used for combustion chamber design. Instead they generally form part of a larger model used to predict the gross performance of an engine.

Work on multi-dimensional combustion models, at least in the diesel field, has first required the development of suitable jet mixing models. Gosman and Johns (45) presented a fully coupled axis-symmetric model, which allowed interaction between the jet and the cylinder flow fields, but were hampered in its development by the need for detailed experimental data. Nevertheless, results obtained were qualitatively representative of injection in an open chamber DI diesel engine. Recently, Watkins and Khaleghi (55) were able to show moderate levels of agreement between a similar three-dimensional coupled model and spray data obtained from a Mirrlees diesel engine.

Predictions obtained from combustion models remain to a large extent unsubstantiated, though experimental work is being performed on simple combustion bombs and stirred reactors as a means of testing the underlying theory for the combustion models. Gosman and Harvey (46) added a combustion model to the "RPM" code and were able to produce qualitatively realistic predictions of the DI diesel combustion process, after appropriate adjustments of the empirical coefficients in the heat release model. Shirakawa et al (56) later showed that during pre-mixed combustion, the model proposed by Gosman

(46) did not predict heat release rates in agreement with results obtained experimentally. They introduced a further empirical coefficient to improve the correlation and were able to provide better understanding of the phenomena that occur in the chamber of a small DI diesel engine. Markatos and Mukerjee (57), using the computer code PHOENICS, examined the in-cylinder processes under motoring and firing conditions for both diesel and petrol engines. Their work also showed the sensitivity of the empirical combustion coefficients to changing conditions as they compared the predicted pressure variation in the cylinder for both 2D and 3D models with experimental data. They concluded that it is still too early to compare predictions with experiments, especially of such complex flows.

All of these multi-dimensional models are very demanding computationally. Brassoli et al (58) required about 20 processing hours using a VAX780 minicomputer. Because of this and the fact that substantiating the combustion models is difficult, Sorenson and Pan (59) proposed an intermediate model for their work on a divided chamber stratified charge engine. The model allowed simulation of non-uniformities, such as air-fuel ratio, within the combustion chamber, without having to resort to full multi-dimensional modelling. A flat flame was assumed to have emerged from the pre-chamber which then occupied the complete cross-section of the chamber geometry as it progressed. Properties were assumed uniform in a plane perpendicular to the flame.

In view of the investigation carried out into the pre-chamber mixing process in the Dorman gas engine, presented in chapter 6, the work undertaken by Benjamin and Weaving (60), in association with CHAM (Concentration, Heat and Momentum Ltd.), is of interest. The paper discusses the development of a mathematical model of flow, heat transfer and combustion in the pre-chamber and main chamber of a stratified charge engine. Although a major part of the combustion takes place in the main chamber, the ignition source for this leaner mixture is the "torch" produced by the expulsion of hot gases from the pre-chamber, in which combustion is initiated by a conventional

spark-plug. The mode of ignition and the precise spread of the flame was not fully understood. Interest was centred on the period 30° either side of TDC. The complex geometry was represented by constructing a 2D model in a plane normal to the main cylinder axis: the movement of the piston being accounted for by time varying boundary conditions (refer to figure 2.14). The advantage cited for this approach is the ability to depict the actual phenomena of the gas dynamics and combustion in space and time, while being more economical in computer time and storage than its three-dimensional counterpart. Results obtained were compared with experimental data obtained from a purposely designed rig. Although the model had the potential to predict flame velocities, which correlated reasonably with the LDA measurements, it was concluded that further development was required, before the model could be used to design combustion chamber geometries having the appropriate level of turbulence to achieve good economy and low pollutant emissions.

Thus, multi-dimensional modelling does offer the means for obtaining reasonably complete flow-structure information that is sufficient for most engineering purposes and unobtainable by any other means. However problems still remain: substantial computer resources are required; there are unresolved questions relating to the modelling of turbulence; the spatial resolution required to produce results that are independent of the mesh density is high, and certain important boundary conditions and/or initial conditions are often unknown for practical conditions (52). The models are also unable to predict "cycle-to-cycle" variability (49). Brandstätter (52) also highlights the need for improved post-processing - colour, interactive viewing of results - to allow better and more immediate visualisation and understanding of the complex 3D flow structures that arise in in-cylinder work.

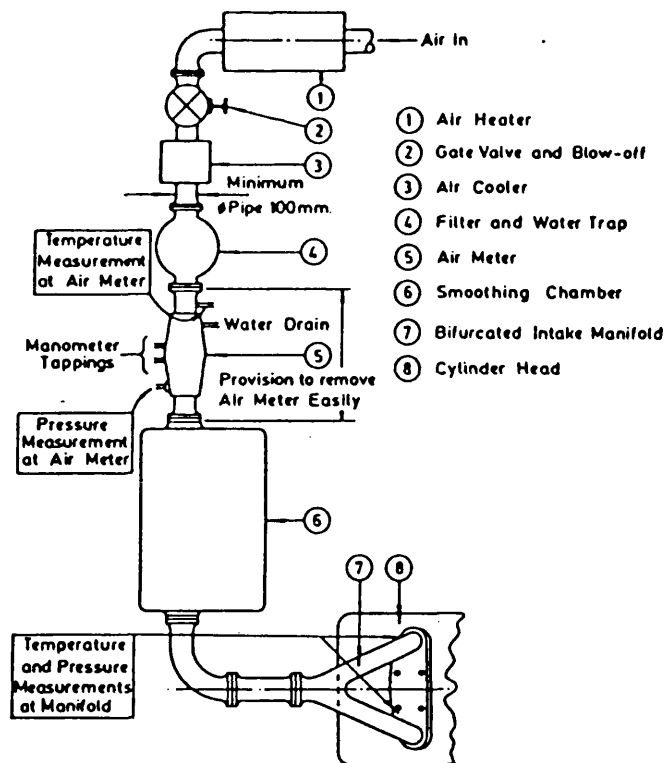


Figure 2.1 Air Intake System on Ricardo Atlas (2)

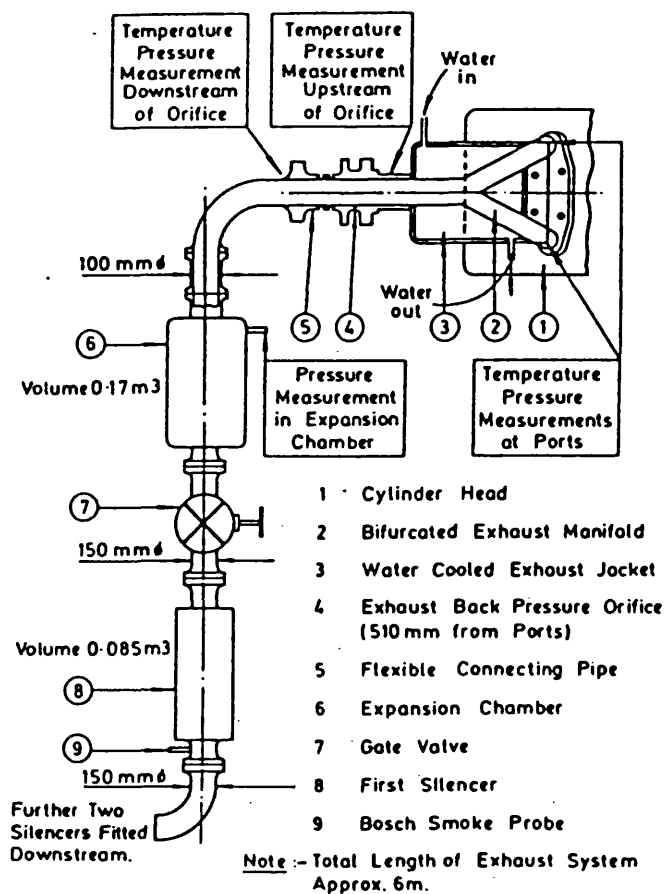


Figure 2.2 Exhaust System on Ricardo Atlas (2)

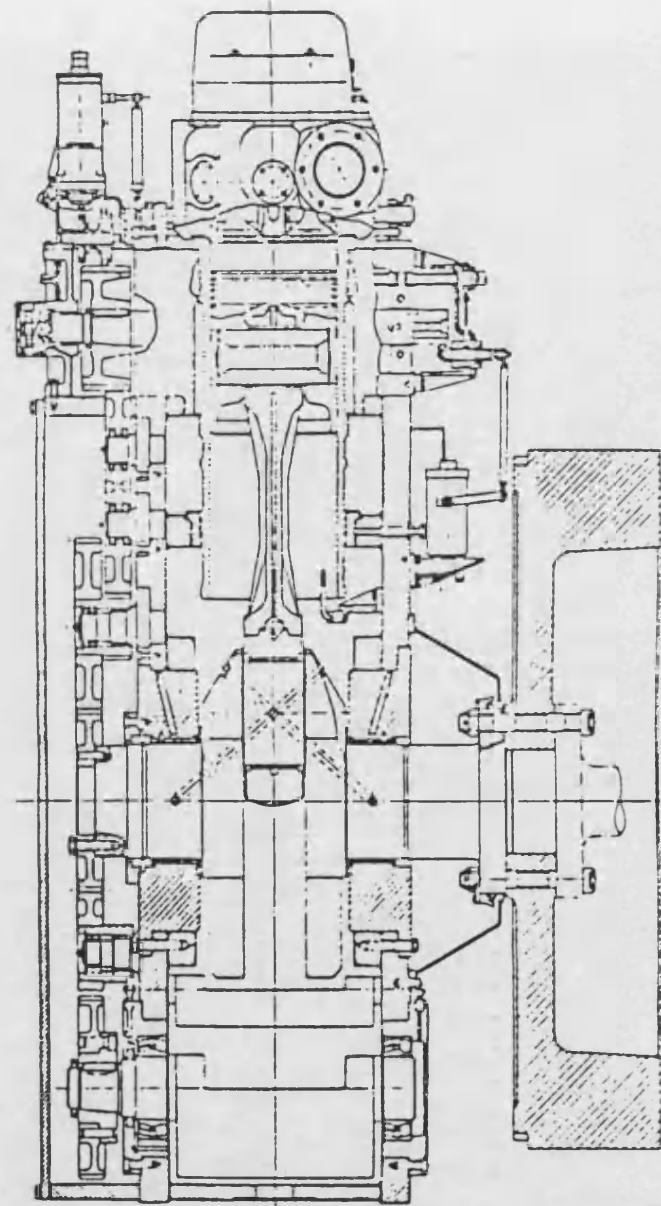
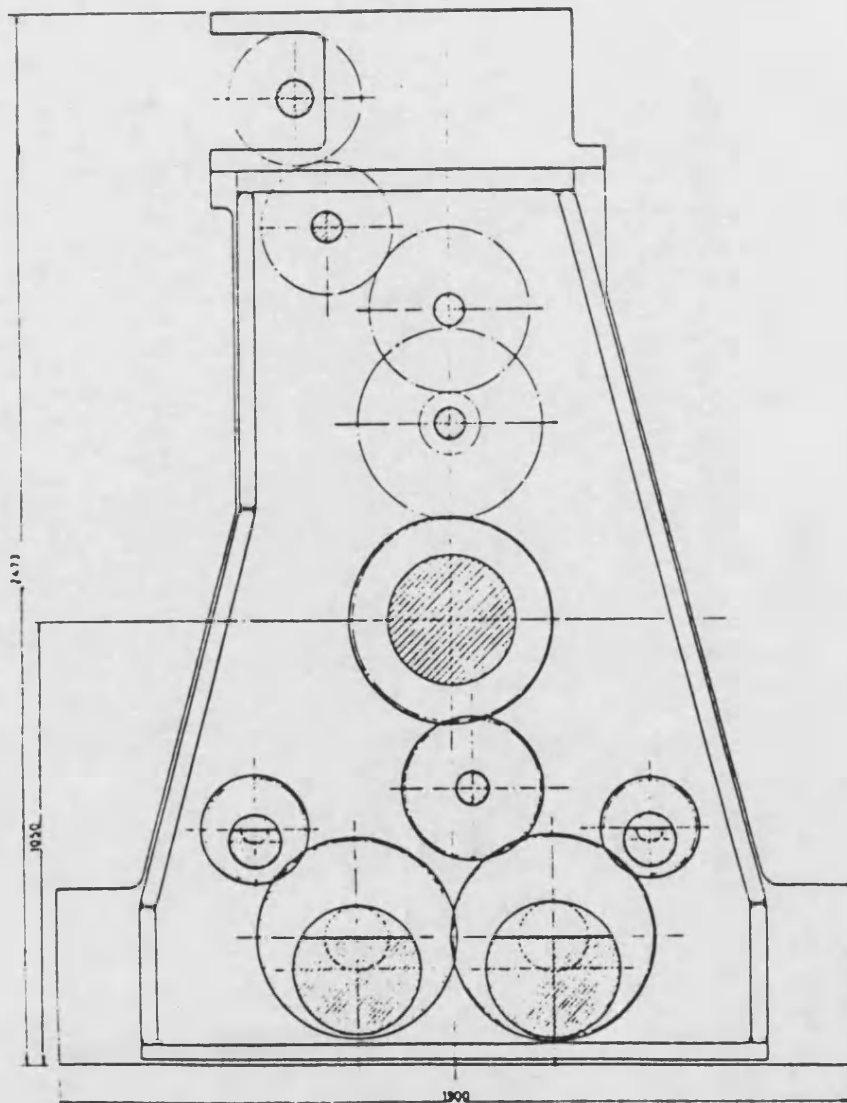


Figure 2.3 Typical Balancer Layout (8)



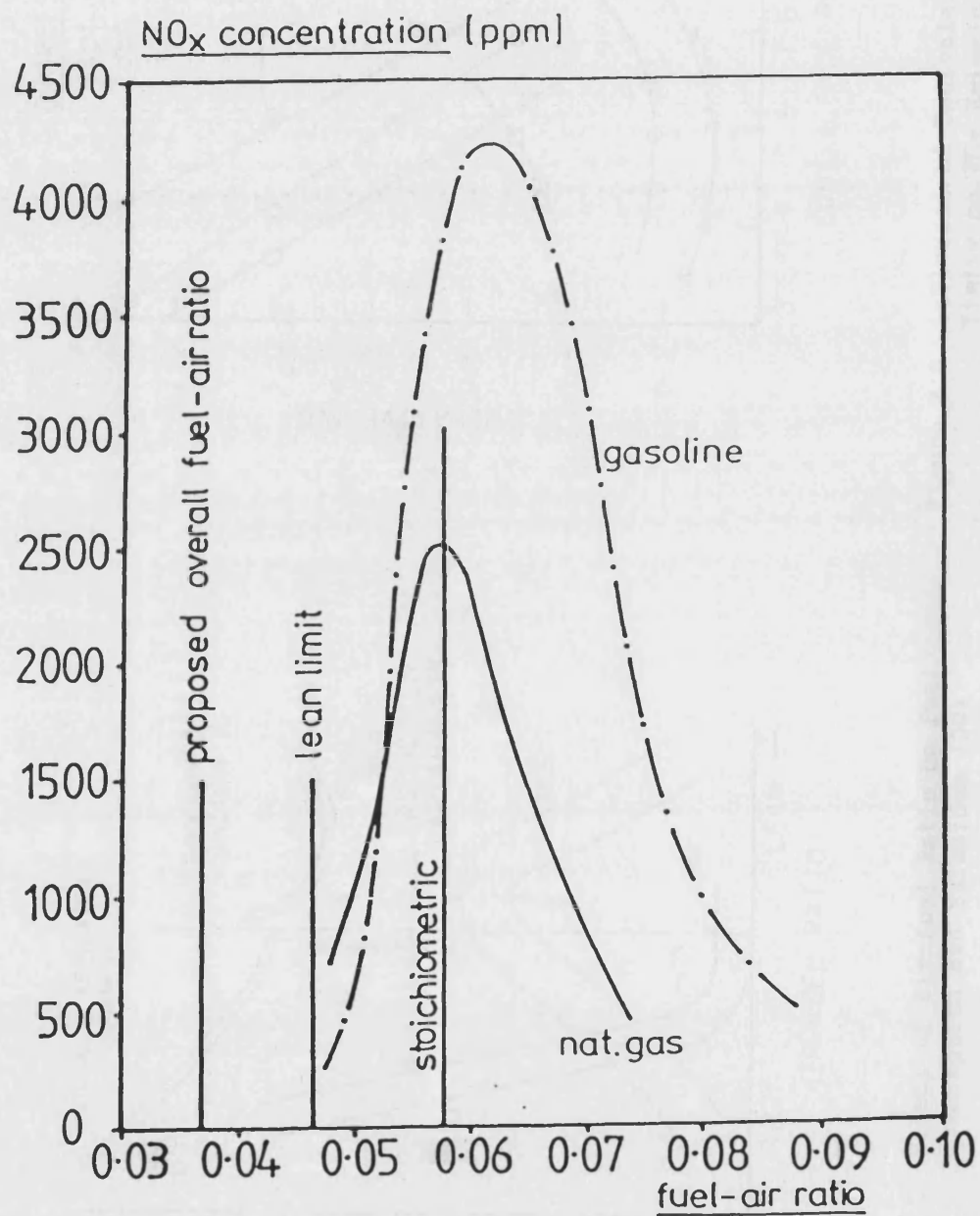


Figure 2.4 Comparison of NO<sub>x</sub> Emissions from a Research Engine fuelled by Natural Gas and Gasoline (29)

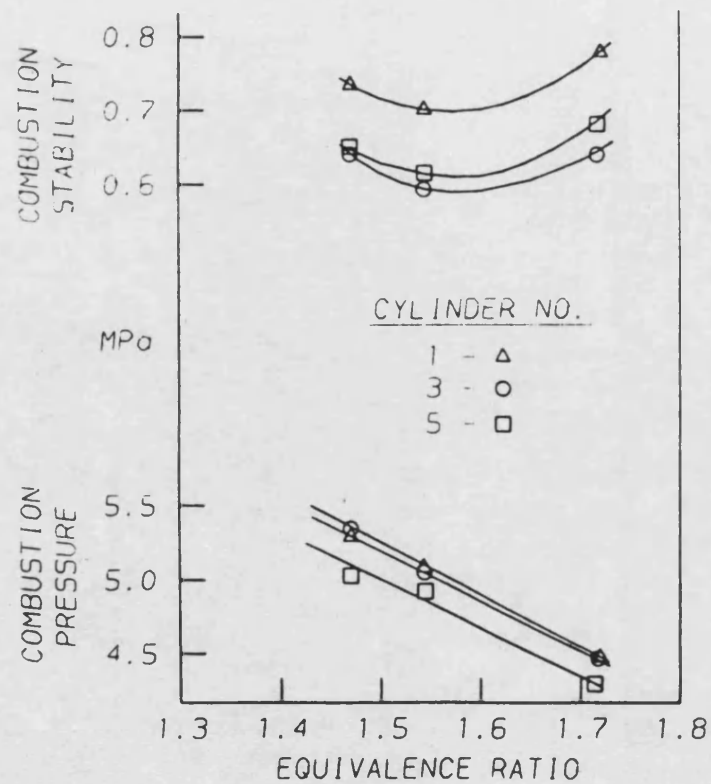


Figure 2.7 Effect of Equivalence Ratio on Firing Pressure and Combustion Stability (30)

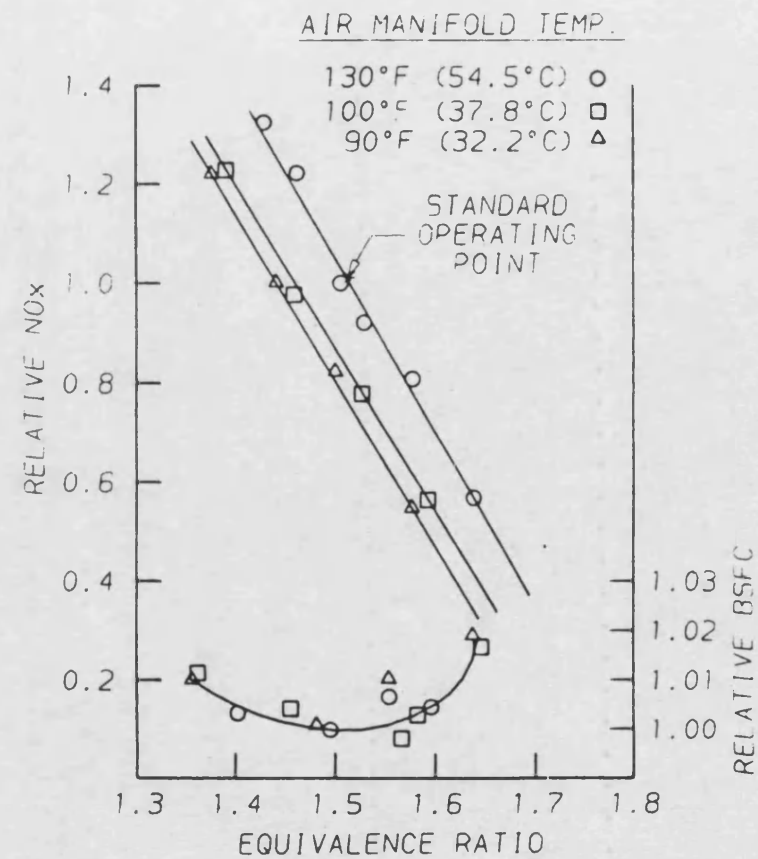


Figure 2.8 Effect of Charge Air Temperature on NOx Emissions and Brake Specific Fuel Consumption (BSFC) (30)

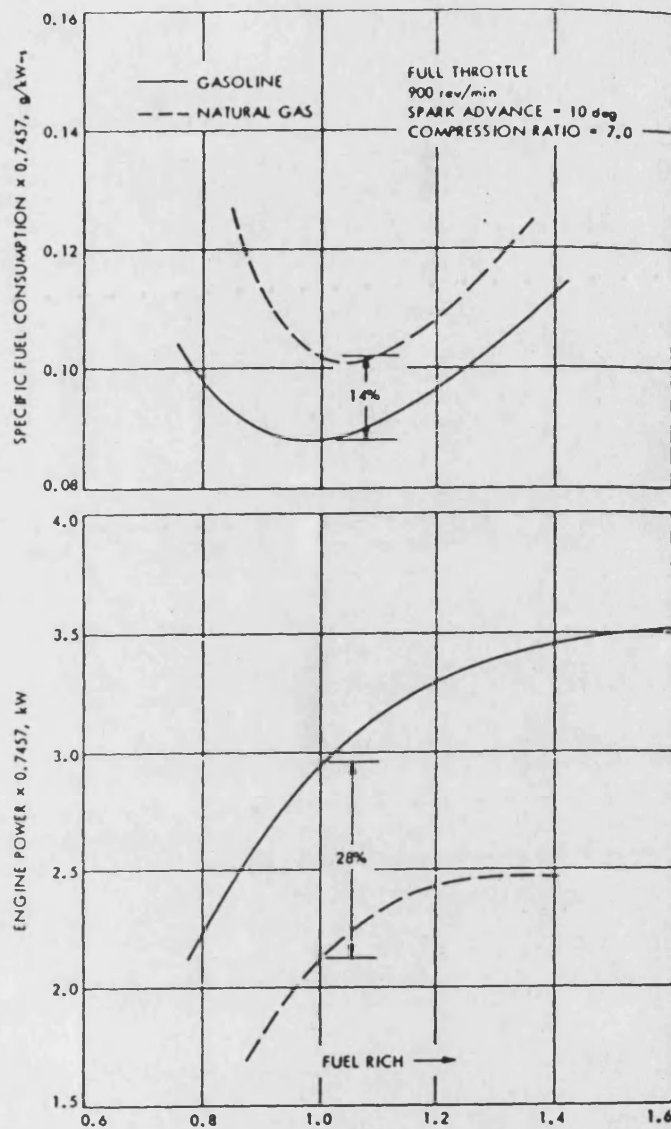


Figure 2.9 Engine Performance as a Function of Fuel Equivalence Ratio with Natural Gas and Gasoline (29)

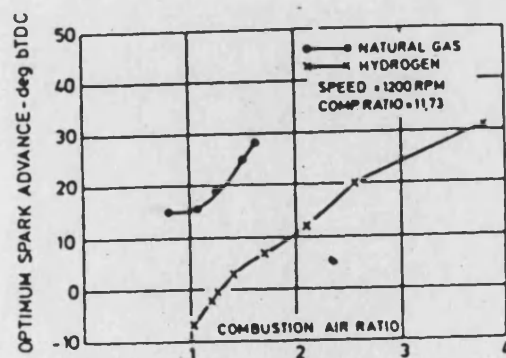


Figure 2.10 Spark Advance Characteristics for Natural Gas and Hydrogen (31)

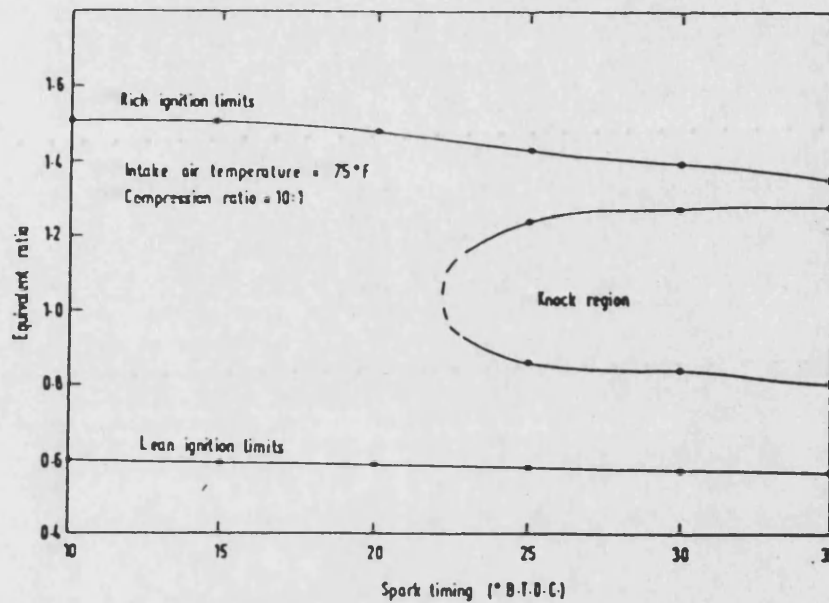


Figure 2.11 Ignition and Knock Limits versus Spark Timing (33)

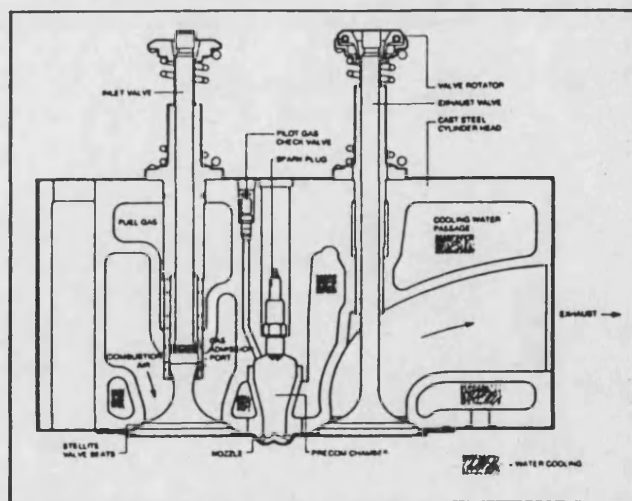


Figure 2.12 Cross-section through Cylinder Head of Delaval Natural Gas Engine (37)

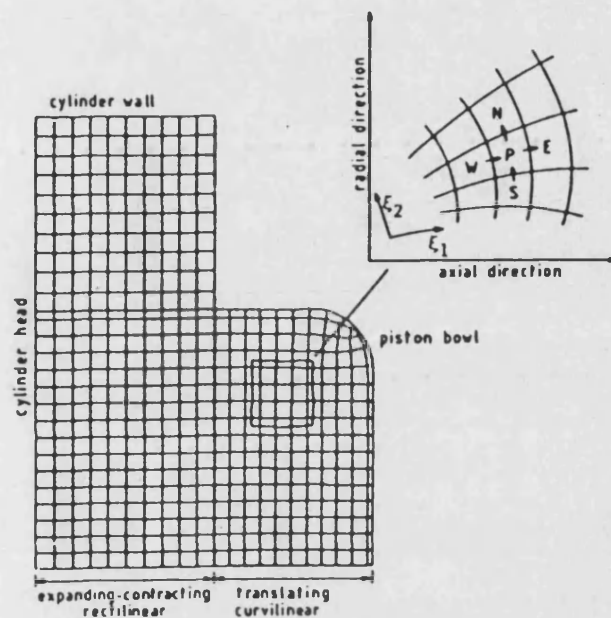


Figure 2.13 Co-ordinate Frame with Moving Grid (45)

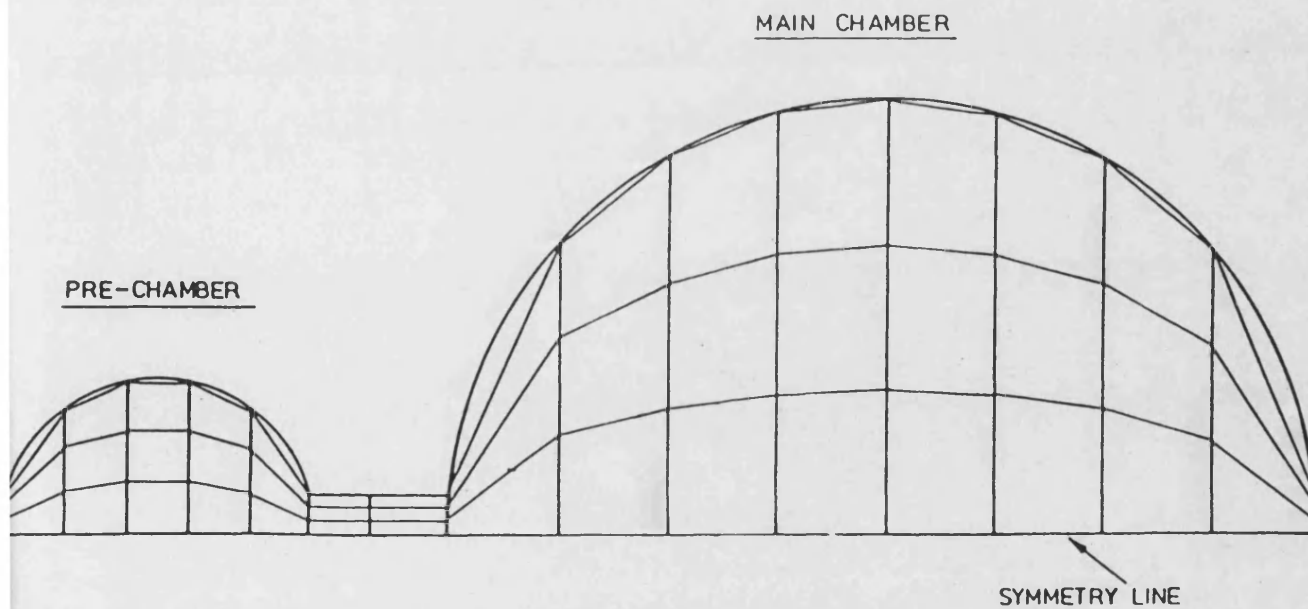


Figure 2.14 Geometry of Stratified Charge Engine and Type of Grid used (60)

# PART II

# CHAPTER 3

### 3. Preliminary Design

This chapter presents an overview of the various aspects which featured in the design of the single cylinder research engine. The aim is to highlight the way the design evolved, the constraints imposed upon it and how these determined the final "shape" of the engine. Presentation of the engine and a detailed discussion of its major components is held over to chapter 4 - "Detailed Design".

Single cylinder engines are widely employed in research and development for all types of engines. In general, they offer economies in costs together with increased flexibility in research compared with multi-cylinder engines. For these reasons single cylinder engines are increasingly being applied to the development of both new and existing multi-cylinder engine ranges. In this role the major constraint is that results are compatible. (The way this can be achieved has been discussed in detail in section 2.1.1). Thus, when used to develop a turbocharged engine the method of simulating pressure charged conditions requires careful attention. Single cylinder engines are also inherently unbalanced. The analysis of the engine balancing requirements is therefore a key feature in any new design.

This latter aspect formed a major part of the initial design work: the success of the engine and the overall design is strongly influenced by the methods of counter-balancing employed. Details of the analysis and the reasons for the adoption of both primary and secondary balancers is discussed in depth in sections 3.2 - 3.4. The chapter is concluded with a summary of the key features of the single cylinder engine.

#### 3.1 Design Outline

The project has been a collaborative (CASE) award with Dorman Diesels, Stafford. The design for the engine was undertaken at the university, in close association with the technical staff at Dorman.



Originally the plan had been for just one engine. Subsequently two were manufactured and assembled.

During the design phase of the project no formal planning was undertaken. (Parts were only scheduled once they were formally taken over by Dorman for manufacture. Those which could not be made "in-house" were sub-contracted out: planning and control of the work being overseen by employees within production control). The order of the design work, after consultation with the Dorman design and production staff, was on the basis of projected lead-times for individual components; the likely design time required; and, obviously, on the natural evolution of the design. No component can be designed in isolation. The design of mating parts must be developed concurrently and to a sufficient level to enable problems and possible methods of solution to be foreseen. Design does not follow a straight path with definite start and end points: it is an iterative procedure. It only stops when the designer is satisfied that the design will work, can be made and will fit together with the other components.

### 3.1.1 Background

The design brief for the single cylinder engine was to produce a versatile research tool which would be used to complement research being done on the existing Dorman "SE" engine range. At the moment the range consists primarily of the 6SE diesel engine, which is available in various builds. A V12 version of the engine (12SE) is also available. An in-line eight cylinder diesel (8SE) and a natural gas version of the 6SE engine, which employs lean burn combustion technology, are also under development.

The Dorman 6SE diesel engines are water-cooled, turbocharged, six cylinder, direct injection diesel engines. Particular features include four valve cylinder heads, unit injectors combining fuel pump and injector in single units and oil-cooled pistons. Technical data for the engine is given in table 3.1. The engine is summarised over:

- **Cylinder Head**      Individual cast iron units secured by four bolts. Two exhaust and two inlet valves are fitted in each head and operated via rocker levers and bridge pieces. A third rocker lever on each head operates the centrally mounted unit injector.
  
- **Piston**              Aluminium alloy pistons fitted with two compression rings and an oil control ring. Casting incorporates oil cooling galleries.
  
- **Fuel Injection Equipment**      Fuel injection is by a Lucas Bryce 'T' size unit injector in each head, operated from a third cam at each cylinder, through push rods and rocker levers.
  
- **Connecting Rod**      Steel forging with detachable bottom cap (45° split).
  
- **Crankcase**            Iron casting. The underslung main bearing caps are retained by high tensile bolts.
  
- **Cylinder Liner**      Centrifugally cast. Synthetic compound 'O' rings are fitted between liner and cylinder block to make a water-tight joint at the lower level.
  
- **Crankshaft and Bearings**      Crankshaft is made from an alloy steel forging. It runs in seven main bearings, which are steel backed with aluminium based alloy running surfaces. Balance weights are secured to a flat seating on the crank webs by bolts and dowels.
  
- **Camshaft and Followers**      The camshaft is supported in the crankcase by seven bearings and is driven from the front of the crankshaft by helical gears. Cam followers are of the roller type.

- **Cooling System**      Engine mounted pumps provide circulation for both jacket and charge-cooler water circuits.
  
- **Lubrication**        An externally mounted rotary oil pump supplies oil for lubrication and piston cooling. Relief valve is integral with pump. Oil is supplied to main bearings and piston cooling jets through rifle drillings in the crankcase.
  
- **Electrical System**      Standard fitment is a 24v alternator, together with regulator and electric starter.

Schematic and cross-sectional views of the engine are shown in figures 3.1(a) and 3.1(b) respectively.

For many years Dorman have converted a proportion of their diesel production for operation as spark-ignited natural gas engines. This has been achieved by reducing the compression ratio and replacing the fuel injection equipment with a spark ignition system and gas carburettor. The main market for this type of engine has been the USA. However, recent emission legislation, particularly against nitrogen oxides ( $\text{NO}_x$ ), means that these engines are becoming unacceptable in this form. The development work at Dorman on the stratified charge lean burn 6SE gas engine is therefore aimed at meeting these low ( $\text{NO}_x$ ) emissions. In view of this the single cylinder engine, denoted 1SE, has been designed such that it may be readily converted to either natural gas or diesel operation. The engine delivered to the university has been set up initially for lean combustion of natural gas; the second engine at Stafford is being used for diesel development work.

### 3.1.2 Design Constraints

To ensure compatibility of results and help reduce costs, common parts have been used as far as possible. In-cylinder components are identical. Also, as the six cylinder engine has unit heads the

single is able to use an existing head (diesel or gas) without requiring any modification. Where on the design it has been necessary to scale down the size of components, for example oil and water pumps, suitable replacements have been selected from other Dorman engine ranges. In reproducing one cylinder versions of six cylinder engine components every effort was made to keep design details as similar as possible. Conceptually the new design was formed by joining the front portion (associated with the first throw) to the rear portion (sixth throw). The "joining line" would be the cylinder centre-line of the respective throws. In this way the new design would allow extensive use of existing tooling, jigs and fixtures.

Throughout the design, the question was asked: can the existing component be used or adapted, before a new design was contemplated. Whilst this approach has obvious benefits in terms of cost, there are also gains in lead-times. It is far easier and quicker to adapt an existing component than design and then have a new component manufactured. Such a philosophy, however, was not allowed to compromise any part of the design. If an "adapted" design was thought likely to be unsatisfactory, it was rejected and a new design drawn up.

### 3.1.3 Engine Services

One of the problems on a single cylinder engine is finding the means to drive and locate the services which are required within a relatively small engine frame. Additionally, the means of simulating turbocharged conditions cause further complication. The installation of the services will be discussed in greater depth in chapter 7.

#### (1) Air Supply and Exhaust Systems

As the SE range consists solely of turbocharged engines the single has to reproduce pressure charged conditions. It is not usually

possible to turbocharge a single cylinder engine; moreover the pressure fluctuations in the exhaust manifold are likely to be unrepresentative of the multi-cylinder engine. Therefore it is normal to provide a supply of compressed air from an external compressor: the delivery pressure and mass flow requirements being dependent upon the cylinder size, engine speed and charge air pressure. An aftercooler is sited after the compressor to adjust the charge air temperature to a representative condition.

Within the School of Mechanical Engineering the infra-structure exists to meet these requirements. The pressurised intake supply is delivered by a large (1500 cfm) Belliss compressor. A large air receiver, mounted externally, acts both as an aftercooler and as the necessary smoothing agent to remove unwanted pulsations in the air delivery.

Exhaust noise from a single cylinder engine has a low frequency and is more objectionable than that from an equivalent sized multi-cylinder engine. Silencers therefore have to be of a considerable size relative to the air flow and at least two are generally necessary. In specifying the exhaust system the aim is to produce conditions after the exhaust ports that are identical to those on the multi-cylinder engine, at least while the exhaust valve is open. The details of the method employed are further dependent on the type of turbocharger operation: constant pressure manifold or pulse turbocharged manifold. The exhaust installation for the 1SE engine is covered in detail in section 4.4 of chapter 4. It is based on the extensive review of this topic by McKenzie and Dexter (2).

#### (ii) Lubricating Oil System

To provide greater test flexibility, and since an engine driven pump can prove difficult to locate, an electrically driven oil pump is often selected. Furthermore, it also helps to reduce the frictional overheads incurred by a single in comparison with the multi-cylinder engine. However, on the 1SE it was decided to drive the oil pump

from the engine. For this purpose one of the primary balancers was used to provide a drive. This would avoid any necessity for "interlocking" - to prevent the engine being started with no oil flow if an electrically driven oil pump were used. Also, in what may be termed the first design phase, it was more important to get the engine running in as short a time as possible. At a later stage the oil circuit could be changed for improved flexibility.

#### (iii) Coolant Circuit

For similar reasons to those above it was again decided that the easiest solution would be to drive the water pump from the engine. This time the pump would be belt driven from a pulley on the front of the crankshaft.

#### (iv) Gas System (Gas Engine Only)

The six cylinder carburettor is too large for it to be used on the single cylinder engine. Instead of selecting a smaller replacement a stepper-motor controlled mixer was designed which would allow easy adjustment of the air-fuel ratio of the main charge. For further flexibility a second smaller mixer would allow control of the pilot charge air-fuel ratio. (Both designs are covered in chapter 7). The natural gas fed to the engine needs to be at a pressure comparable with the boosted air supply to allow mixing to occur in the carburettor (mixer). To achieve this an external installation incorporating gas booster, cooler and numerous safety features was required. The only engine mounted components, besides the mixers, would be the coil and magneto. The magneto would be driven from the second primary balance shaft. The pre-chamber assembly replaces the diesel unit injector in the cylinder head. Governing of the engine is electronically controlled and operates on the butterfly valve.

#### (v) Fuel System (Diesel Engine Only)

On the diesel 1SE, the magneto of the gas engine is replaced by the low pressure fuel pump, similarly driven. The governor now controls the fuel rack setting on the unit injector.

#### 3.1.4 Experimentation

The type of research that will be undertaken on a single cylinder engine also plays a part in shaping the design. When used to support multi-cylinder development the thrust of the experimentation will undoubtedly be aimed at optimising the engine parameters. Compared with the multi-cylinder engine, the single is considerably cheaper to run and allows changes in build to be accomplished more readily. Possible uses in development during the life of an engine family are shown in figure 3.2.

If the single is not necessarily based on a specific engine family, or where it outlives its development requirements, then it can prove very useful in long term research. As well as undertaking research similar to that shown in figure 3.2 more radical areas can be investigated. Thus, the performance work might include such areas as very high firing pressures, high compression ratios, combustion photography and future fuels research. The engine could also be used for component development: for example, the use of ceramics and novel piston designs. Finally the single cylinder engine can be used as a standard test engine to measure the effect of different lubricating oils, fuels and components on mechanical and thermodynamic properties.

Whilst the specification for the 1SE is as a development tool for the SE range, consideration of these other roles is important if the design is to be versatile. Admittedly, in the initial design these considerations were heavily outweighed by the need for compatibility and the need to make maximum use of existing components. It is envisaged that the single at Dorman will be primarily used for SE

development work throughout its life. The university's engine, however, could in future be used for more fundamental research work.

In both cases the need to provide access for instrumentation is fairly apparent: not just for measurement of various performance parameters, but also to enable correlation of results with the multi-cylinder engines. Generally single cylinder engines afford good access, though constraints are imposed by the need to locate all services within just one cylinder.

### 3.1.5 Preliminary Design of Major Components

The longest lead-time items in a new engine design are invariably the crankcase and crankshaft. Thus ideally, initial design work would centre on these components, particularly as a new crankshaft design would have to be manufactured under sub-contract. However the overall design is strongly governed by the balancing requirements for the engine and so could only proceed once the details for the balancer assembly had been finalised. Early evaluation of flywheel requirements and the design for the camshaft was also necessary. In the remainder of this sub-section the preliminary designs for these components, with the exception of the balancer assembly, are discussed. The preliminary balancer assembly design is covered in section 3.4. It is preceded by two sections. In the first, the theory associated with engine balancing and its necessity in a single cylinder engine is presented. The second reviews the various counter-balancing options available before discussing the solution employed on the 1SE.

#### (1) Crankshaft

At an early stage the possibility of using the rear portion of the existing forged 6SE crankshaft was investigated. The sixth throw of the crankshaft transmits the power to the flywheel and also contains the necessary thrust faces. It was thought that by using this



section of a crankshaft, possibly a rejected one, that the cost for a single cylinder crankshaft could be reduced.

The six cylinder crankshaft has a standard firing arrangement 1-5-3-6-2-4 and is therefore inately balanced. To reduce the magnitude of the opposing internal couples it has balance weights on webs 1,6,7 and 12. These, following standard convention, are arranged at 90° to crankpins 2 and 5. This means that the balance weights do not sit immediately opposite the corresponding crankpins, but are canted over at some 30 degrees. The single cylinder requires two weights mounted opposite the crankpin and equally displaced from the cylinder axis.

This meant, that if the six cylinder crankshaft was to be used, provision would have to be made to attach a second balance weight on the eleventh web (crankpin 6). Further, new balance weights would be required having a large overhang to ensure that the combined centre of gravity would lie directly opposite the crankpin. Such a design for the balance weights would have resulted in very high stresses, and there was also the problem of fitting them within the confines of the existing crankcase walls. For these reasons, plus the fact that this extra complication would not result in the cost savings envisaged, this approach was abandoned. A new single cylinder crankshaft was required. To ensure that, as far as possible, existing tools and jigs could be used, much of the design detail of the six cylinder crankshaft was carried over to the single.

#### (11) Crankcase

An important fact in the development of the 1SE single cylinder research engine was that at a very early stage it was established that a single cylinder crankcase could be cast using the pattern equipment of the 6SE. The possibility of a fabricated construction had been very briefly considered, perhaps incorporating the necessary location for the balancer shafts (section 3.4), but was rejected. It was felt that the design would have been too dissimilar to the multi-

cylinder engine; no cost advantage could be envisaged and the lead-time would possibly have been unacceptably long. Further, the design would have been untried and would have warranted considerable analysis, for which there was insufficient time.

By using the rear portion, the sixth cylinder, of the existing mould it would be relatively easy to impart all the necessary rear end detail - thrust faces, main bearing supports, etc. - to the single cylinder. The correct front detailing would be achieved by locating a blanking piece, carrying the same pattern detail as the front of the 6SE mould, immediately before the sixth cylinder. The standard cylinder core block would then be used to give the identical internal details. Having set the "new" pattern the remainder of the mould could then be filled with sand ready for casting. This approach, whereby the single cylinder is merely a shortened version of the 6SE crankcase, had many advantages. With the distances from the cylinder centre line to the front and rear end faces identical to those of the six, the designs for the crankshaft and camshaft were very much simplified. Also because the front and rear ends of the crankcase are unaltered, drilling and machining details of these faces could be kept the same, thus ensuring the use of existing tooling and fixtures.

The crankcase of a single cylinder engine is inherently weaker than that of a multi-cylinder engine because in the multi-cylinder the combustion pressure load is "shared" with adjacent cylinders. To overcome this the material for the 1SE crankcase was upgraded to S.G. (spheroidal graphite) iron.

#### (111) Flywheel

With a single cylinder engine only firing once for every two revolutions of the crankshaft the torque fluctuations are large (61). To combat this and bring the cyclic variation down to the level of the 6SE, the flywheel moment of inertia of the 1SE had to be increased to 3.3 times that of the six cylinder engine. The

necessary increase in inertia was estimated to double the existing weight of the flywheel. Concern was felt as to what effect this increase in static load would have on the rear bearing in the crankcase. To ensure that this would not result in failure of the rear main bearing, details of the proposed design were sent to the bearing manufacturer for analysis. An inadequate oil-film would have serious repercussions: the design of the rear crankcase journal might need altering or provision might have to be made for a second support (out-rigger) for the flywheel. Fortunately their report (62) concluded that the existing bearing would perform satisfactorily.

One solution to increase the inertia of the flywheel would be to shrink a ring onto the existing 6SE flywheel. This was rejected on two counts: the physical size of the ring to be shrunk on would cause manufacturing problems, and that the ring itself would need to be cut from a large section of plate, giving rise to excessive waste material. Some securing bolts would still have been necessary and there was concern over the bolt holes acting as stress raisers.

The simplest solution was to machine a new flywheel from a single plate. A balanced steel (Grade 50B), ultrasonically tested, was chosen. The design was a copy of the 6SE flywheel with the rim enlarged to accommodate the increase in inertia.

#### (11) Camshaft

The 6SE camshaft is supported in the crankcase by seven bearings and driven from the front by helical gears. The proposed design for the new crankcase (11) would maintain the front and rear bearing to cylinder axis distances the same. Thus, the design for a new single cylinder camshaft would be an identical copy of the front portion. Reviewing the options available - new or adapt the 6SE camshaft - it became clear that the more cost effective and easiest solution would be to use the first throw arrangement of the 6SE camshaft. Since this camshaft is a seven bearing design, with the bearings equally displaced, the 1SE camshaft could be manufactured by simply sawing

the six-cylinder camshaft off after the second journal. The camshafts for the diesel and gas engines were both obtained in this way. Using the front end would ensure that all the necessary machining for the location and attachment of the camshaft gear was in the correct place.

### 3.2 Balancing a Reciprocating Engine

In any engine the reciprocating motion of the pistons and the complex motion of the connecting rods set up forces and couples which then react on the engine structure. For every cylinder of the engine there is not only a disturbing force, which acts along the cylinder axis due to the reciprocating motion of the piston and small end, but also a rotating out-of-balance associated with the crankpin, webs and big end of the connecting rod. This force is constant in magnitude, but rotates with the crankshaft.

These forces impose loads on the main bearings and tend to shake the whole structure. In an in-line engine the forces act in planes parallel to one another, and dependent on the crank arrangement used, can lead to pitching, yawing or even rolling of the engine. It is for this reason that during the design phase these forces need careful consideration, not only to eliminate all external forces and couples, if possible, but also to reduce the magnitude of internal couples tending to bend the engine crankcase and overload individual bearings. For an engine to be fully balanced it is necessary to arrange the crank throws such that the resulting net forces and couples transmitted to the structure are zero. Typically this is not the case without resorting to other means.

### 3.2.1 Rotational Balance

The rotational force generated by the out-of-balance mass  $m$  of the crankpin, webs and big end (see appendix 1) with its centroid at a radius  $r$ , and rotating at a speed  $\omega$  rad/sec, is given by:

$$F = m\omega^2 r \quad \dots A2.1$$

The effects of this force on the engine structure may be eliminated either by balancing each throw individually or by considering the engine as a whole. The former is obtained by securing two balance weights directly opposite the crankpin, each weight being symmetrically displaced about the cylinder centre line to avoid the introduction of unwanted couples (see appendix 2). Where the crankshaft is to be made in large numbers these weights may be either forged or cast integrally with the crankshaft. Later machining ensures that balance is achieved. The latter method involves arranging the crankthrows such that at any given time the rotational out-of-balance of one crankthrow is counteracted by the out-of-balance of another throw or combination of throws. Even then balance weights may be added to reduce the size of the internal couples present to avoid overloading of individual bearings and so minimise failure due to an inadequate oil film.

### 3.2.2 Reciprocating Balance

In an internal combustion engine the piston assembly, gudgeon pin and an associated part of the connecting rod (appendix 1) reciprocate in the cylinder bore. As they are accelerated and decelerated at top and bottom dead centres disturbing forces are produced along the cylinder axis. The nature of this force, described in detail in appendix 3, is given by the equation:

$$F = M_{\text{RECIP}} \omega^2 R (\cos\theta + (R/L)\cos 2\theta) \quad \dots A3.3$$

where:

$F$  = reciprocating out-of-balance force

$M_{\text{RECIP}}$  = reciprocating mass

$\omega$  = engine speed

$R$  = crank throw

$L$  = connecting rod centre distance

Thus the force may be seen as being made up of two components, both acting along the cylinder axis; one component arising at engine speed, known as the primary force, and the second at twice engine speed - the secondary force. Whilst clearly being dependent on the reciprocating mass and stroke ( $2R$ ) of the engine, the importance of engine speed should be noted.

In a multi-cylinder engine, therefore, every effort is made to eliminate or at least reduce the size of the resulting disturbing forces and couples. Generally by designing the crankshaft such that the cranks are symmetrically arranged it is possible to eliminate most of the disturbing effects. Thus in a four cylinder in-line engine with firing order 1-3-4-2 there is complete primary force balance. Also as the crankshaft is a mirrored arrangement about its centre the primary and secondary couples produced in each half cancel each other out. Only the secondary forces remain completely unbalanced. As the resultant force is quite low their effect can be reduced to acceptable levels by installing the engine on flexible mountings of low stiffness. For the case of an in-line six cylinder engine the primary and secondary forces and couples may be inately balanced. However, for both engine configurations balance weights are added to the crankshaft to reduce the effect of the opposing couples within the engine structure and hence minimise the crankshaft deflections.

### 3.3 Reciprocating Balance of a Single Cylinder Engine

For full balance it is necessary to eliminate the effects of both the reciprocating and rotational out-of-balance forces and couples. The latter, consisting of the total out-of-balance force of the crankpin, webs and a portion attributable to the connecting rod, is relatively

easily achieved by attaching two balance weights each having a moment equal to half the out-of-balance, with their combined centre of gravity opposite to that of the crankpin. Merely balancing the rotating weight, however, leaves the reciprocating forces acting along the cylinder axis unbalanced.

Many solutions are available to deal with the problem of reciprocating out-of-balance. They do not all necessarily eliminate the problem; some merely reduce the magnitude of the disturbing force transmitted to the surroundings to a level which is acceptable for the particular application envisaged. The route chosen is also largely governed by the size of the disturbing forces themselves. The problem is further complicated by the fact that the disturbing force, as shown in appendix 3, consists of two components, a primary force (engine speed) and a secondary force (twice engine speed). Thus, if it is required to eliminate both components two separate solutions are needed. A summary of the solutions generally used is given in the sections that follow.

### 3.3.1 Primary Balance

There are three generally used alternatives aimed at reducing or eliminating the out-of-balance balance moment  $M_{\text{RECIP}R}$  associated with the primary component of the disturbing force (63).

(1) Over-balance of the rotational forces.

Suppose a proportion  $x$  of the reciprocating out-of-balance is added to the crankshaft opposite to the big end. This will then produce an out-of-balance moment  $xM_{\text{RECIP}R}$  which can be considered as providing a component vertically, i.e. along the axis of the cylinder, equal to  $xM_{\text{RECIP}R}\cos\theta$  and a corresponding moment  $xM_{\text{RECIP}R}\sin\theta$  horizontally, where  $\theta$  is the angle turned through by the crank measured from top dead centre (see figure 3.3). Since the downward component due to the balance weight opposes the upward force due to the reciprocating mass the net out-of-balance along the cylinder axis is:

$$M_{\text{RECIP}} R \cos \theta - x M_{\text{RECIP}} R \cos \theta = (1-x) M_{\text{RECIP}} R \cos \theta$$

It can be seen, however, that if balance weights are added to reduce the primary reciprocating out-of-balance by a proportion  $x$ , a horizontal out-of-balance  $x M_{\text{RECIP}} R \sin \theta$  is simultaneously introduced. In practice half the reciprocating primary out-of-balance is usually balanced as a compromise ( $x = 0.5$ ). This is evenly divided between two weights normally mounted outside the crankshaft journals, as space considerations usually preclude the additional weight being added to the weights used for rotating balance. Generally this method is used for relatively small out-of-balance forces or where the motion induced horizontally is unimportant. It must also be noted that it imposes additional loads on the crankshaft.

#### (ii) Principle of Reverse Cranks.

If two masses having the same out-of-balance of  $0.5 M_{\text{RECIP}} R$  are simultaneously arranged to rotate in opposite directions at the same speed then each of them produces an upward force  $0.5 \omega^2 M_{\text{RECIP}} R \cos \theta$  at a speed of  $\omega$  radian/sec. Referring to figure 3.4 it can be seen that the vertical components are always in phase, and so adding them to one another produces a varying moment  $M_{\text{RECIP}} R \cos \theta$ . In the horizontal direction the components are in anti-phase and so when added cancel one another.

This concept is a useful one since it permits replacing a single harmonically varying moment (or force) acting in one plane only by two counter-rotating vectors each having half the original magnitude. This principle can therefore be applied in the balance of primary and secondary disturbing forces in the case of a single cylinder engine and for dealing with primary and secondary out-of-balance forces and couples where they occur in multi-cylinder engines.

In figure 3.5 the ideal arrangement is shown for balancing the primary forces of a single cylinder engine. Here the balance weights shown on the crankshaft eliminate the rotating out-of-balance only,



but the two balancer shafts are arranged to be rotated in opposite directions at crankshaft speed. If the shafts are equi-distant from the vertical cylinder axis and the centre of mass for the two balancer masses are arranged to be on the longitudinal cylinder axis the primary out-of-balance is eliminated.

#### (iii) Principle of Reverse Cranks - one balancer shaft only.

This is the same as the method above (ii), except that the primary balancer weight rotating in the same direction as the crankshaft is incorporated in the crankshaft balance weight to reduce the size and cost of the engine. The primary out-of-balance force is eliminated, but at the cost of introducing a harmonic rolling couple equal to  $0.5M_{\text{RECIP}}RL$  due to the vertical distance  $L$  between the two balancer shafts (see figure 3.6). Again as in method (i) extra loads are imposed on the crankshaft because of the additional weights.

### 3.3.2 Secondary Balance

The secondary out-of-balance force is given by:

$$\omega^2 M_{\text{RECIP}} (R/L) \cos 2\theta$$

As can be seen this may only be balanced by a force rotating at twice crankshaft speed. The secondary force acts along the cylinder axis, so two balancer shafts rotating in opposite directions must be used in a similar way to the primary balancers in section 3.3.1 (ii).

If the moment to be provided by each balancer shaft is  $M_r$  then

$$\begin{aligned} \omega^2 M_{\text{RECIP}} R(R/L) &= (2\omega)^2 2M_r \\ \Rightarrow M_r &= \frac{M_{\text{RECIP}} R(R/L)}{8} \end{aligned}$$

The balancer masses must be phased to act downwards when the piston is at top dead centre.

### 3.4 Balancing of the 1SE Engine

To be able to decide what form of balancing, if any, is required it is first necessary to calculate the effects of the disturbing forces on the engine test-bed installation.

#### 3.4.1 Excitation Induced by Reciprocating Forces

For engines running at high speeds the resulting out-of-balance forces can be very high giving rise to large amplitudes of vibration. Therefore as a means of assessing the likely magnitude of these vibrations the engine installation may be represented by a simple mass-spring-damper system (figure 3.7), where the disturbing force is due only to the reciprocating mass, i.e. full rotational balance is assumed.

From the detailed derivation undertaken in appendix 4 the maximum resulting amplitude of vibration ( $x_{max}$ ), where the engine, mass  $M$ , is operating well above its natural frequency, is given by

$$x_{max} = \left| \frac{M_{RECIP} R \eta^2}{M(1-\eta^2)} \right| + \left| \frac{M_{RECIP} R(R/L) \eta^2}{M(1-4\eta^2)} \right| \quad \dots A4.10$$

$[x_1] \qquad \qquad [x_2]$

where  $\eta = \frac{\text{forcing frequency}}{\text{natural frequency}}$

As can be seen the resulting amplitude again consists of two components; the first and second terms being due to the primary and secondary out-of-balance forces respectively.

In table 3.2 each component is tabulated separately to highlight the contribution of the two forces. Engine data is taken from table 3.3. It is worth noting the important factors; first, operating the engine well beyond the natural frequency of the installation has little effect on the resulting amplitude. (Engine mounts are normally selected such that the natural frequency of the system is less than a

third of the forcing frequency - i.e.  $\eta > 3$ ). Secondly, the contribution of the primary out-of-balance force is much larger than the secondary. Though the magnitude of the forces only differ by the factor  $R/L$  (approx. 0.3), the contribution to the amplitude of vibration of the primary disturbing force is approximately fifteen times that of the secondary.

To be able to assess whether these values are at all acceptable it is necessary to turn to figure 3.8, due to W. Ker Wilson (64). The normal operating speed of the existing six cylinder 6SE engine is governed by the requirements for electricity generation: 1500 rpm (approx.) for 50 Hz or 1800 for 60 Hz. Allowing for some overspeed protection it is safe to assume, for calculation purposes, that the maximum engine speed will be 2000 rpm, corresponding to a mean piston speed of 12.7 m/s. This will produce an excitation frequency of 2000 cycles/min. due to the primary unbalance, and a further excitation frequency of 4000 cycles/min. due to the secondary unbalance. Ideally, an engine should operate in the normal-smooth region. This is particularly the case for a research engine where there is a requirement for measurements taken from the engine to be accurate and consistent. This can be made difficult where external vibration interferes with transducer readings (5). Thus from the figure the maximum allowable vibration is of the order  $\pm 0.025$  to  $\pm 0.050$  mm ( $\pm 0.001$  to  $\pm 0.002$  inches). This should be compared with the predicted amplitude of vibration for the unbalanced engine of approximately 3 mm; some hundredfold greater!

#### 3.4.2 Reciprocating Balance Solution for the 1SE

From the previous section it has been established that the predicted amplitude of vibration needs to be reduced by a factor of a hundred. It is perhaps helpful therefore to re-write the equation A4.10 to highlight the important factors.

$$x_{max} = \frac{M_{RECIP} R \eta^2}{M} \left[ \left| \frac{1}{(1-\eta^2)} \right| + \left| \frac{R/L}{(1-4\eta^2)} \right| \right]$$

It has already been demonstrated that altering the value of  $\eta$ , i.e. changing the stiffness of the mountings, has little effect on the excitation transmitted (table 3.2). Since the engine components (piston mass, crankthrow etc.) are fixed the only parameter that can be changed is the installation mass  $M$  - the mass of the engine and frame. However, as the equation illustrates, the relationship is purely proportional, so that a hundredfold reduction in the amplitude of vibration requires the sprung mass to be increased by the same factor. This is clearly impractical as this would mean a suspended test-bed of forty tonnes! This is in agreement with Griffin and Wittek (5) where a smaller single cylinder than the 1SE with primary unbalanced forces of 19.4 kN running at 2000 rpm was bolted to over nine tonnes of concrete. It would be possible to bolt the engine and dynamometer together and then mount them as an assembly, but this would not give the mass increase required. Thus the most suitable method available is to counter-react the disturbing forces by the use of balance shafts mounted on or within the engine frame.

Referring to table 3.2 it has been shown that the primary out-of-balance force contributes fifteen times as much to the vibration amplitude, compared to the secondary unbalance, and so balancing the primary unbalance would do much to reduce the problem. However, it is worth noting that complete balance of the primary force would still leave an amplitude of vibration equal to approximately  $\pm 0.2$  mm. This is still a factor of ten too large. The amplitude could be reduced to acceptable levels by then mounting the engine on a concrete plinth weighing four tonnes. Since the design already requires balancing of the primary forces there is much to be said for doing likewise with the secondary forces. The extra complication is small; the secondary shafts being arranged to be driven directly off the primary gears via suitable 2:1 gearing. There is also a case to be made for "over-engineering" the design to ensure that the research engine will run satisfactorily in the future when it is used for applications perhaps unforeseen at the time of conception.

The method of balancing selected for both primary and secondary forces is the principle of reverse cranks, as detailed in section

3.3.1 (ii). This is the only method available for secondary balancing and whilst others do exist for primary balancing they do not fulfil the requirement to the same extent. The layout eventually chosen followed very much the standard practice (2,4,5 and 8); the balancers being symmetrically located below the crankshaft driven by an intermediate idler gear. In fact generally the only variation is the position of the secondary balancers, in relation to the primary balance shafts. This tends to be governed by space considerations.

In the design of the 1SE the standard layout, as illustrated in figure 3.9, was adopted. It has the benefit that the balancer shafts may be separated from the crankcase. This is an important point, as at an early stage it was established that the new single cylinder crankcase could be made from the existing patterns and cores of the six cylinder crankcase, so long as major modifications were not required. Having the balance shafts suspended below the engine as a self-contained unit helps to lower the centre of gravity of the engine, offsetting the fairly heavy cylinder head and rocker gear assembly.

### 3.5 Summary of the Preliminary Design

In the preceding sections the various aspects which have played a part in shaping the 1SE engine design have been discussed. Emphasis has also been placed deliberately on the areas which occupied the majority of the design time. It is now proposed to unify these ideas in summarising the key features of the single cylinder research engine.

- |                          |   |
|--------------------------|---|
| ● In-cylinder Components | These are identical to the respective diesel or gas engine.                                       |
| ● Cylinder Head          | Standard 6SE four valve head, with either a unit injector (diesel) or pre-chamber assembly (gas). |

- Crankcase                    New casting produced from existing pattern equipment. Rear and front details and internal core structure identical to 6SE.
  
- Crankshaft                A new design machined from a solid billet. The journals, front and rear ends are identical to the 6SE crankshaft. Camshaft and balancer assembly gear driven from the front of the crankshaft. Two balance weights are secured to the webs to ensure full rotational balance of the assembly.
  
- Camshaft                  Front portion of either diesel or gas fuelled 6SE camshaft used. Valve train identical with respective engines.
  
- Flywheel                  A new steel flywheel with an inertia 3.3 times the 6SE flywheel. Hub and SAE flange detailing identical.
  
- Balancer Assembly        A fabricated steel housing located below the crankcase. It supports a pair of primary and secondary balancers which are gear driven from the crankshaft via an intermediate idler gear.
  
- Cooling System           Engine mounted water pump, belt driven from the pulley on the front of the crankshaft. Cooling (thermostatically controlled) via a heat exchanger and secondary water circuit.
  
- Lubrication               Oil pump driven from right-hand primary balancer. It supplies high pressure oil for lubrication and piston cooling through rifle drillings in the crankcase. A low pressure tapping feeds the roller bearings in the balancer assembly.

- Electrical System      Engine uses the standard 6SE electric starter. Power is from batteries.
  
- Air Supply              Pressurised air is supplied externally from a large compressor, through an air receiver and smoothing tank, to a standard manifold section.
  
- Exhaust System        Exhaust gases are fed away by a standard manifold section. Turbocharged flow conditions are simulated by an orifice, plenum and gate-valve arrangement. The exhaust system is completed by two large silencers.
  
- Gas System  
  (Gas only)              Mains supply boosted and cooled by an external compressor and cooler installation. Magneto is driven from left-hand primary balancer. Pre-chamber, installed in place of unit injector in cylinder head. The air-fuel ratios of the cylinder charge and pilot pre-chamber supply are independently adjustable by stepper motor controlled mixers.
  
- Fuel System  
  (Diesel Only)          Unit injector in cylinder head operated by push rod and rocker from camshaft. Fuel lift pump driven from left-hand primary balancer.

6SET: Turbocharged (Radiator cooled engine)  
 6SETCR: Air-to-water charge air cooled (Radiator cooled engine)  
 6SETCA: Air-to-air charge air cooled (Radiator cooled engine)  
 6SETCW: Air-to-water charge air cooled (heat exchanger or remote radiator cooled engine)

## TECHNICAL DATA

Combustion system	Direct injection	
Bore	mm	160
Stroke	mm	190
Number of cylinders	6 in-line	
Swept volume	litre	22.92
Compression ratio	13.6:1	
Injection equipment	Unit injector	
Rotation viewed on flywheel	Anti-clockwise	
Oil capacity	litre	113.4
Lubricating oil specification	MIL-L-2104C or	API CC + CD
Fuel oil specification	BS 2689: Class A2	

## Fixed Speed Performance Tables to ISO 3046 (BS 5514) to standard reference conditions (see below)

Continuous Ratings					Specific Fuel Consumption				Lubricating Oil Consumption			
kW <sub>b</sub> (bhp)					g/(kW <sub>b</sub> h)				litre/h			
r/min.	1000	1200	1500	1800	1000	1200	1500	1800	1000	1200	1500	1800
6SET	—	—	392 (526)	—	—	—	209	—	—	—	1.10	—
6SETCR1	273 (366)	331 (444)	446 (598)	446 (598)	232	219	212	219	0.73	0.84	1.10	1.21
6SETCR2	326 (437)	384 (515)	456 (611)	456 (611)	218	216	212	219	0.83	0.96	1.13	1.30
6SETCA1	—	—	484 (649)	484 (649)	—	—	209	224	—	—	1.38	1.44
6SETCA2	—	—	538 (721)	538 (721)	—	—	209	223	—	—	1.62	1.72
6SETCW	—	—	538 (721)	538 (721)	—	—	203	213	—	—	1.62	1.72

One Hour Ratings					Specific Fuel Consumption				Lubricating Oil Consumption			
kW <sub>b</sub> (bhp)					g/(kW <sub>b</sub> h)				litre/h			
r/min.	1000	1200	1500	1800	1000	1200	1500	1800	1000	1200	1500	1800
6SET	—	—	432 (579)	—	—	—	215	—	—	—	1.21	—
6SETCR1	300 (403)	364 (488)	491 (658)	491 (658)	232	219	214	222	0.80	0.92	1.21	1.33
6SETCR2	359 (481)	422 (566)	502 (672)	502 (672)	221	216	214	222	0.91	1.05	1.24	1.43
6SETCA1	—	—	532 (714)	532 (714)	—	—	210	223	—	—	1.51	1.58
6SETCA2	—	—	592 (793)	592 (793)	—	—	212	224	—	—	1.78	1.90
6SETCW	—	—	592 (793)	592 (793)	—	—	205	212	—	—	1.78	1.90

Table 3.1 Technical Data for Dorman 6SE Diesel Range



$\eta$	$x_1$ (mm)	$x_2$ (mm)	$x_{max}$ (mm)
3	2.75	0.18	2.93
5	2.55	0.17	2.72
10	2.47	0.17	2.64

**Table 3.2 Amplitude of Vibration due to Unbalanced  
Primary and Secondary Forces**

#### DATA FOR THE 1SE SINGLE CYLINDER ENGINE

Piston assembly (rings and gudgeon pin)  $M_{\text{RECIP}} = 7.25 \text{ kg}$

Connecting rod: big end  $M_{\text{BE}} = 6.10 \text{ kg}$

small end  $M_{\text{SE}} = 3.05 \text{ kg}$

centre distance  $L = 0.336 \text{ m}$

Stroke = 0.190 m throw  $R = 0.095 \text{ m}$

$R/L = 0.283$

Engine speed: 1500 rev/min (approx)  $\rightarrow 50 \text{ Hz}$

1800 rev/min (approx)  $\rightarrow 60 \text{ Hz}$

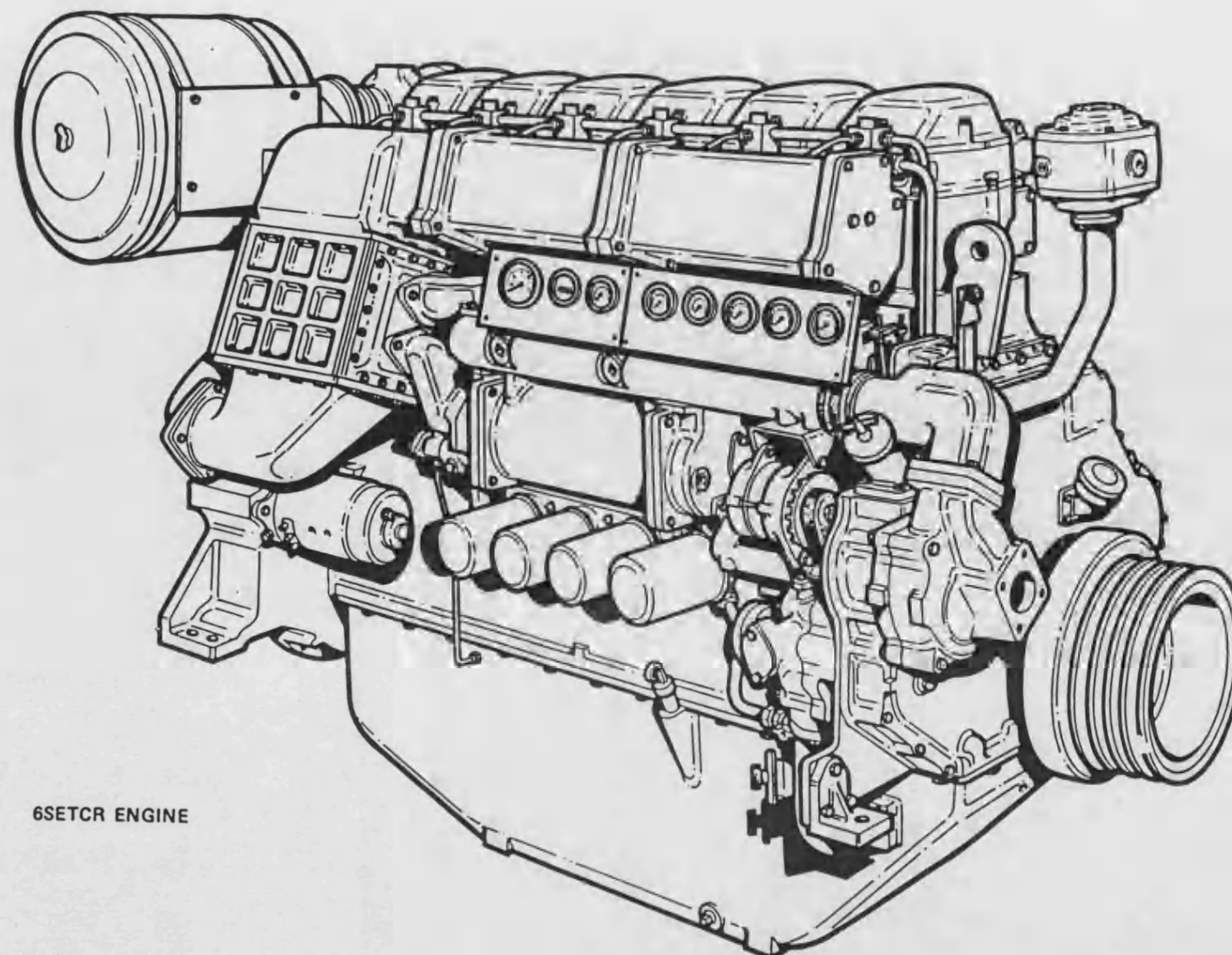
Maximum taken as 2000 rev/min

Firing order: 1-5-3-6-2-4

Engine mass (estimated):  $M = 400 \text{ kg}$

Note: This was based on the 6SE having a mass of  $\approx 2000 \text{ kg}$ . However estimated value is a gross underestimate - the true engine mass is closer to 800 kg. The difference, however, does not affect the validity of the decision taken - the need for both primary and secondary balancers.

Table 3.3 Engine Data for Balancing Calculations



6SETCR ENGINE

Figure 3.1(a) Schematic View of Dorman 6SE Diesel Engine

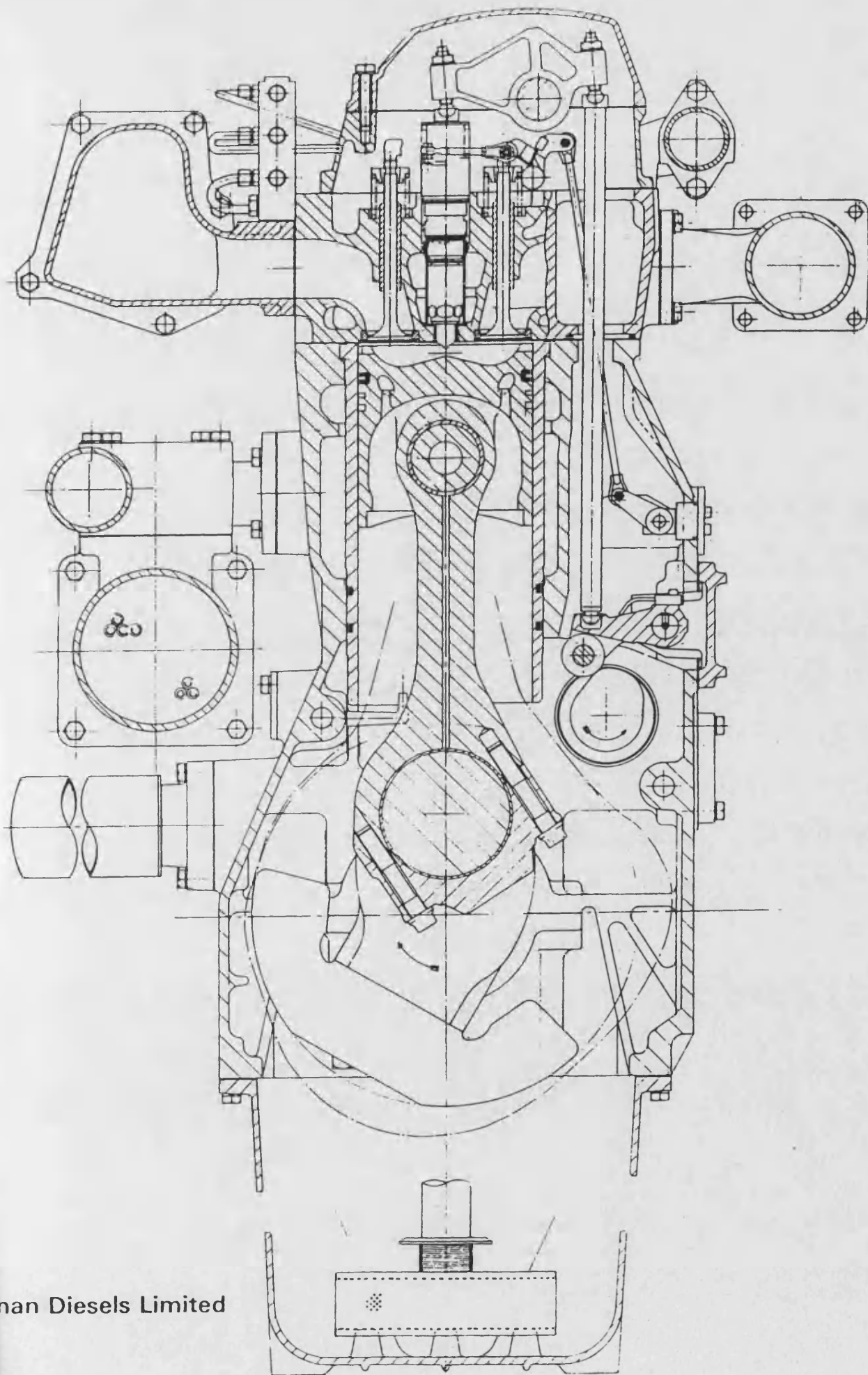
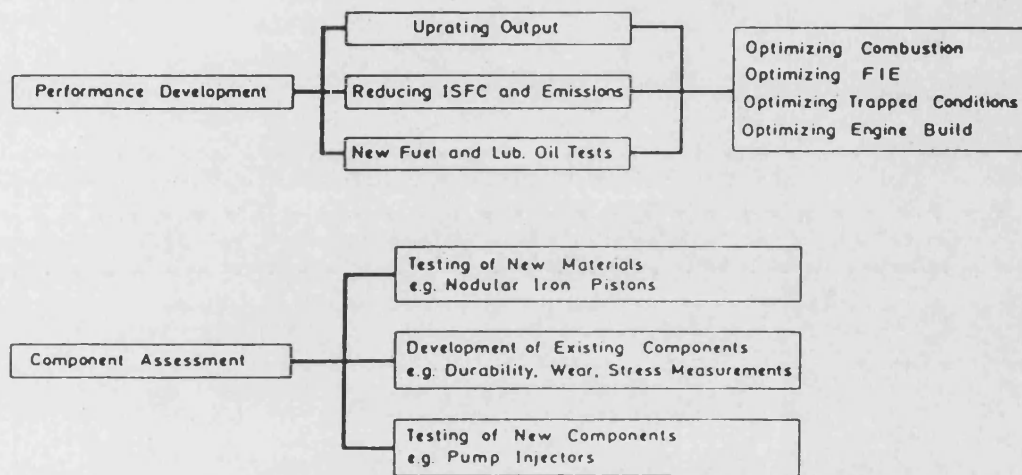


Figure 3.1(b) Cross-section through Dorman 6SE Diesel Engine



**Figure 3.2 Use of Single Cylinder Engine in Developing an Existing Engine Family (2)**

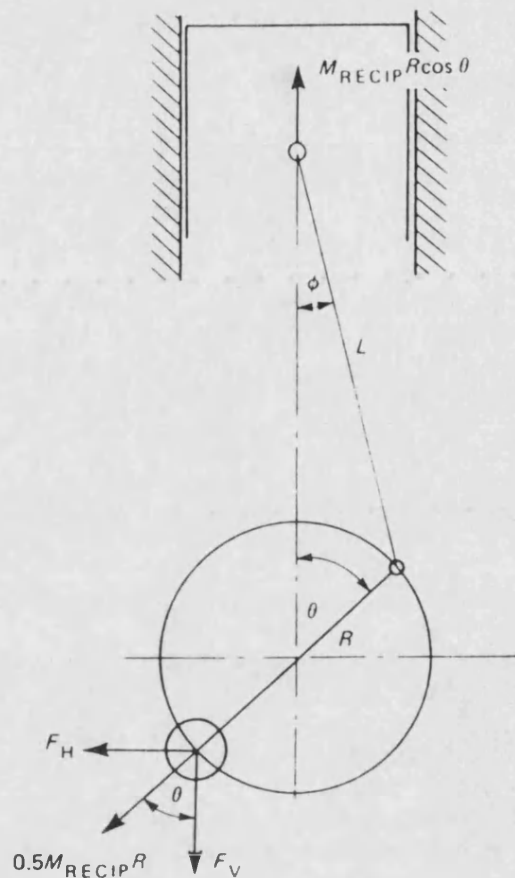


Figure 3.3 Diagram to show Basic Balancing Principles for a Single Cylinder Crank Throw (63)

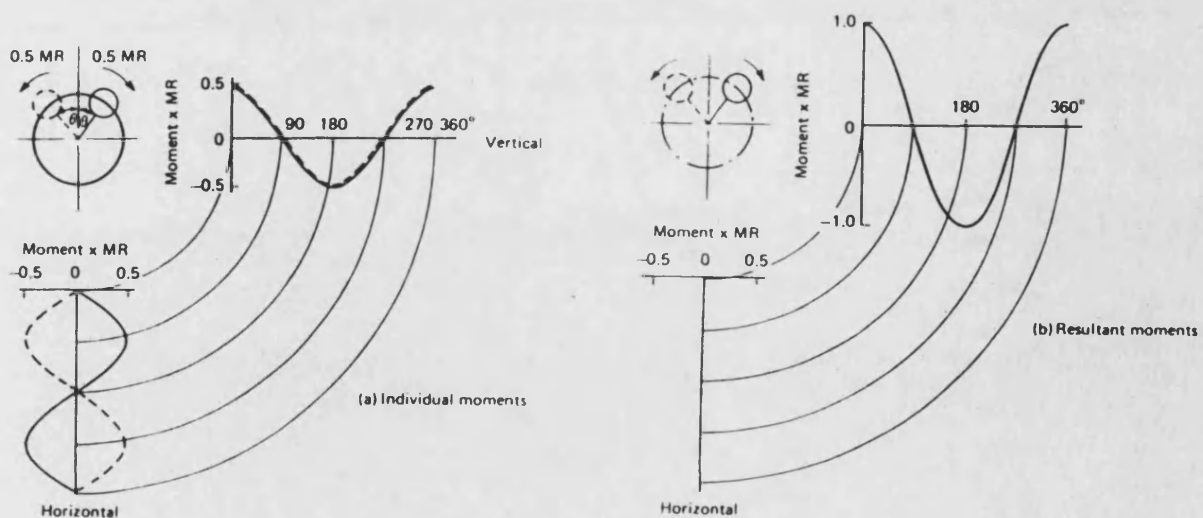
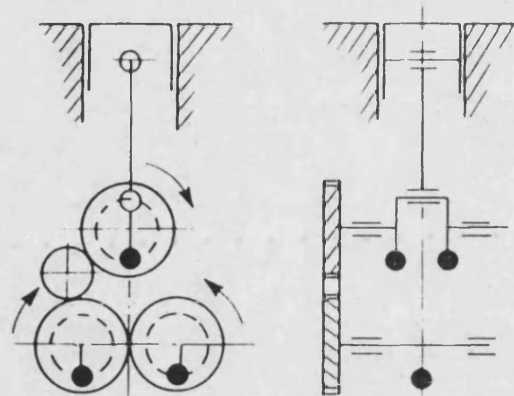
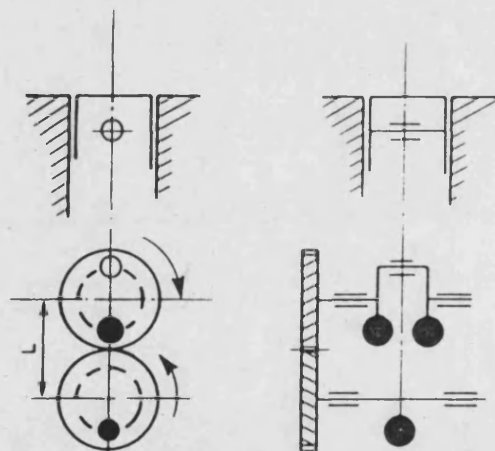


Figure 3.4 Vertical and Horizontal Moments produced by Two Equal Moment Reverse Rotation Masses (63)



Rotating mass =  $M$   
 Reciprocating mass =  $M_{\text{RECIP}}$   
 Crank radius =  $R$   
 Total moment of crankshaft balance weight  
 =  $MR$   
 Moment of each balancer mass =  $m_1 r_1 = 0.5 M_{\text{RECIP}} R$

**Figure 3.5 Primary Balancing of a Single Cylinder Engine using two Counter-rotating Balancer Shafts (63)**



Rotating mass =  $M$   
 Reciprocating mass =  $M_R$   
 Crank radius =  $R$   
 Total moment of crankshaft balance weight  
 =  $mr = \frac{(M + M_R)R}{2}$   
 Moment of balancer shaft weight =  $m_1 r_1 = 0.5 M_R R$   
 Rolling couple introduced =  $0.5 M_R R L$

**Figure 3.6 Compromise Single Cylinder Engine Balance using a Single Balancer Shaft (63)**

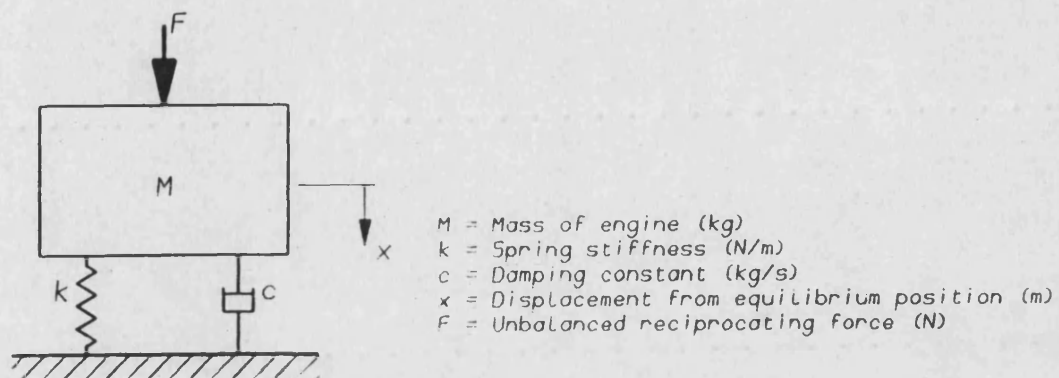


**Figure 3.7 Mass-Spring-Damper System representing Engine Installation**

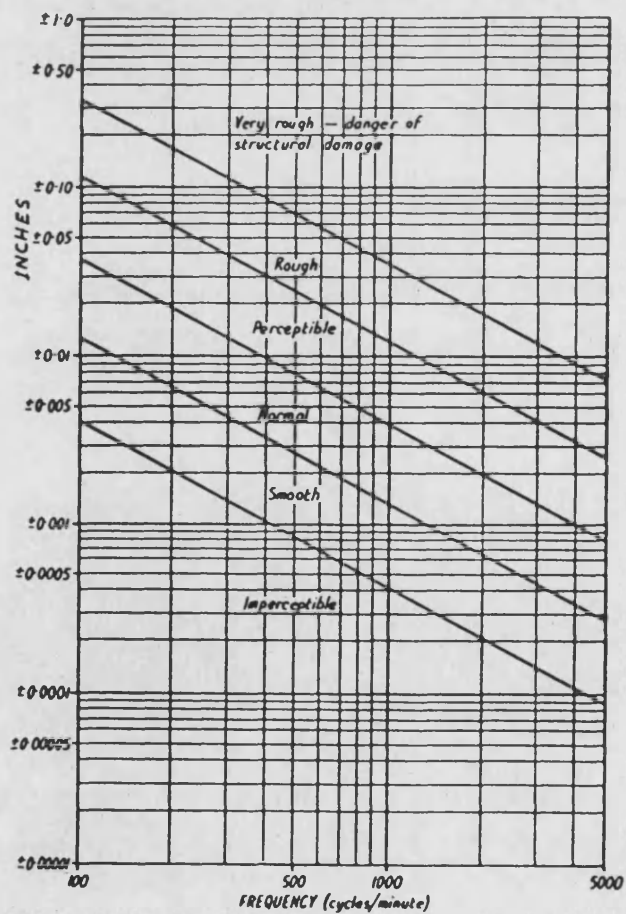
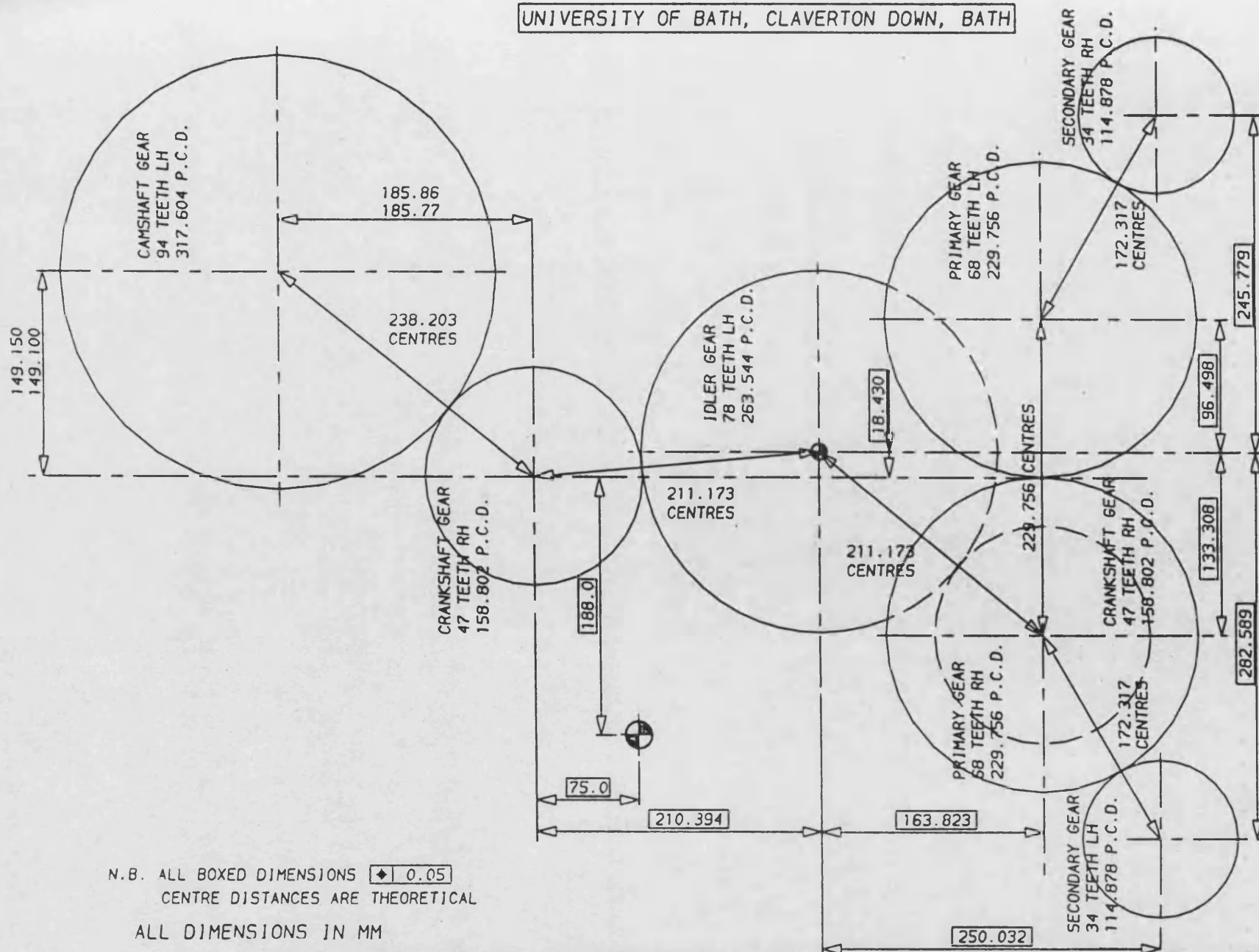


**Figure 3.8 Effect of Engine Vibration (64)**





N.B. ALL BOXED DIMENSIONS  $\pm 0.05$   
CENTRE DISTANCES ARE THEORETICAL  
ALL DIMENSIONS IN MM

Figure 3.9 Geartrain Layout on Dorman 1SR Engine

DO NOT SCALE

#### NOTES

REMOVE ALL BURRS AND  
SHARP EDGES UNLESS  
OTHERWISE STATED

WORK TO  $\pm 0.3$  ON ALL  
DIMENSIONS RELATIVE TO  
M/C SURFACES UNLESS  
OTHERWISE STATED

TAKE CARE! THIRD  
ANGLE PROJECTION

PARTS FOR A SINGLE  
CYLINDER RESEARCH  
ENGINE AT THE  
UNIVERSITY OF BATH  
QUERIES  
(0225) 61244 EXT. 375

# CHAPTER 4

## **4.**

## **Detailed Design**

In the previous chapter the preliminary design work for the single cylinder engine was presented. Having determined the overall design and the important aspects of the key components, the next stage is the detailed design of the engine components. This work is presented here. Obviously there is little point in describing the design details of every component. Instead the discussion in this chapter concentrates on the design methodology (the way the designs were developed), the presentation of the designs for the major components, the selection of the ancillaries, and the analysis of the exhaust installation.

### **4.1 Design Methodology**

All the new design work for the single cylinder engine, with the exception of one or two components, was carried out at the university. With the project being a collaborative venture (CASE award) with Dorman Diesels, Stafford, its success depended on the close co-operation and communication between the company and the university.

During the project the design of most components was developed in the same way. Initially, rough layouts and sketches were made, which were discussed in some detail with the technical people at the company during the regular visits there. These were on an informal basis; the visits being arranged to coincide with the need to resolve or discuss a particular problem. They also provided the ideal opportunity to gather any necessary information; for example, details of company standards or copies of relevant drawings of the six cylinder 6SE engine. On average these visits occurred monthly, though their frequency increased towards the end of the design phase, where the momentum of the project, plus the need to draw the design work to a close, resulted in far more activity. Smaller queries, such as the need for further drawings or minor problems with the designs, were adequately resolved over the telephone.

Once the important features of a design were established it was usual to detail the component on the MEDUSA draughting and modelling workstation within the School of Mechanical Engineering. At the start of the project there had been no firm intention to undertake the design work on a CAD (Computer Aided Design) system. Whilst Dorman have CAD workstations they are not compatible with the MEDUSA system and most of the design and detailing work still occurs on drawing boards. Use of the CAD system started as a feasibility study: the system was new to the school and whilst the general benefits of such a system are well known, the lack of any previous CAD experience might have offset any expected gains. Inevitably, progress was slow during the learning process, but it quickly became apparent that the system would offer many advantages.

With Dorman manufacturing most of the engine it was to be expected that design changes would be required; either to suit existing tooling or to allow the use of an existing component. Here the use of a CAD system proved invaluable; allowing details to be readily changed as the design progressed. It was also easy to ensure that, at all times during the design phase, two copies of each drawing were available - one at Dorman, the other at the university. The copies at the company served two purposes: they made the discussion of particular problems over the telephone far easier, but more importantly allowed the design and production staff more time to study and evaluate the designs. It would have been impractical and unreasonable to expect them to have sufficient time to do the necessary checking during the visits to the company, particularly when the two or three key personnel, closely involved with the project, were also responsible for the day to day running of the respective departments. It was more effective to use the time at the company to discuss the broader aspects of the designs for the individual components, rather than become tied down in fine details. These could be examined later when more time was available. Minor alterations were usually pencilled on the drawings, which were then returned to the university for updating on the CAD system. More major problems that occurred were either discussed over the telephone or held over to be resolved during the next visit.

A further advantage of the CAD system was the inclusion of a powerful solid modeller within the MEDUSA package. This allows complicated models of components to be constructed using a variety of Boolean operations. The ability to generate a solid representation of a component proved extremely useful in determining the important geometric properties. This was extensively used during the design of the balance shafts and crankshaft assembly. In many cases the modeller proved to be the starting point for drawings, because from the solid model it is possible to generate both ordinary orthogonal views and plane sections.

## 4.2 Engine Component Design

In the sub-sections that follow, the designs for the primary and secondary balancers, along with that for the crankshaft assembly are described in some detail. The section is concluded with a summary of the key design points for the remaining more major components of the 1SE engine. A schematic view of the engine (diesel version) is shown in figure 4.1.

### 4.2.1 Primary and Secondary Balancers

In sections 3.4.1 - 3.4.2 the need for balancers on the 1SE has been clearly demonstrated. The disturbing force arising from the reciprocating motion of mass  $M_{\text{RECIP}}$ , occurring in an engine running at a speed of  $\omega$  radians per second is given by:

$$F = M_{\text{RECIP}}\omega^2 R \cos\theta + M_{\text{RECIP}}\omega^2 R(R/L) \cos 2\theta \quad \dots A3.3$$

Taking the maximum engine speed as 2000 rpm and using the engine data taken from table 3.3 (previous chapter), the maximum primary and secondary forces, and corresponding out-of-balance moments are summarised in table 4.1. The required out-of-balance moments for the individual balancer shafts are also included for completeness. Once these had been determined the detailed design of the balancers became

an iterative process which is influenced by many factors. This is best illustrated by reference to figure 4.2.

The simplest way to create an out-of-balance is to bolt a weight onto a shaft. This method has the further advantage that the balance weight can be altered to suit changes in the reciprocating mass. Pursuing this method the general dimensions of the shafts were determined by the size and type of bearings required to deal with the high radial loads, and the length of the crankcase, which limits the length of the shafts, since the balancer box must bolt onto the bottom of the crankcase. The bearings eventually chosen, following the maker's recommendations, were a pair of single row cylindrical roller bearings. At one end of the shaft a "four-lipped" type was used to provide axial location and also to take up the small axial loads imposed by the use of helical gears. To allow for possible growth of the shaft in relation to the bearing housings and the build up of manufacturing tolerances a standard "shoulderless" type was mounted at the other end.

The balance weight is a half ring in section, counter-bored around the four bolt holes to provide a clamping surface for the 'Durlok' bolts used to secure the weight to the shaft. As this is an easily defined shape geometrically, determining the size required for the correct out-of-balance is straight forward. However, getting the correct out-of-balance moment is fairly critical and so allowance was made for the out-of-balance of the bolt heads when determining the balance weight dimensions. These were then calculated so that the overall balancer assembly is slightly over-balanced to allow small drillings to be made after assembly to correct for general machining tolerances. A simple MEDUSA model of the primary balance weight with its geometric properties overlaid is shown in figure 4.3.

As the designs developed some dimensions were changed to allow the use of existing components from the "SE" or other Dorman engine ranges. For instance, the original shaft diameter for the secondary balancer was 30 mm; determined by the bearing bore diameter. By changing this to 35 mm and selecting the next bearing up in the same

range the design could then use existing gears, spacers, washers and securing nuts, saving not only design time, but also cost.

By pursuing this approach further it was possible to reduce the design effort required without compromising the overall design. It was even possible to use the existing idler gear on the 6SE to transfer the drive from the crankshaft gear to the balancer shafts. In this way, of the six gears in the balancer geartrain only two were completely new. At a late stage in their design the primary balancers were modified to drive the oil pump on the one side and the fuel pump (diesel) or magneto (gas) on the other; the ancillaries all requiring to be driven at engine speed. The final designs for the primary and secondary balancers are given in figures 4.4 and 4.5.

#### 4.2.2 Crankshaft and Balance Weight Assembly

For full rotational balance of a single cylinder engine two crankshaft balance weights are required; each having an out-of-balance moment equal to half the combined out of balance of the crankshaft and big end of the connecting rod.

##### (1) Crankshaft

In section 3.1.5 the reasons for a new single cylinder crankshaft, machined from a solid billet, rather than adapting a six cylinder crankshaft, were discussed. In the new design, much of the design detail of the six cylinder crankshaft was carried over, to ensure the use, as far as possible, of existing tooling and jigs.

Initial analysis of the likely out-of-balance moment of the crankshaft and big end, arrived at from information drawn from the 6SE crankshaft and early MEDUSA models, showed that the existing balance weights could be used, if slightly reduced in size. This meant that the new web design could be kept simple; there was no need to reduce the web thickness in the area of the crankpin. Once the form of the crankshaft had been finalised a detailed model was

generated, see figure 4.6, enabling the out-of-balance moment to be calculated using the MEDUSA geometric properties utility. The model then formed the basis for the detailed manufacturing drawing: orthogonal views and plane sections being generated from the model, which were then dimensioned and detailed in the usual way. Minor changes were also made to the design to bring it in line with the latest revisions on the 6SE crankshaft. Having established the exact out-of-balance of the crankshaft and knowing the out-of-balance moment of the big end it was then a simple task to determine the size of the new crankshaft balance weights.

#### (11) Balance Weights

The existing balance weights are manufactured from steel plate using a profile flame cutter. As the rotational out-of-balance required for the new weights was approximately 85% of the old ones, the simplest way to achieve the reduction is to decrease the width of the weight, whilst keeping the same profile.

Neglecting the effect of any holes or drillings the advantage of this method is that the out-of-balance is then proportional to the width of the weight; the position of the centre of gravity remains the same. In this way it was possible to calculate the new width required. The weight was then modelled on MEDUSA to check the out-of-balance moment. Some fine tuning work was required to allow for the drillings, and for the contribution of bolts and dowels in the crankshaft assembly. Taking these into account at the design stage limits the amount of corrective drilling which is usually necessary when the whole assembly is dynamically balanced. Because of manufacturing tolerances it is clearly impractical to achieve full rotational balance without some form of correction work. For this reason the weights were designed so that the whole assembly would be slightly "overbalanced" i.e. the contribution of the weights is greater than required. This was done because it is easier to bring dynamic balance to within the desired limits by drilling the balance weights, than by drilling the crankshaft. Drilling of the crankshaft



at the assembly stage could not only give rise to unwanted stress raisers in the crankshaft, but could lead to local distortion if machining is attempted through the case-hardened surface. The crankshaft assembly - with balance weights attached - is shown in figure 4.7.

#### 4.2.3 Balancer Box

The balancer box involved the most extensive design work, and proved the most difficult of all components to manufacture - more so than the crankcase and crankshaft. The basic design of the balancer box was determined by the positions of the balancer shafts and the need to be able to bolt the box onto the bottom of the crankcase. Geartrain layouts other than the one shown in figure 3.9 were considered. Layouts with the secondary balancers mounted above the primary ones were tried in that they seemed to offer a more compact design, but were rejected for a variety of reasons: new gears would have to be made, securing the box to the crankcase would be difficult, or the final balancer box design would be very difficult to fabricate. The final design is to a certain extent a compromise. The layout is not the most compact, giving rise to increased weight, but it does allow the use of many existing components. As the engine is a one-off - it is not intended for mass production - the latter point is of considerable importance, enabling the cost to be kept down.

The main problem in the design was to ensure accurate positioning of the gear centres. The problem manifests itself particularly in the joint region between the balancer box and crankcase, where a build up of machining tolerances could lead to misalignment between the crankshaft and idler gears (refer to figure 3.9). The problem is further compounded by the need for an oil tight seal in this area. A gasket could not be used because of its dimensional instability. The solution was to machine the top face of the box, or if necessary the base of the crankcase at assembly time, to ensure that the gear centre distances would be correct. A proprietary liquid sealant

would be used to prevent oil leakage. To reduce local distortion in the top face of the balancer box, the top flange was bolted, as well as welded, to the front and rear faces. This meant the size of the weld required could be reduced. The use of the bolts had the further advantage that they would take some of the dynamic load imposed on the welded joints due to the primary and secondary balancer weights.

With the balancer shafts and balancer box forming a sub-assembly, there was a danger during the engine build that the secondary gears could be damaged, if the box was laid flat on its base. To prevent this, the area around the secondary bearing housings was extended downwards to ensure sufficient clearance beneath these gears. Drillings also had to be carefully located in the box to lubricate not only the double pairs of primary and secondary roller bearings, but also the idler gear stub shaft. Oil would be fed to these areas direct from the oil pump, via a restrictor, through a network of external copper pipes. The balancer box design is given in figure 4.8. The additional holes in the front face are to save weight; a problem highlighted by a MEDUSA model of the box.

#### 4.2.4 Crankcase

The decision to cast the single cylinder crankcase using the existing six cylinder pattern equipment very much simplified the design work; not only of the 1SE crankcase, but also of other components - crankshaft and camshaft. Because the new crankcase was merely a shortened version of the 6SE crankcase, with the front and rear face detailing almost identical, valuable time was saved in not having to present a full set of manufacturing drawings. Instead only external views were required, showing the new locations of the oil and water inlets and other small changes, such as new tapped hole positions. All other detailing was cross-referenced to the existing six cylinder 6SE crankcase drawing sheets.

Such a short engine presented problems in the re-location of the oil and water inlets. A large flywheel at the rear of the engine and a

gearcase at the front limits access to the two sides. With the pushrods and control rods running up the right-hand side, viewed from the front, entry to the water gallery is therefore restricted to the left-hand side. For the water feed a new boss was required; this was achieved by removing sand from the mould at the appropriate position. The location of the boss proved difficult in that any pipe fittings would have to avoid the starter and governor actuator which are on this side - refer to figure 4.1. Any drillings would also have to miss the crucial area around the cylinder head bolt bosses. The oil supply represented less of a problem; it could be fed directly into the main oil gallery which is lower down in the crankcase.

To improve serviceability a crankcase door was included. This affords access to the big end bolts, which can then be undone to allow the removal of the piston and connecting rod through the top of the engine. This is a necessary feature because the alternative of removing them through the engine base would mean dismantling the gearcase and balancer box assembly.

The decision to upgrade the casting material to S.G. iron required consultation with the foundry personnel. The slightly different pouring characteristics of this material meant that extra feeder bosses were required on the mould. Where these would interfere with any fittings on the crankcase they would simply be removed at the machining stage. The location of the extra bosses was left to the judgement of the foundry department and were not included on the manufacturing drawings. With there being less experience of casting S.G. iron, it was decided, as a precautionary measure, to cast three crankcases. Further, all would be machined until either a critical flaw was detected, or machining was sufficiently advanced on two of the crankcases that no further work would be required on the third.

On the 6SE engine the underslung bearing caps are cast in the same material as the crankcase. Whilst it would have been feasible to use them, it seemed sensible to also upgrade these in line with the crankcase. Unfortunately, it was not a simple matter of casting new

bearing caps in S.G. iron. The very small quantities could not justify this. Instead a simplified design, which retained all the essential features, was manufactured from a single thickness of steel plate. The design for this was undertaken by design staff at Dorman.

#### 4.2.5. Flywheel

The various constraints imposed on the design, discussed in section 3.1.5 (iv), meant that a new flywheel had to be manufactured from a single thickness of plate. For this a balanced steel (Grade 50B), ultrasonically tested, was chosen. This has the advantage of a yield strength over twice that of the cast grey iron material (Grade 260) used on the 6SE flywheel.

In the new design, as far as possible, details were carried over from the six cylinder engine: the existing starter ring was retained. Increasing the inertia some threefold meant a dramatic increase in the overall size of the flywheel; from a diameter of 530 mm on the 6SE to a new outside diameter of 780 mm on the 1SE. The resulting stresses were checked, with the assistance of Dr. Charlton, by analysing an axi-symmetric two-dimensional representation of the flywheel on a finite element package available on the School of Mechanical Engineering's VAX 11/750 computer. The results, which were corroborated by further analysis at Dorman, confirmed that stress levels in the Grade 50B material were acceptable. The maximum recommended running speed was calculated based on the maximum permissible stress in the bore being one quarter of the yield stress of the material. A contour plot of the hoop stress for the flywheel is shown in figure 4.9. It can be seen that the maximum stress level occurs at the front edge of the bore. This is due to the combined effects of the centrifugal loading and the bending moment, caused by the additional material at the flywheel rim.

A MEDUSA model of the flywheel was also generated. The property utility was used to check the moment of inertia. It confirmed the supposition that the mass of the new design, at 230 kg, would be

approximately double that of the 6SE, and therefore justified the earlier analysis of the main bearing loads (see section 3.1.5 (iii)).

To provide more security, in the event of a catastrophic failure leading to the engine seizing, two extra 25 mm dowels were included in the hub of the flywheel. A similar number of dowel holes were added to the crankshaft flange.

#### 4.2.6 Gearcase

The existing cast aluminium gearcase could not be used because of the addition of the balancer box and the cut out around the starter. A new gearcase was therefore designed which was of a fabricated construction. In the top portion details were carried over from the existing gearcase. It was then extended downwards to enclose the balancer gears and to provide support for the oil pump and magneto or fuel lift pump. The ancillaries, driven directly by the primary balancers, are mounted on separately bolted plates. These allow some movement and thus ensure accurate alignment of the driving tangs on assembly. The same method was adopted to allow the crankshaft seal to be positioned accurately.

#### 4.2.7 Sump

The new sump was designed to bolt directly onto the bottom of the balancer box with the front being brought forward to form a joint with the gearcase. With a volume of 24 litres the capacity of the single is a nominal one sixth that of the 6SE sump (113 litres); extra capacity being allowed for the roller bearings in the balancer box and the geartrain requirements. The simple welded construction features support legs. These do not support the engine on the test-bed, but were included to ease assembly during the engine build, when the engine often stands on the sump. In the installation the engine is bolted to the test-bed frame using the four feet mounted on the front and rear suspension plates.

#### 4.2.8 Suspension Plates

The suspension plates carry the weight of the engine. The design of the 6SE front suspension plate was adapted, by extending it downwards to give extra support for the balancer box, and to provide a means of attaching the new gearcase. The flywheel housing on the rear of the 6SE engine had to be replaced by a new rear suspension plate because it was now too small for the larger flywheel. Guarding of the flywheel and flexible coupling to the dynamometer is achieved by enclosure under a steel mesh.

#### 4.3 Engine Ancillaries

All the ancillaries used on the 1SE single cylinder engine were either obtained from the 6SE engine range or from smaller Dorman engines. Whilst this had obvious cost benefits, it also ensured that other necessary mating components were available. Pumps were selected on the basis of their flow capacities being approximately one-sixth of the flow requirements on the 6SE six cylinder engine. It had already been decided, in the first design phase at least, to arrange for all ancillaries to be engine driven (refer to section 3.1.3). The selection of the various ancillaries is discussed below. Description of the circuits for the services is covered in chapter 7. The layout of the engine-mounted components was finalised at the time of the engine build.

##### 4.3.1 Oil Pump

The oil pump capacities for the 6SE and the requirements for the 1SE engine are summarised in table 4.2. The 6SE pump (SE 116D) is gear driven. The most suitable oil pump for application in the 1SE engine was taken from the "DA" engine range, from which the the sump oil filter and pipe-work were also obtained. The advantage of using this pump was that it came complete with driving-tang, enabling it to be

mounted off the end of a shaft. The right-hand balancer was chosen to provide the drive as its direction of rotation was correct for the pump, which is uni-directional, and would ensure sufficient flow capacity when rotating at crankshaft speed (1500 rpm). In fact, as can be seen from the table, the pump supplies excess capacity at this speed. This is desirable because oil-flow requirements on the 1SE are likely to be higher than the nominal one-sixth capacity of the 6SE; oil is still required for the geartrain and additionally for the roller bearings in the balancer box. Oil from the pump is fed to an engine mounted oil stabiliser and filter unit with integral relief valve. This unit is taken from the "L" engine range.

#### 4.3.2 Water Pump

The gear-driven water pump on the 6SE was replaced by a belt driven pump of smaller capacity. This pump, with integral pulley, is normally found on the "L" series engines. Technical data is summarised in table 4.3. The "L" water pump is located on the left-hand side of the engine, the belt being tensioned by mounting the pump through slots. The standard 6SE pulley, mounted on the front of the crankshaft, normally drives the radiator fan. It had to be altered to accommodate the different belt profile of the "L" water pump pulley. To avoid an unduly large overhang at the front of the engine, the 6SE pulley was also mounted back-to-front allowing the driving belts to be kept closer to the front of the gearcase.

#### 4.3.3 Starter

Compared with other ancillaries on the 1SE the criteria for the selection of the starter are less well defined. On the one hand, in comparison with the 6SE engine, the torque required to overcome pumping and frictional effects is less, thus suggesting a smaller starter unit. Conversely, there are fewer firing strokes per revolution and so more crankshaft revolutions may be required before combustion is initiated. The starter also needs to accelerate the

considerable extra inertia of the flywheel and balancer assembly. It was therefore decided to employ the same electric starter as on the 6SE engine. This had the advantage that it enabled the location of the starter position to be copied over from the 6SE engine; simplifying the design for the rear suspension plate, and allowing the use of the 6SE starter ring.

On the development test-beds at Dorman, an equivalent capacity air-starter is used, allowing multiple starts without fear of draining batteries. This alternative was considered, but rejected: there were doubts whether the air requirements could be met (at the university) and also it is a bulkier unit. Allowance had to be made for the size of the existing electric starter. It is longer in length than the single cylinder crankcase and so the front suspension plate and gearcase had to be designed to pass around the rear portion. Re-charging of the batteries would be from an external source. An engine driven alternator, as on the 6SE, was not considered.

#### 4.3.4 Governor-Actuator

On the 6SE either an electronic (Heinzmann) or gear-driven hydraulic governor is available. For the single cylinder engine the Heinzmann governor was selected: it offered more flexibility for mounting. On the diesel version of the 1SE it is located in the same place as on the 6SE. This was done to allow maximum use of existing components, though this did restrict access on the left-hand side of the engine (refer to section 4.2.4 and figure 4.1). In this position the actuator operates the fuel "rack" of the unit injector, via the standard 6SE control linkage, which runs from left to right inside the gearcase.

The gas version of the engine has the actuator located on the end of the inlet manifold. It directly controls the position of the butterfly valve, mounted downstream of the mixer body. The signal for the governor, in both engine builds, is provided by a magnetic pick-up mounted off the gear-ring on the flywheel.



#### **4.3.5 Fuel Lift Pump (diesel) and Magneto (gas)**

The left-hand primary balancer shaft was designed such that, dependent on engine build, it could be used to drive either a fuel lift pump or a magneto unit. The change-over is achieved by swapping the respective adapter-retaining plates. The adapter plates are matched to the driving tangs of either the magneto or fuel lift pump and are simply bolted to the end of the primary shaft. They also serve to retain the gear and bearing in position (figure 4.4). The fuel lift pump, in common with the oil pump, is taken from the "DA" engine range. It provides the necessary 2.5 litres per minute delivery rate. The "Altronic III" magneto is a self-contained capacitor discharge ignition system, designed for lean mixtures, and which when linked to a varying timing unit allows the spark-timing to be altered by simply rotating a dial.

#### **4.4 Parametric Simulation Study of Exhaust Conditions**

To ensure compatibility between results from the single and multi-cylinder pressure charged engines, McKenzie and Dexter (2) introduced five conditions - refer to section 2.1.1. Of these, the fifth criterion, to match conditions after the exhaust ports during the open part of the cycle, proves most difficult to satisfy. For a constant pressure manifold reasonable accuracy can be achieved in simulating the exhaust conditions on a single cylinder engine. However, the same is not true with a pulse turbocharged engine or one with "compact" manifolds.

##### **4.4.1 Single Cylinder Pressurised Exhaust Installation**

The Dorman 6SE engine features a "compact" manifold (65). Instead of a large manifold for a constant pressure system, the compact manifold has a comparatively small bore with pulse converter junctions at each

port. All the cylinders are connected together by a single pipe (for an in-line engine) which results in reduced production costs.

In their paper McKenzie and Dexter (2) suggest that exhaust conditions for a compact or modular pulse converter manifold may be simulated as a constant pressure system. This is easiest achieved by placing an orifice plate or gate-valve in the exhaust system. The orifice size is selected to give the correct turbine characteristics. Unfortunately, an orifice can only approximate the turbine at one particular load and speed. Thus, to operate the engine over a wide range of load and speed conditions, a range of orifice sizes are required. A gate-valve, capable of operating at high exhaust temperatures, therefore seems to offer greater flexibility: its flow area is easily altered to suit different engine loads and speeds. However, with the compact manifold being somewhat of a hybrid between a constant pressure and pulse turbocharged system, the methods of reproducing pulse turbocharged manifold conditions were also considered.

Simulation of a pulse exhaust manifold is more complex, with no solution proving wholly satisfactory (2). McKenzie and Dexter considered six alternatives. They suggested that the best method, when the primary aim is to investigate closed cycle conditions, is a system which incorporates an orifice plate, plenum chamber and gate-valve. The size of the orifice is chosen to control the shape of the exhaust pulse, whilst the gate-valve after the plenum volume is used to alter the mean exhaust pressure. The large plenum chamber volume serves to damp out pulsations before the gate-valve

Though the above installation is tailored to pulse exhaust systems, it was felt it offered greater flexibility - an important factor in research work - than the simpler orifice or gate-valve installation for a constant pressure exhaust system. By careful selection of the orifice size and fine adjustment of the back pressure valve it ought to be possible to simulate compact manifold conditions. The correct reproduction of the pressure pulse on the single cylinder engine is important in that it governs the scavenge air flow. For simulation

of diesel engines, which have large overlap periods, this is critical if in-cylinder conditions are to be similar to those on the six cylinder engine. Fortunately, the installation has, at least initially, to reproduce exhaust conditions on a gas engine. Thus, the exact setting of the exhaust parameters can be relaxed: the overlap period is only  $32^\circ$  ( $16^\circ/16^\circ$  either side of TDC).

As a means of assessing the feasibility of this approach and to provide valuable insight into the characteristics of the above installation, a brief parametric study of the installation was undertaken using the engine simulation package "SPICE". The aim of this theoretical work was to match the exhaust conditions of the single cylinder research engine to those of the 6SE engine. Ideally, the exhaust manifold pressure on the 1SE would have been compared with experimental data for the 6SE. Unfortunately, no such data was available and so the investigation had to compare results obtained by simulation.

#### 4.4.2 Simulation Models using SPICE

The computer program SPICE, available in the School of Mechanical Engineering, is a large FORTRAN based diesel engine simulation program. The essence of the method employed is that the engine is represented as a system of thermodynamic control volumes, flow junctions and shafts. Thus, each manifold or cylinder will be a unique control volume, which is successively filled and emptied as mass passes through the engine - hence the term "filling and emptying" applied to these models. The precise arrangement of the elements depends on the engine being modelled.

The method of solution involves the construction of differential equations for stagnation temperature, fuel-air ratio and mass within each control volume and for the speed of each shaft, based on the conservation principles of mass, energy and momentum. From the initial values given, the set of first order coupled differential equations are then solved at discrete time steps for each control

volume. The "unpredictable" aspects of engine performance - those not amenable to theoretical analysis, such as ignition delay, combustion processes and heat transfer - are modelled using empirical formulations

Engine models are constructed by defining the engine parameters (bore, stroke, valve timing, etc.) in a base data file, which for the case of a turbocharged engine simulation is then linked to two additional data files (compressor and turbine). Numerical printout of results and plot data is controlled by parameters within the base engine file. Further information on the program is available in reference 66.

#### (1) Simulation Model of the 6SE Gas Engine

The 6SE was modelled as a full six cylinder engine with compressor and turbine. The SPICE program is currently only able to model diesel combustion, and so the gas engine had to be fired as a "diesel". This meant that the fuelling and air-fuel ratio in the simulation were chosen to predict similar performance levels to early experimental data obtained from the 6SE gas engines on Dorman test-beds.

A further simplification was enforced when modelling the compact manifold. Because wave action in the manifolds is ignored in the program, the effects of the single compact manifold were approximated by two exhaust manifolds feeding a twin-entry turbocharger turbine. A schematic representation of the model is shown in figure 4.10. Whilst this clearly raises doubts as to the validity of the model this approach was justified in that the single cylinder model would be similarly restricted. The aim of the study was not to match theoretical data to experimental results, but to use the predictions to help design the single cylinder exhaust installation, particularly the sizing of the orifice.

#### (11) 1SE Simulation Model

The model for the 1SE engine is shown in figure 4.11. Pressurised charge conditions were simulated by applying boosted boundary conditions at the entry to the inlet manifold (junction 3). In attempting to match the exhaust pressure pulses the fuelling level was kept identical to that on the 6SE, whilst the effects of varying the exhaust manifold volume (vol. 3) and the orifice size (junction 4) were examined. For the early work the large plenum (80 litres) was removed. Its volume had been sized on the recommendations of McKenzie and Dexter (2), who suggested a volume equal to 20 x swept cylinder volume. Such a large volume caused problems with the convergence of solutions: pressure changes occurred very slowly which meant, that if the initial boundary conditions were inaccurate, the simulation needed to perform many cycles before a satisfactory solution was reached. The plenum was included in the model once the approximate sizes for the orifice and exhaust manifold volume were determined. Fine tuning of the installation could then be undertaken with the boundary conditions better defined, from the earlier simulations.

#### 4.4.3 Simulation Results

Initially the six cylinder model was run to obtain the exhaust manifold pressure trace shown in figure 4.12. The curve is from volume 5 (see figure 4.10) and the middle peak corresponds to the first cylinder. The single cylinder model (figure 4.11) was then run and the following parameters varied:

- exhaust manifold volume (vol. 3);
- orifice size (junction 4); and
- gate-valve opening (junction 5)

to try to match the exhaust pulse shape obtained from the 6SE model.

In the initial model, with plenum removed, the exit pressure boundary condition was set to 1.5 bar. This ensured that the base level of the pressure trace would correspond with the lowest point on the 6SE trace - refer to figure 4.12. (In the full 1SE model, with plenum, and on the installation, this base pressure level would be achieved by restricting the flow area after the plenum: equivalent to closing the gate-valve). Removing the plenum (and gate-valve) at this stage, allowed the effect on the shape of the exhaust pulse of orifice size and manifold volume to be studied in isolation.

#### (i) Exhaust Manifold Volume

The six cylinder model employed two manifolds of eight litres each, representing a total exhaust volume of sixteen litres. On the basis that the 1SE is a one-sixth model, the exhaust volume in the 1SE installation model was initially set to 3 litres. However, with some thought it is apparent that for matching purposes this is an invalid assumption. On the six cylinder simulation, only one cylinder exhausts into one of the two manifolds at any one time during a cycle. The same pattern is maintained on the single, thus to ensure the same pulse shape in the single cylinder exhaust manifold its volume has to be set equal to the split manifold volume of the 6SE (8 litres). This is confirmed by figure 4.13, where the exhaust pressure pulses for two different manifold volumes (6 and 9 litres) on the 1SE installation are compared with pulses obtained from the 6SE simulation. A smaller exhaust manifold causes a sharper rise in the initial pressure peak following the opening of the exhaust valve. The shape of the second "hump" is determined by the orifice area. In the subsequent studies this was investigated; with the manifold volume being kept constant.

#### (ii) Orifice Size

The results of varying the orifice size are shown in figure 4.14. Reducing the orifice size has two effects: on the the firing stroke,

with the exhaust valve open, the peak pressure in the manifold is slightly increased, and on the exhaust stroke the flow at the orifice becomes "choked", leading to the formation of a second peak. It also extends the decay in pressure in the manifold to beyond the point of EVC (exhaust valve closure), markedly altering the back pressure during the overlap period. However, the figure clearly demonstrates that a match is possible by careful selection of the manifold volume and orifice size.

The next stage was to study the effect of the plenum chamber and gate-valve. This combination is used to set the correct back pressure, which in the previous cases had been artificially set by adjusting the exit boundary condition.

#### (iii) Gate-valve Position

The gate-valve was treated as a simple orifice; the closing effect being simulated by reducing the orifice area. The plenum chamber volume was fixed at 80 litres. Figure 4.15 shows that as the flow area through the valve is reduced the pressure curve is lifted vertically, thus clearly demonstrating the way the gate-valve can be used to set the correct back pressure.

A final study looked at running the engine at a different load condition (the engine is designed for fixed speed operation). In the six cylinder and single cylinder engine models the fuelling was reduced to a level corresponding to a 3/4 load condition for the gas engine. (The gate-valve "opening" was left unaltered from the full load case). The pressure pulses in the respective exhaust manifolds are shown in figure 4.16. Again, a reasonable match is achieved. Some adjustment of the gate-valve is required to lower the single cylinder pulse during the overlap period.

From the simulation work the feasibility of the installation has been shown, though there were doubts over the assumptions made, particularly those relating to the modelling of the compact manifold. Nevertheless, the study has enabled the approximate sizing of the orifice required, allowing an orifice plate, plenum and gate-valve to be designed. The design for the gate-valve is presented in chapter 7.

On the installation, techniques available to match conditions are less sophisticated. Ideally, the aim would be to log the single cylinder pressure trace with a high speed data acquisition system and compare it with a previously stored six cylinder trace. Adjustment of the gate-valve, and perhaps initially use of different orifice plates, would then ensure a good match. However, the lack of such a pressure trace from the six cylinder gas engine obviates this approach. Instead, corresponding exhaust conditions have to be approximated by scheduling the mean back pressure, for which experimental data is available, on the basis of engine boost levels. Fortunately, the short overlap period on the gas engine means that matching conditions are less critical than they would be for a diesel engine.



	Primary	Secondary
Maximum Out-of-balance Force (kN)	42.92	12.13
Out-of-balance Moment (kgm)	0.9785	0.277
Out-of-balance moment for each Balancer (kgm)	0.4893	0.0346
Rotational Speed for Balancers	1 x engine	2 x engine

**Table 4.1 Primary and Secondary Out-of-balance Forces and Moments**

	pump speed (rpm)				
flowrate	1000	1200	1500	1800	
l/sec	-	-	1.70	2.00	6SB engine (SE 116D)
l/sec	-	-	0.28	0.33	1SB req.
l/sec	0.33	0.40	0.50	0.57	DA116A pump

**Table 4.2 Oil Pump Requirements**

	pump speed (rpm)				
flowrate	1000	1200	1500	1800	
l/sec	-	-	10.0	10.6	6SB engine (SE 145K)
l/sec	-	-	1.7	1.8	1SB req.
l/sec	1.6	1.8	3.5	3.6	L145BP pump

**Table 4.3 Water Pump Specification**

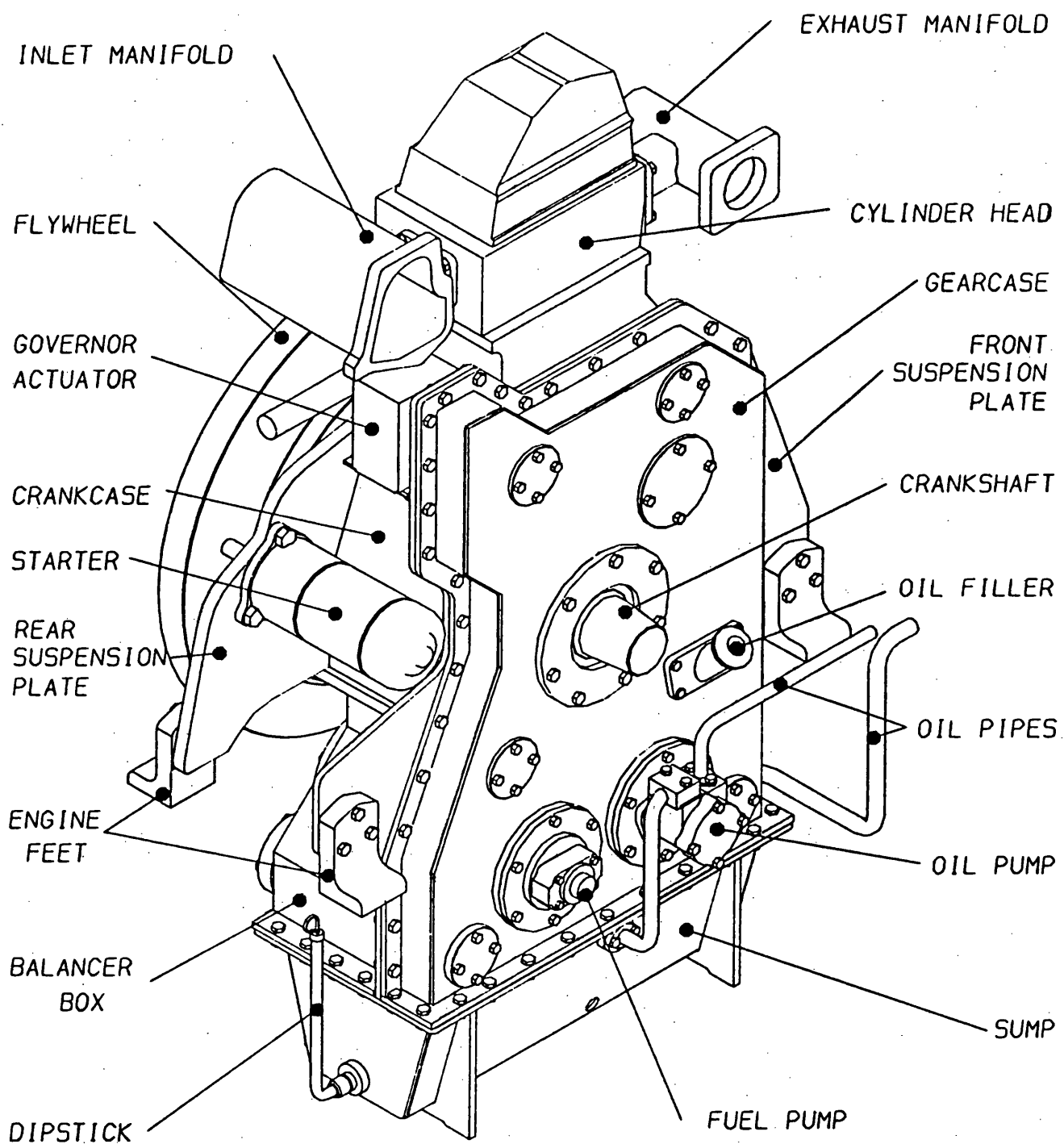


**Figure 4.1 Schematic View of 1SB Single Cylinder Research Engine (Diesel Version)**

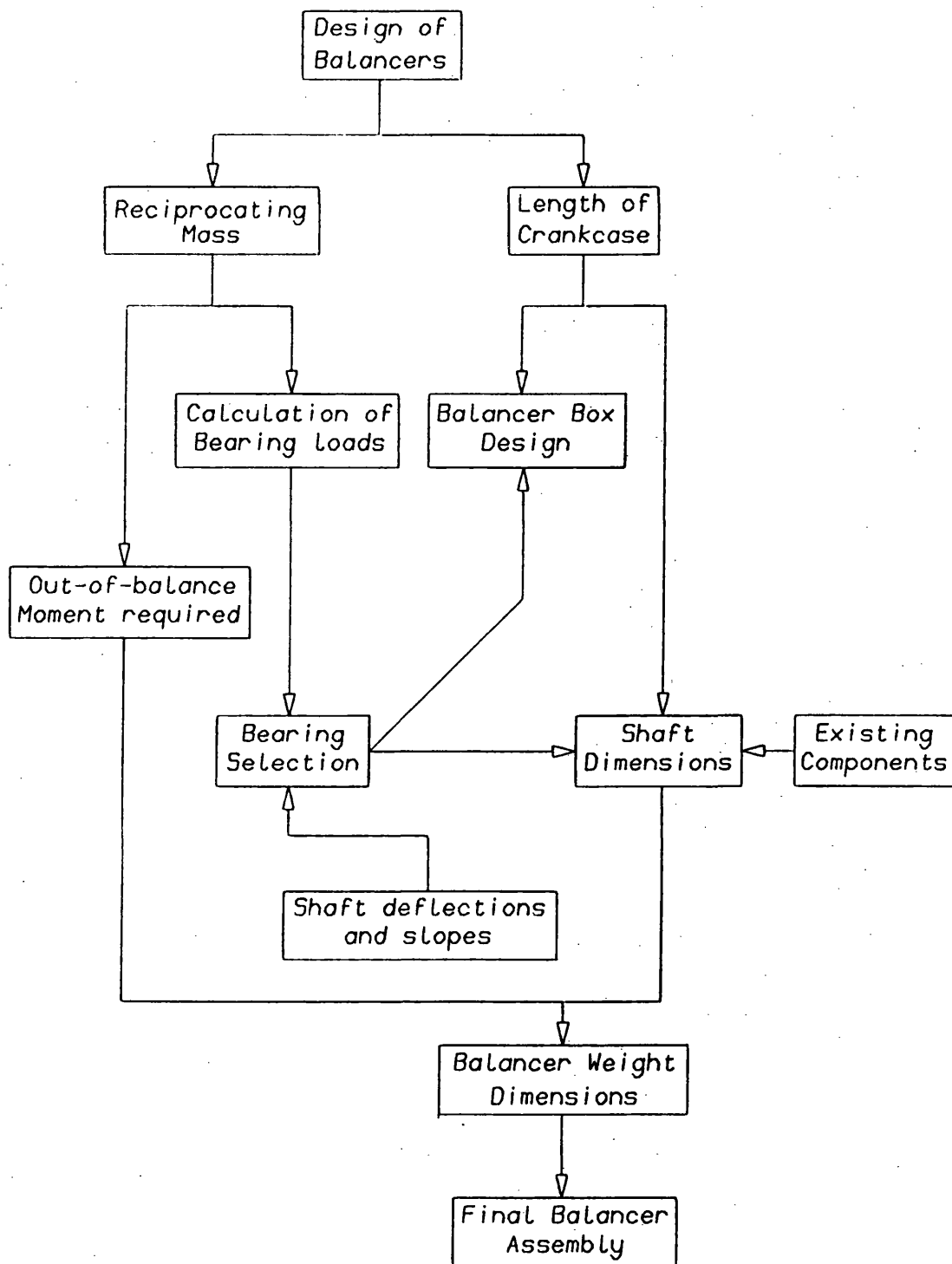
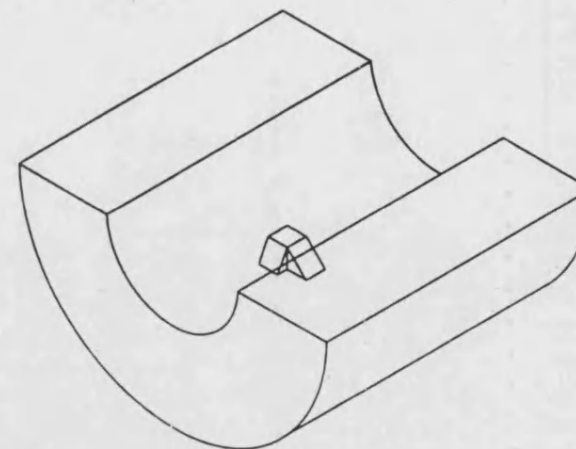
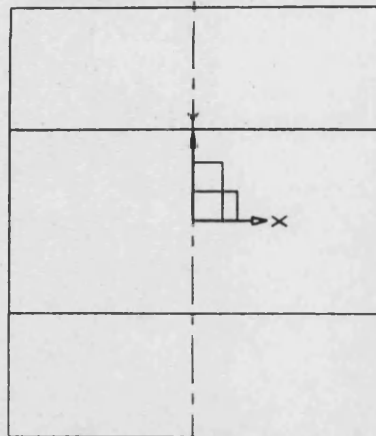


**Figure 4.2 Factors Influencing the Design of the Primary and Secondary Balancers**

CLASS  
UFD

TITLE PRIMARY BALANCE WEIGHT



FIT 0.8

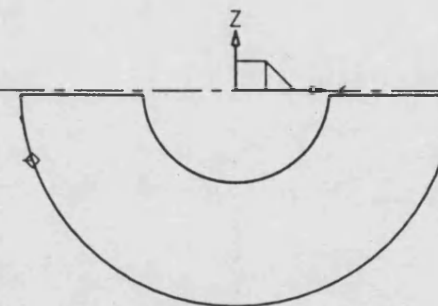
NODRAW

NODRAW

Model Name : 1340A.MOD

Object Name :

Volume	:	0.14420E+07	cubic mm
Surface Area	:	0.91927E+05	square mm
Centre of Gravity	:	-0.45687E-04	mm
	:	-0.19347E-04	mm
	:	-42.7445	mm
Density	:	0.78000E-02	g/cubic mm
Mass	:	0.11247E+05	g
Moments of Inertia about	:	0.51022E+08	g.square mm
	:	0.47080E+08	g.square mm
	:	0.46119E+08	g.square mm
Radius of Gyration	:	67.3528	mm
	:	64.6989	mm
	:	64.0348	mm



UNIVERSITY OF BATH  
ENGINEERING DESIGN GROUP  
CIS-MEDUSA

A3

MODEL:

MODEL:

MODEL:

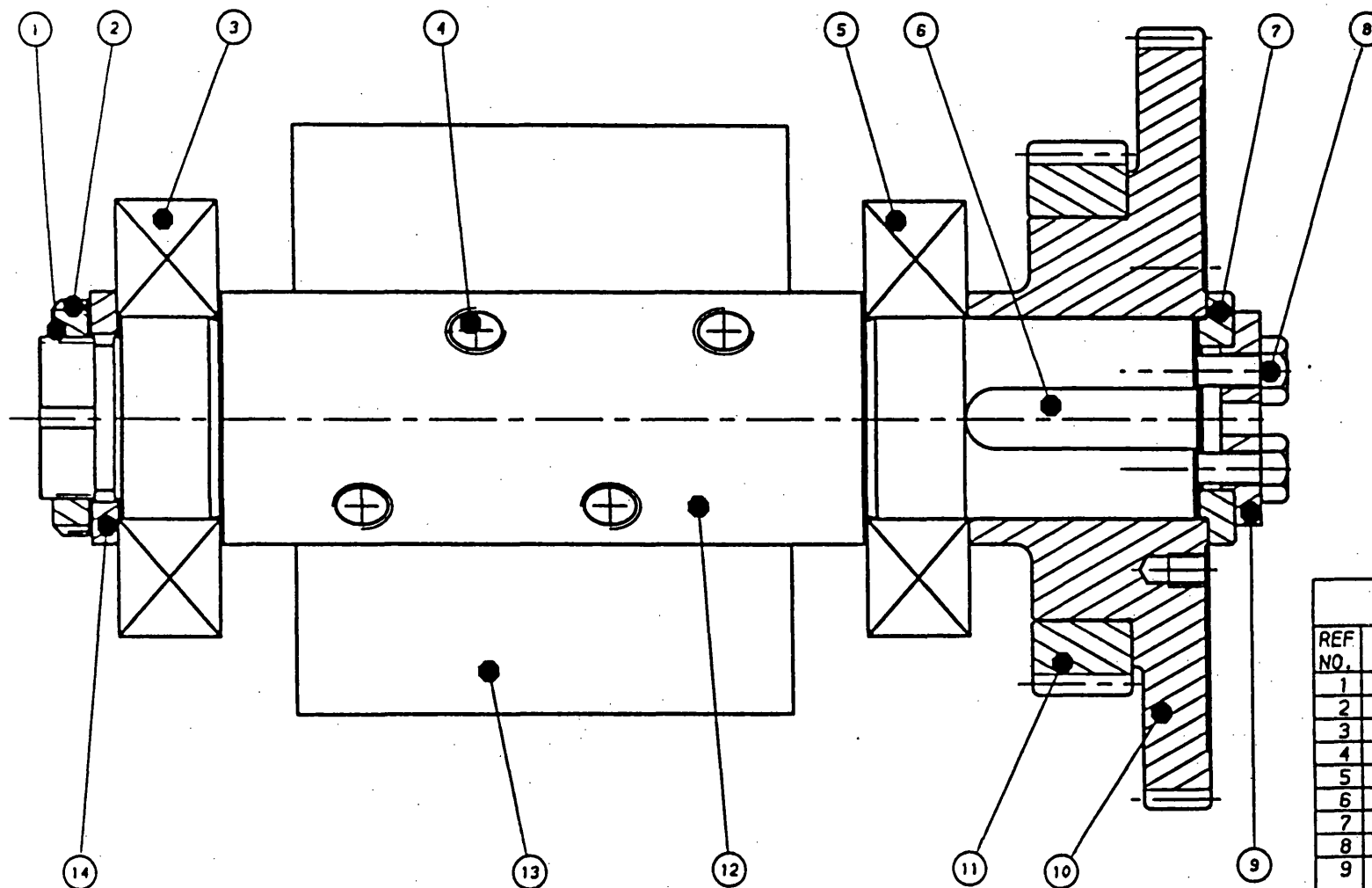
ISSUE N°

1340A

DRG N°

MODEL: CHOTOL

Figure 4.3 MEDUSA Model of Primary Balance Weight  
with Geometric Properties overlaid



## NOTES

REMOVE ALL BURRS AND SHARP EDGES UNLESS OTHERWISE STATED

WORK TO  $\pm 0.3$  ON ALL DIMENSIONS RELATIVE TO M/C SURFACES UNLESS OTHERWISE STATED

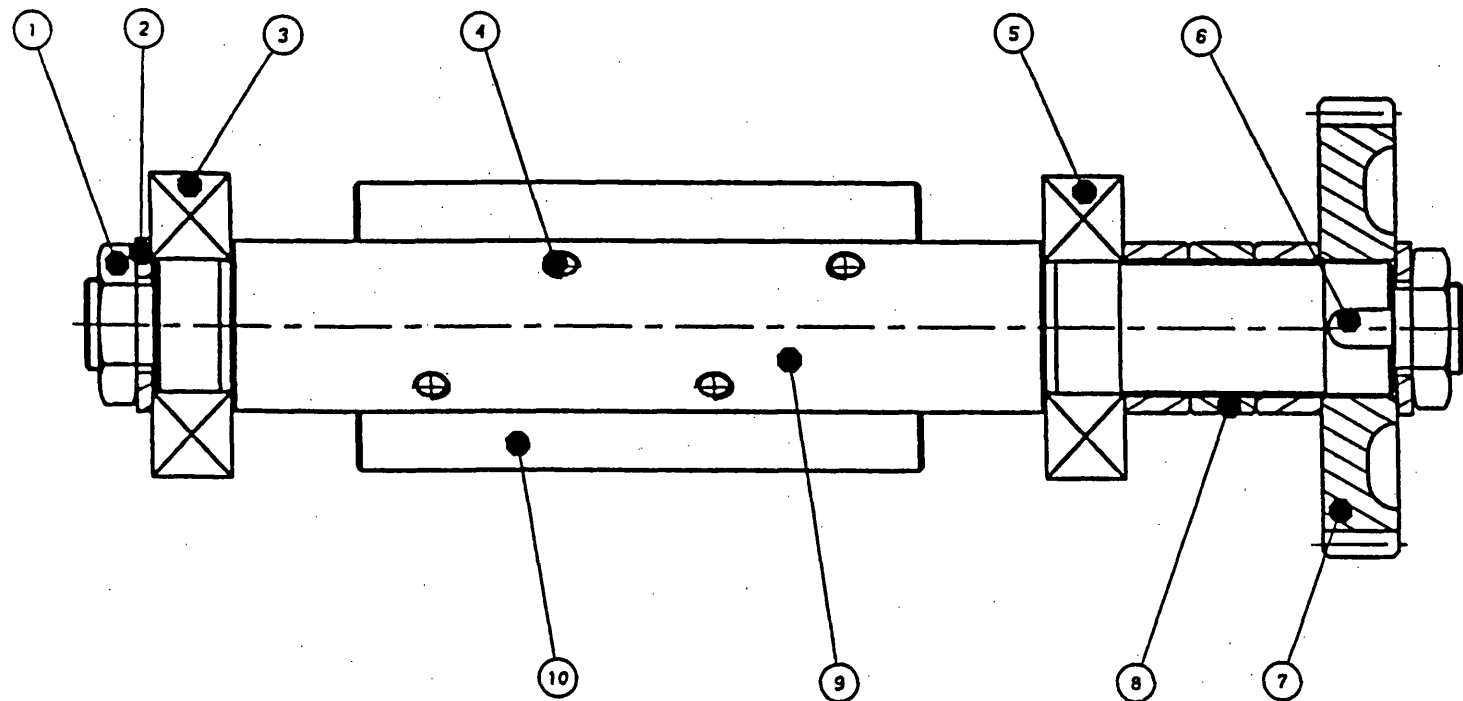
TAKE CARE! THIRD ANGLE PROJECTION

PARTS FOR A SINGLE CYLINDER RESEARCH ENGINE AT THE UNIVERSITY OF BATH  
QUERIES  
(0225) 61244 EXT. 375

## PARTS LIST

REF NO.	PART/DRG NO.	DESCRIPTION	NO. OFF
1	KM 10	INTRA NOTCH NUT	1
2	MB 10	INTRA LOCK WASHER	1
3	NUP 312	RHP ROLLER BRG	1
4	2116/090	M16 SELF LOCKING SCREW	4
5	NU 312	RHP ROLLER BRG	1
6	353/378	PARALLEL KEY	1
7	1349A	ADAPTER WASHER	1
8	312/065	M10 SETSCREW	2
9	1344A	FUEL LIFT PUMP AND GEAR RETAINING PLATE	1
10	1347LA	PRIMARY GEAR (LEFT)	1
11	SE 96C	CRANKSHAFT GEAR	1
12	1345A	PRIMARY BALANCE SHAFT	1
13	1346A	PRIMARY BALANCE WEIGHT	1
14	1342A	SPACER	1

Figure 4.4 Primary Balancer Shaft (left)

NOTE

\*ONE GEAR MUST HAVE A LH HELIX THE OTHER  
A RH HELIX AS SHOWN IN DRG. 1360A

Figure 4.5 Secondary Balancer Shaft

## NOTES

REMOVE ALL BURRS AND  
SHARP EDGES UNLESS  
OTHERWISE STATED

WORK TO  $\pm 0.3$  ON ALL  
DIMENSIONS RELATIVE TO  
M/C SURFACES UNLESS  
OTHERWISE STATED

TAKE CARE! THIRD  
ANGLE PROJECTION

PARTS FOR A SINGLE  
CYLINDER RESEARCH  
ENGINE AT THE  
UNIVERSITY OF BATH  
QUERIES  
(0225) 61244 EXT. 375

## PARTS LIST

REF NO.	PART/DRG NO.	DESCRIPTION	NO. OFF
1	2524/200	THIN NUT	2
2	88/562	RETAINING WASHER	2
3	NUP 307	RHP ROLLER BRG	1
4	2110/050	M10 SELF LOCKING SCREW	4
5	NU 307	RHP ROLLER BRG	1
6	353/340	PARALLEL KEY	1
7	SE1168/15	OIL & WATER PUMP GEAR*	1
8	374/1227	SPACER	3
9	1355A	SECONDARY BAL. SHAFT	1
10	1356A	SECONDARY BAL. WEIGHT	1

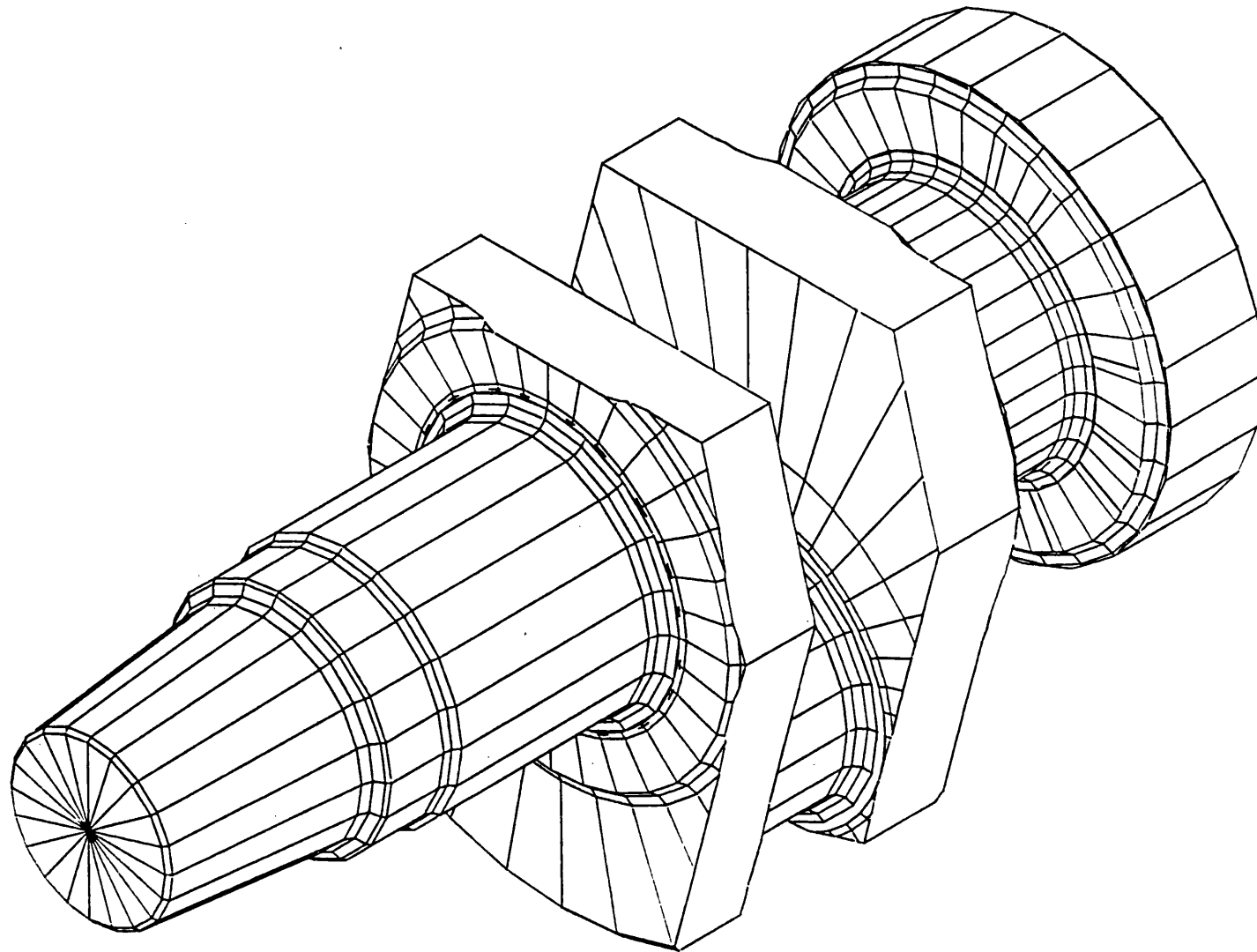


**Figure 4.6 MEDUSA Model of 1SE Crankshaft**



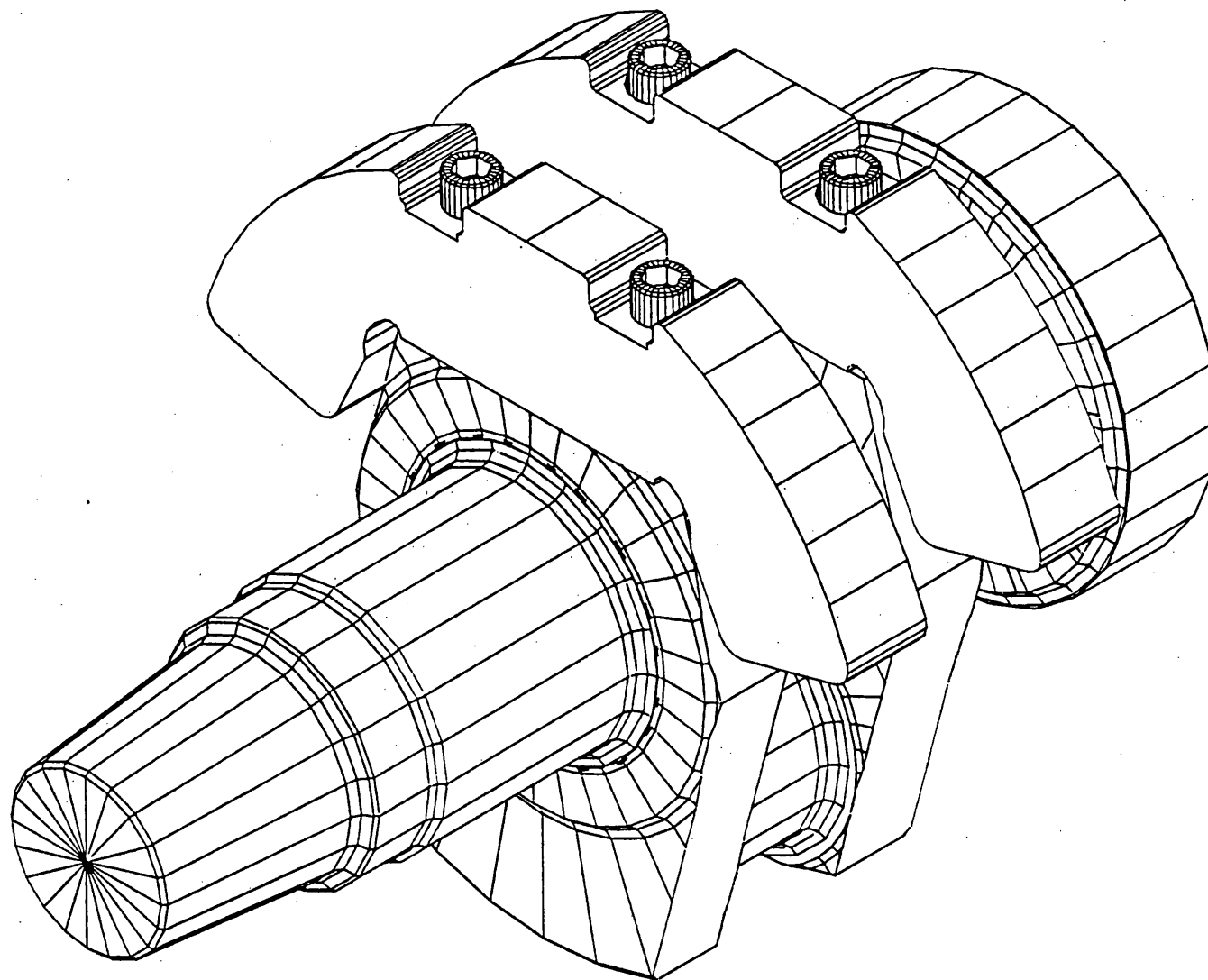


Figure 4.7 MEDUSA Model of 1SE Crankshaft Assembly

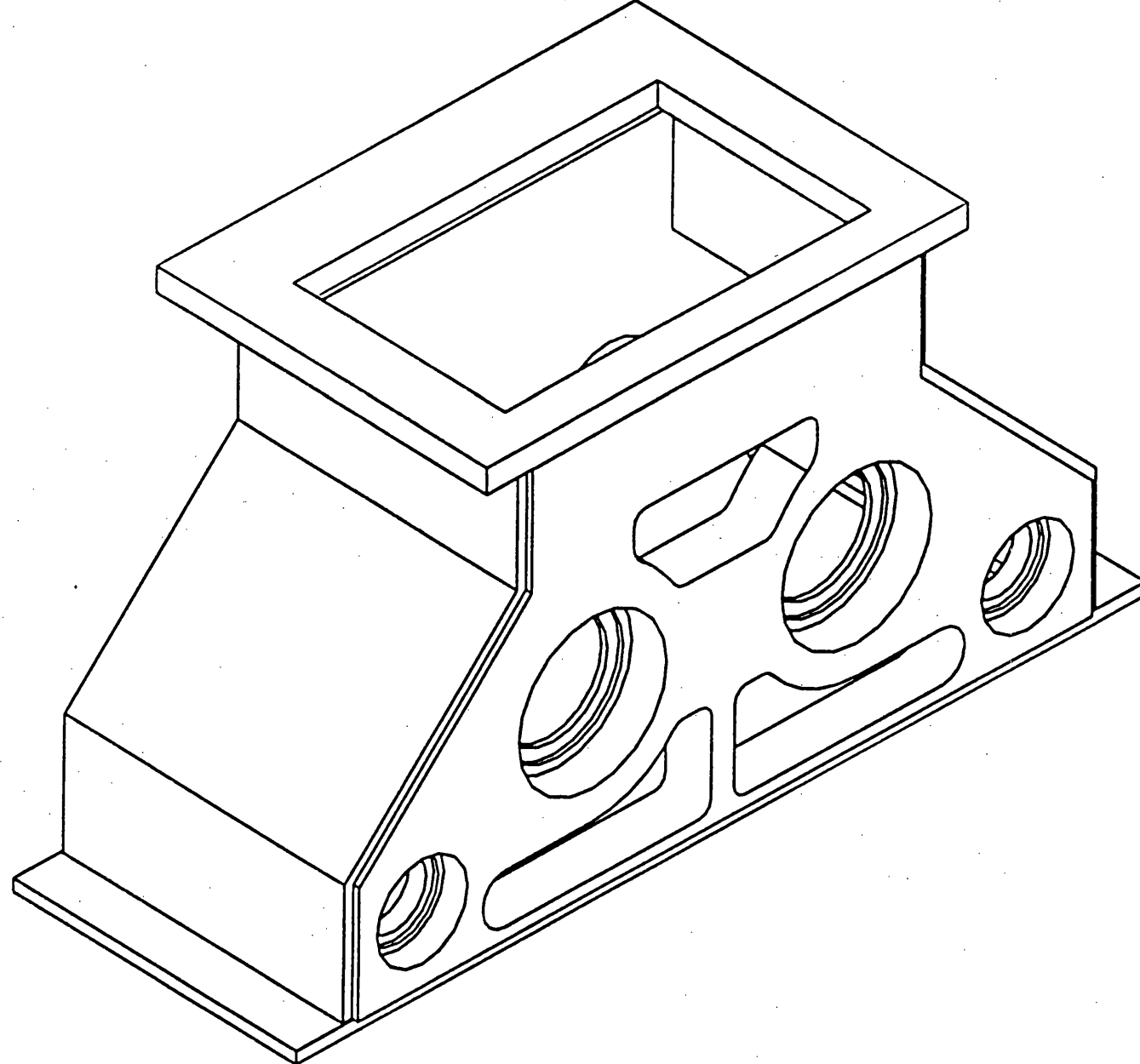
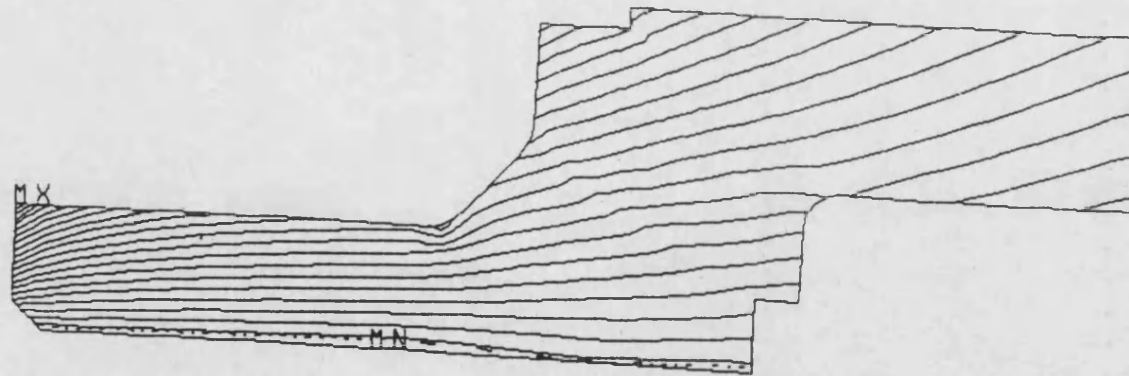


Figure 4.8 MEDUSA Model of Balancer Box

Figure 4.9 Contour Plot of Hoop Stress obtained from  
an Axis-symmetric Model of 1SB Flywheel

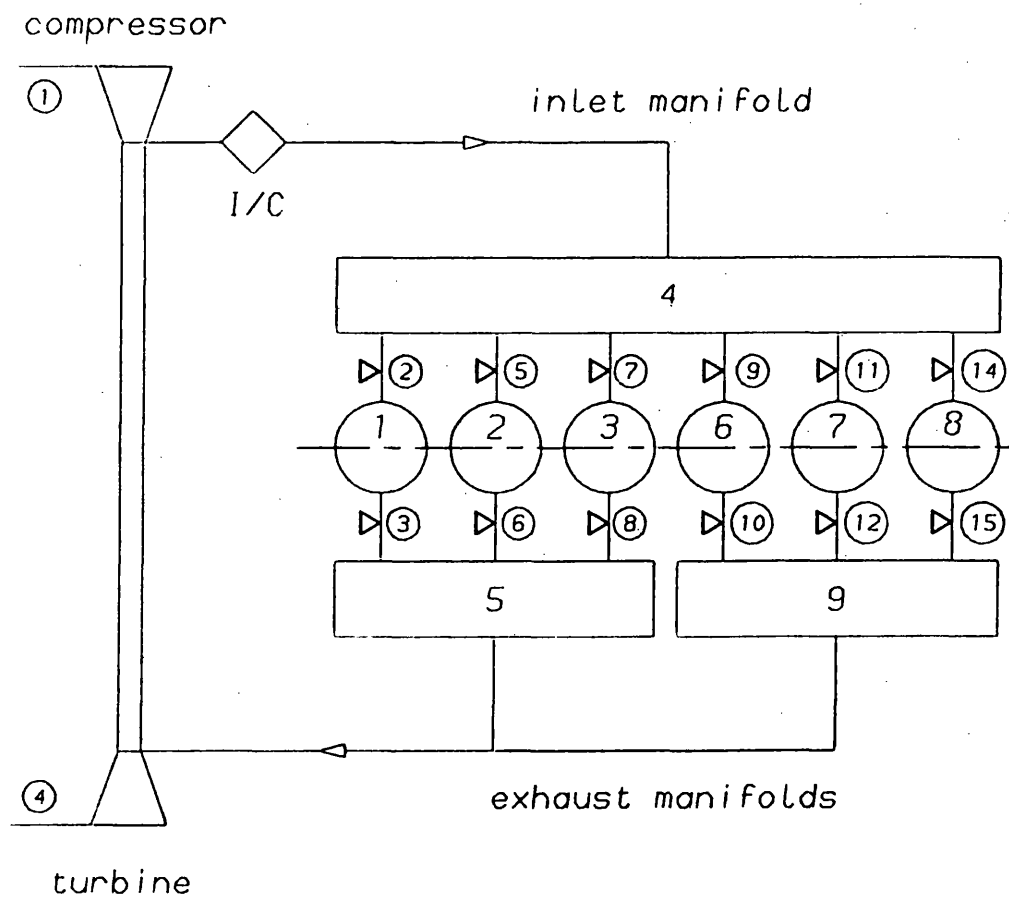
POST1 -INP=



1 1SE FLYWHEEL STRESS MODEL

ANSYS 4.2  
APR 14 1986  
17:11:34  
POST1 STRESS  
STEP=1  
ITER=1  
S2  
STRESS GLOBAL

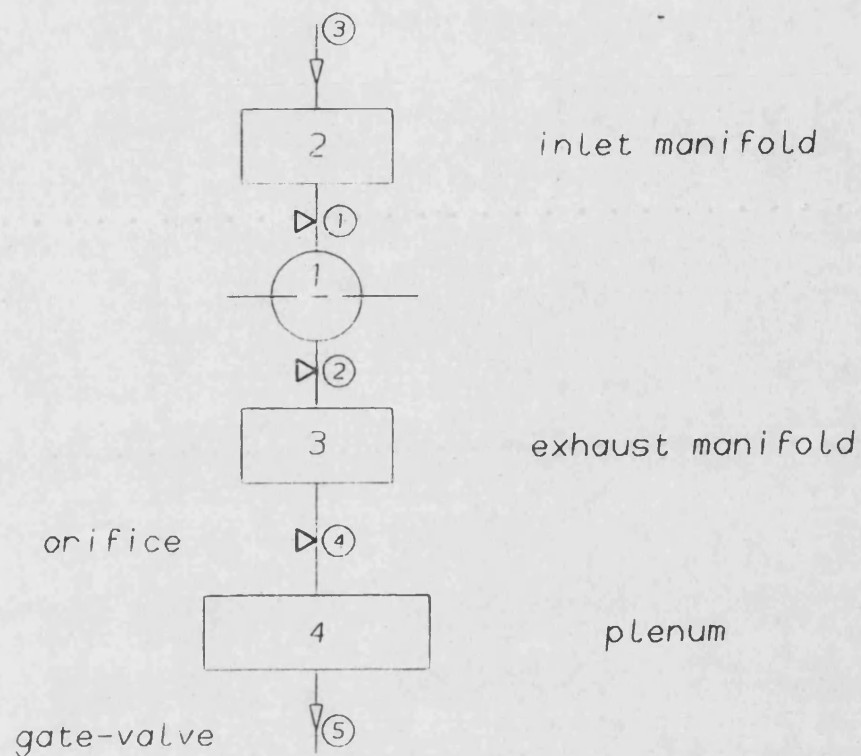
ZV=1  
DIST=187  
XF=220  
YF=54.3  
EDGE  
MX=53341  
MN=-1998  
NCON=20  
VMIN=630  
VINC=2636



Volume 4 = 18 litres  
 Volume 5 = 8 litres  
 Volume 8 = 8 litres

Entry Conditions (Junct. 1)  
 pressure = 1.0 bar  
 temperature = 298 K  
 Exit Conditions (Junct. 4)  
 pressure = 1.0 bar  
 temperature = 298 K

**Figure 4.10 SPICE representation of 6SE Engine**



Volume 3 = 6 litres  
 Volume 3 = varied  
 Volume 4 = 80 litres

Entry Conditions (Junct. 3)  
 pressure = 2.1 bar  
 temperature = 306 K  
 Exit Conditions (Junct. 5)  
 pressure = 1.0 bar  
 temperature = 700 K

**Figure 4.11 SPICB representation of 1SE Engine Installation**

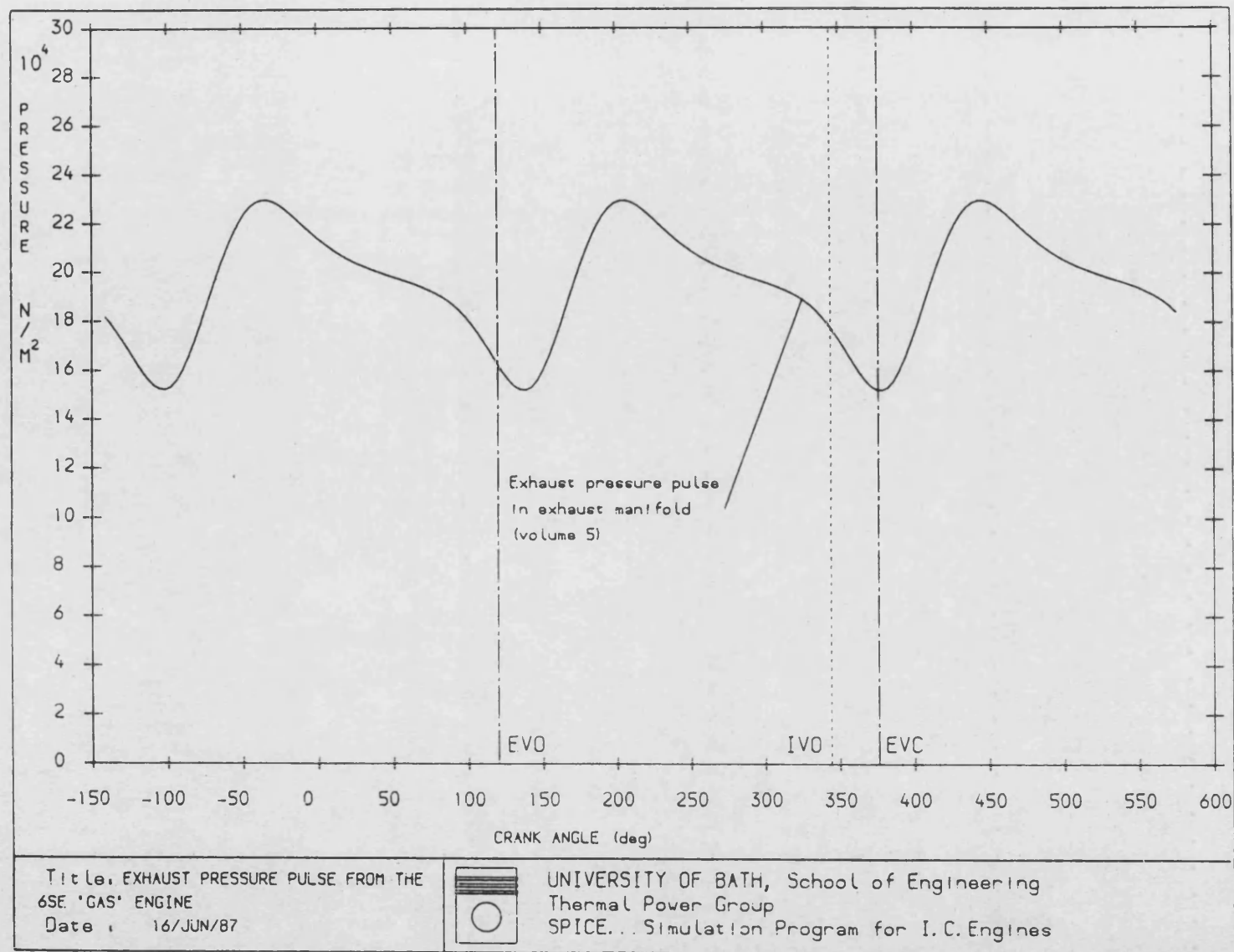


Figure 4.12 Exhaust Pressure Curve from 6SE SPICE Model

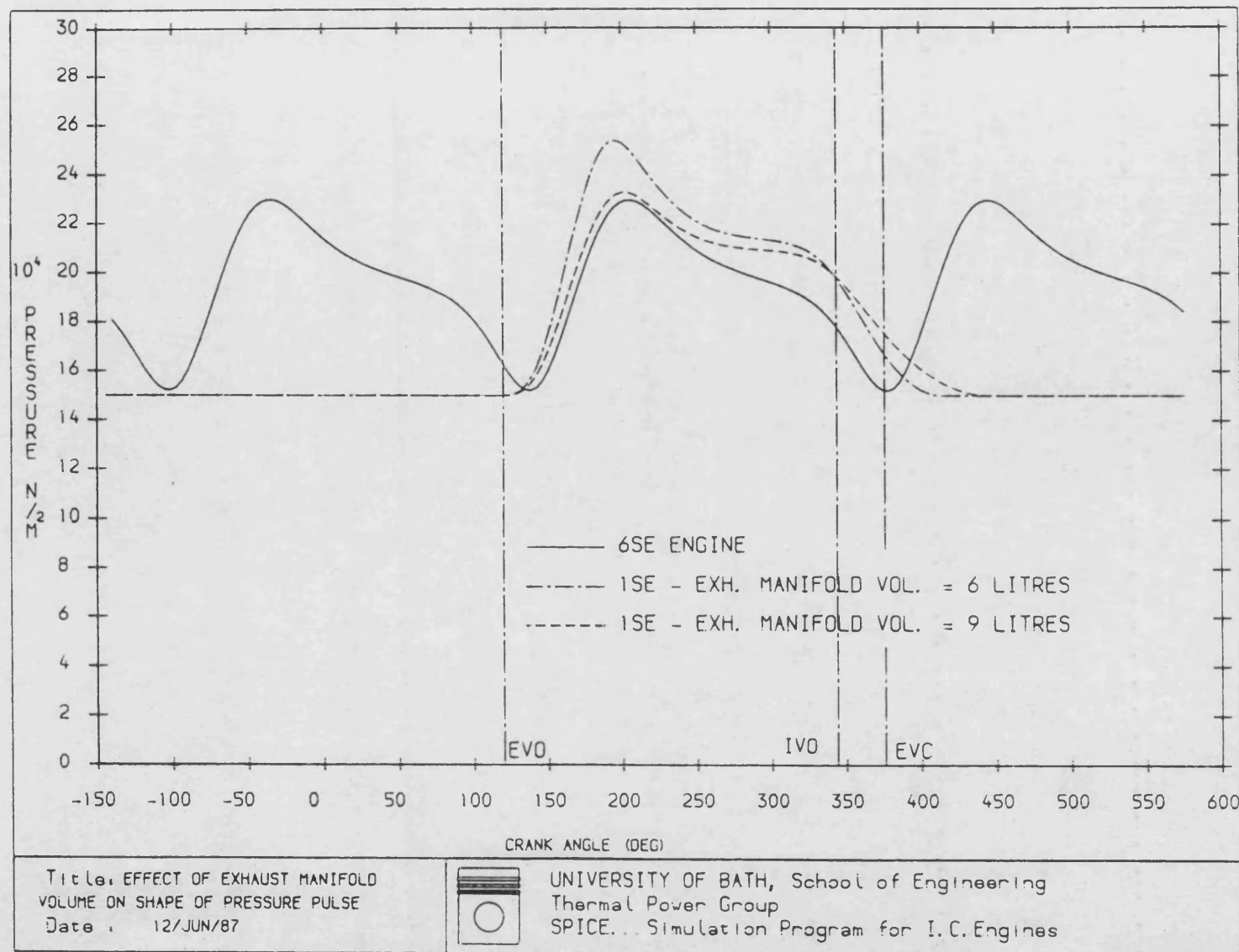


Figure 4.13 Effect of Exhaust Manifold Volume on Pulse Shape for 1SE Installation

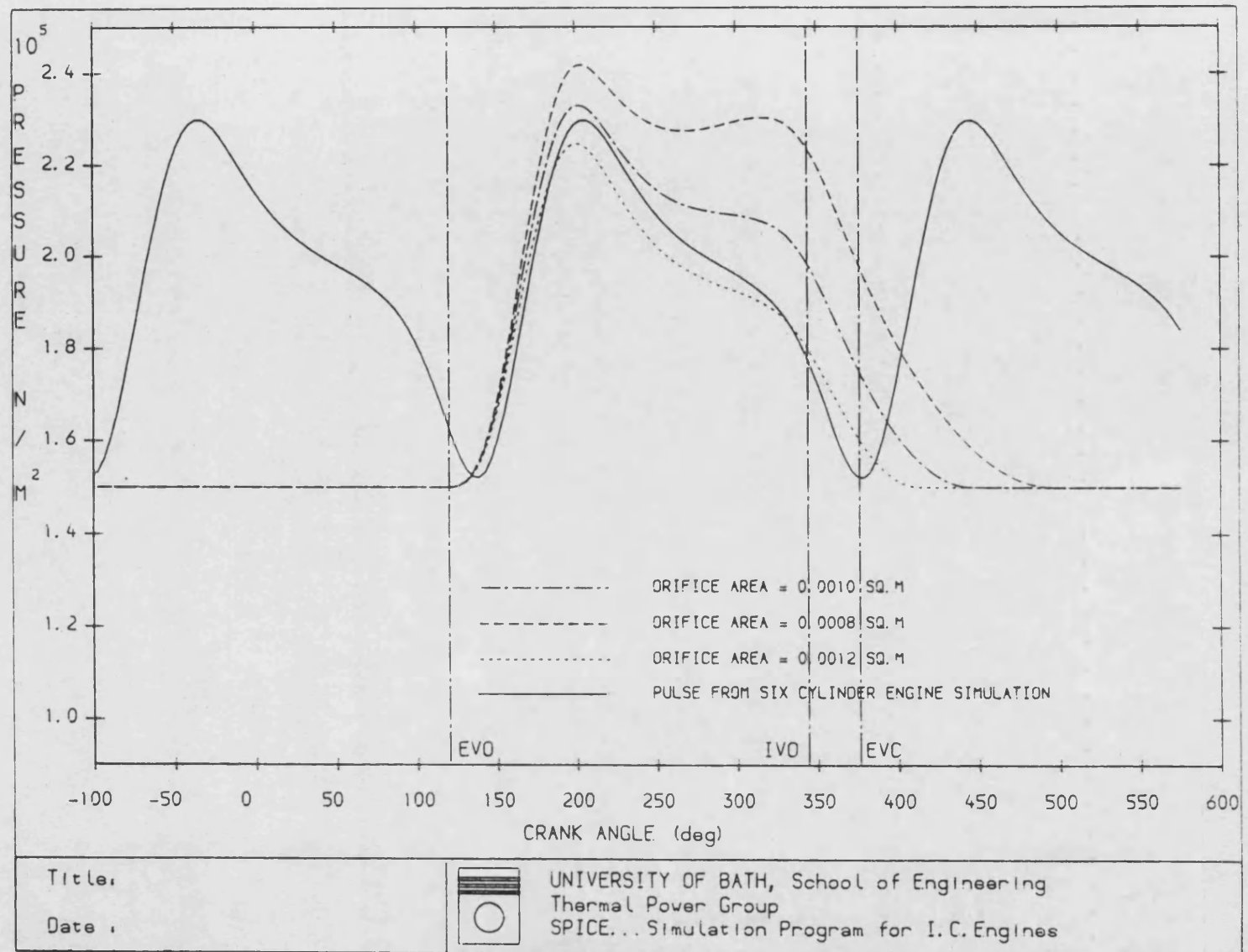


Figure 4.14 Effect of Orifice Size on Exhaust Pulse Shape for 1SB Installation



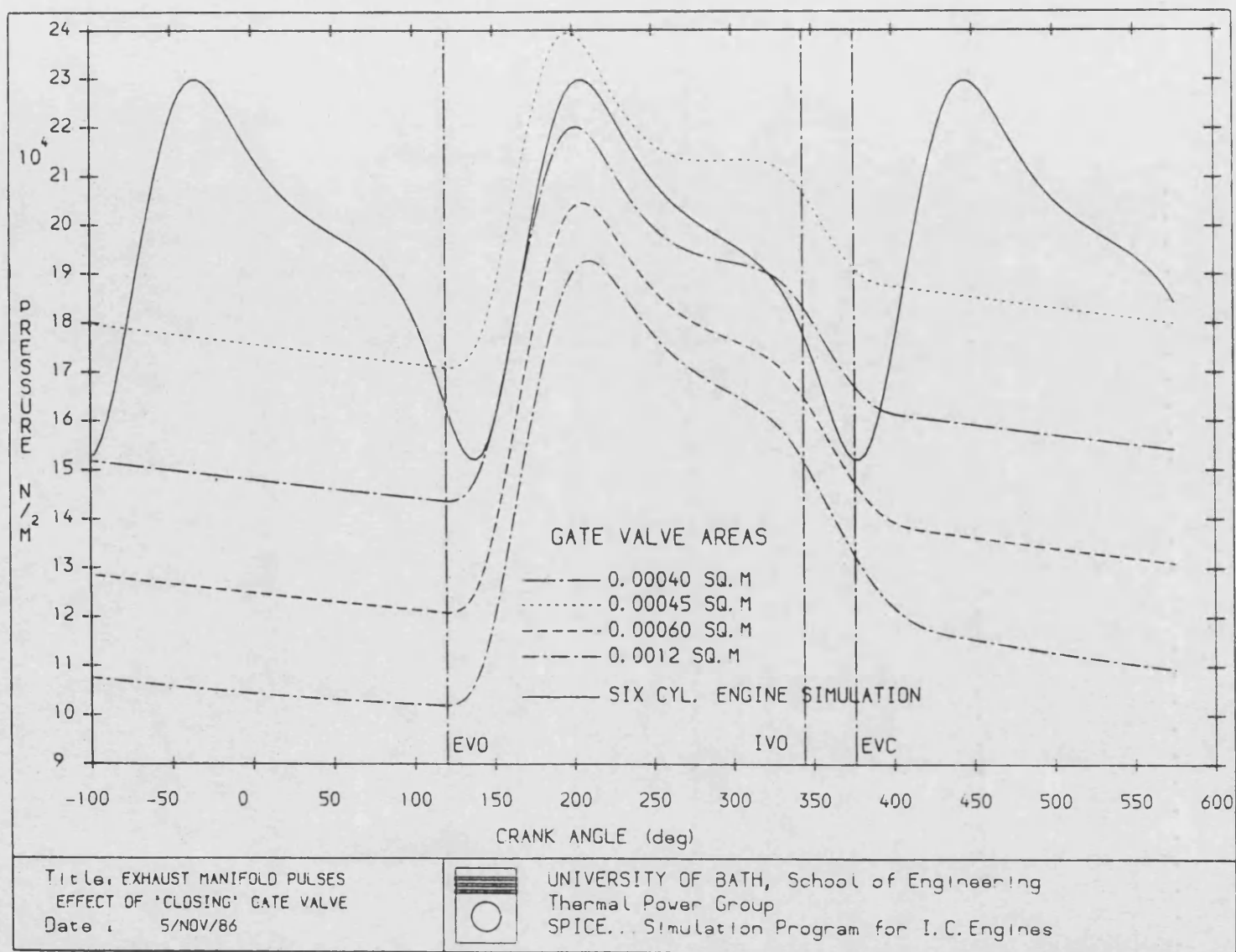


Figure 4.15 Use of Gate-valve to control Mean Back Pressure for 1SB Installation

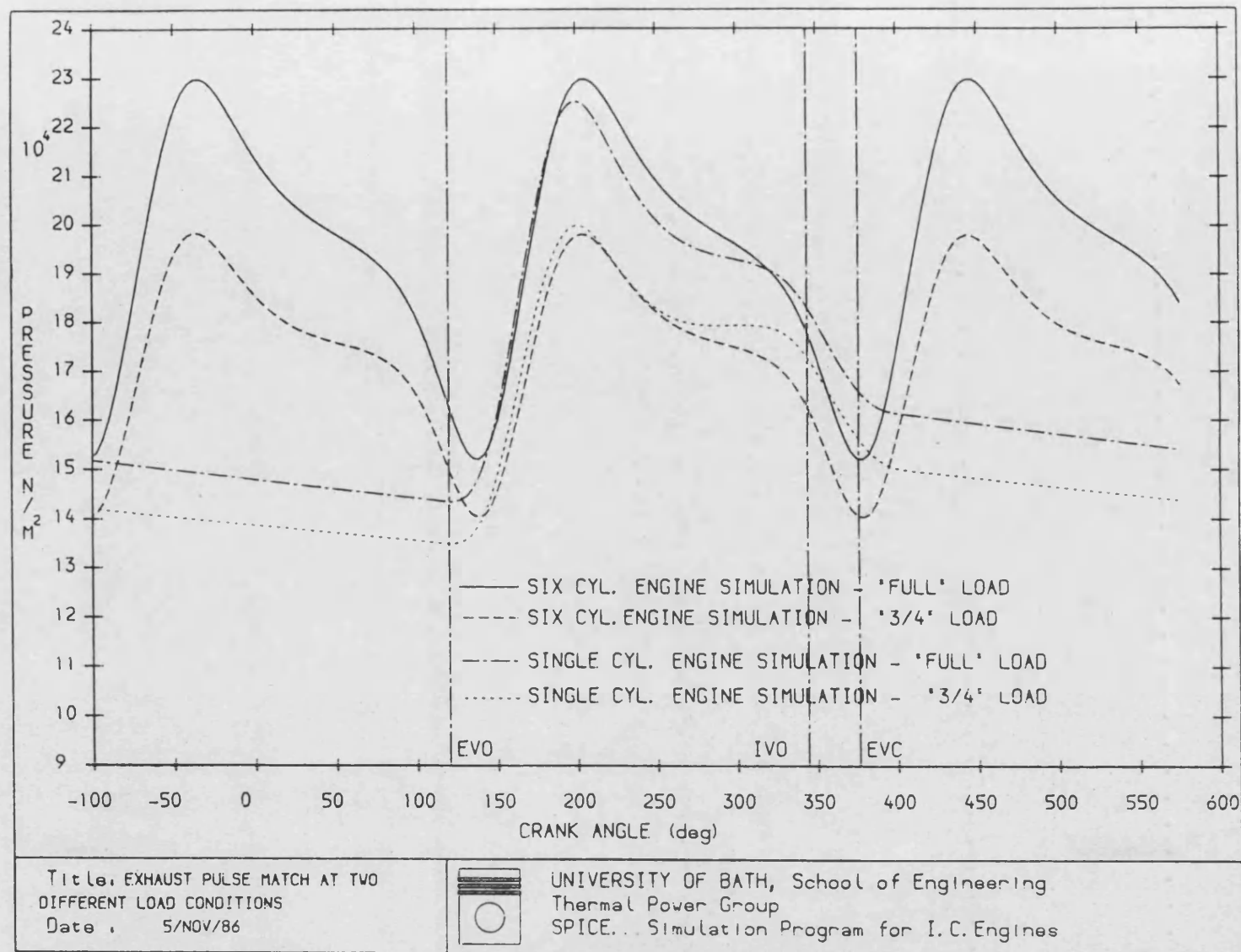


Figure 4.16 Comparison of 1SB and 6SB Exhaust Pressures at Full and 3/4 Load Conditions

# PART III

# CHAPTER 5

## 5. Description of the PHOENICS Fluid Dynamics Program

The Dorman gas engine was designed for "lean-burn" combustion of natural gas, with the aim of reducing  $\text{NO}_x$  emissions. The key to achieving this is in ensuring the reliable combustion of a very lean mixture (equivalence ratio 1.6). The design incorporates a small pre-chamber (5% of clearance volume) in which a near stoichiometric mixture is ignited by a conventional spark plug. The flame thus produced acts as a high energy source or "torch" to ignite the lean mixture in the cylinder.

The in-cylinder mixing and combustion processes are of vital importance to the success of this type of lean-burn combustion system. The main problem is the achievement of a mixture close to stoichiometric in the pre-chamber at the point of ignition, over a wide load and speed range. A relatively small quantity of gas is fed to the pre-chamber (pilot supply) through a non-return valve, whilst a lean mixture is carburetted into the manifold to feed the main chamber. During the compression stroke it is essential that the over-rich mixture in the pre-chamber is correctly diluted by, and mixed with, the lean mixture drawn in from the main chamber.

Much of the initial design work for Dorman was undertaken by Ricardo (67), who identified the pre-chamber as a key area for development work. They recommended that an investigation of the design and size of the pre-chamber should form a part of the early experimental program. There was also a need to establish the parameters which influence the formation of a combustible mixture within the pre-chamber at the time of ignition. In view of this and the importance of this area to the success of the engine it was felt a theoretical study would provide valuable insight.

For this work it was proposed to use the fluid flow program PHOENICS which is accessible on the university's main-frame computer. The aim was to investigate the parameters which affect the mixture formation and distribution in the pre-chamber. It was not proposed to

investigate combustion. Present combustion models are not as widely applied or as sophisticated as fluid flow models; they are generally empirical models which require tuning of combustion "parameters" and are very demanding computationally (46,57,58). In the following sections a description is given of PHOENICS and of the simulation work undertaken.

### 5.1 The PHOENICS Fluid Dynamics Program

PHOENICS is a general-purpose computer code for the simulation of fluid flow, heat transfer, mass transfer and combustion processes. The name is an acronym standing for: Parabolic, Hyperbolic or Elliptic Numerical - Integration Code Series. The first three terms are mathematical classifications of partial differential equation types and all arise in the analysis of fluid flow. Examples of each class are given below:

- Parabolic - single predominant flow direction, where downstream boundary has no effect. e.g. diverging jet
- Hyperbolic - "shock-wave" problems, e.g. supersonic jet mixing; and wave propagation problems, e.g. manifolds.
- Elliptic - recirculating, confined flows. e.g. air motion in a cylinder.

The code uses standard finite difference procedures applied to the fundamental conservation laws of physics (mass, momentum and energy) as expressed by the Navier Stokes equations. For turbulent flows similar conservation equations are solved for the turbulence parameters ( $K$  and  $\epsilon$ ). All these equations are applied over a finite difference grid, into which the domain has been artificially divided.

The version of PHOENICS at Bath is a relatively early generation of the code. This means it does not have the later "body-fitted" coordinate system or the improved data input practices. Thus, flow

modelling is restricted largely to cartesian or cylindrical polar flow regions. Irregularities are accounted for by prescribing regions of the finite difference grid which are not accessible to flow ("blocked"). An example of this method in comparison with a body-fitted coordinate system is shown in figure 5.1. Data input to this version is by insertion of assignment statements into a skeleton FORTRAN program. This subsequently writes data files which are accessed by a general solution procedure. Sophisticated data preparation - such as the prescription of "blockages" in the flow domain or non-uniform flow fields - requires more elaborate FORTRAN programming.

#### 5.1.1 Solution Method

The solution method employed by PHOENICS is based on the finite difference technique. This requires the region of interest to be formed into a finite difference grid over which the differential equations representing the physical laws governing the "conservation" of mass, momentum and energy are applied. All these equations can be expressed in a common form, namely:

$$\frac{\partial}{\partial t}(\rho\phi) + \frac{\partial}{\partial x_j}(\rho u_j \phi) = \frac{\partial}{\partial x_j}(\Gamma \phi \frac{\partial \phi}{\partial x_j}) + S_\phi$$

accumulation      convection      diffusion      source  
rate

where:       $\phi$  : any of the dependent variables  
               $\rho$  : density  
               $u_j$ : velocity component ( $j = 1-3$ )  
               $S$  : source term  
               $\Gamma$  : diffusion coefficient

PHOENICS then solves discretized versions of the equations; applying them over the sub-domains, or cells, into which the region has been divided. Each cell is topologically cartesian; thus in the general 3D case has six sides and eight corners. Within a cell is a typical point - called a grid node - for which the fluid property values,

$\phi$ 's, are regarded as representative of the whole cell. The velocity components are stored on the faces of the cells and thus collectively constitute a staggered grid as shown in figure 5.2. Thus, the velocity nodes are midway between the pressure nodes. The pressure difference is seen as a driving potential for the velocity.

Integration over each cell leads to "finite-domain" equations, with each grid point  $\phi$  connected with seven neighbouring  $\phi$ 's, namely those at the north, south, east, west, high, low and previous time locations. In algebraic form the relation runs:

$$a_P \phi_P = a_N \phi_N + a_S \phi_S + a_E \phi_E + a_W \phi_W + a_H \phi_H + a_L \phi_L + a_T \phi_T + S$$

wherein the subscript P denotes grid point; subscripts N, S, E, W, H, L, T denote neighbours in the above mentioned order and S is the source term.

The " $a_i$ " coefficients express the influences of convection and diffusion processes across the cell boundaries. It is convenient to regard  $a_T$  as "convection in time". Thus the value at P is a weighted average of the values of the neighbouring cells and the previous value in the cell. In evaluating the dependent variables,  $\phi$ 's, at P only inward convection is allowed to influence the values. This is known as an "upwind" formulation. The equations to be solved are non-linear - the dependent variable  $\phi$  appearing in the coefficients. Further they are "fully-implicit" - the unknown appearing on the left and right hand sides of the equations. Thus iteration techniques must be used rather than direct matrix inversion.

### 5.1.2 Solution Procedure

The solution of the finite-difference equations is performed, as stated above, by means of an iterative procedure employing pressure and velocities as the main flow variables. The "staggered" grid is used to link the pressure fields and velocity. The sequence of the numerical solution may essentially be listed as follows:



- (i) the pressure field is guessed;
- (ii) the corresponding velocity fields are computed - from the momentum equations;
- (iii) the resulting errors in the continuity equations are computed;
- (iv) these are then used to correct the pressure field;
- (v) re-calculate velocities from momentum equations.

These ideas may be elaborated. During the solution PHOENICS employs what are called repeated z-direction sweeps through the integration domain. The whole set of cells is regarded as consisting of one-cell-thick slabs, extending in the x and y directions, and piled on top of one another in the z-direction. A sweep starts at the bottom (low-z) slab using the existing values in the cells. The finite domain equations are solved for all the cells in the slab, the value of  $\phi$ 's (dependent variables) at the next higher slab being regarded as known. Attention then moves to the next higher slab, the  $\phi$  values adjusted in reference to those slabs above and below. The process is continued until the sweep is completed.

At the end of a sweep the continuity errors are computed. Each dependent variable must satisfy a continuity type equation. For some the equation is clear - species conservation equations solved to find the mass fraction. For others the relationship is less obvious: the "correct" pressure field is that which will ensure that mass is conserved throughout the flow domain. After the first sweep the final solution will not have been achieved so the process is repeated until the difference in  $\phi$  between successive sweeps falls within specified limits. In the program the number of sweeps to be performed at each time-step can be set. Thus, once this number has been achieved the solution will automatically move on to the next time-step regardless of whether the continuity errors have fallen to within the desired limits. Clearly some experimentation is required to set the optimum number of sweeps for any particular problem. A high number of sweeps will result in improved accuracy but there will be a trade off in the length of the computer run times.

### 5.1.3 Program Structure

The PHOENICS program has three elements (refer to figure 5.3):

- (i) "EARTH" - the central equation solver.
- (ii) "Satellite" - a separate program supplying problem-defining data to cause "EARTH" to simulate the required process. It does not interact with "EARTH": it writes the data files which "EARTH" reads.
- (iii) "Ground-Station" - a further separate program allowing modification of properties or boundary data as the program is running. It does interact with "EARTH".

#### (i) EARTH

The numerical solution scheme is an independent computer code which, as already indicated, constructs and solves the equations representing the balance of the various physical quantities over each of the sub-domains or "cells". Thus, on reading in the data file created by the satellite program the "EARTH" code is tailored to the solution of a particular flow configuration. The intention of the originators of the PHOENICS program is to standardise the numerical solution of flow problems. As part of the philosophy the "EARTH" code is not accessible to the user and is meant to be considered as a "black box".

#### (ii) Satellite

The satellite consists of a main program SATLIT and a further subroutine FLDDAT. It is in the main program SATLIT that the basic problem is defined through the insertion of executable statements. In a related data file - DEFA - "default" values of all data items which the satellite will transmit to EARTH are supplied. The FLDDAT part of the subroutine is used to prescribe non-uniform initial fields - i.e. values in each grid-cell - of all the dependent

variables with which the computation will be started. These are the "initial values" in a transient-flow calculation, and "initial guesses" in a steady-flow one. (In the steady-state the initial fields do not influence the converged solution, but may affect the convergence rate). Uniform fields can be supplied directly in SATLIT. Having defined the problem the information is made available to the solution program EARTH through three output data files:

GUSI - general information; mesh geometry, etc.

PRSI - blockages

FIEL - non-uniform fields

In setting up the model initially, it is necessary to work through the various groups of the SATLIT program setting variables and including FORTRAN code to define the problem properly. Usually the user will have access to a relevant PHOENICS demonstration report (PDR), which would serve as a guide, when working through the satellite. Perhaps the best way to illustrate how a model can be set up and to give an indication of what can and cannot be done in the satellite is to highlight the key features. Attention is drawn to the satellite skeleton frame work shown in appendix 5. (The text in parentheses refers to the group numbers in the SATLIT program).

Satellite - basic problem definition

Type of flow (Group 1)

By default PHOENICS anticipates an elliptic-type flow. Where the problem is of a parabolic nature, e.g. boundary layer, the defaulted setting should be changed. This permits economies of both computer storage and computer time.

Time - dependence (Group 2)

Except where the model is to be used for a steady-state solution it is necessary here to include details of the transient simulation. The start and end times need to be set as well as details of the size

of the time steps and their distribution. For example when modelling the rise of a piston towards top dead centre the initial step size would probably be relatively large with size decreasing as top dead centre is approached.

#### Coordinate system (Group 1)

Two coordinate systems are available: cartesian or cylindrical polar. It is important for the latter case that the x-direction is set as the circumferential one, with the z-direction running parallel to the axis of rotation (see section 5.1.2). The grid spacing for the x, y and z directions are defined in groups 3, 4 and 5 respectively. In each case the overall size must be given along with the fractions into which they will be divided. It is not necessary to employ even grid spacing, but large changes between adjacent cells should be avoided.

#### Moving grid (Group 6)

The EARTH program contains a number of moving grid options, in which the grid, or a portion of it, is expanded or contracted in the z-direction. These built-in options include settings for piston in cylinder calculations, pressure effects within a gun barrel and the option of a constantly expanding grid.

#### Blockages (Group 7)

To be able to model complicated flow domains it is required to block certain regions, such that they are inaccessible to flow. This is done by specifying "porosity" settings for each of the grid cells. There are four porosities for each cell: the cell (or volume) porosity represents the proportion of the cell volume available for occupancy by the fluid; and the other three, the east, north and high porosities, represent the fraction of the respective face area which is available for flow. Porosity values of unity correspond to no blockage, whilst values of zero mean that the cell is completely

blocked. Partial blocking - a value between zero and unity - is also possible.

#### Properties (Groups 8-10)

In groups 8 and 9 those variables for which a solution is required need to be set. In the default setting nothing is solved! Group 10 is specifically used to select various built-in options for evaluating density. These include: constant density, density as a function of pressure, etc. If none of the options fit the user's needs then the density formulation has to be prescribed in the GROUND subroutine.

#### Initial Fields (Group 13)

Before the solution commences the initial fields of all the variables to be solved for must be set. If the fields are non-uniform they need to be described in the FLDDAT subroutine.

#### Boundary/Internal Conditions (Groups 14-24)

If no action is taken the EARTH program will act as though the fluid is confined within a container, the boundaries of which are impenetrable to the flow of mass, momentum or energy. In real flow problems such boundaries do occur; the axis of symmetry for example. Also where wall effects are relatively minor compared with effects away from the walls then these default conditions may be sufficiently accurate, e.g. events in a combustion chamber.

Where it is necessary to identify "special" boundary conditions then this is done through up to ten regions which the user defines. This is done by specifying the start and end grid cells for each region. In this way, it is possible to introduce wall functions, and to include inflow and outflow of mass. This should only be done in the satellite if the conditions do not vary during the solution (e.g. fixed pressure exit or fixed inflow rate). Varying conditions need to be entered via the GROUND subroutine.

All boundary conditions are inserted as sources and sinks into conservation conditions on flow properties (section 5.1.1). These are represented by linear expressions of the form:

$$\text{source} = C_{\phi} (V_{\phi} - \phi)$$

where  $C_{\phi}$  and  $V_{\phi}$  are the "coefficient" and "value" which are prescribed separately for each region. The term  $\phi$  is the calculated local grid-node value of the variable in question. It is important to realise when providing a boundary condition which involves mass inflow or outflow that it is also necessary to include those properties associated with mass (enthalpy, concentration, velocity components) as sources too. When wall functions are specified, they are introduced either with turbulent or laminar profiles - dependent on the Reynolds number. (The shear stress is evaluated - from laminar or log-law relationships - and its components are then included as source terms for the velocity components parallel to the wall).

In the remaining groups it is possible to set the various parameters controlling the solution procedure. i.e. number of iterations, convergence criteria, etc (Groups 26-28) and to organise the type of solution output required.

#### (iii) Ground-station

During the course of the numerical solution it may be necessary to modify features requiring interaction with EARTH. Examples of these include:

- (a) introducing complex non-linear boundary conditions
- (b) providing any required property formulae for densities, enthalpies, etc. which are not available as built-in options
- (c) writing special output not included as standard.

A skeleton ground-station is listed in appendix 6.

Provision is made for this contingency in the subroutine called GROUND. Like the satellite the GROUND subroutine is divided into sections or "chapters". These are called at particular stages in the EARTH solution sequence; for example at the start and end of a time-step or end of an iterative loop. It is important to know when each chapter is accessed so that any modifications included will be read in by EARTH at the correct time. The FORTRAN coding in GROUND will vary considerably from problem to problem, and so it is not proposed to work through each chapter. Instead, the more commonly used ones will be highlighted.

#### "Chapter 5"

This is the chapter where any source-term modifications are made. It is called during the solution for each variable at the z-slab in question. Information is not transferred directly between EARTH and GROUND but via connecting subroutines; for example ADD, which is used to set source terms. In this way information can be read from arrays in the EARTH code, manipulated in GROUND and then returned in modified form to EARTH. It is left to the user to provide the FORTRAN coding to introduce the sources at the correct areas of the domain. Examples of the types of sources which may be added are:

- an internal heat source, and
- inflow or outflow of mass.

#### "Chapter 7"

This chapter is called at the end of operations at a slab, just before the solution moves to the next slab. Two typical examples of its use are:

- to compute the total masses of gas and air for the slab and their sum; and
- to store local velocity components for later plotting of velocity fields.

## "Chapter 9"

With this chapter being accessed at the end of each time step - for a transient flow only - it is here that the user can organise output, specific to the problem, for writing to separate files.

## "Chapter 10"

The chapters 10-16 perform different functions to those discussed so far. They are provided specifically for the adjustment of material properties. Chapter 10 has been highlighted because it is used to prescribe special density formulations not covered by the built-in options of the satellite. Thus, if the simulation is concerned, for example, with more than one gas, then it is here that the coding for the density calculation for the mixture of gases is included.

### 5.2 Initial In-cylinder Air Motion Model

In the description that follows it is important to stress that using PHOENICS has been very much a learning process. Setting up the model - defining the geometry, boundary conditions, etc. - is perhaps the easiest part. The difficulty arises in assessing the validity of the assumptions made and results obtained. Throughout the work a step-by-step approach was adopted. At each stage some attempt was made to verify results from the model before advancing to the next stage. Where possible simple checks were performed and where this was not the case every attempt was made to ensure that the results were at least plausible! Only in this way was it possible to gain confidence in the predicted results as the simulation models became more complex.



### 5.2.1 Construction of the Piston In-cylinder Model

The basis for the construction of the initial model was a PHOENICS Demonstration Report (68). The model detailed is concerned with the air motion in the combustion chamber of a diesel engine during a part of the cycle when the valves are closed and in which compression and expansion occurs. Having no experience of running PHOENICS this was felt to be a sound starting point: much of the information contained in the report would be relevant and initial changes would be limited to alterations in geometry. Importantly the use of the moving grid option was demonstrated (see section 5.1.3).

Following the procedure highlighted in previous sections the necessary information was entered into the satellite. For simplicity the model was taken as axi-symmetric and so a two-dimensional calculation would suffice. Chemical reaction and heat transfer were not considered, but the air turbulence was simulated by use of a two-parameter model ( $K-\epsilon$ ). In this model, in common with others (50,51), forced vortex flow around the cylinder axis with a uniform turbulence - solid body rotation - is assumed to represent the induction swirl when the inlet valve closes. For piston in cylinder simulation work the convention in PHOENICS is that the grid is specified at BDC, irrespective of the starting angle of the calculation. Compared with the actual geometry of the Dorman engine, the model is very much simplified. Without resorting to a 3D model, combined with partial blockages, details such as the valve cut-outs and complex piston bowl shape are impossible to model. However, it was important that the correct clearance height in the cylinder be maintained and so the bowl volume was adjusted to ensure that the compression ratio remained at 12:1. The finite-difference grid is shown in figure 5.4. At the numbered boundary regions shown no-slip conditions (zero velocity at the wall) were applied, and "wall functions" included for the near wall values of the dependent variables (see section 5.1.3).

### 5.2.2 Assessment and Validation of Results

Having run the program and ensured that it was working correctly it then clearly became necessary to verify the validity of the output. With no relevant experimental data available, validation was limited to examining output which could be easily checked. Certainly no means were available to check swirl and velocity components against experimental measurements: for these particular variables all that was practicable was to check flow directions and velocity magnitudes based on examination of the internal pressure gradients.

The main basis for comparison was the pressure variation with crank angle. Not only is pressure one of the key dependent variables in the solution procedure, but the pressure values obtained could be reliably compared with perfect gas law theory. This was made easier by the fact that the simulation did not involve combustion and was run only over the part of the cycle when the valves were closed. A further check was provided by results from a simple single cylinder engine model constructed on the engine simulation package (SPICE), available in the School.

In each case the initial conditions at inlet valve closing were as follows:

pressure (bar)	1.17	stroke	190mm
temperature (K)	300	conrod length	336mm
compression ratio	12:1	bore	80mm
inlet valve closing (IVC)	40 deg	(0 deg = BDC on the	
exhaust valve opening (EVO)	300 deg	compression stroke)	

For PHOENICS the initial pressure is the value set in each "cell" at the start of the computation, whilst for the perfect gas law formulation ( $PV^\gamma = \text{const.}$ ) and the SPICE model the value is the starting point for the calculations.

A comparison of the pressure predictions is shown in figure 5.5. The main points to note are:

- (i) the close agreement between curves obtained from simple theory (PV $\gamma$ ) and SPICE (variable  $\gamma$ );
- (ii) lower peak pressure (26.8) predicted by PHOENICS;
- (iii) difference in these values  $\approx 18\%$ .

Analysis of the monitor printout - containing information on convergence continuity errors, etc. - obtained from the PHOENICS model indicated that the solution had converged. However, this is only the first stage. In solving a finite-difference problem various factors influence the solution (57), namely:

- (a) number and distribution of grid points;
- (b) number and distribution of time-steps;
- (c) limits set on termination criteria; and,
- (d) sweep and iteration numbers.

In optimising the parameters for a particular problem there is no quick and easy method. The only guide-line is to experiment with settings until a point is reached where further refinement results in no significant changes being noted. However, it is possible, especially as the number of grid nodes and time-steps is increased, to reach a point where further numerical accuracy is offset by unacceptable computational expense (47).

Calculations based on the data given in the PHOENICS Demonstration Report (PDR 6) showed that the error between the pressure value predicted at TDC and that evaluated from perfect gas law theory to be approximately 12%. In the example the PHOENICS prediction proved to be the higher value. The report itself did not attempt to verify any of its predictions, beyond checking that they were plausible, nor did it cover the effect of grid and time-step refinements.

It was felt, however, that for the initial Dorman model an investigation into the effect of grid spacing, and size and

distribution of time-steps would prove useful. It could perhaps provide early information on the likely number of cells and the time-steps that would be needed for later more complex models. There was not time for an extensive exploration, but some of the findings are outlined below.

#### a) Effect of Grid Spacing on the Solution

Two refinements were explored:

- (i) increasing the number of cells in the moving grid; and
- (ii) adding more cells in the radial direction.

In the initial model (see figure 5.4) the moving grid was only divided into five regions resulting in the cell volumes at BDC being correspondingly large. This should be compared with Ikegami (51), who employed a 20x16 grid for the moving part and a further 10x12 for the bowl, and Matsuoka (50), who divided the cylinder radius into 24 pitches with the axial direction being divided into 20 - 8 outside the bowl and 12 inside. By sub-dividing the moving grid further it was thought that convergence would be improved, leading to better agreement between the predictions of the cylinder pressure. The subsequent results showed a marginal improvement, but not the improvement that was desired. This was perhaps to be expected. In the few degrees of crank angle either side of TDC the moving grid cells are compressed into a very small space and so refining the grid has no real effect on the pressure value. It does of course provide for better flow definition.

The second option - more cells radially (y-direction) - was adopted for similar reasoning as above. There was also the feeling that wall effects and no slip conditions could be affecting the solution, especially in view of the fact that initially they were applied over the one y-slab above the piston crown. However, these modifications plus the previous grid alterations, which combined made up a grid of 20x24 - following Matsuoka (50) - only produced a final pressure

value of 27.0 bar (vis. 26.8 bar). This was certainly not the increase that was sought and so it was concluded that other parameters must be affecting the solution more markedly.

Examples of the predicted velocity fields in the r-z plane, as the piston rises to TDC then recedes, are shown in figures 5.6(a-d). Whilst it was not possible to validate the results, the figures do illustrate squish and reversed-squish patterns similar to those produced by others (50,51). No work was undertaken on the effect of swirl ratio, although Matsuoka et al. (50) had shown this to affect the predicted squish patterns.

#### **b) Effect of the Size and Distribution of Time-steps on the Solution**

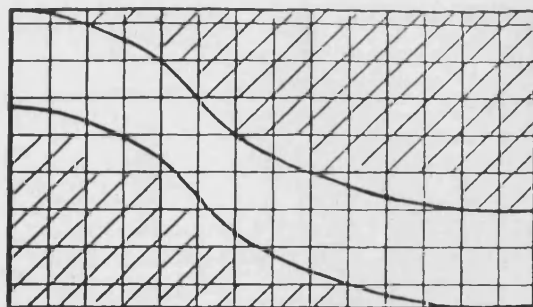
Numerical accuracy depends not only upon how many time steps are employed, but also upon how they are distributed. In most cases common sense is the best guide! At the start, the size of the time-steps and their distribution had been chosen to limit the changes in pressure between steps. Thus, initially the steps were in ten degree intervals, then decreasing in stages, until around TDC the step size was down to half a degree. This is illustrated in figure 5.7.

Benjamin et al. (60) in their combustion model employed time-steps of half a degree throughout the cycle, whilst Matsuoka (50) employed steps as small as one sixth of a degree. Whilst small time-steps do not entail additional computer storage they do result in large computation times. With the computer resources available such small steps could not be justified; instead a run with 160 steps (120 x 1°, 40 x 0.5°) from IVC to TDC was investigated. As the computation proceeds the program only stores previous and current time-step values and thus too coarse a time interval initially could ultimately affect the final solution of the dependent variables. The results obtained, however, indicated that the original time step distribution had been appropriate: no change in the pressure at TDC was observed.

In view of the poor agreement between the pressure values obtained from PHOENICS and the "zero-dimensional" models, and with a need to be satisfied that the grid settings in the satellite had been entered correctly, additional FORTRAN coding was included in GROUND to output the total enclosed volume at each time-step. Although great care had been exercised when defining the original grid it might have been possible that a number of rounding errors could be enough to sufficiently alter the geometry and thus change the compression ratio. The output obtained showed that the difference between the desired compression ratio and that used in the PHOENICS program to be less than one percent: not enough to explain the 18% error in TDC pressure values.

The cause of the error was traced at a later date to the constants set in the density formulation. As was explained in an earlier section (5.1.3) a number of fixed density options are available to the user. The one chosen here, and used in the CHAM example, PDR 6 (68), was of the form:  $\rho = A p^B$ , where A and B are constants, independent of temperature; and where  $\rho$  and p are respectively the density and pressure.

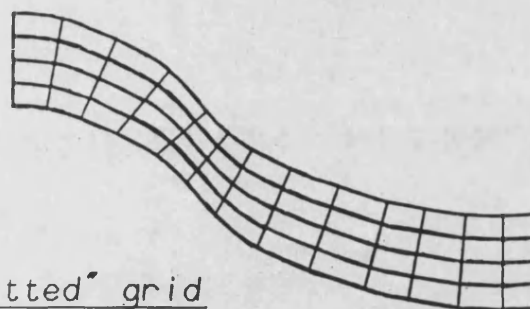
This was appropriate for a closed adiabatic compression and expansion. In the PHOENICS documentation inadequate information is given on the setting of these constants: it is not pointed out that they need to be altered for different initial conditions. An attempt was made to evaluate the constants set in the satellite based on the PDR 6 report. Unfortunately, when comparing with the report, insufficient data on the initial conditions was available to be able to make accurate calculations. New values were therefore set based on the initial conditions for the Dorman geometry. The pressure value at TDC (33.7 bar) subsequently predicted proved to be within 4% of that obtained from SPICE (variable  $\gamma$  with temperature), and more importantly when this value was compared with PV $\gamma$  the error proved to be less than one percent.



shading indicates fully  
blocked cells

(boundary cells can be  
partially blocked to  
improve accuracy)

regular grid



"body-fitted" grid

**Figure 5.1** Illustration of Difference between "Body-fitted" and Regular Grid Coordinates to represent curved Geometry

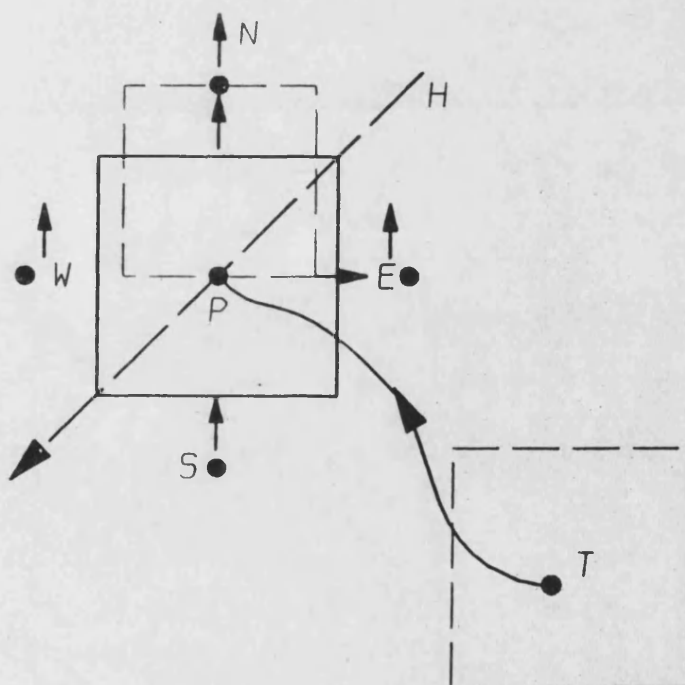
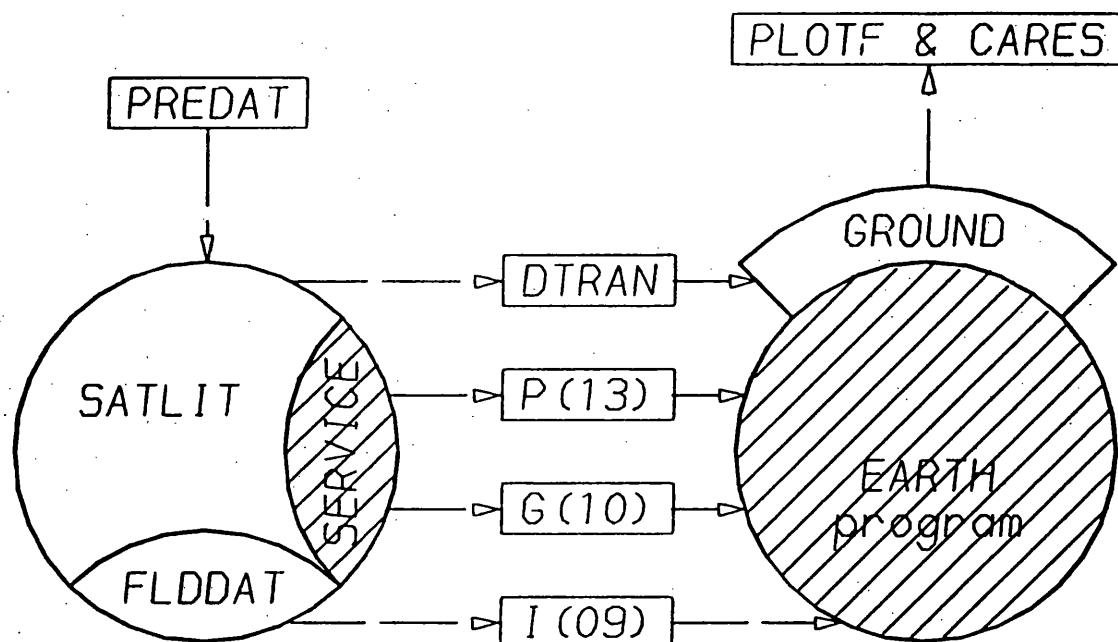


**Figure 5.2** Cell Definition within the PHOENICS Program



Meanings of annotations are as follows:

- = Data File, with logical-unit numbers
- G = General (GUSSI) Data
- P = Porosity Data (PRSI)
- I = Initial-Fields Data (FIEL)
- DTRAN = Original Data File (PREDAT)
- = Data link

PLOT & CARES are the purpose written plotting and output files

PREDAT is a purpose written data input file

**Figure 5.3 Relations between the PHOENICS Programs and Subroutines**



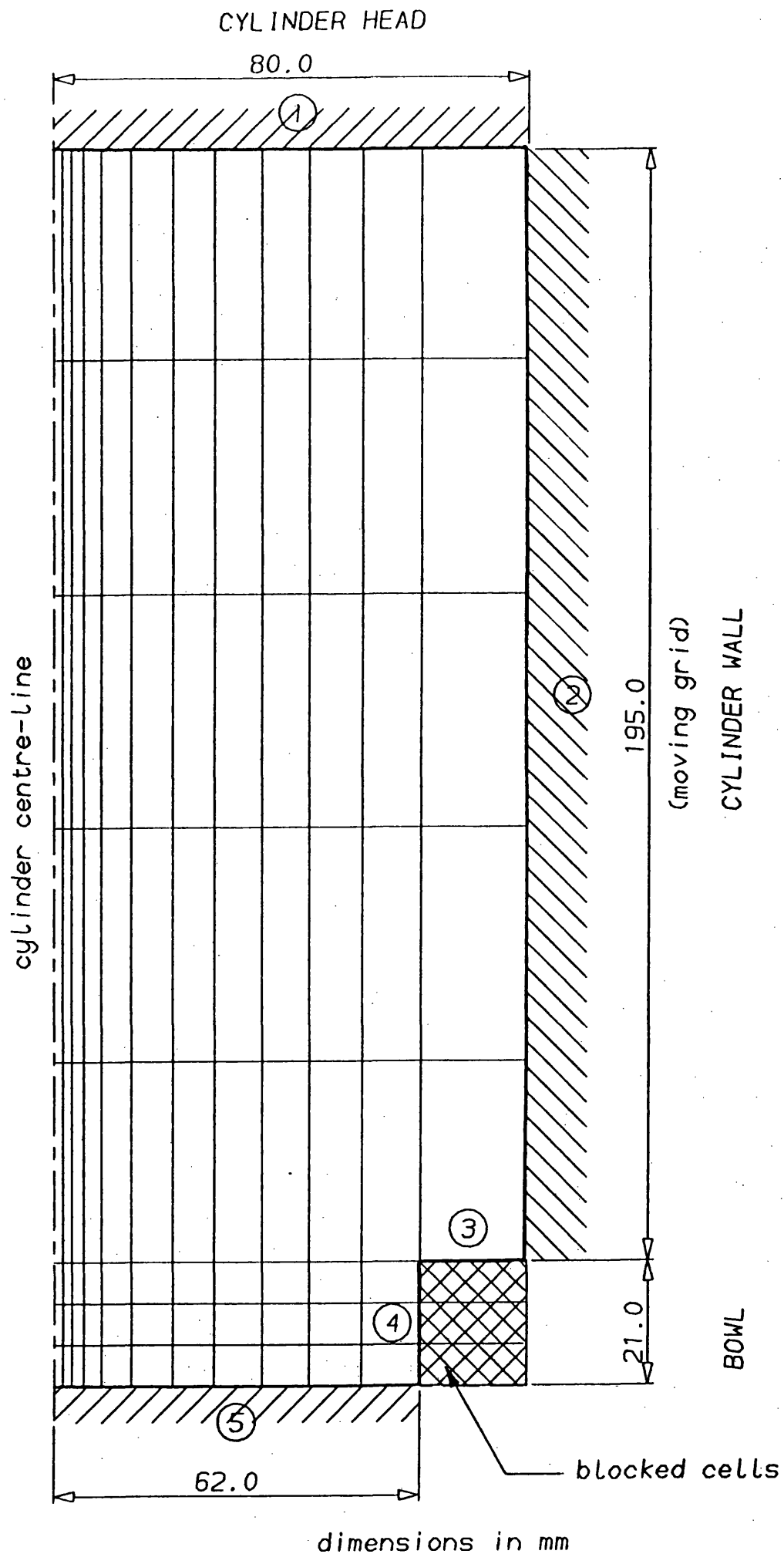


Figure 5.4 Finite Difference Grid for Piston In-cylinder Model

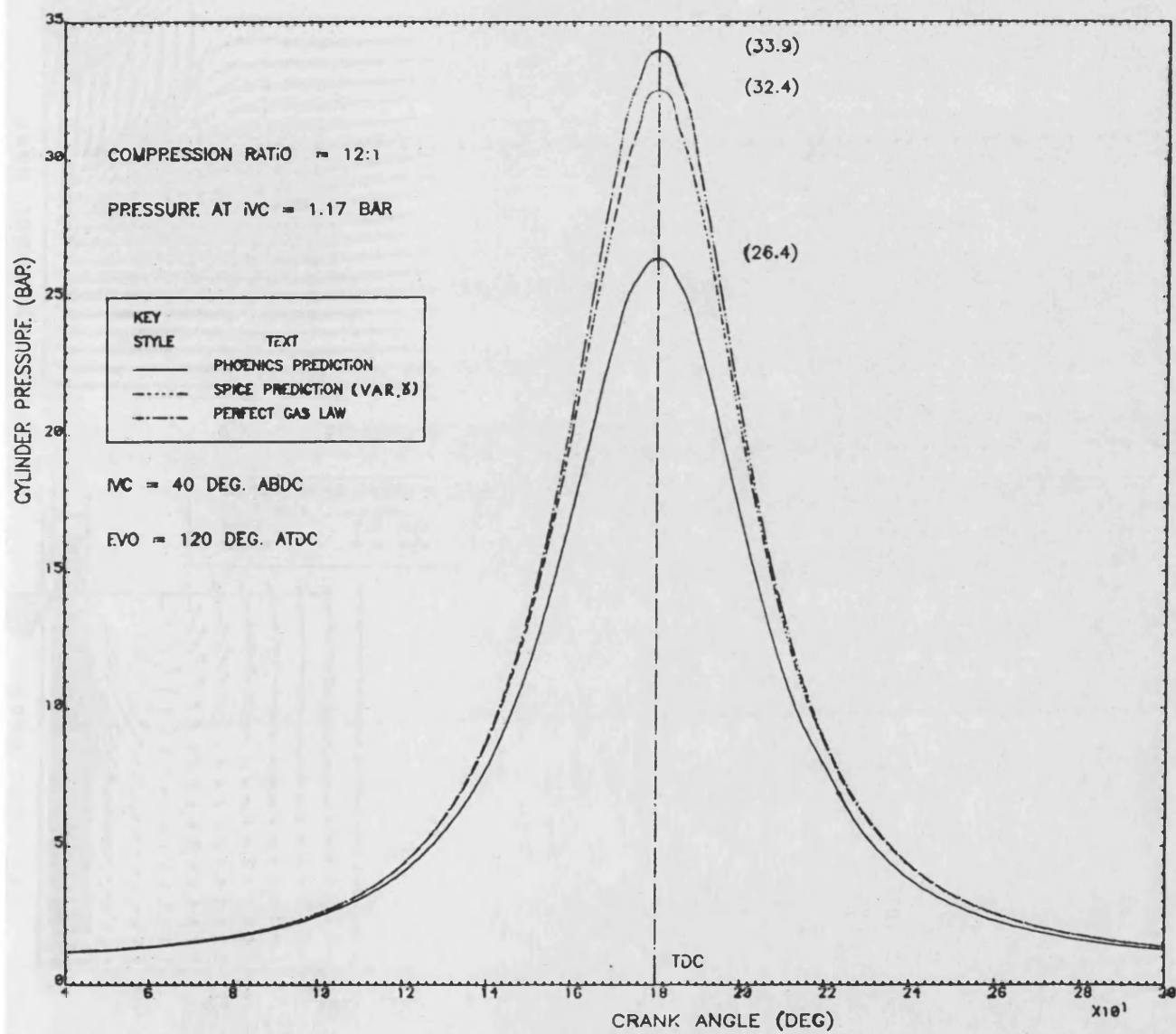


Figure 5.5 Comparison of Predicted Motored Cylinder Pressure

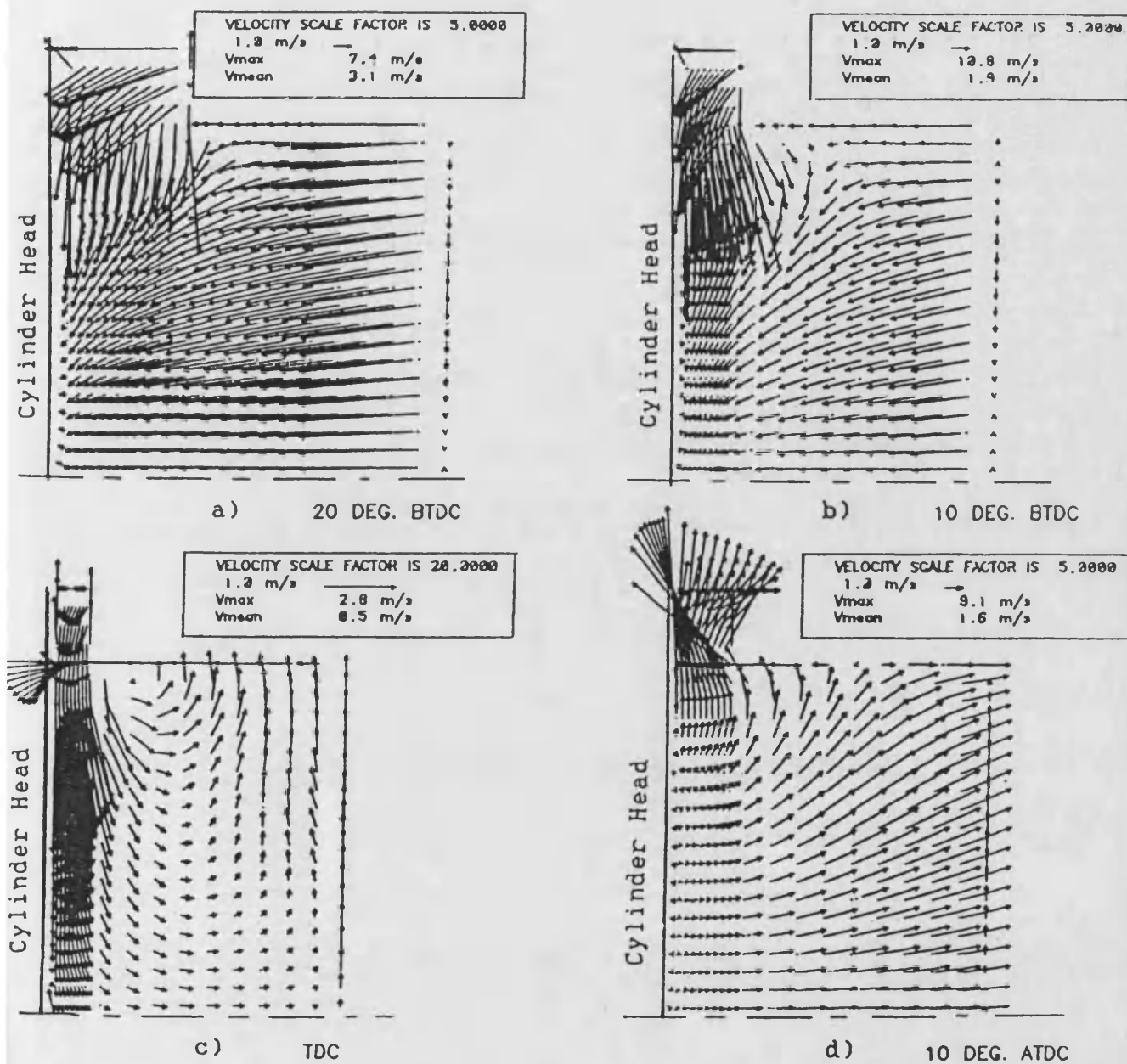
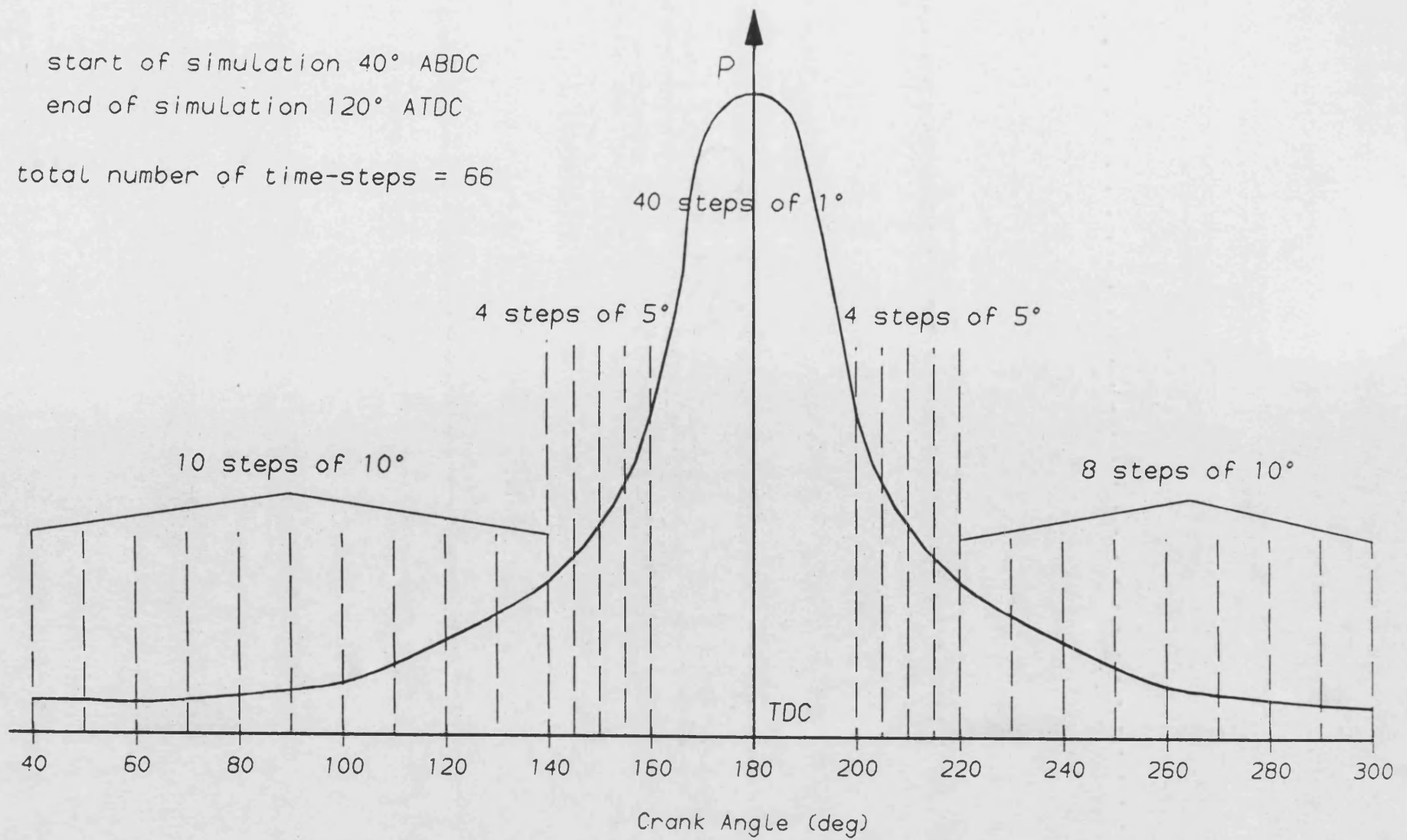


Figure 5.6 Velocity Fields around TDC showing Squish and Reverse-squish Patterns (Compression Ratio 12:1)

Figure 5.7 Indication of Size and Distribution of Time Steps



# CHAPTER 6

## **6. Computational Study of Pre-chamber Mixture Formation**

As was stated in the introduction to chapter 5 the reason for using PHOENICS was to investigate the mixing and distribution in the small pre-chamber. The study described at the end of the previous chapter was concerned with a piston in cylinder model and served primarily for familiarisation. This chapter describes two models: the first, an extension of the two-dimensional axi-symmetric piston in cylinder model, in which a pre-chamber was added to the top of the model; and the second, a separate 3D model of the pre-chamber. The latter model enables the geometric features such as the one-way gas valve and nozzle holes to be properly described.

### **6.1 In-cylinder Model with Pre-chamber**

Initially the pre-chamber was modelled very crudely; no attempt was made to represent the sloping walls in the finite difference grid. Also the pre-chamber nozzles were replaced by a simple straight through connecting hole. The overall volume of the pre-chamber (15cc) was correct. The grid used is shown in figure 6.1. For comparison purposes with the work described in chapter 5, the coarse grid from the early piston in cylinder model (figure 5.4) was used as a basis. Since at this point the applicability of the model was more important than the numerical accuracy of any results obtained, using the "coarse" grid had the added advantage of reducing the computation time. Also to avoid having to re-run the early piston/cylinder model the original values of the density constants were kept. (This density formulation would need to be changed later to allow for temperature effects and for a mixture of gases).

As expected the cylinder pressure values obtained are very similar to the earlier simple piston in cylinder model. A slight reduction in the highest value is predicted due to the small decrease in compression ratio because of the addition of the pre-chamber volume. What is perhaps more striking in figure 6.2 is the way the pre-chamber pressure fails to follow the cylinder pressure, as it did on

the compression stroke, but remains at around 7 bar. This was surmised to be due to the outflow discharge coefficient not being equal to the inflow coefficient because of the narrow restriction and sharp corners in this model.

To investigate this last point it was necessary to refine the pre-chamber geometry. The sloping sides were modelled by partially blocking those cells in this region and prescribing the appropriate cell faces as inaccessible to flow. The pressure curve drawn from the subsequent run confirmed the supposition (see figure 6.2). An interesting feature here is the way that the pre-chamber pressure curve crosses that of the cylinder before TDC. With the pressure in the pre-chamber just before TDC being greater than that in the cylinder an outflow would be expected. However, this ignores the momentum imparted to the air by the piston which allows the air to continue to enter the pre-chamber. This is confirmed by analysis of the monitor print-out: whilst the pressure difference between the chambers is negative, viewed from the cylinder, the velocity direction is into the pre-chamber. After TDC is reached the pressure in the main chamber begins to fall producing an outflow from the pre-chamber. Because of the nozzle restriction the pre-chamber pressure curve lags behind that of the cylinder pressure on the expansion stroke.

Examples of the developing velocity fields as the air is compressed and forced into the pre-chamber are shown in figures 6.3(a-e). The maximum velocity attained through the nozzle is approximately 160m/s. From these figures it is just possible to detect the re-circulation which is formed by the air entering the pre-chamber at high velocity. Once inside, the air is forced along the top wall, down the sides and then diverted around as it comes into contact with further in-rushing air.

Whilst the initial results were encouraging they already served to highlight some problems: a finer grid would be needed in the pre-chamber for better flow definition. This would necessarily imply a finer grid in the cylinder which would lead to very large computation

times. This did not seem justifiable in that the bulk of the grid and hence the majority of the solution is taken up with merely supplying boundary conditions to the pre-chamber. Furthermore at some stage it would be necessary to simulate the valve overlap and induction periods - the time in the cycle when the pilot gas enters the pre-chamber.

An attempt was made to include FORTRAN coding in the ground-station to describe the valve data and timing, but this proved to be difficult and computationally very expensive. With the valves modelled initially by "switches" - allowing flow over fixed areas at certain relevant periods of the cycle - the predicted cylinder pressure did not exhibit the expected behaviour. Rather than seeing the usual dip through overlap and induction, the pressure settled quickly to the boundary pressure set at the valve - effectively the manifold pressure. This response is undoubtedly due to the instant opening of the valves. To model the effective flow area would entail introducing a time varying boundary condition which might be chosen to mimic the observed pressure variation in the cylinder.

With the need for a 3D model to describe the geometry fully, the decision was taken to build a separate 3D model which would only include the pre-chamber geometry. The effect of the piston motion, overlap and induction, and the pilot gas flow through the one-way valve would be simulated by varying boundary conditions applied over the appropriate cells of the finite difference grid.

## **6.2 Separate 3D Pre-Chamber Model**

In the previous section some of the problems associated with the 2D piston in cylinder model with pre-chamber were highlighted. Whilst most of the problems could have been resolved, the separate pre-chamber model was felt to offer many advantages:-



- (i) Pre-chamber geometry can be described more accurately with a three dimensional model without undue computational expense.
- (ii) Geometric changes, e.g. varying pre-chamber volume, can be easily accommodated.
- (iii) The angled nozzle holes can be simulated. This would be extremely difficult in the pre-chamber/cylinder model.
- (iv) A finer grid is possible resulting in better flow definition.
- (v) Effect of compression ratio can be easily investigated.

The effect of the piston motion was modelled by applying time dependent boundary conditions over the nozzle holes in the pre-chamber. These boundary conditions were obtained, with the exception of the cylinder pressure values, from the earlier simulation work on the cylinder with pre-chamber model. Since it was necessary to run the simulation through the overlap period of the cycle the pressure values could only be obtained from concurrent simulation work carried out using SPICE (66). The boundary conditions relevant to the flow of pilot gas through the disc valve were assumed not to vary during the cycle.

### 6.2.1 Pre-chamber Geometry

In figure 6.4 schematic views of the pre-chamber assembly are shown. The carburetted mixture in the cylinder enters the pre-chamber through four equi-spaced holes which are angled at  $60^\circ$  to the vertical. The disc valve and spark plug both lie in the same plane and are offset from the central axis. In defining the three dimensional grid to represent the pre-chamber, the grid spacing was chosen to allow the key elements to be readily incorporated (figure 6.5). Thus whilst it was not feasible to model the holes as circular, by careful setting of the relevant grid fractions it was possible to ensure that the hole areas over which the flow enters were the same. One further consideration here was that the grid divisions were also positioned so as to allow half-blocking of the cells in the sloping wall region. No attempt was made at this stage to allow for the protrusion of the spark plug into the pre-chamber.

## 6.2.2 Setting of the Pre-Chamber Boundary Conditions

### (i) Nozzle

To simulate the effect of the piston, time dependent boundary conditions were applied over the appropriate cells at the end of the nozzle. The values of the dependent variables - pressure ( $p$ ), turbulence kinetic energy ( $K$ ), turbulence dissipation rate ( $\epsilon$ ), enthalpy ( $H$ ) and gas concentration ( $c$ ) - were taken from selected cells in the cylinder with pre-chamber model; the cells being located close to the cylinder head just below the pre-chamber nozzle.

In the program the values of the dependent variables are held in data sets in a specially written interpolation subroutine - INTPOL, which is accessed from the ground station. At each time-step (crank angle) during the solution a value of each of the independent variables is calculated using a linear interpolation routine. These boundary conditions are then communicated to the main EARTH module via a call to a PHOENICS service subroutine called ADD.

Although the pressure values, as stated earlier, were obtained from SPICE simulation work - based on the gas engine valve timing and compression ratio - they were included as boundary sources in an identical manner. Through the overlap period, where no values of  $K$ ,  $\epsilon$ , and  $H$  were available, values were assumed based on the limited trends available. Whilst the values of enthalpy ( $H$ ) could be set with some certainty - knowing that temperature fluctuations during this period were not large - setting of the correct turbulence kinetic energy and dissipation rate was felt to be important in that they could possibly control the mixing process. A subsequent study - refer to section 6.2.3 (v) - indicated that the turbulence assumptions had no observable influence on the mixing within the pre-chamber, which is dominated by pressure effects.

Initially, for simplicity, the flow between the cylinder and the pre-chamber was assumed to pass through a single centrally located hole. The evaluation of the rate of inflow or outflow is determined by the

pressure gradient at the nozzle i.e. the difference between the boundary pressure set and the value in a near-boundary cell. This is expressed within the program as follows:

$$\text{source of mass, } m = C_m(V_m - p)$$

Thus the value  $V_m$  has the physical significance of an external pressure; and the coefficient  $C_m$  that of the reciprocal of a flow resistance between the internal grid node, where the pressure is  $p$ , and the external pressure  $V_m$ . Whilst the setting of  $V_m$  is obvious: it is the boundary value of the pressure read in from the INTPOL subroutine, the setting of  $C_m$  is less straightforward. It is generally not possible to calculate the correct value and setting the wrong value can lead to convergence problems or the mass flows being evaluated incorrectly. For this work the PHOENICS literature (69) served as a guide: the value of  $C_m$  being set approximately as:

$$C_m = 1000 \times (\text{expected mass flow rate} / \text{external pressure})$$

The expected mass flow rate is based on simple analysis of the local density and flow velocity determined from the pressure difference, modified to incorporate a discharge coefficient, estimated equal to 0.65 (70).

It is important to recognise that it is not sufficient just to set the mass flow value. It is also necessary to set values for all the dependent variables because mass flowing into a cell convects with it these "exterior" values. Hence, source terms must be added for all the variables not just those for continuity. Thus once the boundary (cylinder) pressure rises above the pre-chamber pressure inflow occurs, and at this point the uniform mixture of gas and air from the cylinder (AFR = 27:1) is assumed to enter.

With the final nozzle cell being located at the last z-slab there is no corresponding velocity value associated with the cell, due to the velocity components being stored on a staggered grid (see section

5.1.1). Thus, in this case, the velocity in the z-direction (w component) must also be set in the penultimate z-slab.

Attempts to achieve this were unsuccessful. The PHOENICS manual provided insufficient information on this point and all runs attempted ran into convergence problems which caused the problem to fail: after repeated investigations this approach was abandoned. In any case the straight through nozzle did not represent the pattern of nozzle holes required.

The alternative method proved to be quite straightforward and furthermore modelled the true geometry with greater accuracy. Instead of introducing the piston boundary conditions at the bottom of the nozzle (final z-slab - NZ) the sources were added over the faces of four cells in the penultimate z-slab (NZ-1). These cells were equi-spaced in the x-y plane with the grid being divided such that the flow face area of each cell corresponded to the true hole area (see figure 6.5). By adding the sources at NZ-1 the additional call to the ADD subroutine had been avoided. The angle of the nozzle holes was defined by resolving the velocity into two components (v and w) which were then added as sources.

#### (ii) Disc Valve

The inflow through the disc valve of the supply mixture was modelled in very much the same way as above: dependent variables were added as sources over a number of cells having a total area equal to the flow area of the disc valve. With all the values being regarded as constant the FORTRAN coding in the ground-station proved to be far more straightforward than for the nozzle. The disc valve acts as a one way valve and this was simulated by comparing the local pressure in a cell directly under the inflow region with the externally set pilot pressure. Once the pre-chamber pressure exceeded the pilot pressure, the part of the subroutine in which the pilot supply sources were added would no longer be accessed.

### 6.2.3 Assumptions Made in the Model

In simulating the mixing process in the pre-chamber several assumptions had to be made, either because of the need for simplicity or because exact values of boundary conditions were not available.

#### (i) Density formulation

The mixture in the pre-chamber was regarded as being made up of three constituents: air, natural gas and residuals, which were assumed to behave as perfect gases. From the Gibbs-Dalton law of partial pressures the local density in each cell was calculated using the equation given below:

$$\rho = \frac{p}{R_0 T} \left\{ \frac{1 - c_1 - c_2}{M_{AIR}} + \frac{c_1}{M_{GAS}} + \frac{c_2}{M_{RES}} \right\}^{-1}$$

where:  $\rho$  = density,  $p$  = pressure,  $T$  = temperature,

$R_0$  = Universal Gas constant,

$M_{AIR}$  = mol. mass of air,  $M_{GAS}$  = mol. mass of natural gas,

$M_{RES}$  = combined mol. mass of residuals,

$c_1$  = fraction of natural gas in each cell, and

$c_2$  = fraction of residuals in each cell.

Within the framework of the PHOENICS program it is necessary to deduce the temperature  $T$  (in a cell) from the computed enthalpy  $H$ . Since  $H = C_p T$ , where  $C_p$  is the local specific heat capacity at constant pressure for the mixture, the temperature is estimated from an iterative procedure in which an initial guess at specific heat  $C_p^0$  gives rise to a temperature,  $T^0 = H/C_p^0$ . A new specific heat  $C_p'$  is introduced assuming a linear dependence of specific heat upon temperature for each of the constituents:

$$C_{PMIX} = c_1 C_{PGAS} + c_2 C_{PRES} + (1 - c_1 - c_2) C_{PAIR}$$

where  $C_{PMIX}$ ,  $C_{PGAS}$ ,  $C_{PRES}$  and  $C_{PAIR}$  are the specific heats at a particular temperature of the mixture, natural gas, residuals and air

respectively. Then the new temperature estimate is  $T' = H/C_p'$ , and the process is continued to convergence.

It will be noted that the density formulation used applies to incompressible flows only. This was felt to be sufficiently accurate. Analysis of the Mach number through the nozzle using the SPICE program had shown the maximum value to be approximately 0.35, with the value being less than 0.1 for the majority of the cycle. At this low value the error due to the absence of any compressibility factor is less than half of one percent (71).

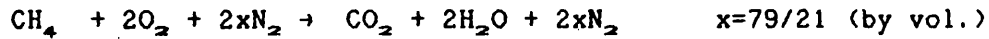
#### **(11) Pilot Mixture Entry into Pre-chamber**

The simulation starts at inlet valve opening (IVO). From the motored pressure curve (figure 6.6) it was postulated that with combustion the cylinder pressure before IVO would always be greater than the pilot supply pressure. Since the pre-chamber pressure trace follows closely that of the cylinder, the assumption was made that a gas/air mixture would only enter the pre-chamber through the disc valve during the overlap and induction periods. Dependent on the relative values of supply pressure to cylinder pressure, gas continues to enter until a point is reached on the compression stroke where the rise in pre-chamber pressure closes the disc valve.

The above assumption was to a certain extent confirmed by SPICE simulation work. Whilst it was not possible to simulate a fired lean burn natural gas engine, particularly with a small pre-chamber, it could be approximated by firing the gas engine as a diesel i.e. the compression ratio and timing were for the gas engine, but fired (without a pre-chamber) using diesel fuel: the fuelling per cycle being chosen to give the same power output as for the gas engine (approx. 50kW per cylinder). The results are shown in figure 6.7. The maximum gas supply pressure is the value at the disc valve and is based on the maximum likely available gas pressure on site - without resorting to an engine driven booster.

### (iii) Initial Conditions at IVO in the Pre-chamber

On the previous cycle complete stoichiometric combustion is assumed to have taken place in the pre-chamber, such that the only products are carbon dioxide ( $\text{CO}_2$ ), nitrogen ( $\text{N}_2$ ) and water vapour ( $\text{H}_2\text{O}$ ): dissociation products such as CO and  $\text{NO}_x$  being ignored. Thus in evaluating the molecular mass and specific heat of the residuals, as in the density formulation above, the values are calculated based on the weighted average of the molecular masses obtained from the chemical reaction:



Note: the composition of natural gas (29,33) is for simplicity represented as methane ( $\text{CH}_4$ ).

With complete combustion taking place in the pre-chamber the peak gas temperature will be around 2000K. During the power stroke the gas expands lowering its temperature. Heat is also lost to the water surrounding the pre-chamber. At IVO the temperature of the residuals was therefore estimated to be approximately 800K.

### (iv) Simulation of Different Engine Load Conditions

The effect of different loads was investigated at values corresponding approximately to full, three-quarter and half load. From early development work on the six-cylinder engine at Dorman Diesels these loads could be translated into corresponding manifold pressures, which were then set as initial conditions in the SPICE simulation program. The motored cylinder pressure curves obtained are shown in figure 6.8. As has been stated earlier these then formed the basis of the cylinder pressure boundary conditions at the nozzle end of the pre-chamber.

Clearly it would have been possible to include a separate set of data points for each load case, though this would have been somewhat

tedious and cumbersome. Instead only the lower curve (manifold pressure = 1.17 bar - half load) was held in the INTPOL subroutine (see section 6.2.2); the other loads being simulated by applying a suitable scaling factor to the base curve. For the purposes of any parametric study this was felt to be sufficiently accurate (see figure 6.8), whilst at the same time affording benefits in ease of computer coding and the setting of different load cases. Additionally, the setting of the boundary conditions of the other independent variables ( $H$ ,  $K$ ,  $\epsilon$  and  $c$ ) were left unchanged with load.

Since the simulation was only run over the unfired part of the cycle the enthalpy values,  $H$ , set as external boundary conditions are dependent only on the compression ratio: the values rising and falling with compression and expansion. Obviously the concentration of the lean gas/air mixture that is forced into the pre-chamber from the cylinder is independent of load: the amount of the two constituents varies - determined from the pressure difference (section 6.2.2)- but the relative proportion remains the same.

#### (v) Boundary Values of Turbulence Parameters

During the early part of the work concern was felt as to what extent the setting of the turbulence parameters were influencing the mixing process within the pre-chamber. A brief study was therefore undertaken, in which different values were prescribed at the beginning of each time-step. In figure 6.9 two cases are presented. In the first example (i), the respective boundary values of  $K$  and  $\epsilon$  were set constant ( $K=60\text{kgm}^2/\text{s}^2$ ;  $\epsilon=3000\text{s}^{-1}$ ) at the start of each time step. For the second example (ii) the turbulence parameters were interpolated ( $K=60\text{--}1700\text{kgm}^2/\text{s}^2$ ;  $\epsilon=3\times 10^3\text{--}18\times 10^6\text{s}^{-1}$ ) at each time step using values taken from the nozzle region of the earlier piston with pre-chamber model (figure 6.1).

Figure 6.9(a) shows the contours of turbulence kinetic energy ( $\text{kgm}^2/\text{s}^2$ ) at 12 deg BTDC for the two cases. The fields are identical, with the maximum values occurring in the region of



entrainment around the incoming jet, i.e. the area of maximum shear. The values set in the nozzle do not determine the values in the pre-chamber which are dominated by pressure effects. (It is for this reason that the setting of the turbulence boundary conditions could be left unchanged with load - as stated above (iv)). Consequently, the set values of  $K$  and  $\epsilon$  may be regarded as rough estimates at the start of each time step. Not surprisingly, with the turbulence fields being identical, the corresponding mixture distributions, as illustrated by the air-fuel ratio contours in figure 6.9(b), are also identical.

#### (vi) Heat Transfer

For simplicity the mixing process in the pre-chamber was assumed to take place under adiabatic conditions. Whilst this is clearly not the case in the engine, it was felt that this simplification did not invalidate the model, in that the simulation does not involve combustion. Clearly if this were the case it would have been necessary to include heat transfer. Further it could be argued, that with temperatures generally being relatively low, little could be gained from the extra complication of adding heat transfer because, without accurate data, doubts would then arise over the setting of the heat transfer coefficients.

### 6.3 Parametric Study

The simulation work undertaken was in the form of a parametric study in which the main variables considered were:

- (i) engine load (inlet manifold pressure)
- (ii) pilot mixture ratio to pre-chamber; and
- (iii) pilot pressure.

The effect of changing the pre-chamber volume (10cc, 15cc or 20cc) was also briefly investigated.

### 6.3.1 Input and Output Files

To allow the parameters to be easily changed a simple data file was written - PREDAT - from which the various variables are subsequently read in by the main PHOENICS program (refer to figure 5.3). This was complemented by a purpose written output file - CARES - in which the important global parameters are recorded at each time-step during the simulation. Useful visual insight into the mixing process was provided by a plotting file - PLOTf. This stored the local values of velocity components (r-z plane) and air-fuel ratios in each cell. From this, velocity fields and concentration fields in the pre-chamber could be displayed at nominated time-steps; usually chosen to coincide with particular points of interest in the cycle.

#### Input file - PREDAT

The input file is a simple seven line file which allows easy setting of initial conditions, size and distribution of time-steps and the points at which plotting fields are required. It also allows limited control of the solution procedure. An example file is shown in table 6.1. The explanation of each line is:

line 1 initial pressure, initial enthalpy - at start of simulation.

line 2 no. of sweeps at each time-step, no. of time-steps, starting point of simulation (deg), end point (deg).

The first two values were primarily used for debugging work and for determining the optimum setting of the sweep number.

A high sweep number results in improved accuracy, but incurs extra computational expense following the law of diminishing returns.

line 3 number of different time settings (max.=10).

line 4 number and size of each of the step lengths.

i.e. 28 steps of one degree, followed by one step of six degrees, etc.

line 5 height of pre-chamber body, overall height of pre-chamber.

These two values allow the pre-chamber volume to be changed without having to re-define the finite difference grid.

line 6 gas supply pressure, gas temperature, concentration of mixture (c). A value of 1.0 implies pure gas; 0.2 an AFR equal to 4:1.

line 7 time-steps at which plotting field output is required.

#### Output file - CARES

The output file stores values of those parameters which were considered important in assessing the mixing in the pre-chamber (see table 6.2). The header contains a summary of the input data, as explained above. An explanation of each column is given below:

- |           |   |
|-----------|---|
| 1 (P)     | The first column shows the time-steps at which plotting fields are available (P=1). These can be readily changed in the input file.   |
| 2 (STP)   | The time-step number  |
| 3 (CA)    | Indicates progress of the simulation, in crank angle degrees, through the cycle.  |
| 4 (PEXT)  | This is the value of the pressure boundary condition, at the start of each time-step, set at the nozzle holes. The values set correspond to overlap, induction and compression. |
| 5 (PPRE)  | The pre-chamber pressure close to the disc valve.   |
| 6 (TEMP)  | Mean temperature in the pre-chamber (K) calculated from the individual values of enthalpy and specific heat in each cell.   |
| 7 (MFT)   | This is the total mass of fuel that has entered through the disc valve. Once the disc valve closes this figure remains constant.  |
| 8 (MFPRE) | Overall mass of fuel in the pre-chamber at any given time, evaluated by summing up the local value in each  |

"unblocked" cell of the finite difference grid. Before mixture from the cylinder enters the pre-chamber the difference between this figure and the one above (MFT-MPRE) is the amount of fuel that has been lost to the cylinder.

- 9 (MRPRE) An indication of the extent to which the pilot mixture purges residuals out of the pre-chamber overlap and induction. At the start of the simulation the pre-chamber is assumed to be fully occupied with residuals.
- 10 (AFR) The global air-fuel ratio, calculated from the concentrations of natural gas and air in each cell.
- 11 (R%) Percentage of residuals to total mass of mixture in the pre-chamber at each time-step.

As a means of testing the output to ensure that the cell-by-cell values were being computed correctly - particularly the amount of gas and the air-fuel ratio - the model was run without gas entering through the disc valve. Instead a known mass of gas was introduced in the pre-chamber by the setting of a non-uniform initial field in the FLDDAT part of the satellite (see section 5.1.3).

Complete listings of the pre-chamber satellite and ground-station are given in appendices 7 and 8.

### 6.3.2 The Pre-chamber Mixing Process

Before going on to discuss those factors which influence the formation of a near stoichiometric mixture in the pre-chamber and the way that they do so, it is proposed to illustrate the sequence of events which occur within the pre-chamber. Basically the mixing is determined by two distinct periods: the initial gas entry through the disc valve, followed by the diluting charge entering from the cylinder. This is best explained by referring to the series of figures 6.10 (a-e).

At inlet valve opening (IVO) or just after, depending on the relative values of pre-chamber pressure to pilot supply pressure, the disc valve opens allowing gas to enter. At 20 deg AIVO (figure 6.10(a)) the residuals from the previous cycle are mixing with, and being displaced by the incoming gas feed. This process continues through the induction period (figures 6.10(b-c)) causing the residuals to be drawn out of the pre-chamber, along with a proportion of the gas. Eventually the increase in pre-chamber pressure due to the in-rushing pilot mixture and the rise of the piston in the cylinder closes off the disc valve (figure 6.11). This is generally around inlet valve closing (IVC) at which point the pre-chamber is predominantly filled with gas or the gas/air mixture introduced through the valve: residuals have been nearly completely purged out (see figure 6.12). The percentage of residuals in the pre-chamber continues to fall after this point, not because of further purging, but due to the increase in combined total mass of the other constituents. Note also the extent by which the temperature in the pre-chamber falls before rising again on the compression stroke (figure 6.13). The initial fall is due to two effects: the entry of the cold gas (300K) and the fact that most of the residuals (hot) have been purged out. A second dip occurs as cooler charge from the cylinder enters the pre-chamber.

At 96 deg BTDC (figure 6.10(d)) a flow of lean mixture is entering from the cylinder through the nozzles. At this stage the pre-chamber represents less than one percent of the volume above the piston. Thus despite the piston being close to its maximum velocity the gas velocity into the pre-chamber is less than 100m/s. At 12 deg BTDC (figure 6.10(e)) the incoming jet of lean mixture has strengthened having a well developed profile, which indicates entrainment of the surrounding gas. Around the jet is a recirculation zone which helps to mix the pure gas and lean mixture.

### 6.3.3 Presentation and Discussion of Simulation Results

In the sections that follow, the influence of the various parameters on the mixing process in the pre-chamber are discussed. For all the

results presented here, the pre-chamber volume was kept constant at 15 cc; the engine compression ratio being 10:1. (A constant inlet manifold mixture ratio of 27:1 was also assumed throughout, as this is the target lean mixture ratio for the engine). The results were obtained over a long period: each simulation taking some 5000 central processor seconds to run on the SWURCC (South Western Universities Regional Computer Centre) ICL 3980. This invariably meant that it was only possible to submit a single job at a time. In view of this the study was broken down into three logical sections.

#### (1) Variation of engine load (inlet manifold pressure)

Three load (boost) levels were considered:

full load - 2.00 bar inlet manifold pressure,  
3/4 load - 1.64 bar, and  
half load - 1.17 bar.

For each set the supply pressure to the pre-chamber was held constant at 1.75 bar. Figure 6.14 shows the predicted variation of overall (spatially averaged) air-fuel ratio from IVO to TDC for the three boost cases for a pure gas supply. Not surprisingly the overall air-fuel ratio at TDC varies more or less proportionally with boost pressure. At higher loads the pressure in the pre-chamber through induction is higher and hence the disc valve is open for a shorter duration. Thus the amount of gas admitted through the valve is less - see figure 6.15. This is to a certain extent counteracted by more gas entering from the cylinder under higher loads, but this brings with it a proportionate increase in mass of air; the mixture entering at a constant air-fuel ratio (AFR = 27:1). Since ignition should occur at 10-15 deg BTDC the levels of overall air-fuel ratio achieved, that is 7-14:1, appear to be rather rich for effective ignition and combustion; the stoichiometric ratio for natural gas being approximately 17:1.

### (11) Varying the supply pressure to the pre-chamber at constant load

With the amount of gas entering the pre-chamber being an important influence on the final air-fuel ratio at TDC a series of runs were performed whereby the engine load was held constant and the gas supply pressure varied. Results, for pure gas, at full load (2.0 bar) and 3/4 load (1.64 bar) are shown in figure 6.16. The air-fuel ratio (AFR) plotted is the spatially averaged value at TDC.

As would be expected, as the pilot pressure is increased more gas enters through the disc valve and so at constant load the final AFR is lower. In the limit the AFR would tend to zero - pure gas only: backing off the pressure results in an asymptote being reached. This figure, different for each load, is determined by the lowest pressure in the cylinder (pre-chamber) during induction. If the gas pressure is lower than this the disc valve never opens and so the air-fuel ratio at TDC would correspond to the figure carburetted into the cylinder - i.e. AFR = 27:1. It should be noted that the required overall air-fuel ratio may be achieved by adopting quite low pilot pressures (1.5-1.7 bar) but the curve is exceedingly steep in this region, making control rather difficult

### (111) Feeding a homogeneous gas-air mixture through the disc valve

From a theoretical analysis of the mixing process, on the compression stroke, between the pre-chamber and the cylinder - see appendix 9 - a formula was derived to predict the final air-fuel ratio, based on simple assumptions of the initial conditions, the engine geometry and the properties of the constituents:

$$f_{P2} = \frac{M_{GAS} + CR f_{MIX} M_{AIR} + (f_{MIX}/f_{P1}) M_{GAS} (CR-1)}{M_{AIR} (CR-1) + (f_{MIX}/f_{P1}) M_{AIR} + (1/f_{P1}) CR M_{GAS}}$$

where:  $M_{GAS}$  = mol. mass of Methane (16) = natural gas

$M_{AIR}$  = mol. mass of air (29)

CR = compression ratio (10:1)

$f_{MIX}$  = 1/AFR of mixture in the cylinder

$f_{P1} = 1/\text{AFR}$  of mixture in the pre-chamber at BDC

$f_{P2} = 1/\text{AFR}$  of mixture in the pre-chamber at TDC

If the following assumptions are made about the mixtures:

- (i)  $f_{\text{MIX}} = 1/27$  the value carburetted into the cylinder,
- (ii)  $f_{P1} = \infty$  pre-chamber is assumed full of pure gas; the residuals having been purged out,

then by substituting for the other values it can be shown that the predicted value of AFR at TDC is around 10:1 ( $f_{P2} = 0.1$ ). Ideally a stoichiometric value is sought. This suggests that air needs to be introduced into the pre-chamber. An idea of how much, can be calculated by re-arranging the formula given above. Thus:

$$f_{P1} = \frac{M_{\text{GAS}} \text{ CR } (f_{P2} - f_{\text{MIX}}) + f_{\text{MIX}} (M_{\text{GAS}} + f_{P2} M_{\text{AIR}})}{M_{\text{AIR}} \text{ CR } (f_{\text{MIX}} - f_{P2}) + (M_{\text{GAS}} + f_{P2} M_{\text{AIR}})}$$

Assuming  $f_{P2} = 1/17$  (stoichiometric), the above formula predicts that to achieve this, a gas/air mixture having an air-fuel ratio of 2.7:1 ( $f_{P1} = 0.36$ ) is needed. Whilst figure 6.16 suggests that a stoichiometric mixture is possible with a pure gas mixture - at full load, supply pressure = 1.6 bar, or at 3/4 load, supply pressure = 1.5 bar - it also clearly illustrates the critical dependence on the pilot pressure. It was therefore felt that by introducing air with the gas at low air-fuel ratios (AFR = 2-5:1) that this would lead to the formation of a near stoichiometric mixture which is less sensitive to changes in load and pilot pressure.

The study therefore involved feeding a homogeneous mixture of gas and air to the pre-chamber, firstly varying the mixture ratio at a fixed supply pressure and secondly, varying the pilot pressure with a fixed mixture ratio. The results for the first part of the study are shown in figure 6.17, in which the overall air-fuel ratio is plotted against crank angle over the range IVO to TDC. For comparison purposes the equivalent results for a pure gas feed are given. The effect of providing a 2.3:1 air-fuel ratio to the pre-chamber is to



raise the overall air-fuel ratio at TDC from 7.5:1 to 15.9:1 at 50% load and from 14.1:1 to 21.2:1 at 100% load.

Figure 6.18 compares the extent of the mixing, in the form of AFR contours for the two pilot feeds above at 50% load. It is of interest to match the contour patterns with the velocity fields shown earlier (figure 6.10(d-e)). At 96 deg BTDC the incoming lean jet has not properly penetrated the pre-chamber. For the pure gas feed (figure 6.18(a)) the greater part of the volume contains mixture at a ratio less than 4:1. At 12 deg BTDC the lean jet has penetrated the pre-chamber, but failed to mix adequately enough for reliable combustion. The mixture is overall rather rich and extremely inhomogeneous. At the spark plug location the mixture ratio is between 6 and 8:1, which is well below the flammability limits.

For the 2.3:1 pilot mixture (figure 6.18(b)) the contour levels are, as expected from figure 6.17, generally leaner. At 12 deg BTDC all the mixture in the pre-chamber lies between the flammability limits - AFR = 10-24:1. (The flammability limits of natural gas lie between equivalence ratios ( $\phi$ ) 0.6 and 1.4 (29,33)). Compared with the pure gas feed the variation in air-fuel ratio is narrower, and this time the mixture ratio in the region of the spark plug is very close to stoichiometric, being in the range 16-18:1.

Results for the latter part of the study - investigation of a range of supply pressures at a fixed load of 75% - are shown in figure 6.19. The main effect of the pilot air-fuel mixture is to raise the TDC overall air-fuel ratio by about 8 ratios for supply pressures above 1.7 bar. This has the advantage of flattening the curve in the critical region close to stoichiometric. Thus with a gas/air mixture fed to the pre-chamber the formation of a combustible mixture is less susceptible to the exact setting of the correct supply pressure.

Clearly from the above results the achievement of a near stoichiometric mixture at TDC is highly dependent on the three main parameters - inlet manifold pressure (load), pilot pressure and pilot

mixture. Whilst the manifold and pilot pressures are independent of one another, their relative values govern the opening and closing of the disc valve. This inter-relation may be conveniently expressed as a pressure ratio; defined as the pilot pressure divided by the manifold pressure. Thus, when the previous results for pure gas, at three load settings and various pilot pressures are plotted in this form, against the AFR at TDC, the points obtained collapse onto a single curve - figure 6.20.

The figure itself appears very similar to figures 6.16 and 6.19 highlighted earlier. However, instead of the positions of the vertical asymptotes depending on the inlet manifold pressure there is now just one asymptote at a pressure ratio of 0.73. This is the ratio of the lowest pre-chamber pressure through induction to the inlet manifold pressure.

By repeating this for the results already obtained with a supply mixture having an air-fuel ratio equal to 2.3:1, and by extending the study to cover other air-fuel ratios, the series of curves shown in figure 6.21 are obtained. As expected each curve emanates from the same point and then falls away to a value, which in the limit, is the air-fuel ratio of the mixture as it enters the pre-chamber. (At the limit the pressure in the pre-chamber would always be too high for any mixture to enter from the cylinder).

For combustion to take place in the pre-chamber the equivalence ratio  $\phi$  must lie between 0.6 and 1.4 - i.e. AFR = 10:1 to AFR = 24:1. Also for the engine to run at full load a supply pressure around 2.0 bar is required (at the disc valve) since a lower supply pressure would be insufficient to allow pilot mixture to enter the pre-chamber during the overlap and induction periods. A supply pressure of 2.0 bar translates to a pressure ratio of 1.0 at full load and, assuming the supply remains constant, a pressure ratio of 3.0 at 1/4 load. From these four points it then becomes possible to define an operating envelope, as shown in the figure. (It should be remembered that these air-fuel ratios take no account of spatial variations within the pre-chamber).

With a constant supply pressure of 2.0 bar and a gas/air mixture having an air-fuel ratio between 2.3 and 4.0 the figure suggests that it would be possible to operate within this envelope. However, in practice the flammability limits are probably too wide. For stable combustion in the pre-chamber the upper limit would be around 20:1, whilst for practical reasons the lower limit would be set at 15. Richer mixtures could lead to the disc valve sticking due to the build up of carbon. Thus, to ensure stable combustion over the entire load range, the aim would be to operate the pre-chamber in the shaded region shown in the figure.

Faced with trying to remain within this reduced envelope, two options seem to be available:

(i) at a fixed air-fuel ratio.

When the load (inlet manifold pressure) is reduced, the pressure ratio goes up - for a fixed supply pressure, and so the operating point moves along the curve to the right. To keep the operating point within the desired flammability limits the supply pressure must therefore also be reduced. This is equivalent to moving back along the curve. The better the control, the closer the mixture in the pre-chamber, at the ignition point, can be held to stoichiometric over the whole load range.

(ii) at a fixed supply pressure.

In this case as the load decreases the pre-chamber supply mixture needs to be diluted by additional air. This results in the operating point moving vertically upwards.

In practice the second option would be difficult to implement successfully; a pressure is being used to control a flow rate. The former option is a control technique already in regular use. A regulator is used to vary the one pressure (pilot) with reference to a second pressure (inlet manifold).

#### (iv) Effect of varying pre-chamber volume

At the start of the section on the parametric study mention was made of a limited investigation into the effects of pre-chamber volume on the mixing process. In the original feasibility study (67), conducted by Ricardo's for Dorman, it was suggested that an area for development work would be to try pre-chambers of differing volumes: 10 cc, 15 cc and 20 cc. Whilst with the PHOENICS model it would be easy to assess different volumes with regard to the mixing process, the pre-chamber model could not, of course, provide information on the energy and formation of the "torch" produced, once combustion has been initiated. Questions such as whether a larger volume pre-chamber would promote a higher energy ignition source would remain unanswered.

In section 6.3.3 reference was made to appendix 9, in which the derivation is given for a formula to predict the AFR at TDC, based on perfect gas theory and making certain assumptions about the mixtures in the pre-chamber and cylinder at BDC. What is interesting is that during the derivation the pre-chamber volume cancels out from the equation; thus implying that the pre-chamber volume is a non-governing factor.

The PHOENICS investigation consisted of running the model under constant conditions (manifold pressure = 1.64 bar, supply pressure = 2.5 bar, supply mixture AFR = 4.0:1) and merely altering the pre-chamber volume. The results are shown in figure 6.22. At TDC the final air-fuel ratios for each case almost exactly correspond; confirming the analytical supposition. In view of this no further investigative work under different loads or supply pressures was undertaken.

```

0.2450E+06 0.1004E+07
19 85 344.0 720.0
10
28.0 10.0 1.0 6.0 6.0 5.0 10.0 2.0 40.0 1.0
0.2460E-01 0.5600E-01
0.2450E+06 0.3000E+03 0.0200E+01 0.37E-01 0.1402E+01
8 20 28 50 73 000 000 000 000 000

```

Table 6.1 Input Data File - PREDAT

PRESAT DATA:		P1	H1	LSWEEP	LSTEP					
		0.245E+06	0.100E+07	19	85					
PREGRO DATA:		PSUP	TFUEL	GAS IN	CFTIN	PREVOL				
		0.250E+06	0.300E+03	0.200E+00	0.370E-01	0.157E-04				
P	STP	CA	PEXT	PPRE	TEMP	MFT	MFPRE	MRPRE	AFR	R%
0	1	354.00	2.12	2.44	758.7	0.3995E-06	0.4792E-06	0.1514E-04	4.0	86.3
0	2	364.00	1.89	2.41	696.9	0.8987E-06	0.1064E-05	0.1294E-04	4.0	70.9
0	3	374.00	1.66	2.38	636.4	0.1476E-05	0.1610E-05	0.1084E-04	4.0	57.4
0	4	384.00	1.48	2.36	594.8	0.2110E-05	0.2042E-05	0.9169E-05	4.0	47.3
0	5	394.00	1.40	2.35	569.4	0.2777E-05	0.2372E-05	0.7901E-05	4.0	40.0
0	6	404.00	1.32	2.34	552.7	0.3467E-05	0.2636E-05	0.6885E-05	4.0	34.3
0	7	414.00	1.24	2.33	540.3	0.4175E-05	0.2862E-05	0.6013E-05	4.0	29.6
1	8	424.00	1.20	2.32	530.7	0.4896E-05	0.3064E-05	0.5241E-05	4.0	25.5
0	9	434.00	1.21	2.32	523.3	0.5616E-05	0.3249E-05	0.4566E-05	4.0	21.9
0	10	444.00	1.22	2.32	517.3	0.6334E-05	0.3413E-05	0.3974E-05	4.0	18.9

Table 6.2 Sample of Output File - CARES

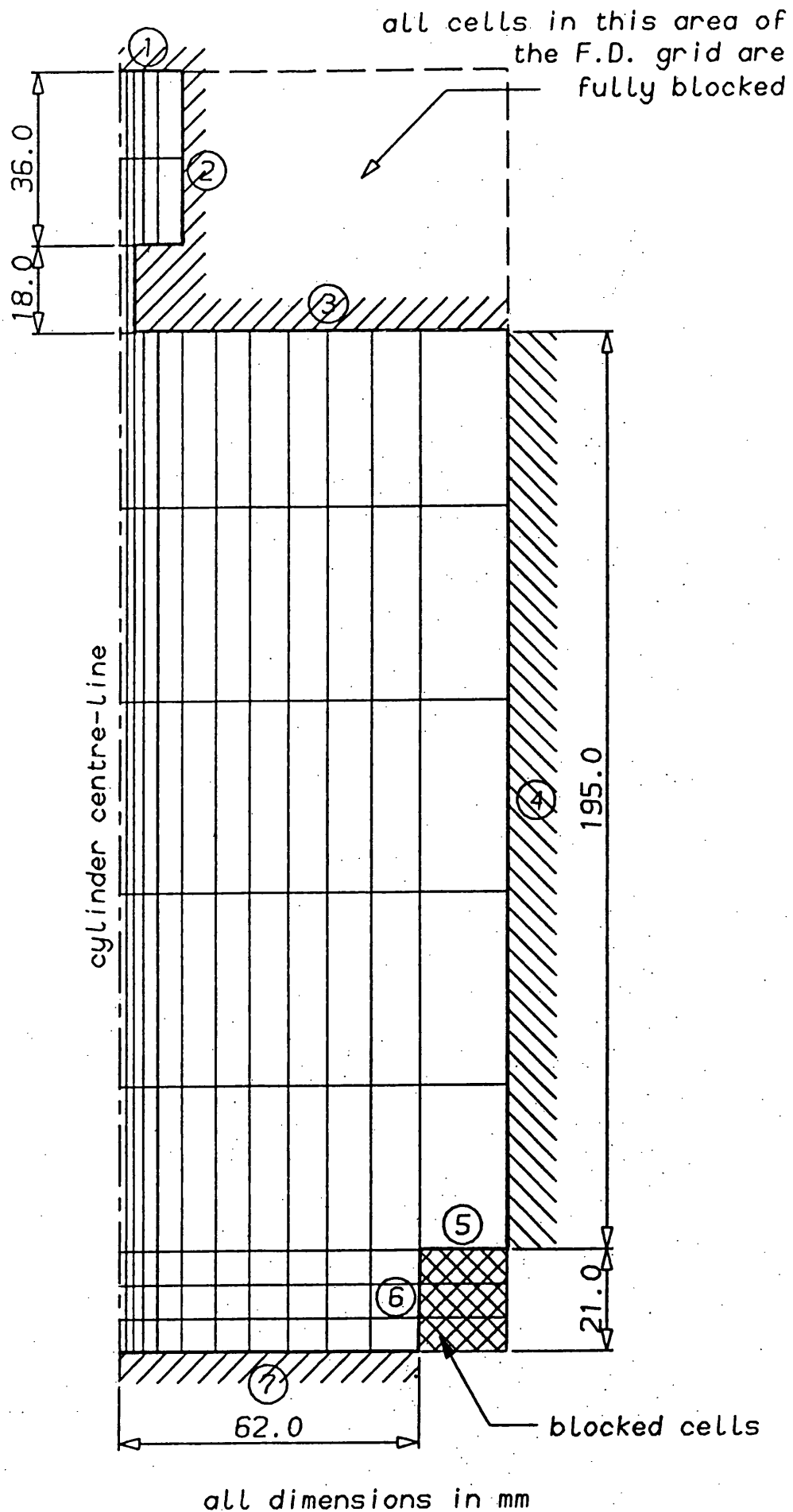


Figure 6.1 Finite Difference Grid for Piston In-cylinder Model with Pre-chamber (ref. figure 5.4)

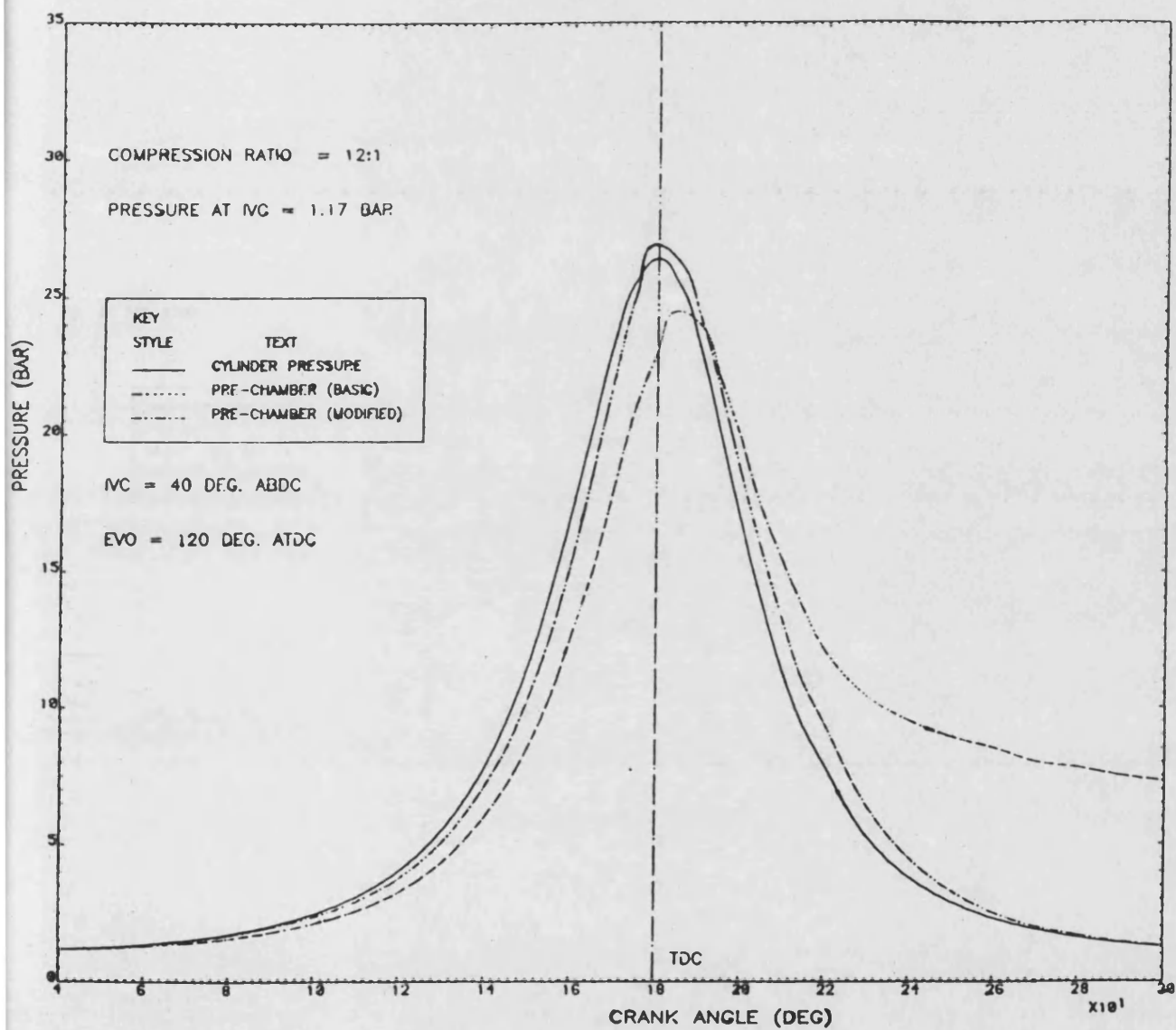


Figure 6.2 Motored Pressure Values in the Cylinder and Pre-chamber (basic and modified)

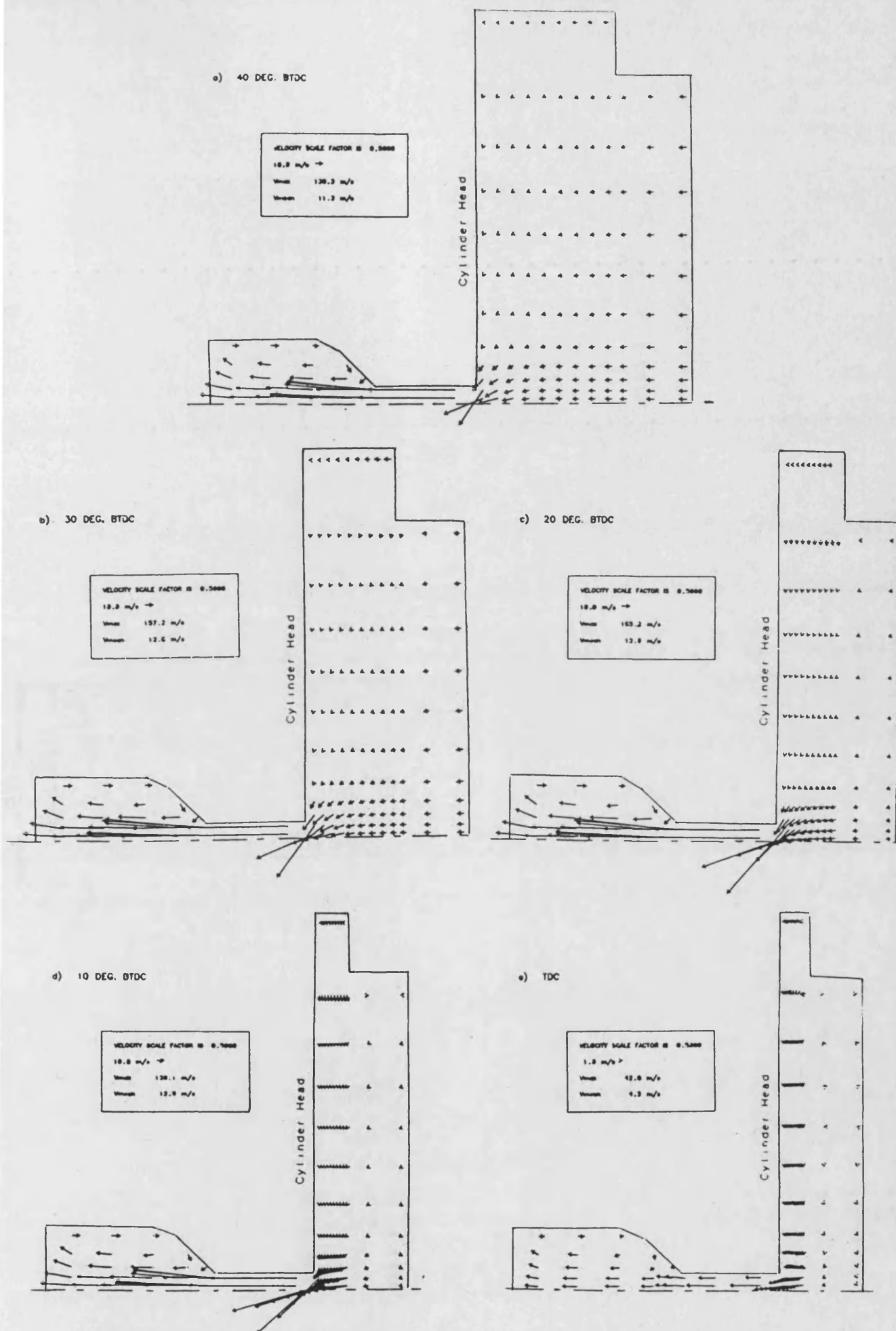
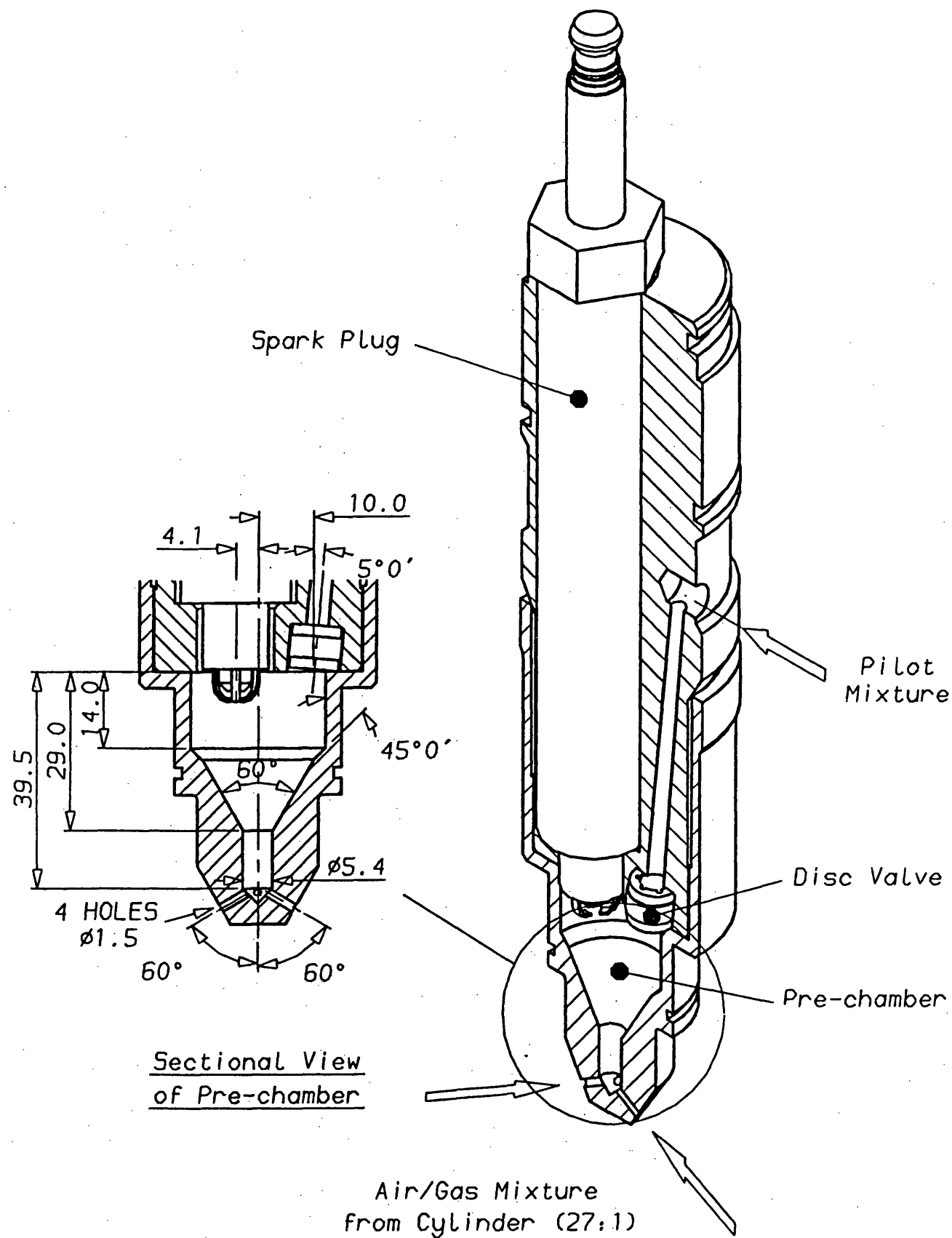


Figure 6.3 Velocity Vector Fields in the Cylinder and Pre-chamber at and before TDC





**Figure 6.4 Schematic and Cross-sectional Views of the Pre-chamber Assembly**

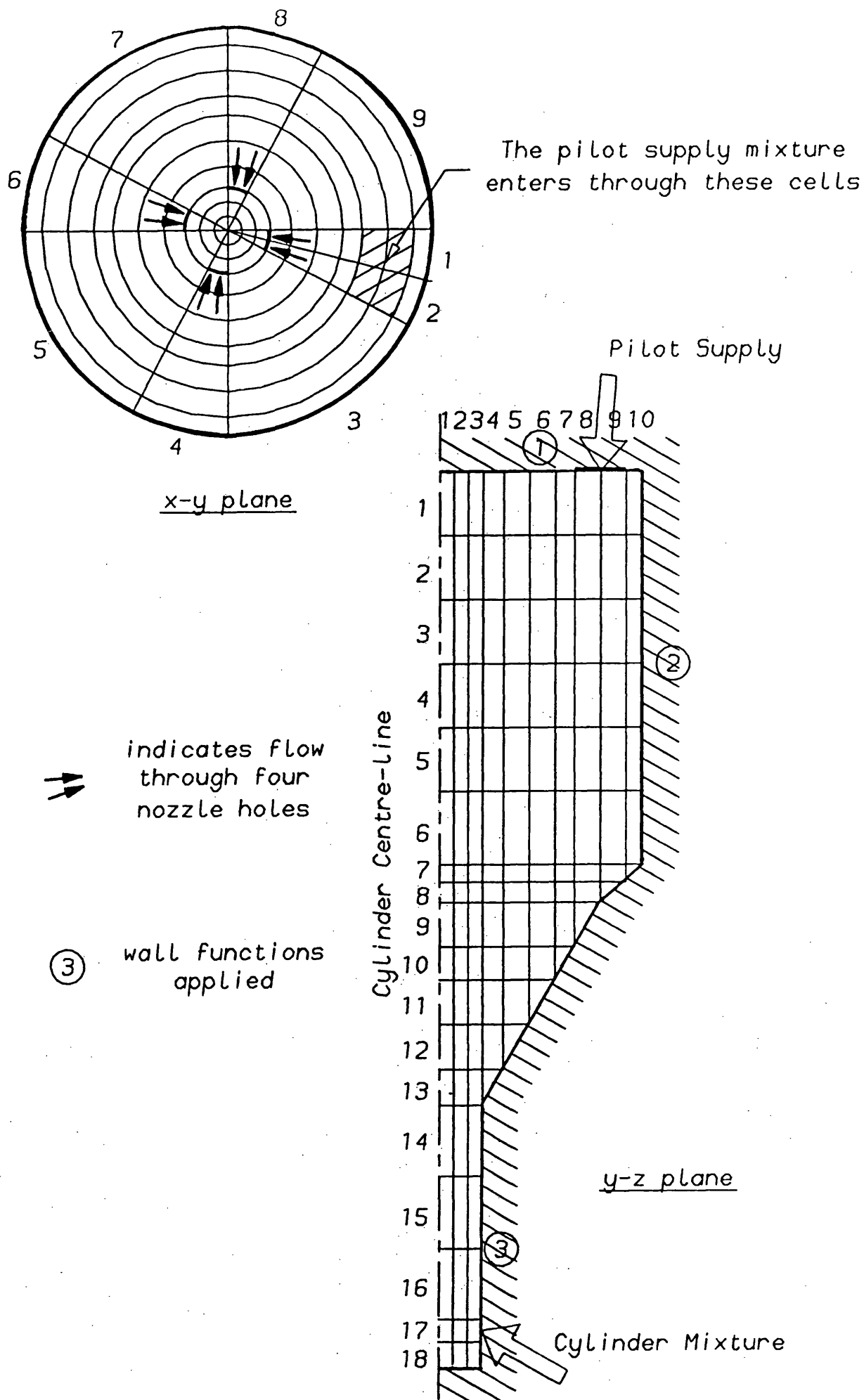


Figure 6.5 Three-dimensional Finite Difference Grid for Separate Pre-chamber Model

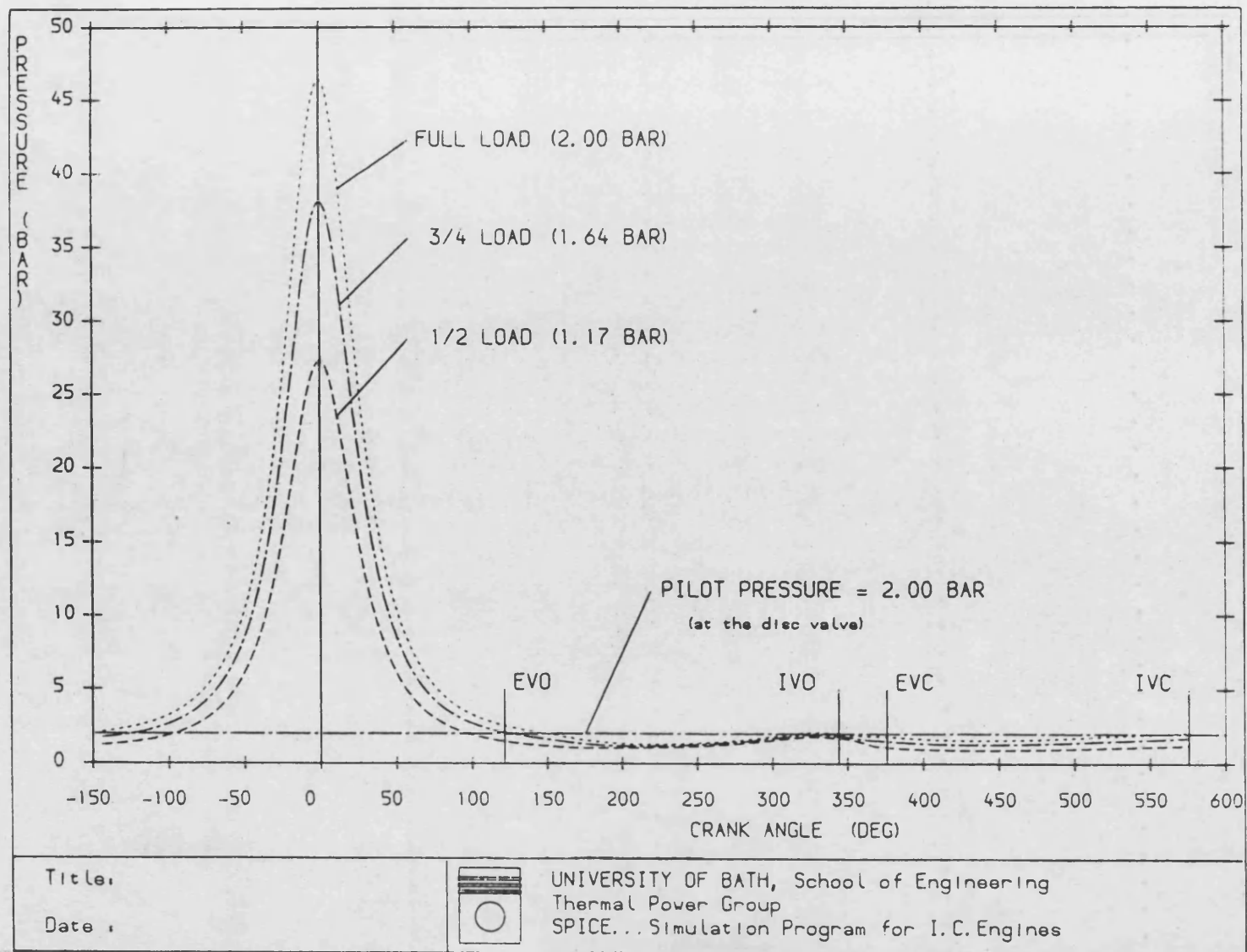
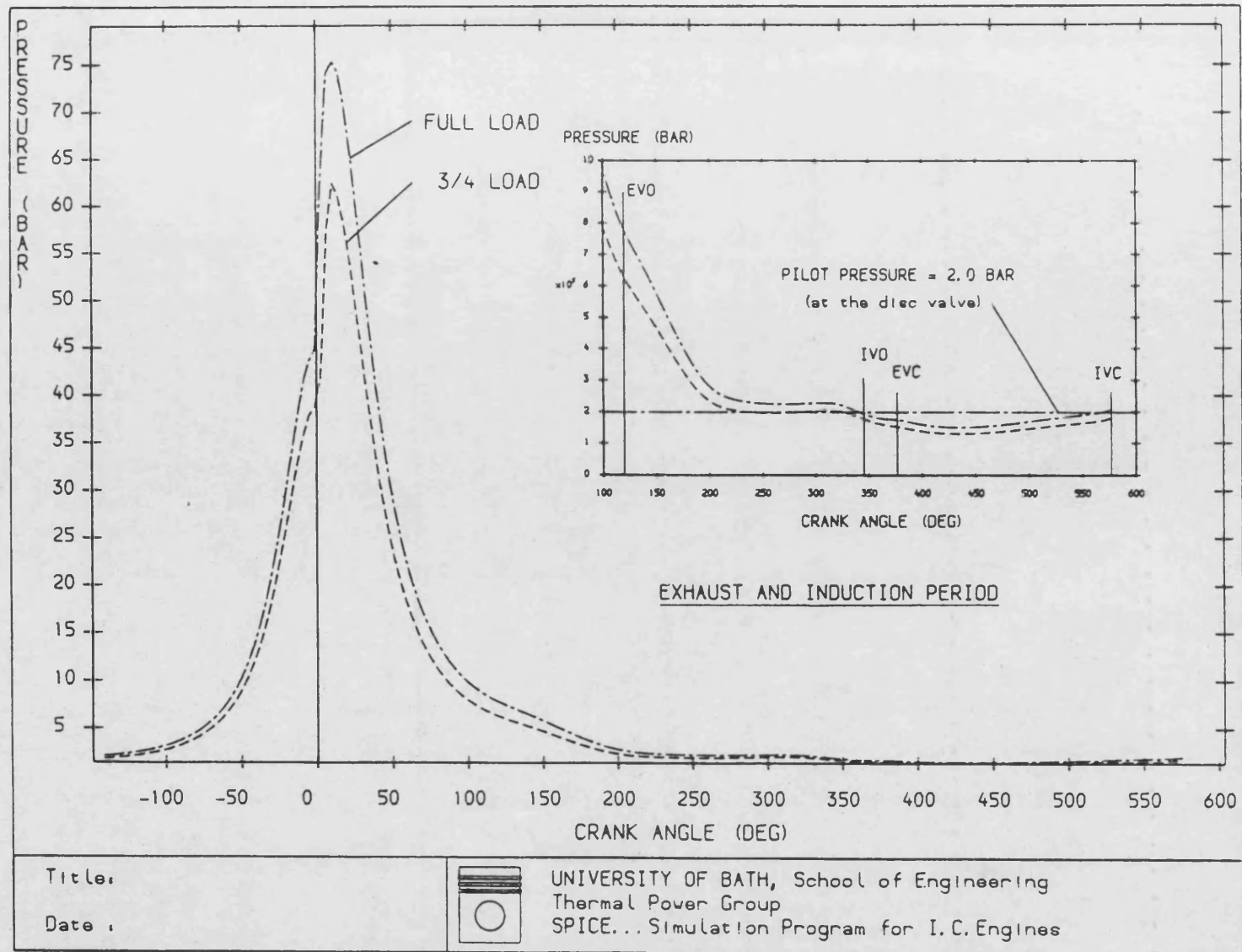


Figure 6.6 Motored Pressures from SPICE at Full, 3/4 and 1/2 Load Conditions



**Figure 6.7 Gas Engine "fired" as Diesel to indicate Cylinder Pressure through Exhaust Period**

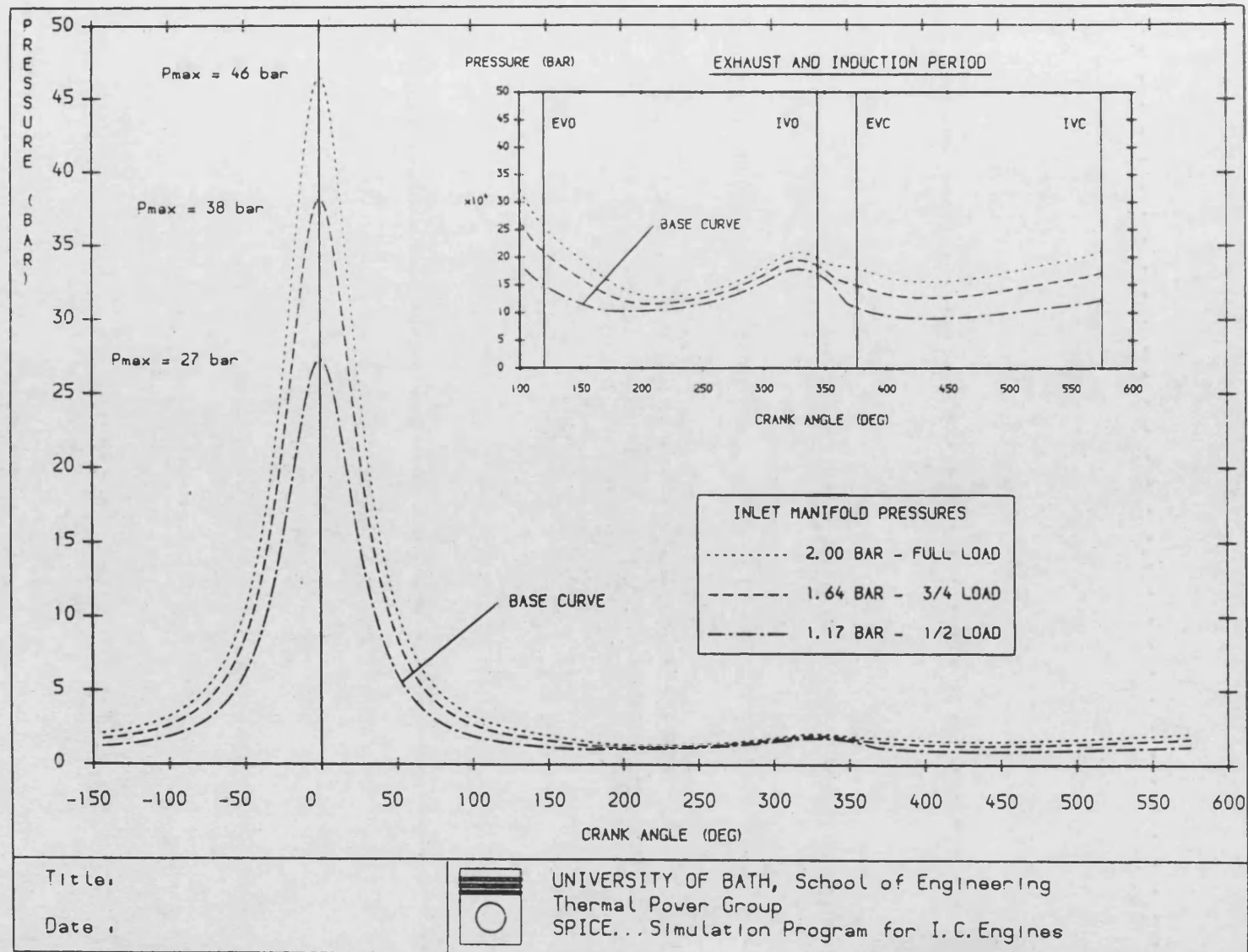
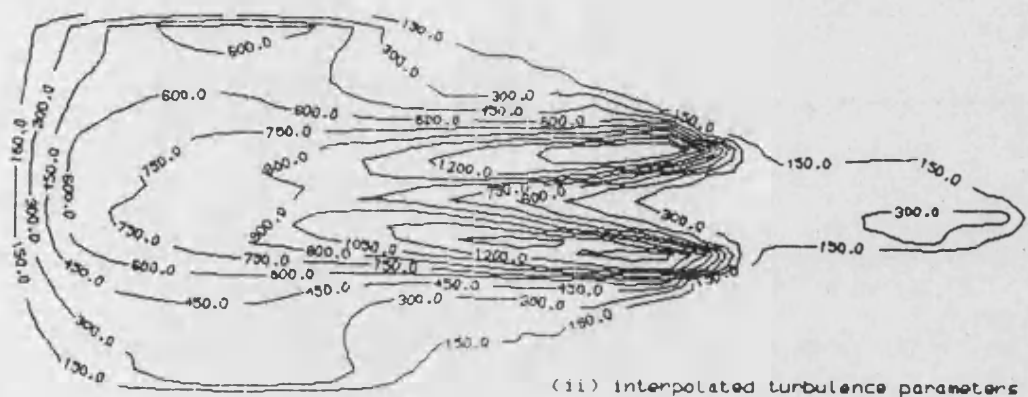
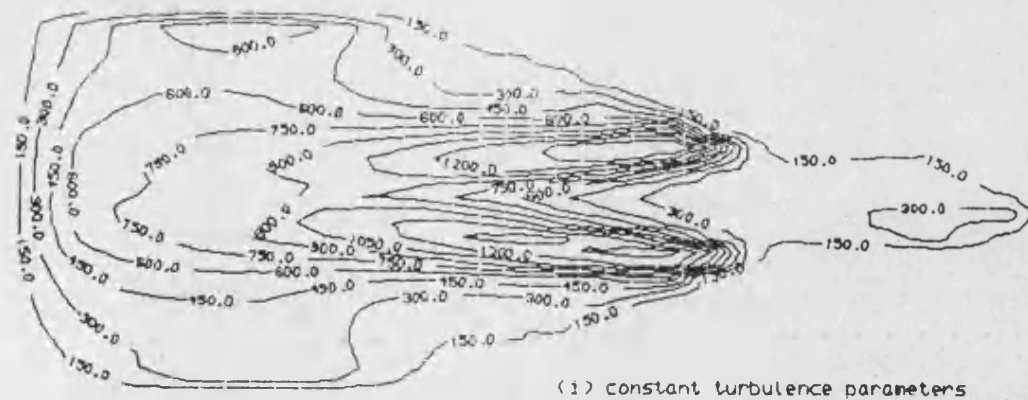
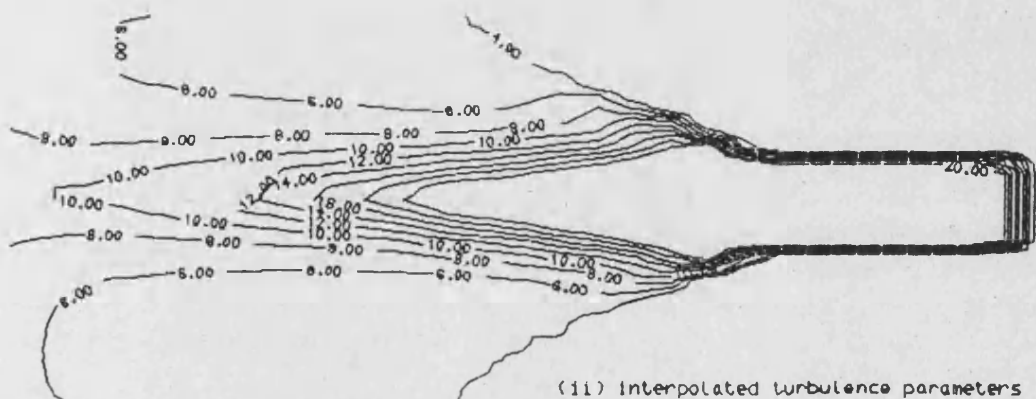
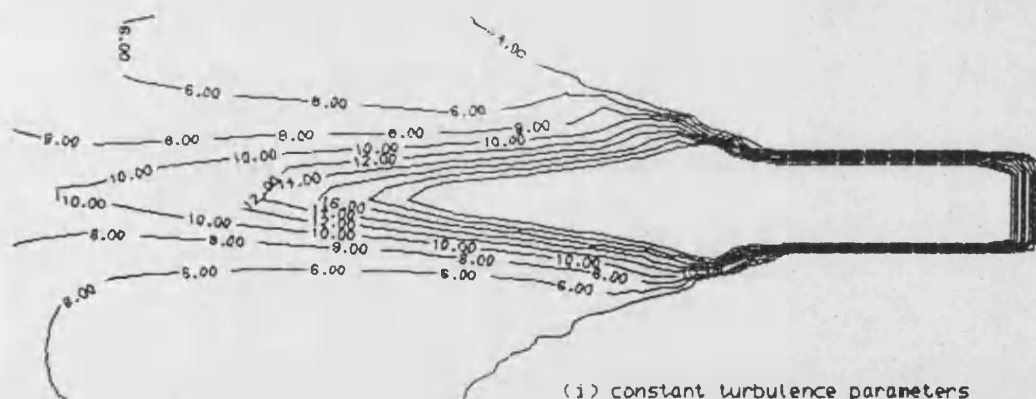


Figure 6.8 Motored Pressure Curves indicating how higher Loads may be scaled from a Base Curve



a) Turbulent Kinetic Energy Contours



b) Air-Fuel Ratio Contours

**Figure 6.9 Turbulent Kinetic Energy and Air-Fuel Ratio Contours at 12 deg BTDC**

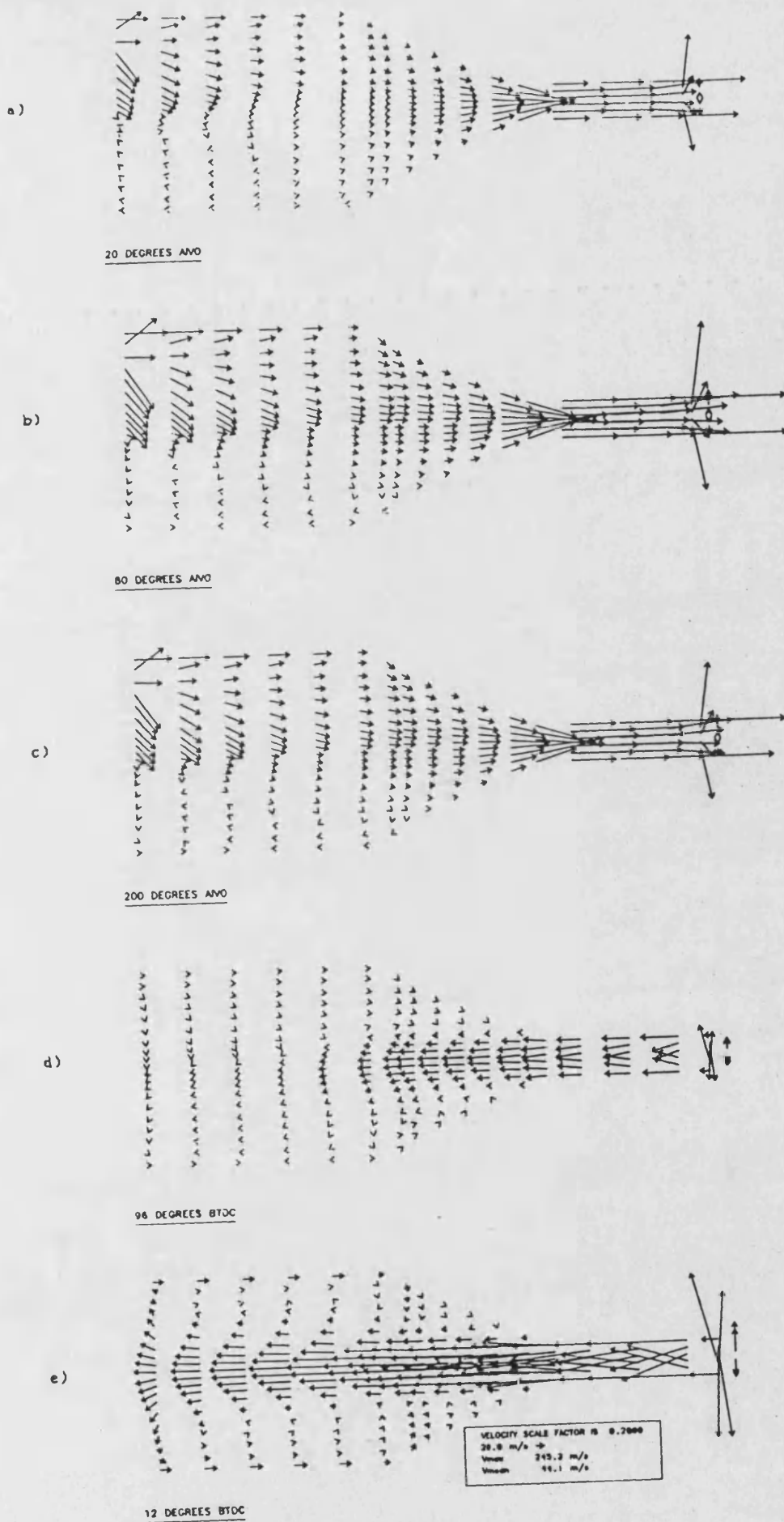


Figure 6.10 Velocity Vector Fields at a Number of Points during Induction and Compression

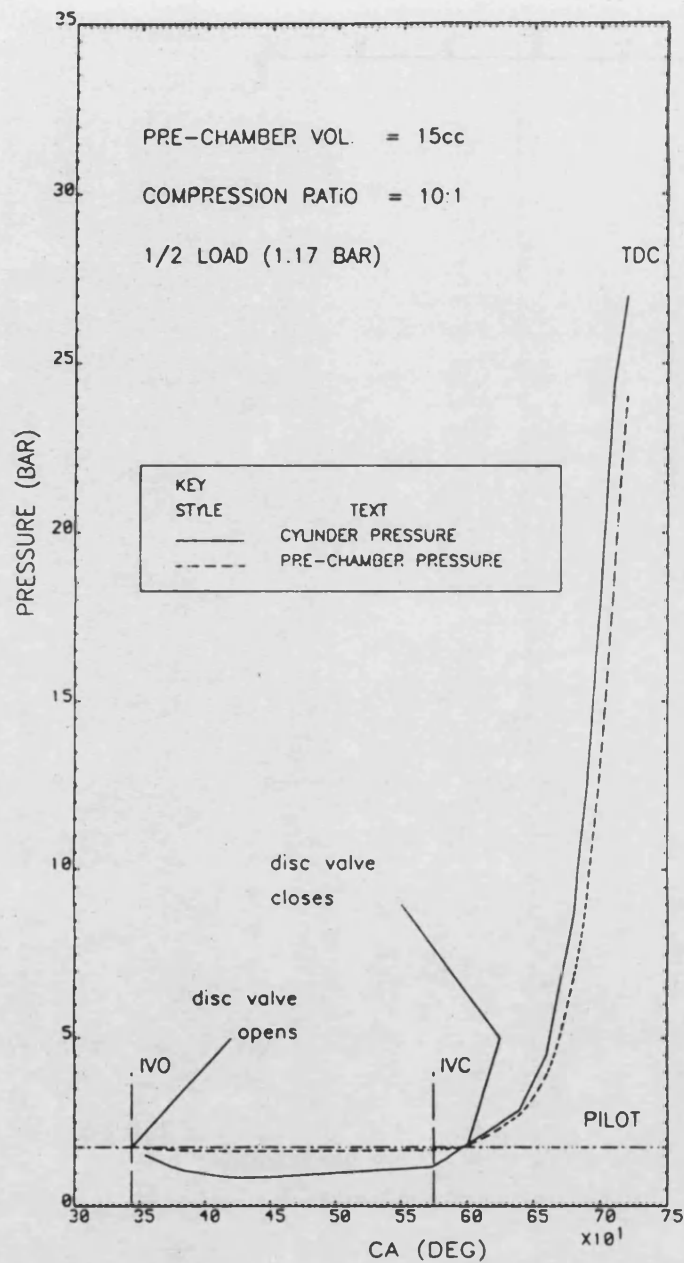


Figure 6.11 Pressures governing Opening and Closing of the Disc Valve

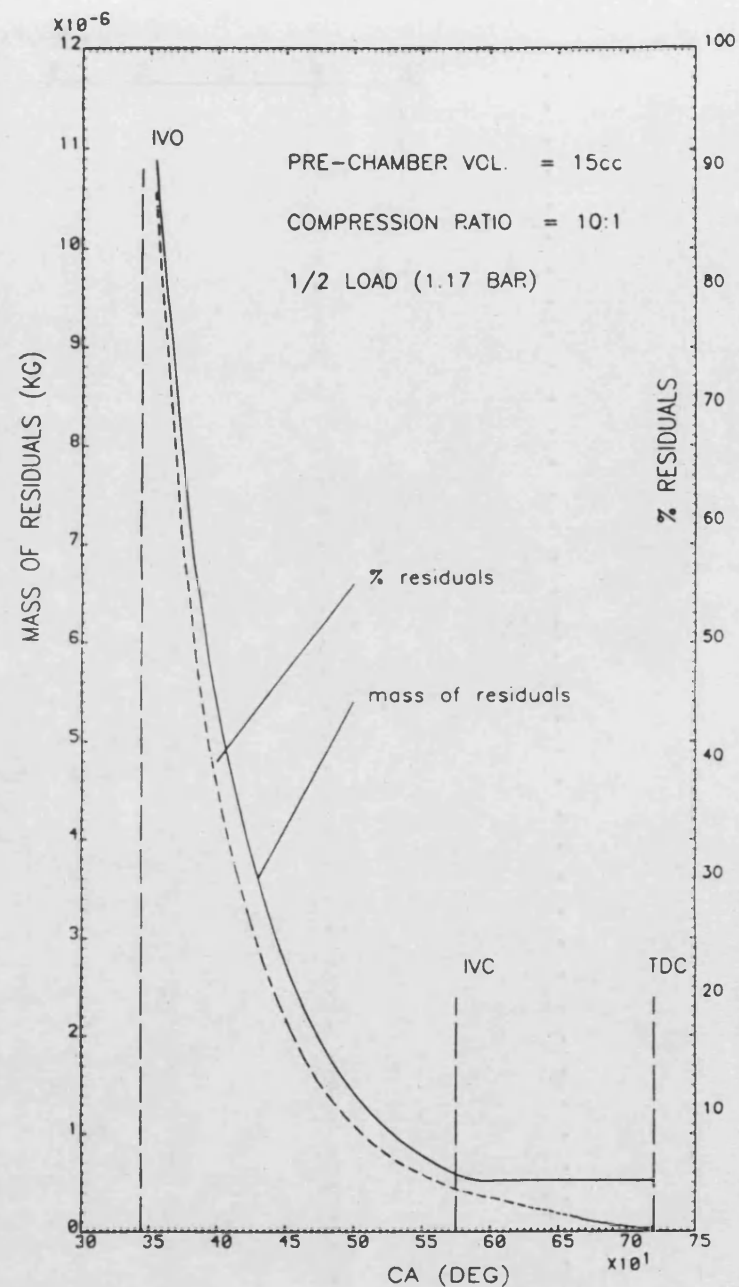


Figure 6.12 Purging of the Residuals from the Pre-chamber



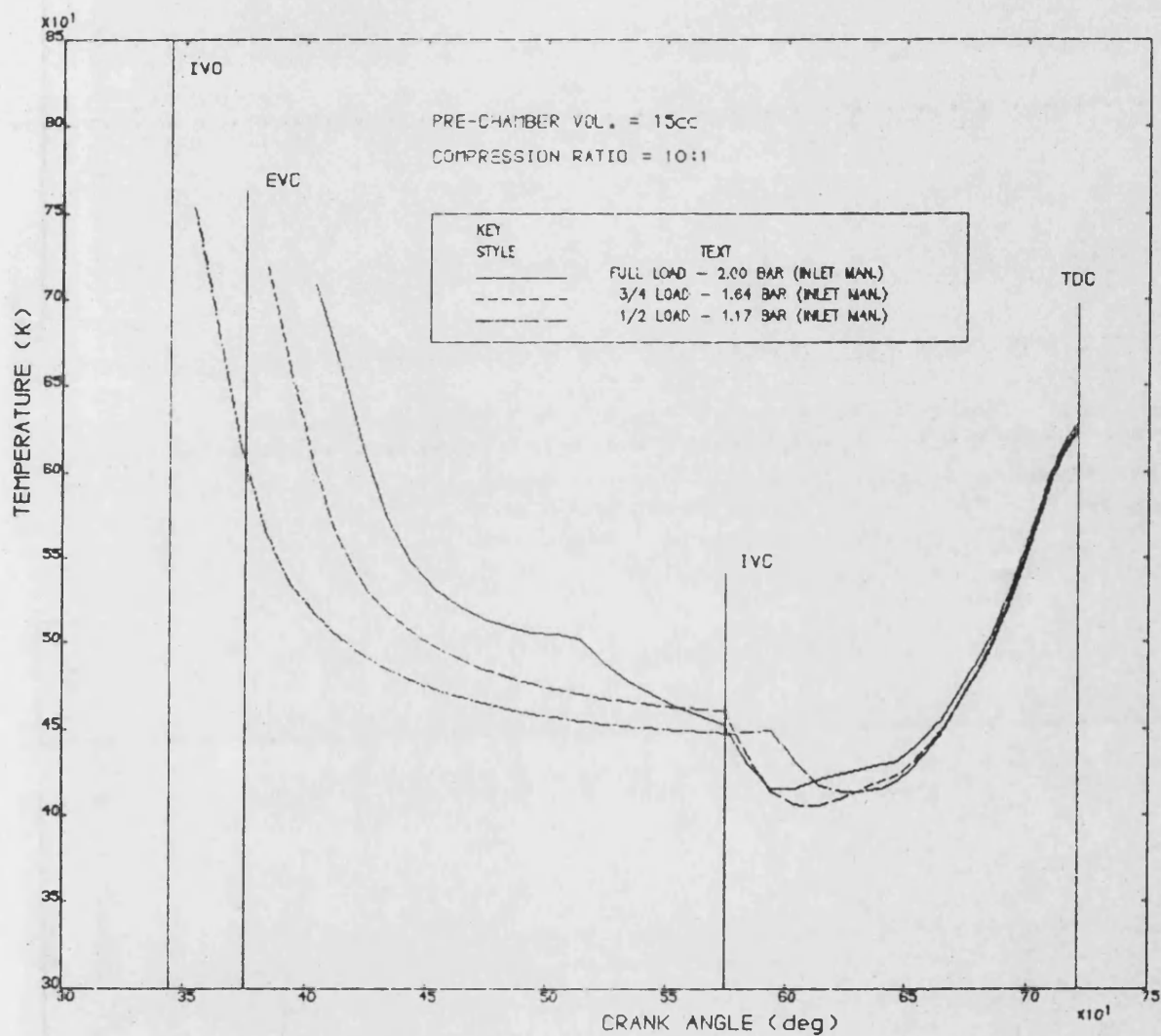


Figure 6.13 Temperature in the Pre-chamber through Induction and Compression

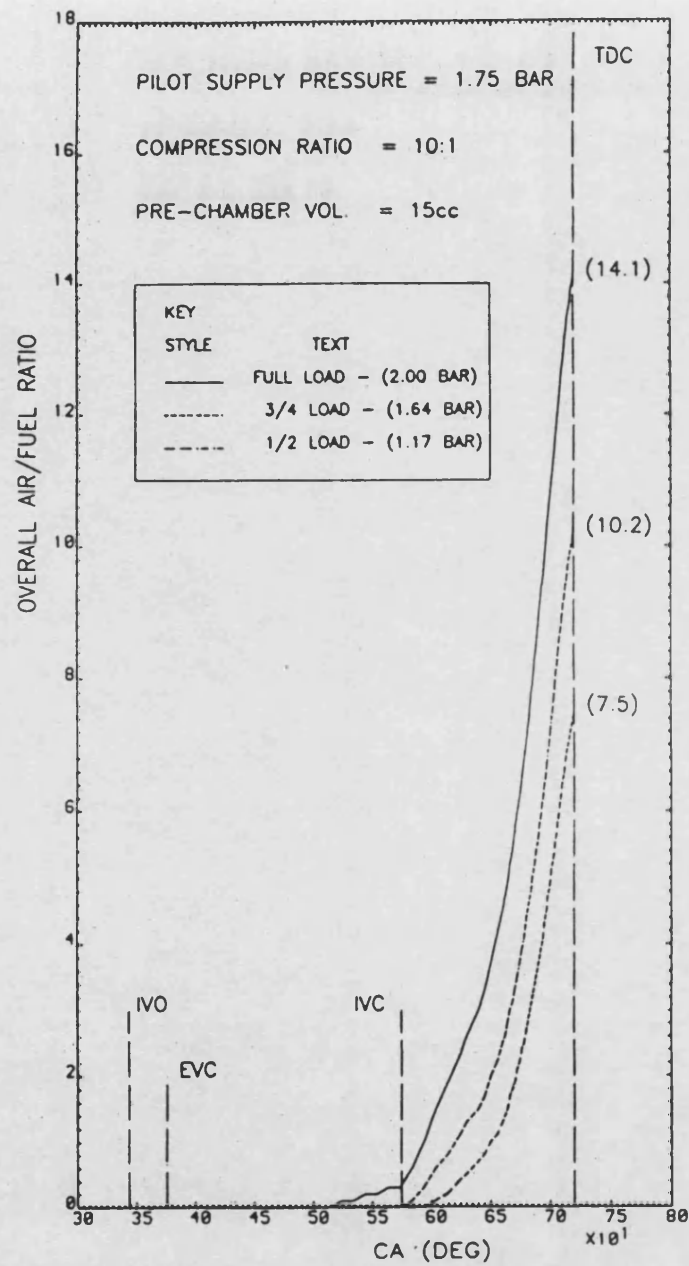


Figure 6.14 Variation of Air-Fuel Ratio with Engine

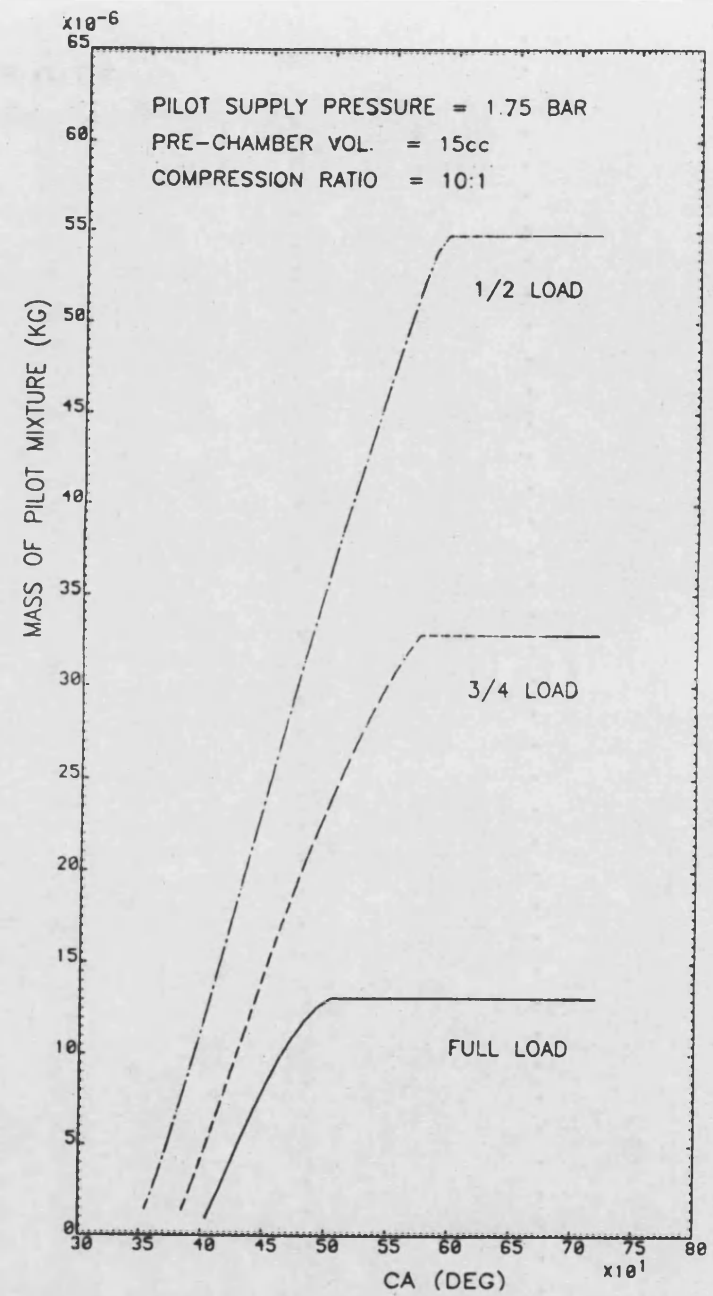


Figure 6.15 Pilot Gas admitted under

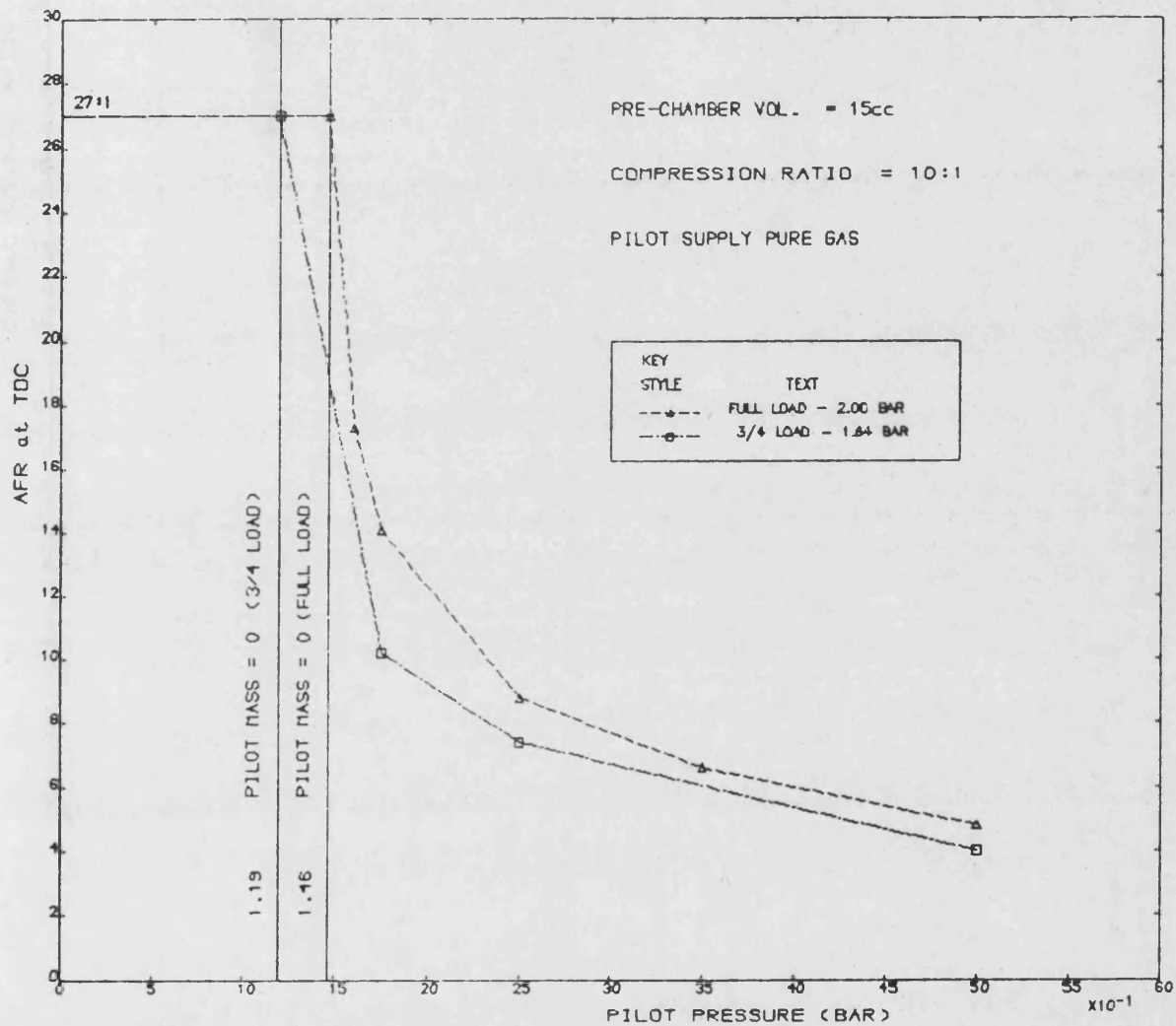


Figure 6.16 Variation of Overall Air-Fuel Ratio at TDC with Pilot Pressure under Full and 3/4 Load Conditions

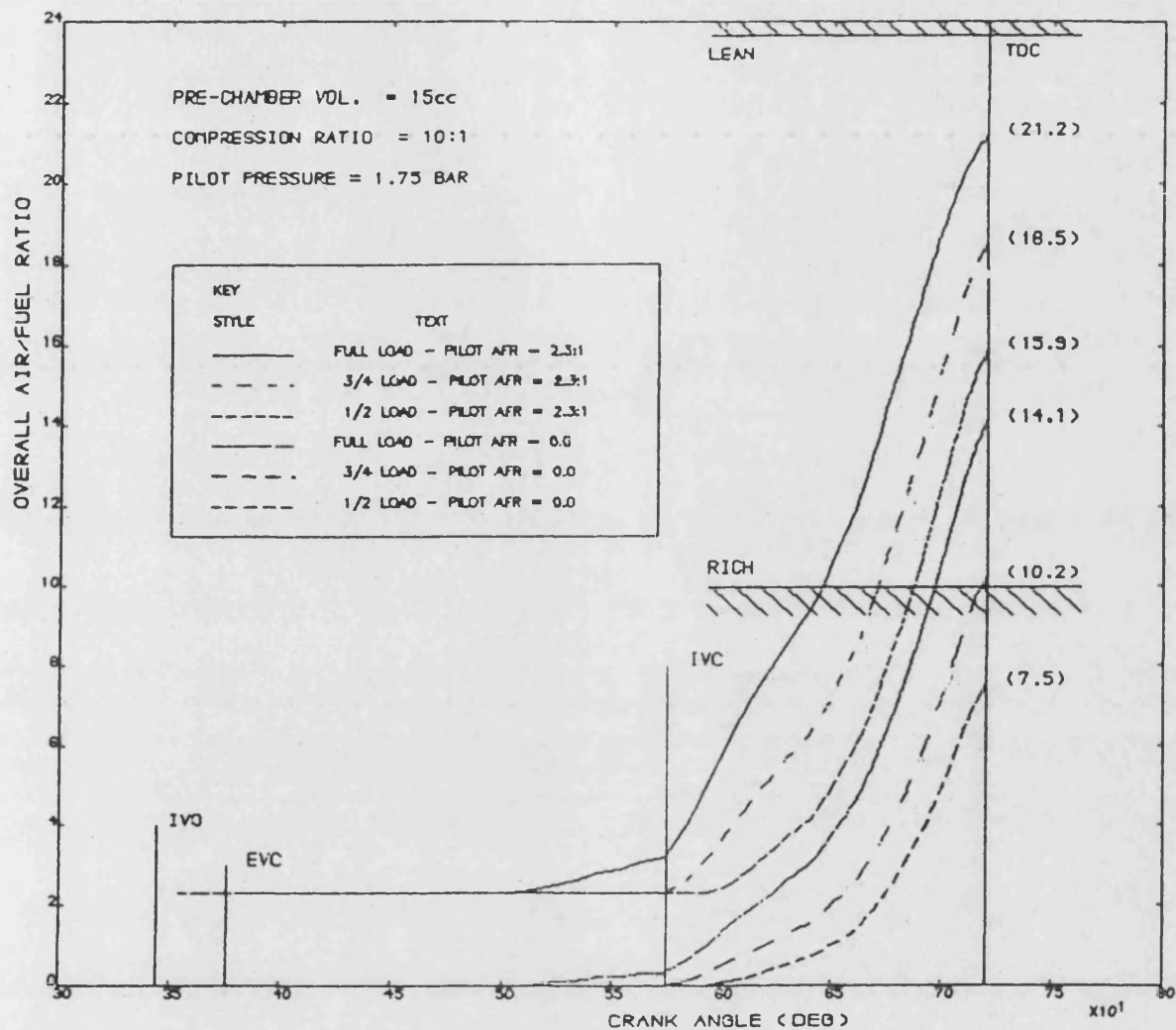
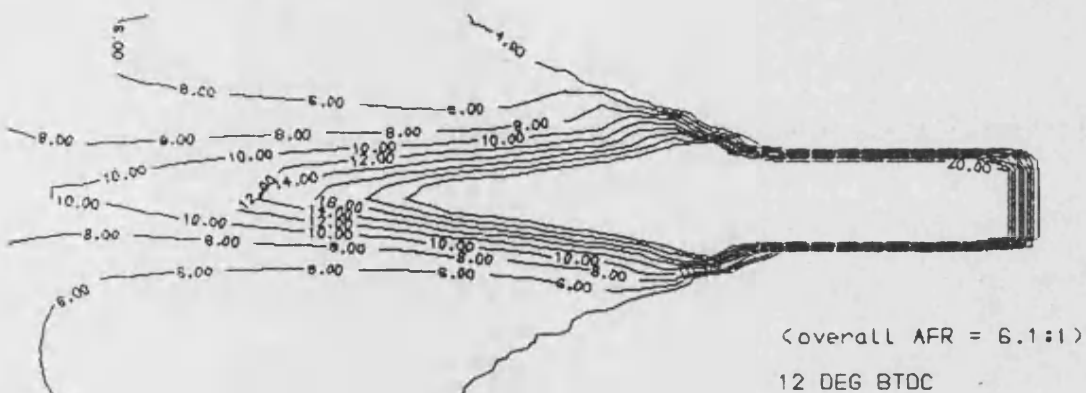
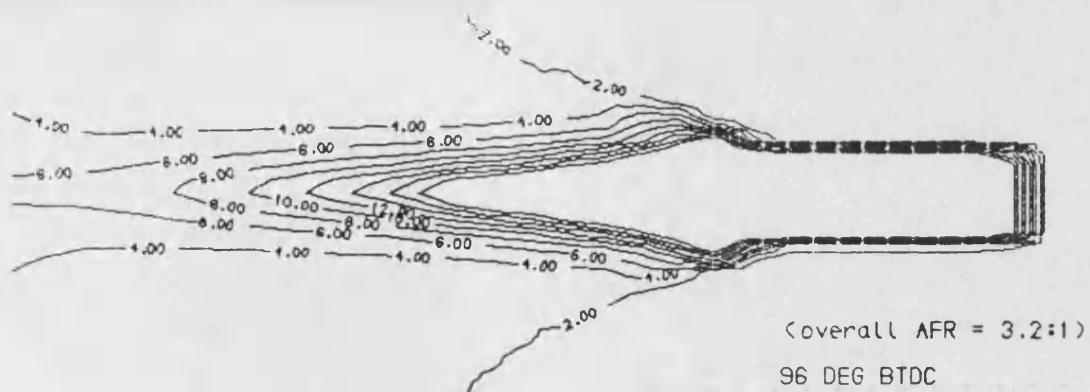
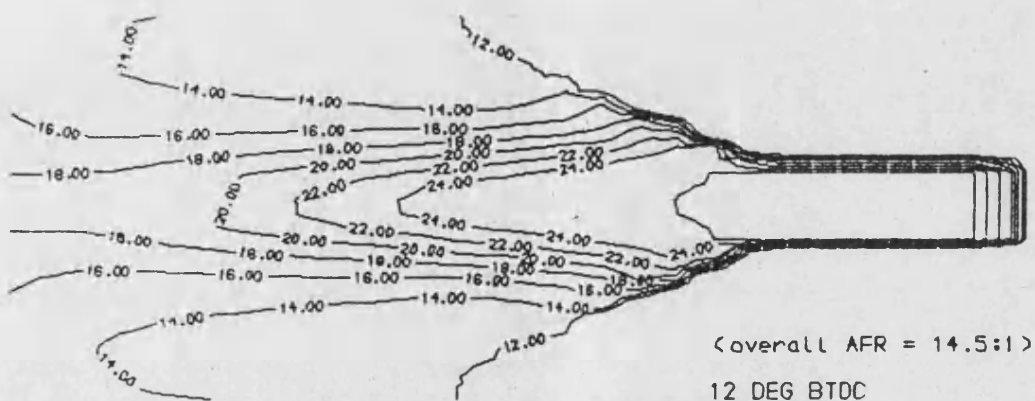
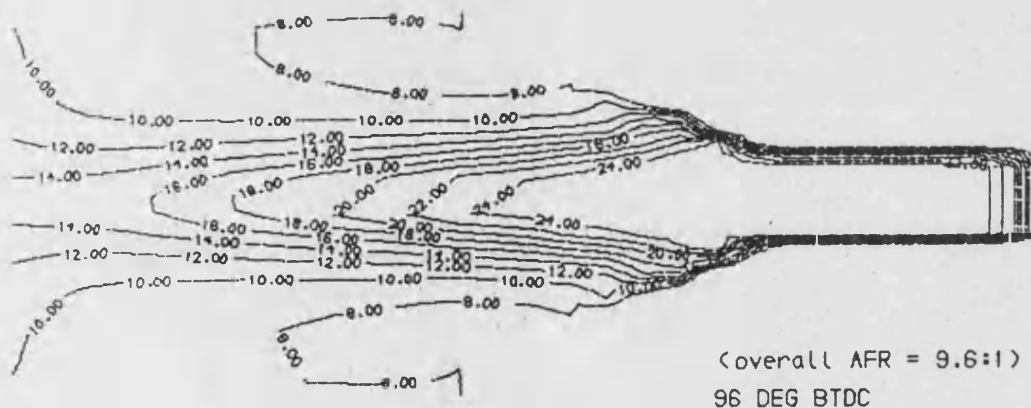


Figure 6.17 Variation of Overall Air-Fuel Ratio with Crank Angle for a Range of Engine Loads and Pilot Supply Mixtures



a) pilot air-fuel ratio = 0.0



b) pilot air-fuel ratio = 2.3:1

Figure 6.18 Contours of Air-Fuel Ratio for Pure Gas and an Air/Gas Mixture at 2:3:1

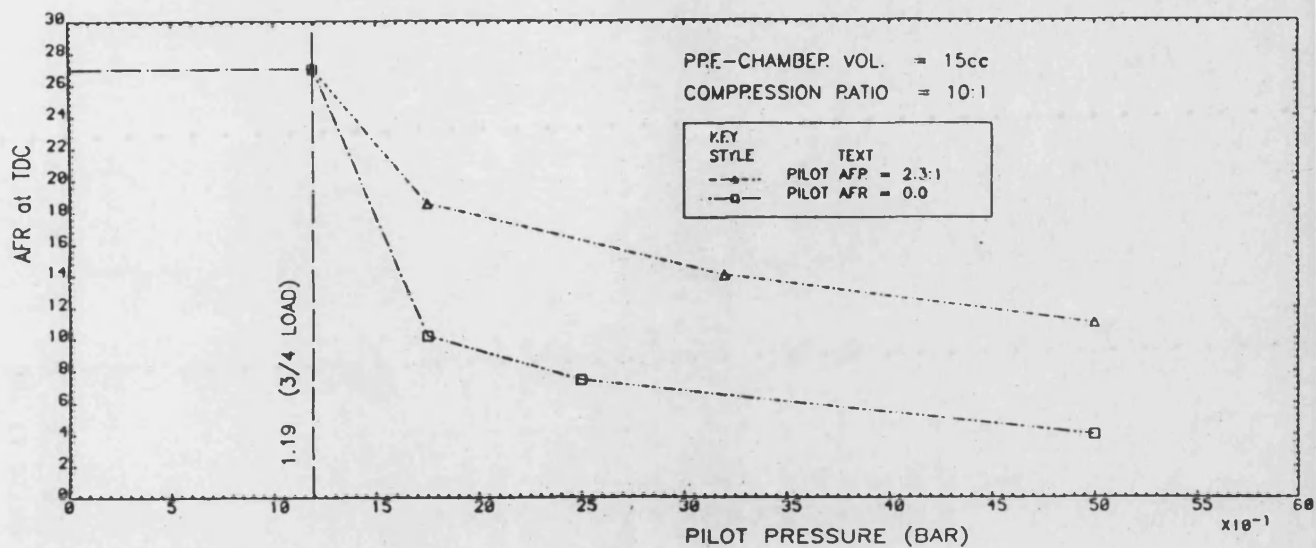


Figure 6.19 Dependence of Pre-chamber Air-Fuel Ratio on Pilot Supply Pressure and Mixture at 3/4 Load

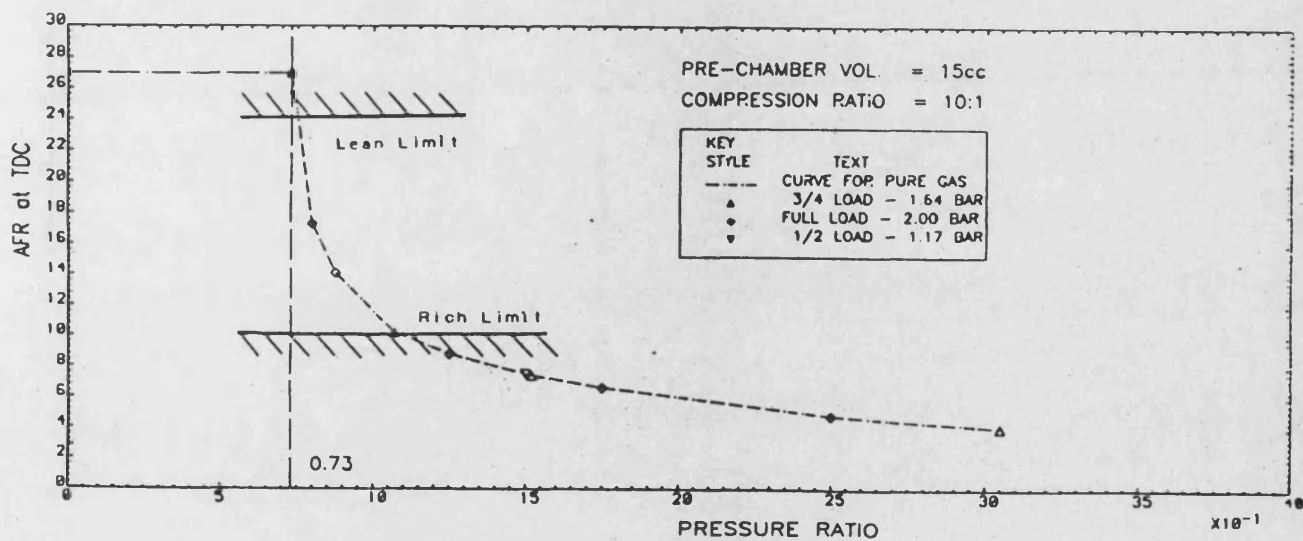


Figure 6.20 Relationship between overall Air-Fuel Ratio at TDC and Ratio of Pilot Supply Pressure to Boost Pressure for a Pure Gas Supply

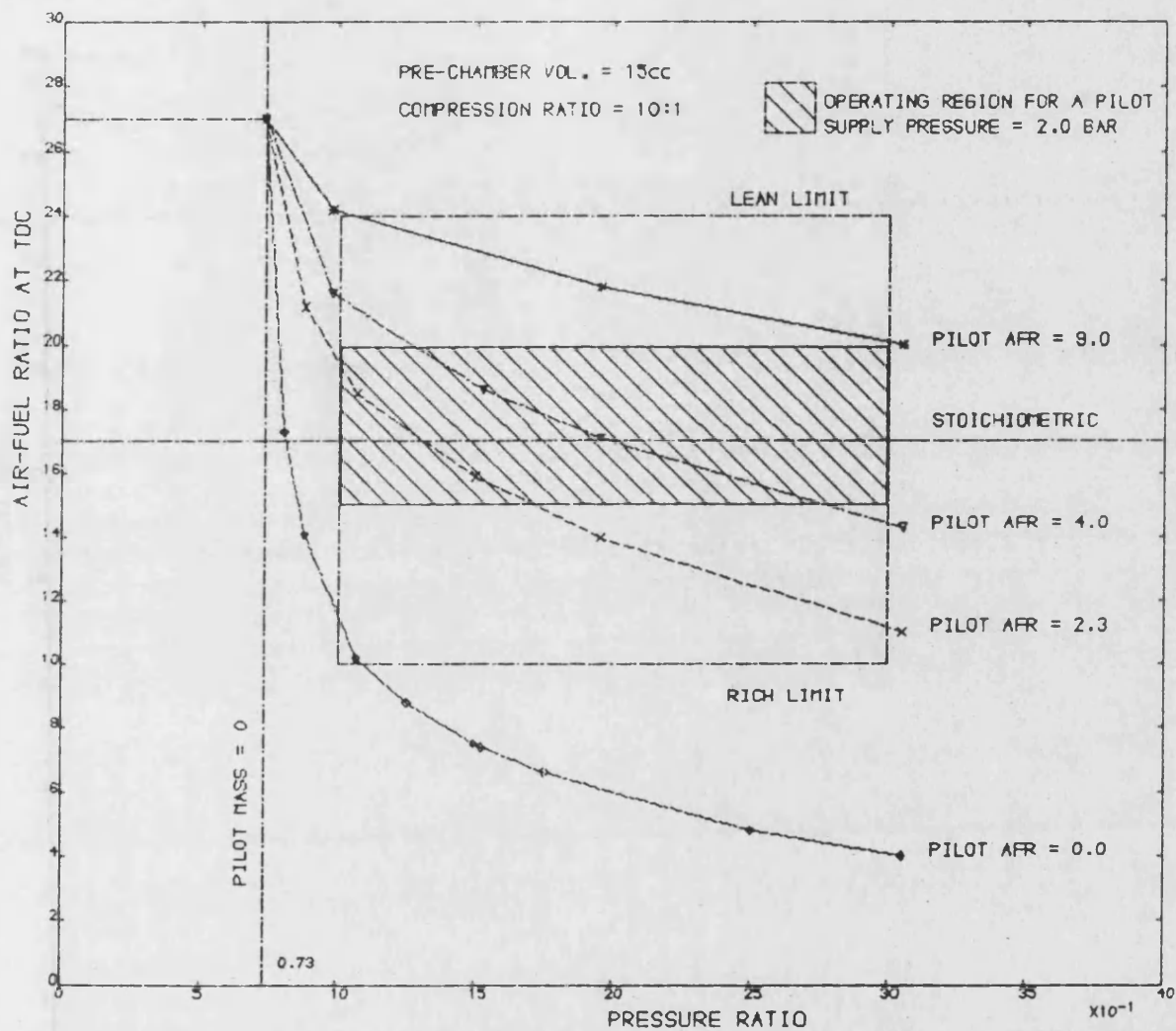


Figure 6.21 Mixture Preparation versus the Ratio of Supply Pressure to Boost Pressure for a Range of Supply Mixture Ratios. The shaded Region is where the System should operate for effective Combustion in the Pre-chamber.



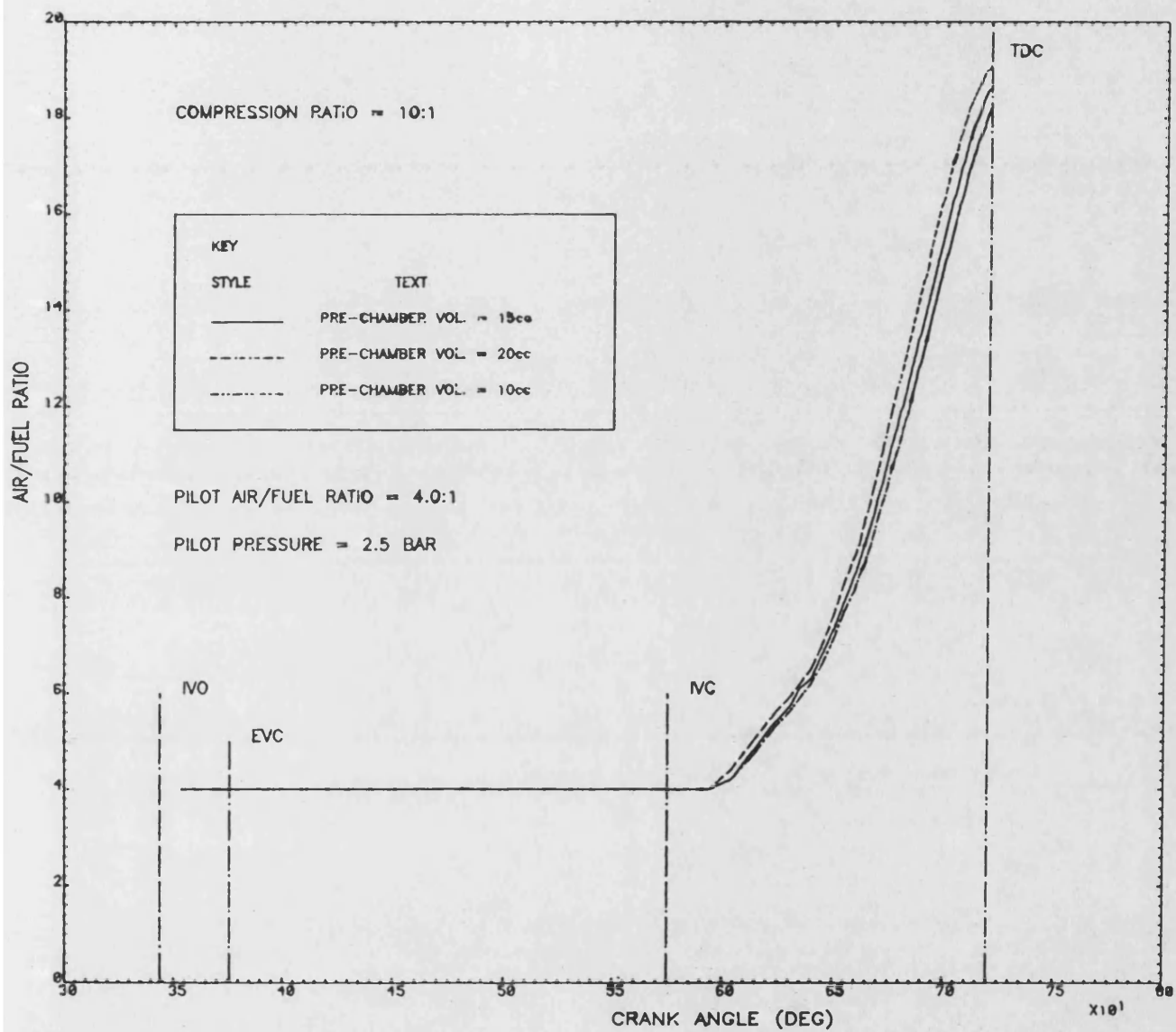


Figure 6.22 Effect of Pre-chamber Volume on Mixture Preparation



# PART IV

# CHAPTER 7

## **7. Test Rig Installation and Instrumentation**

This chapter details the experimental rig and its instrumentation. The rig is described in section 7.1 in terms of the normal supply systems (air, exhaust, cooling, and fuel). Instrumentation is covered in section 7.2. At this point the rig is in the process of commissioning: the main aim being to allow initial running of the new engine as quickly as possible. Instrumentation is, correspondingly, rather basic.

It is envisaged that the next phase of the project will involve a thorough test program; the objectives of which would be to explore the operating parameters of the installation and establish the various criteria to allow matching of the 1SE engine to its multi-cylinder counterpart. It is also intended to undertake an investigation of the pre-chamber mixing parameters with the aim of validating the theoretical work presented in the previous chapter. Consequently, in installing the engine an attempt has been made to allow for these future activities. The instrumentation would be developed accordingly to meet these requirements.

### **7.1 Rig Description**

The overall layout of the rig is illustrated schematically in figure 7.1, with the actual installation and engine shown in figures 7.2(a) and 7.2(b) respectively. The engine is the lean-burn natural gas version of the Dorman 1SE single cylinder research engine, the design of which has been described in detail in chapters 3 and 4. The engine is secured to a channel-sectioned frame which is flexibly mounted on four elastic elements, incorporating overload and rebound washers. Drive to the dynamometer is via a splined cardan shaft and two flexible couplings. The assembly was selected on the basis of the manufacturer's recommendations; having undertaken a torsional vibration (TV) analysis of the system (72). This precaution was felt necessary because of the uneven firing loads of a single cylinder

engine and the large flywheel inertia which tends to dominate the torsional vibration system. The Froude hydraulic dynamometer, which had to be mounted on a second frame to bring its impeller shaft in-line with the crankshaft, is bolted directly to the test-cell floor.

The need to simulate turbocharged conditions required far more elaborate supply systems than would be found on the test-bed of a naturally aspirated single cylinder engine. On the induction side elevated temperatures and pressures are required to reproduce similar manifold conditions to those of a compressor and intercooler. Similarly, at the exhaust port, conditions should mimic the presence of a turbocharger turbine, particularly the pressure pulses which strongly influence scavenging in the engine. And finally, a complete installation is required to compress the natural gas supply from a relatively low mains pressure to a level slightly above engine boost requirements.

#### 7.1.1 Induction System

The complete induction system is shown in figure 7.3. Air at elevated pressure is supplied from the large external "Belliss" compressor at a constant pressure of 6.4 bar (80 p.s.i. gauge). The inlet manifold pressure is regulated by adjusting a simple hand-operated air valve which in turn controls a large dome valve. The desired air temperature is achieved using heater elements (18 kW) which are regulated by a proportional-integral-differential temperature controller via thyristor switching units.

The large air receiver is used to dampen pressure pulsations within the manifold so presenting the flow measuring orifice plate with a steady flow rate. The receiver was sized using the recommendations of McKenzie and Dexter (2): they suggest a capacity approximately equal to 40 x swept volume. For the 1SE engine this equates to a volume of 155 litres. A proprietary unit of slightly smaller capacity (127 litres) was readily available and so was chosen as it

could be easily adapted for wall mounting; saving valuable space in a test-cell rapidly becoming overcrowded with service requirements.

After leaving the air receiver the air flow is divided: the majority feeds into the inlet manifold with the remainder being led, via a small variable area ("Rotameter") flowmeter, to the pre-chamber. The cylinder air is mixed with the gas prior to the inlet manifold in a purposely designed mixer. The design for the mixer is shown in figure 7.4. A linear actuator (stepper-motor with integral lead-screw) is used to control the movement of a small cone which in turn regulates the flow of gas into the mixer. Adjustment of the cone's position is by three simple toggle switches: direction (open and close), jog (a single stepper pulse) and run (continuous pulses for large movements). These enable the mixture strength to the cylinder to be varied over a wide range; something that could not have been easily achieved with a small conventional carburettor.

The theoretical investigation into the mixing in the pre-chamber (chapter 6) highlighted the requirement to feed a gas/air mixture to the pre-chamber. To allow a range of mixtures to be studied a second much simpler mixer (refer to figure 7.5 ) was added into the pre-chamber supply line. This is controlled in the same manner as the larger main chamber mixer. A shut-off valve is included in the air line to enable, if desired, only pure gas to be fed to the pre-chamber.

#### 7.1.2 Exhaust System

The design for the exhaust system has been discussed in detail in chapter 4 (section 4.4). Exhaust back pressure is controlled by a cable operated, 30mm diameter gate-valve - refer to figure 7.6 - located downstream of the exhaust plenum. To ensure "fail-safe" operation the simple valve cannot completely close off the exhaust restriction and has been designed such that, in the event of the cable breaking, the weight on the pivot arm returns the valve to the open position. A parallel by-pass line, incorporating a "bursting

disc" arrangement, is also included in the gate-valve assembly. The disc is set to rupture should the pressure differential across it exceed 2.0 bar. The exhaust plenum (80 litres) was manufactured from a section of large-bore pipe welded to domed end sections: the assembly being pressure tested.

The orifice, sited before the plenum, serves to shape the pressure pulse in the exhaust manifold and is thus intended to mimic the characteristics of the turbine nozzles. The orifice diameter was calculated using the results from a parametric study (refer to section 4.4) and should be regarded as a "best-guess" in the absence of any experimental data. (A detailed investigation of the exhaust system would form a major part of the work involved in matching the 1SE to the six cylinder engine). From the study a suitable flow area for the orifice had been determined. This was converted to a nominal diameter (48mm) by applying an appropriate discharge coefficient based on BS1042 (fluid flow in closed conduits). To withstand the high exhaust temperature (c. 850K) the orifice plate was manufactured from stainless steel.

The parametric study had also shown the importance of the volume prior to the orifice. For best matching results the exhaust manifold and pipe volume on the single should be identical to the total exhaust manifold volume of the 6SE. At this stage, this has not been achieved on the rig. In linking the engine exhaust to the wall mounted orifice, plenum and gate-valve assembly, the pipe runs required have resulted in a larger volume than desired.

The exhaust installation is completed by two silencers: the first a triple-chamber design in which expansion and diffusion take place in the first two sections, and attenuation of the high frequencies of the exhaust noise in the final section. The second, is a "straight-through" unit for further noise absorption. The total volume of the silencers is approximately eighty times the swept cylinder volume.

### 7.1.3 Natural Gas System

The requirement for gas pressures comparable with the engine boost levels necessitated a separate gas installation prior to the engine. The circuit is shown in figure 7.7 and is in accordance with the British Gas Codes of Practice (IM/17). Gas from the mains supply (5" water gauge) is compressed by a vane compressor, driven by an electric motor. Gas which is surplus to the requirements of the engine is fed back to the low pressure side of the compressor via a return loop. To avoid the gas being continually heated as it cycles around and to ensure the correct delivery temperature to the engine the gas is passed through a heat exchanger. The cooling medium is the secondary water circuit.

The gas installation is interlocked with high and low pressure switches and various engine parameters, such as flywheel overspeed (set at 1900rpm), high engine water temperature and low oil pressure. An emergency isolating button is also incorporated. The gas pressure switches act on the solenoid operated shut-off valves. These are closed automatically and the compressor motor isolated should the mains supply fall below atmospheric pressure (low), or if the pressure after the compressor exceeds a set maximum (high). The engine parameters are similarly wired. In all cases, the detection of a fault condition causes the engine to stop. The engine can only be re-started once the shut-off valves have been manually reset. To negate the serious consequences of an explosion in the inlet manifold, a 38mm diameter bursting disc is built into the manifold end plate. A further pressure switch mounted on the manifold is used to detect the rapid rise in pressure.

Following the pattern of the air installation the gas supply is also divided in two. Each supply - cylinder and pre-chamber - passes through a flowmeter, gas regulator and mixer. The regulators ensure that the gas pressure to the mixers is maintained at a set level above the air pressure. To achieve this, air at boost pressure is fed to one side of the diaphragm within each regulator. In addition, changing the springs within the regulators enables the cylinder and

pre-chamber gas supply pressures to be set independently of one another. The charge mixtures fed to the two chambers can be individually altered by the positions of the cone and needle within the respective stepper-motor operated mixers (refer to figures 7.4 and 7.5).

#### **7.1.4 Engine Coolant System**

The cooling system consists of a closed primary loop (cooling the engine) and an open secondary circuit (cooling the primary). Water for the secondary circuit is pumped from a large cooling pond, outside the test-cell building, to which it returns after passing through the engine mounted heat exchanger. At this stage the primary system is completely contained on the engine, with the water pump belt driven from the crankshaft. The circuit is shown in figure 7.8. It follows conventional engine practice: during start-up, i.e. when the water temperature is low, the water by-passes the heat exchanger and returns directly to the pump. As a means of stabilising the oil temperature, the engine water passes through an oil stabiliser-cooler before entering the crankcase. A high water temperature sensor is incorporated before the thermostat. In the event of the maximum temperature limit being exceeded ( $98^{\circ}\text{C}$ ), through perhaps failure of the water pump, then the engine is automatically stopped.

#### **7.1.5 Engine Oil System**

The oil system, like the primary water circuit, is contained on the engine. This was done for reasons of simplicity and speed of installation at the early stages of the engines design (refer to section 3.1.3). From the engine driven pump (right-hand primary balance shaft) oil is fed to the oil cooler which features an integral filter unit and relief valve. (The primary engine coolant flows through the other side of the heat exchanger). High pressure oil is fed directly to the main bearings for lubrication. Low pressure oil feeds the cylinder head rocker assembly, the geartrain,



piston cooling jet and the roller bearings in the balancer box. All the oil drains back to the sump. The oil circuit is shown in figure 7.9. An oil pressure switch, integral with the high water temperature sensor, shuts down the engine - by isolating the gas supply - should the oil pressure fall below 2.5 bar (22 p.s.i.).

## 7.2 Instrumentation

At this early stage the instrumentation on the rig is rudimentary and incomplete. In the limited time available only basic requirements, such as gas and air flowrates and some pressure measurements, could be recorded. They served primarily to provide feedback during the early running of the engine: flowrates could be observed, but could not be corrected to standard conditions because of the absence of temperature and pressure measurements.

In the next phase, as stated earlier, the instrumentation will be developed in line with experimental requirements; with the majority of instruments being linked to a PC (personal computer) based data acquisition system. The system will incorporate both high speed data sampling, to allow logging of transient parameters, for example cylinder pressure, and a low speed setting for recording of steady-state conditions. At this early stage, however, only the recording of cylinder pressure has been attempted. This and the other instrumentation are described, in brief, below.

### (1) Air Mass Flow

The total air mass flowrate to the engine is measured by means of a standard bevel-edged orifice plate, diameter 36mm, with D and D/2 tapings upstream and downstream, corresponding to BS1042. The differential pressure is measured by a vertical water manometer; the flowrate being calculated using the relationship:

$$q_m = K \sqrt{\Delta p \rho_1}$$

where:  $q_m$  = mass flowrate (kg/s)

$K$  = constant, based on orifice geometry ( $m^2$ ) = 0.00087

$\Delta p$  = differential pressure (N/m<sup>2</sup>)

$\rho_1$  = density at upstream location (kg/m<sup>3</sup>)

The small proportion of air fed to the pre-chamber is measured by a variable area flowmeter. The flow of air into the cylinder is the difference between these two readings.

#### (ii) Gas Flowrate

The proportions of gas fed to the cylinder and pre-chamber are individually measured by appropriately sized variable area flowmeters.

#### (iii) Engine Speed

During these early stages the engine speed was measured by a hand-held tachometer: the speed is registered from a reflective marker placed on the crankshaft pulley.

#### (iv) Engine Torque/Power

The engine torque is recorded by the weight added to the lever arm of the Froude hydraulic dynamometer. This value is then converted to engine power using the manufacturer's conversion given below:

$$\text{Power (hp)} = W.N/K$$

where:

$W$  = weight (lb)

$N$  = engine speed (rev/min)

$K$  = dynamometer constant = 200

#### (v) Cylinder Pressure Measurement

Measurement of the cylinder pressure was by a piezo-electric pressure transducer (Kistler 6121), mounted in the flame deck of the cylinder head. (The head had been pre-drilled in the development department at Dorman). The transducer was held in place by an adapter which in turn was clamped by a securing nut. The signal from the transducer was fed to a charge amplifier which was linked into the data acquisition system. With the pressure trace being the only signal entering the system, triggering had to be achieved internally; resulting in the x-ordinate being the system time base. Generally an external trigger is used; commonly using the signal obtained from a crankshaft encoder. This allows the trace to be displayed against crank angle, rather than time, with positions such as TDC being easily identifiable.

#### (vi) Gas Pressures

Simple vertical water manometers were used to record the pressure differential of gas to boost air prior to the mixers. This was to ensure that the regulators were functioning properly. If the gas pressures were too low it would be difficult for mixing to take place.

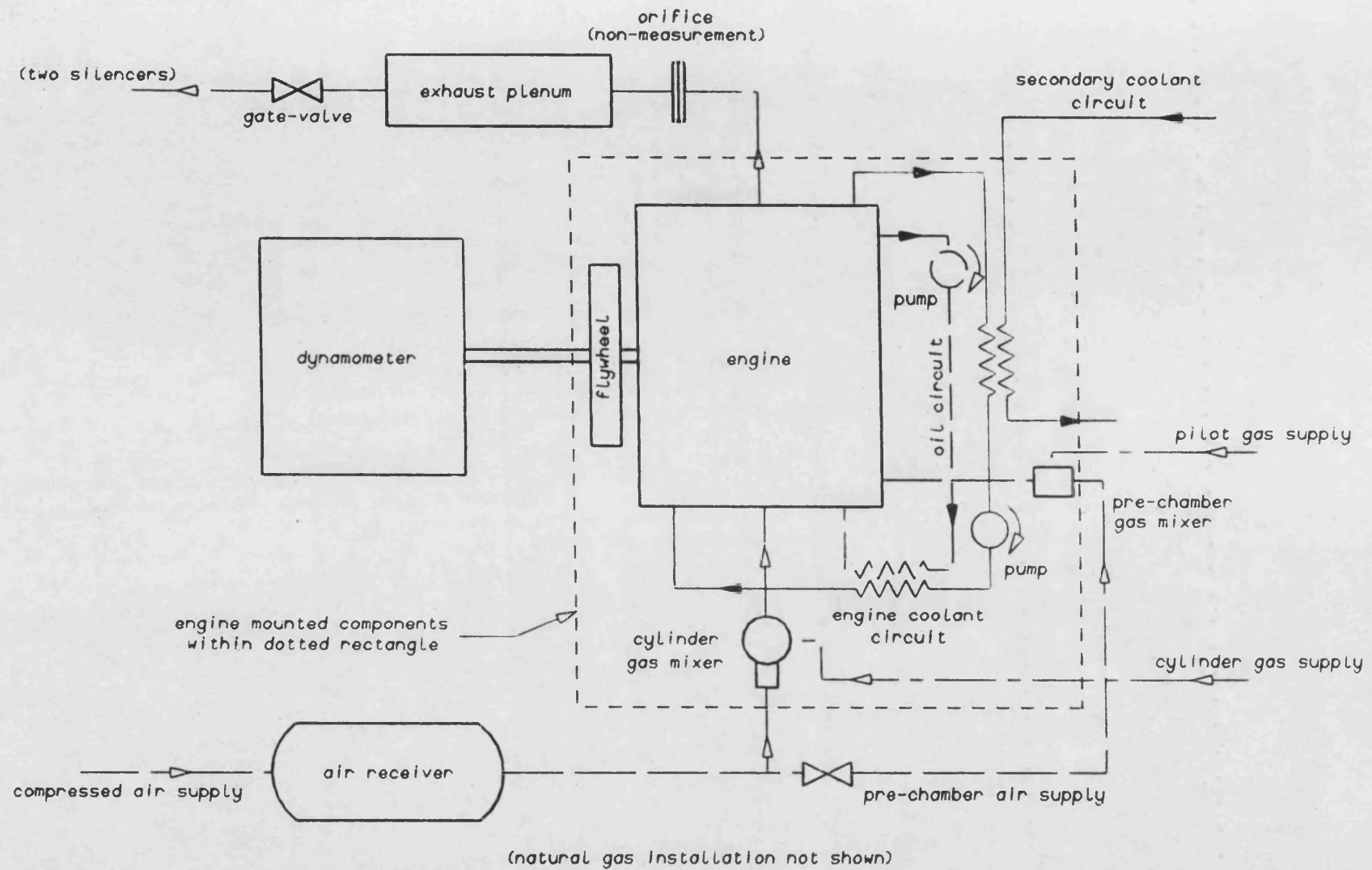


**Figure 7.1 Schematic Representation of Rig Installation**

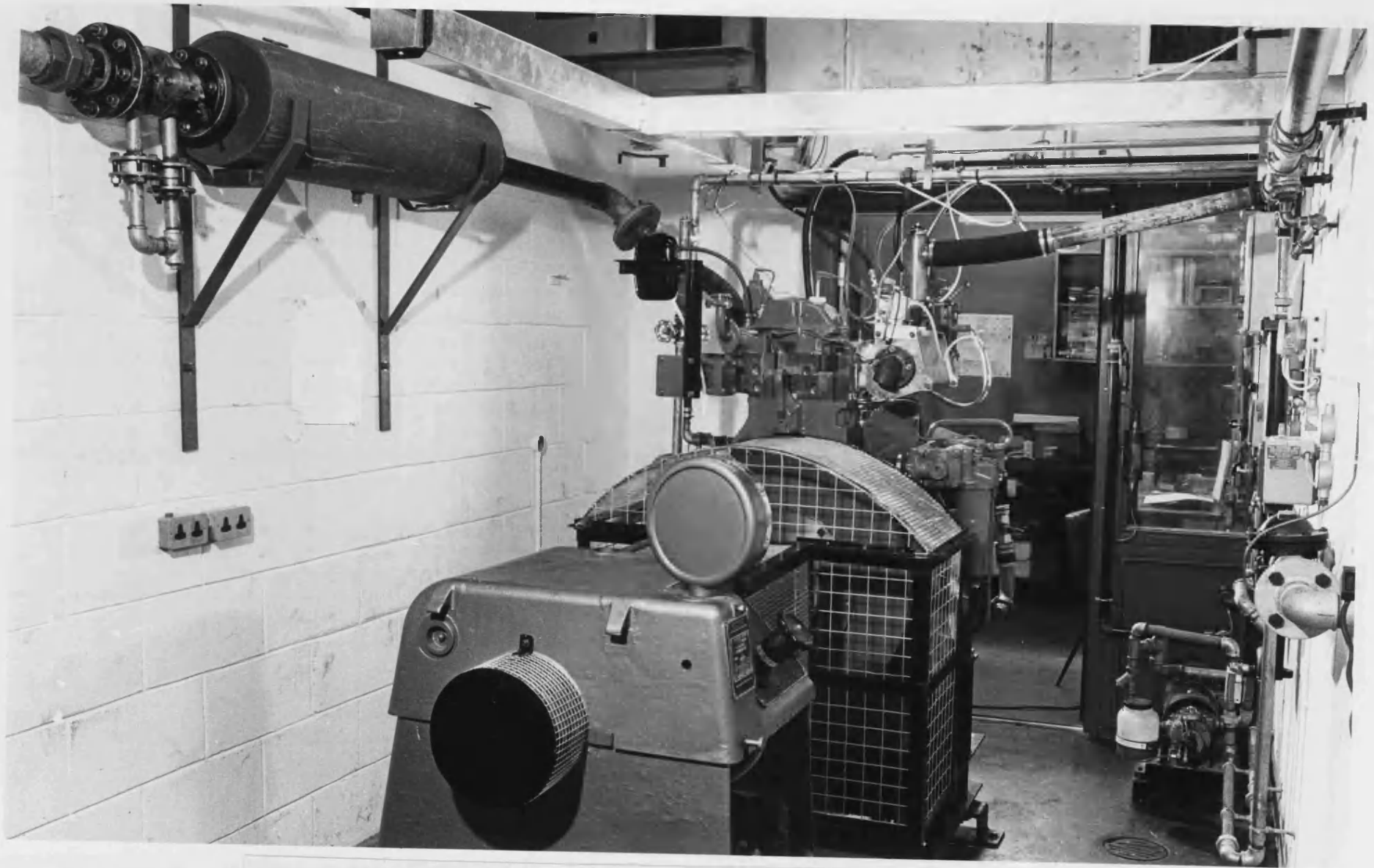


Figure 7.2(a) Overall Rig Installation at Bath University

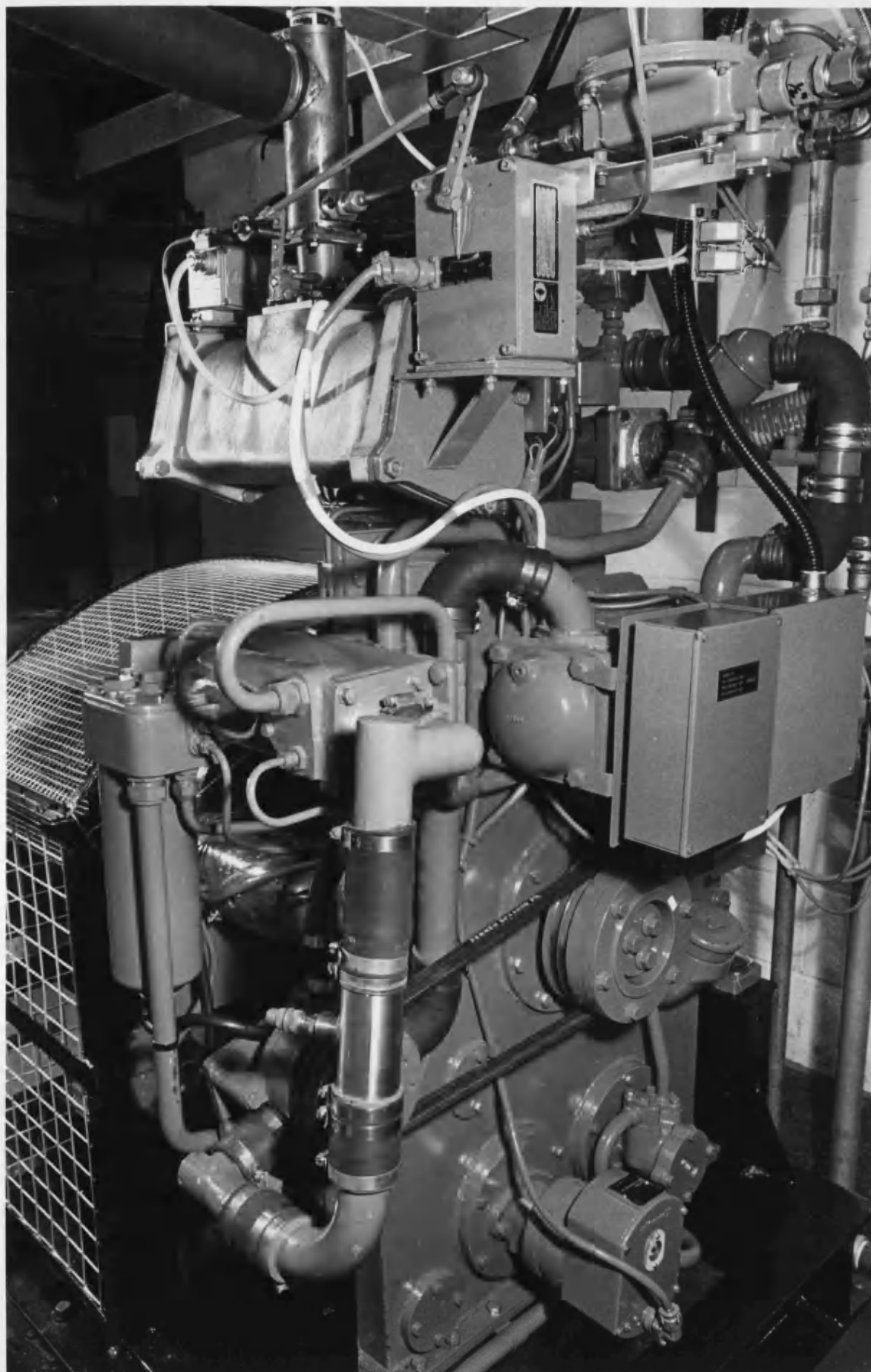


Figure 7.2(b) Lean Burn Natural Gas Version of 1SE Engine

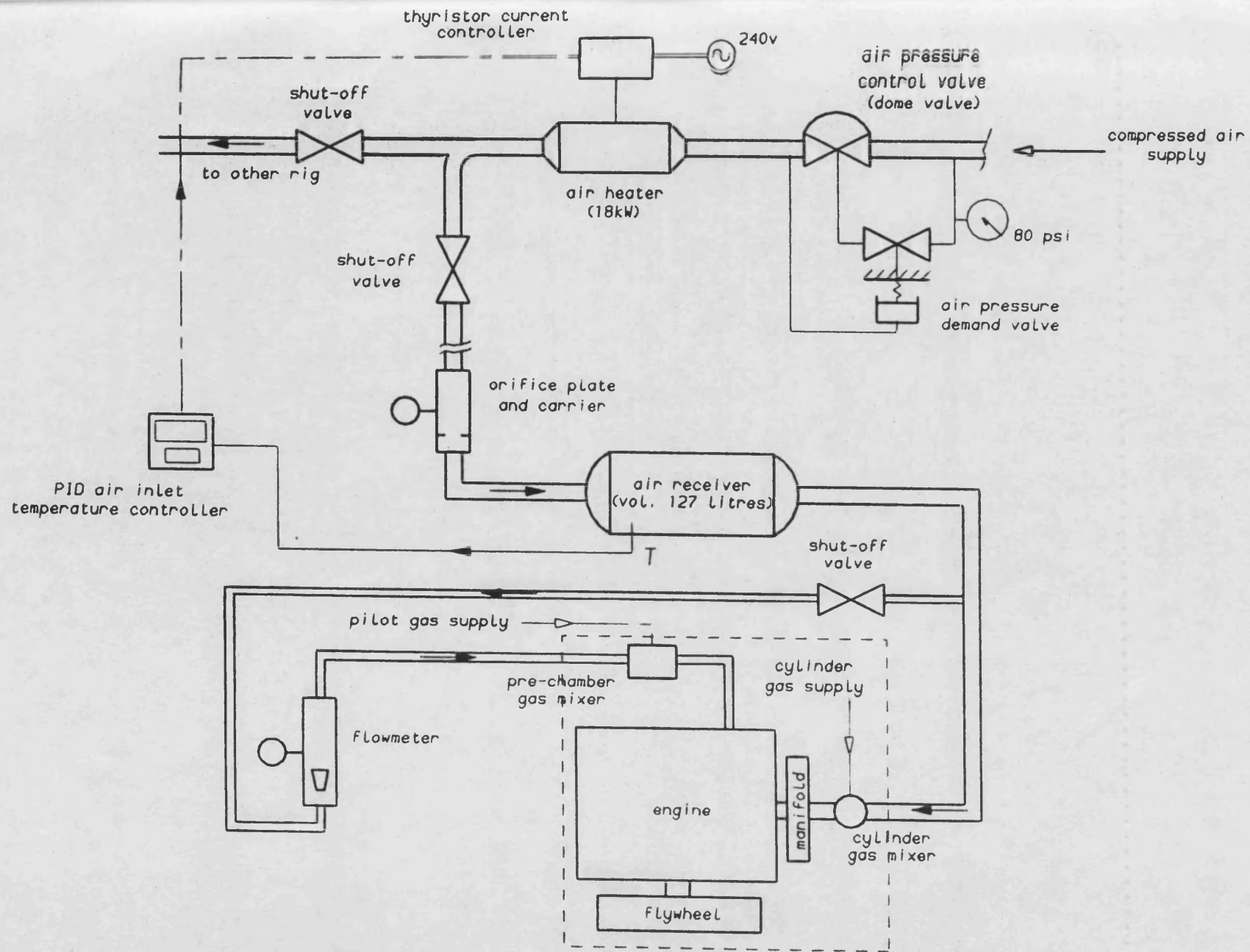


Figure 7.3 Induction System

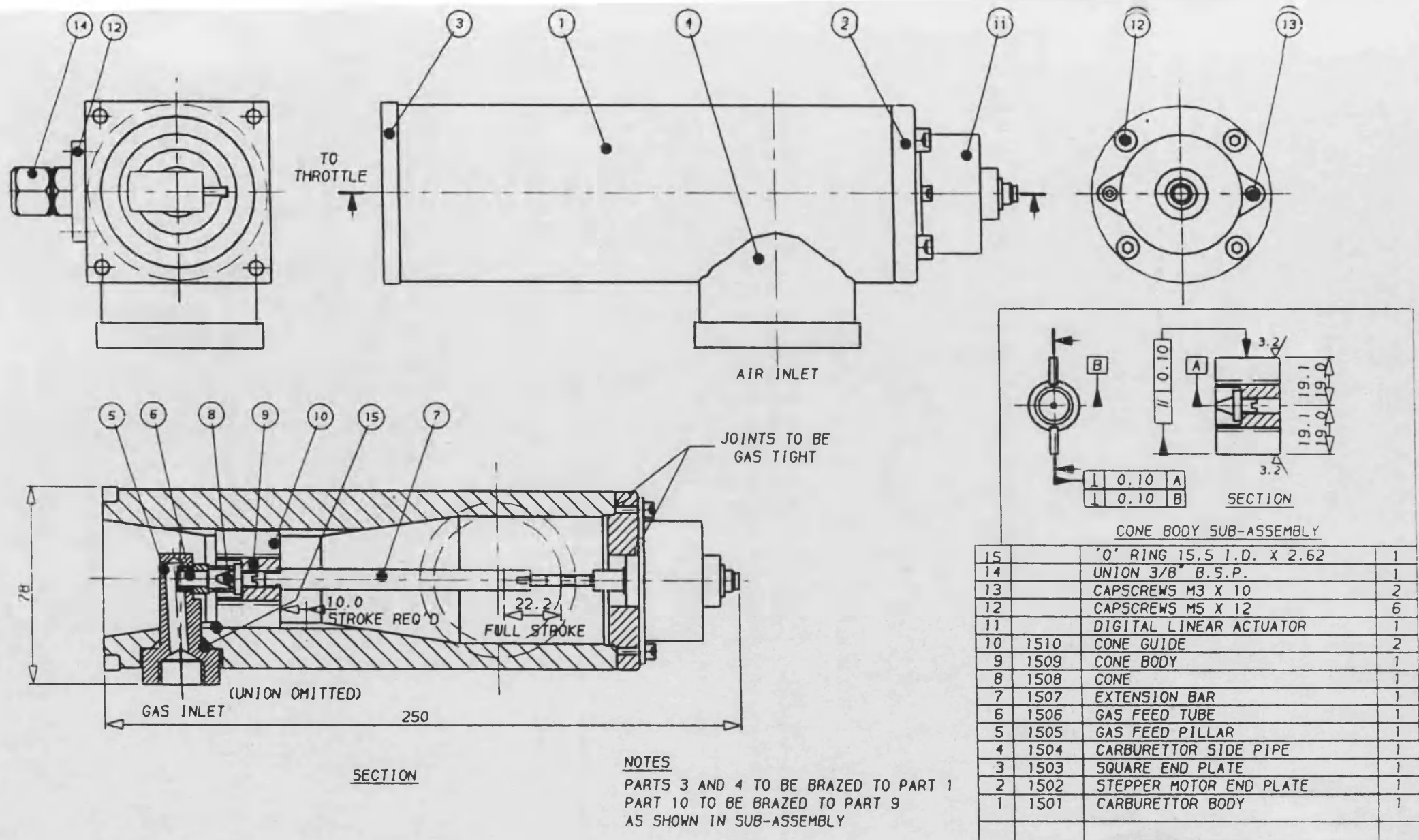


Figure 7.4 Main Chamber Gas Mixer



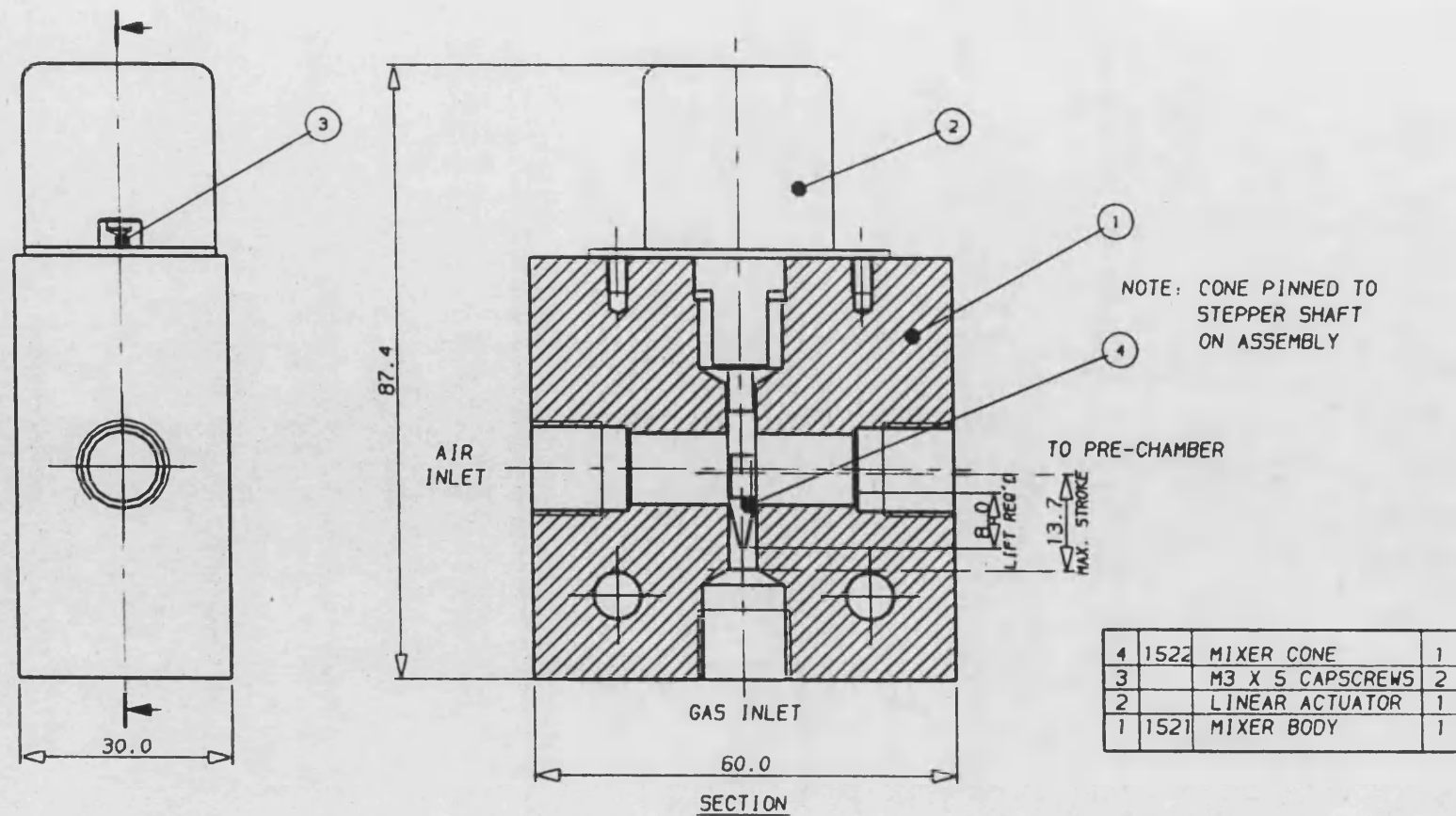


Figure 7.5 Pre-chamber Gas Mixer

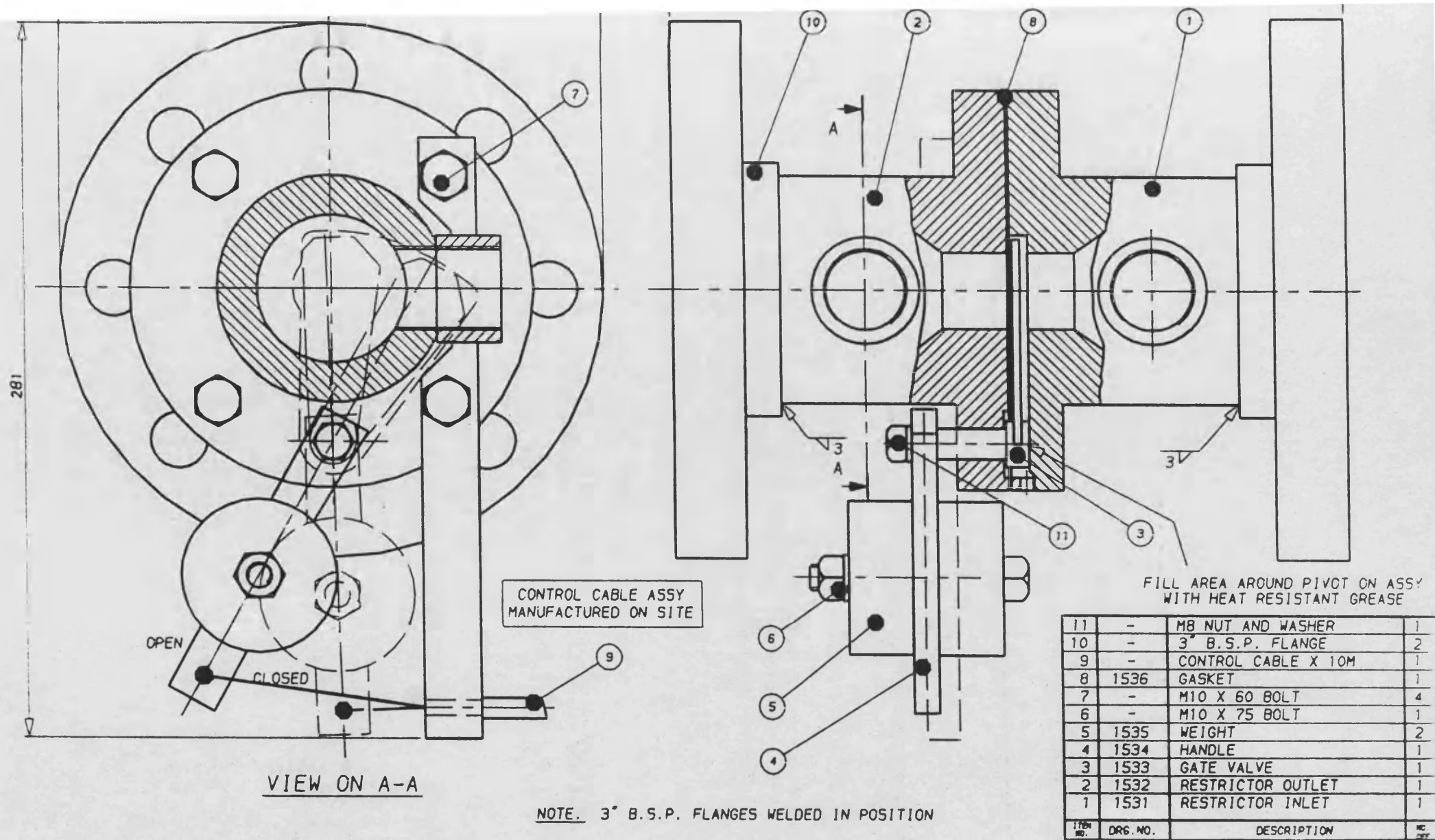


Figure 7.6 Exhaust Gate-Valve Assembly

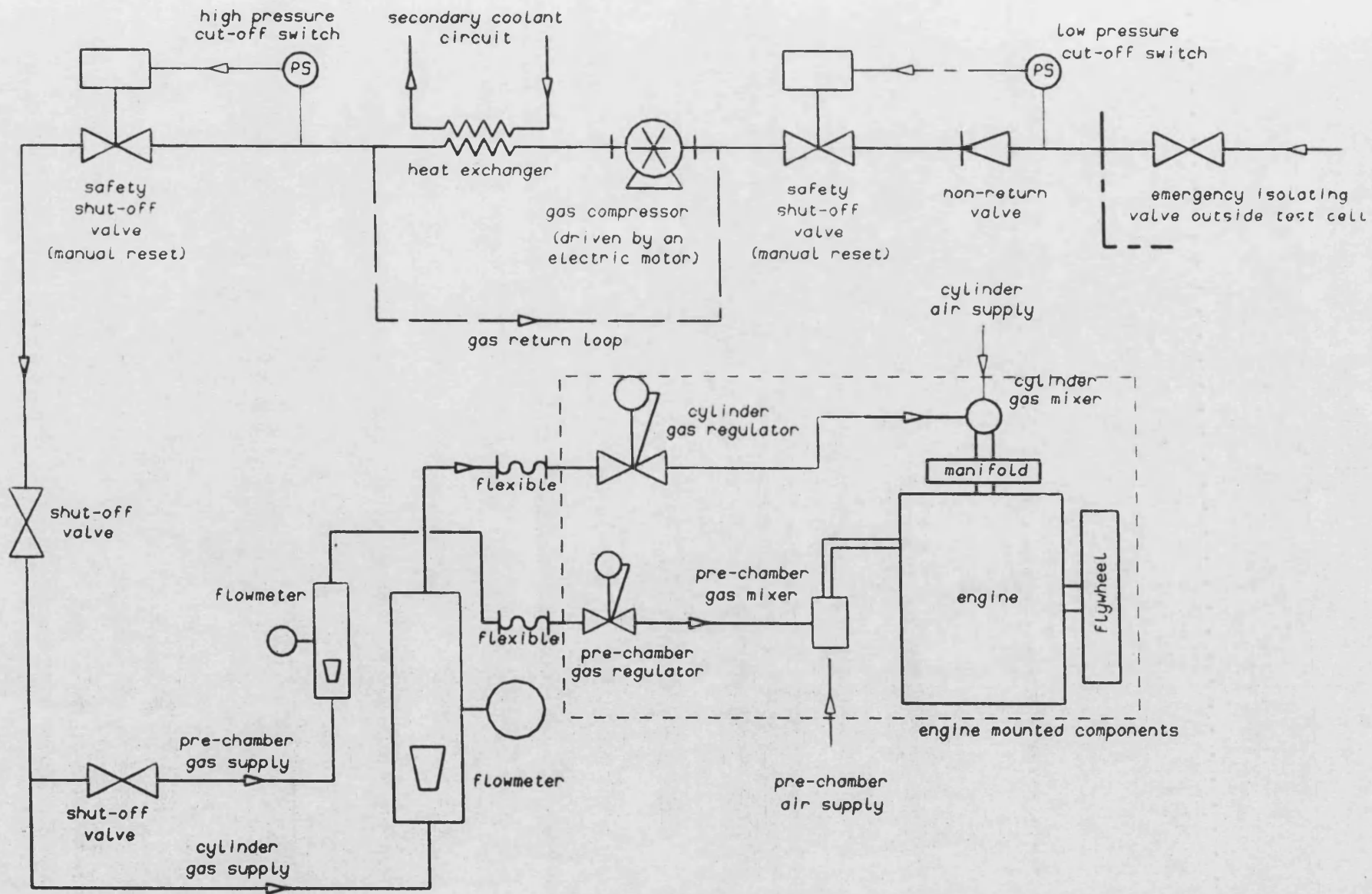


Figure 7.7 Natural Gas System

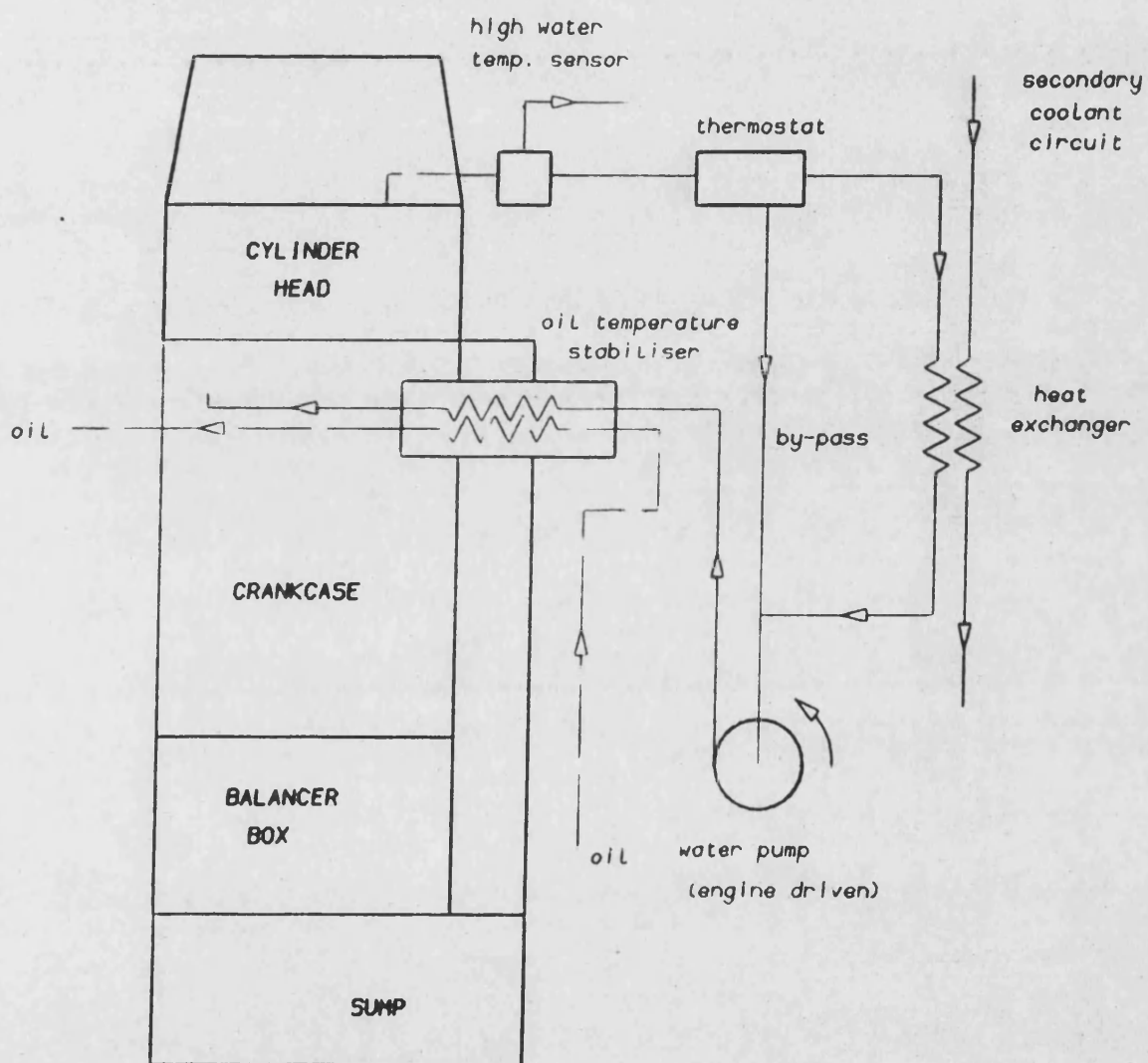
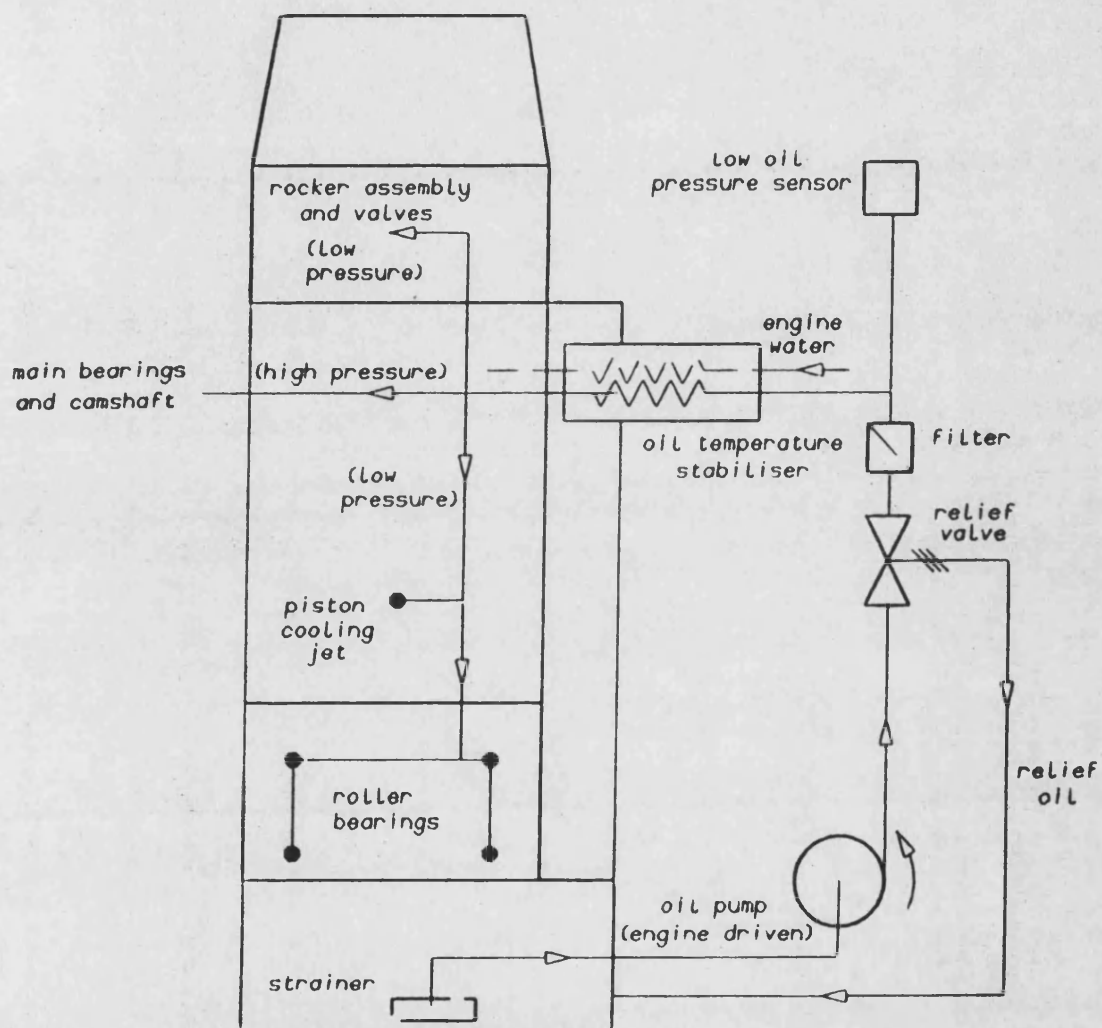


Figure 7.8 Engine Coolant System



Note. All oil drains back to the sump

On engine filter and relief valve  
are integral with the oil  
temperature stabiliser unit

**Figure 7.9 Engine Oil System**

# CHAPTER 8

## 8. Early Running Experiences of the 1SE Gas Engine

After completion of the design work and the manufacture of the engine, it had been hoped that there would be sufficient time towards the end of the project to allow limited commissioning of the engine, perhaps even a parametric study of the pre-chamber mixing process, guided by the earlier PHOENICS investigation. Ultimately, these goals were too ambitious, and only limited running of the engine took place. In total, running time on the gas engine has amounted to just four hours. (Only on one occasion did the engine run long enough for the thermostat to open). The time was used to gain confidence in the rig and installation, and to iron out the inevitable early problems. These experiences are discussed in this chapter: no formal results are presented.

### 8.1 Starting the Engine

One of the early concerns expressed was on the problem of starting the engine. As explained in chapter 7, the engine has two independently controlled gas/air mixers: each allowing a wide range of air-fuel ratios. Whilst this flexibility would offer many advantages in mapping the engine performance, it was felt that it could also make starting extremely difficult. Unlike a carburettor, they are not geared to maintaining a specific air-fuel ratio and so until the engine is running there is no means of knowing the relative proportions of gas and air. Once the engine has started then the air-fuel ratio may be determined from the readings on the flowmeters. The setting of the correct air-fuel ratio, particularly to the main chamber, was considered critical if the engine was to start successfully. (Initially only gas would be admitted to the pre-chamber, as on the Dorman 6SE gas engine).

Fortunately, the engine proved unexpectedly easy to start. Under naturally aspirated conditions, starting was achieved by feeding pure gas to the pre-chamber, with just air introduced into the cylinder.

Any attempt to add a tiny fraction of gas with the main chamber air, once the engine was running, caused the engine to stall, suggesting that the engine was operating very close to the rich limit. Nevertheless, the engine always started reliably under these conditions and would continue to idle, if somewhat unevenly, between 350 and 400 rpm.

## 8.2 Operation of the Mixers

The successful operation of both the pre-chamber and main chamber mixers is essential if the engine performance is to be mapped over a wide range of air-fuel ratios. First attempts to alter the mixer settings resulted in both cones becoming jammed. The faults were soon rectified by removing burrs and sharp edges left over from machining, but the sticking of the mixers did serve to highlight an early problem. With no indication of the position of the cone, movement could only be detected by the readings on the flowmeters.

This was fraught with difficulties. The flows, especially to the pre-chamber, oscillated wildly at low speeds. This is very much a function of the opening and closing of the disc valve in the pre-chamber. (A reservoir tank - capacity 0.7 litres - was later added to the pre-chamber gas supply, but resulted in only a marginal improvement). Also, with no load, the gas flow into the main chamber hardly registered on the flowmeter. It was easier to detect the effect of altering the mixer settings by carefully monitoring the engine response.

From idle, the engine speed could apparently be increased, without load, by solely increasing the boost pressure of the air. (To simplify the engine operation the governor-actuator controlling the throttle position was disconnected and the throttle held in a fixed position). Under these conditions it was impossible to tell whether main chamber gas was also being admitted because, as stated earlier, the flow was too small to register on the flowmeter. It could have been that gas was "leaking" into the mixer, despite the cone being in



the closed position, since as a function of the regulator, an increase in boost pressure causes a corresponding rise in the gas pressure. Ultimately, a point was reached where further increases in boost resulted in no further speed rise, and if continued caused the engine to misfire; perhaps suggesting that a lean limit had been reached in the pre-chamber. To raise the speed further, now required a definite input of main chamber gas each time, though in very small proportions (equivalent to a single step of the stepper controller). Too large a movement and the speed would fall away. By carefully balancing the requirements of gas and air the engine was run up to a maximum speed of 1000 rpm. It was thought unwise to go beyond this under no-load conditions.

In contrast with the main mixer, relatively large movements were required in the position of the pre-chamber cone setting before any change was detected in the engine's response. When admitting gas and air into the pre-chamber the total flow appeared to remain constant, such that a reduction in gas flow was balanced by an increase in air flow. This is perhaps to be expected since the pre-chamber has a fixed flow capacity at any given speed.

Despite the early problems the mixers performed satisfactorily, though they could be improved if feedback was introduced on the cone positions. This would afford greater confidence when controlling the mixers and enable a degree of repeatability.

### 8.3 Engine Load

The limited test period did not allow more than a cursory examination of the engine under load. Certainly no attempt was made to run at targeted ratings (approx. 50kW at 1500 rpm). In any case results taken at this stage would be unreliable. In setting up the installation the secondary water circuit was plumbed to both heat exchangers (gas and engine) and the dynamometer. As a consequence, the valve settings to the heat exchangers adversely affected the flow to the dynamometer. This led to load settings drifting and at one

stage it became impossible to add load at all. The solution is clearly to link the dynamometer to a separate supply.

Under load the engine ran to a maximum speed of 1135 rpm with a power output of 12kW. From a no-load condition the speed was adjusted, as before, by carefully controlling the boost air pressure and main chamber gas mixer. Vibration appeared well contained. Any gross inaccuracies in the reciprocating balance calculations should have been apparent at the higher speeds.

Generally, the present dynamometer facility is unsatisfactory. The load control appears rather insensitive and has to be done from within the test-cell.

#### **8.4 Engine Shut-down**

For safety reasons, shut-down of the engine is achieved not by grounding the spark, as on a car engine, but by isolating the gas supply. Thus, no matter whether the shut-down is under controlled conditions or through detection of a fault, the solenoid valves are closed and the compressor stopped. Ignition is allowed to continue. This is to ensure that the engine and installation is completely purged of possible combustible mixtures.

During testing the engine was shut down frequently; generally in a controlled manner, though the safety system was occasionally tripped by a fault. This was invariably the oil pressure, when an incorrect mixture setting caused the engine speed to fall below the critical level for the oil pump to provide sufficient pressure. When the engine did shut down, it was by no means instantaneous. It took over 30 seconds. This appears inordinately long, but is due to the combination of the volume of gas in the pipework, after the solenoid valves, which the engine continues to draw in and burn, and the large flywheel inertia. Isolating valves sited closer to the engine would reduce the run down time but at the cost of leaving large quantities of gas trapped in the installation.

## 8.5 Acquisition System

The PC based AIMS acquisition system was used, at this stage, only to log the cylinder pressure but, in future, it is intended that it will be a key element in the instrumentation of the rig. Initial reactions to the system were favourable: it being easy to use and commendably quick to understand.

The signal from the pressure transducer was fed to a charge amplifier which was linked to the A/D card in the computer. Processing of the signal, however, was unreliable. This was due to the absence of a reliable trigger. Normally, the signal from a crankshaft encoder is used but here an internal trigger had to be employed. This relied on detecting a certain signal condition. Various modes were tried: scanning for a voltage level, a particular slope condition, or continuous triggering (as on an oscilloscope), but results proved generally erratic.

To calibrate the signal properly, it is necessary to know not only the charge amplifier conversions but also the signal base-line position, to enable the trace to be positioned correctly on the vertical axis. Some early results are shown in figures 8.1-8.5. The pressure values are, at best, estimates using the charge amplifier calibrations and a knowledge of the compression ratio. (The curves have been aligned vertically by assuming the cylinder pressure just prior to the exhaust valve closing is equal to atmosphere. The crank positions were calculated from the engine speed and the estimated position of the peak compression pressure).

For future work these problems can be readily overcome. A crankshaft encoder will provide consistent triggering, as well as allowing the pressure trace to be displayed accurately against crank angle. A simple manometer to measure the manifold pressure will enable the correct base level to be set; making the assumption that pressure through the gas exchange process is approximately equal to the manifold pressure.

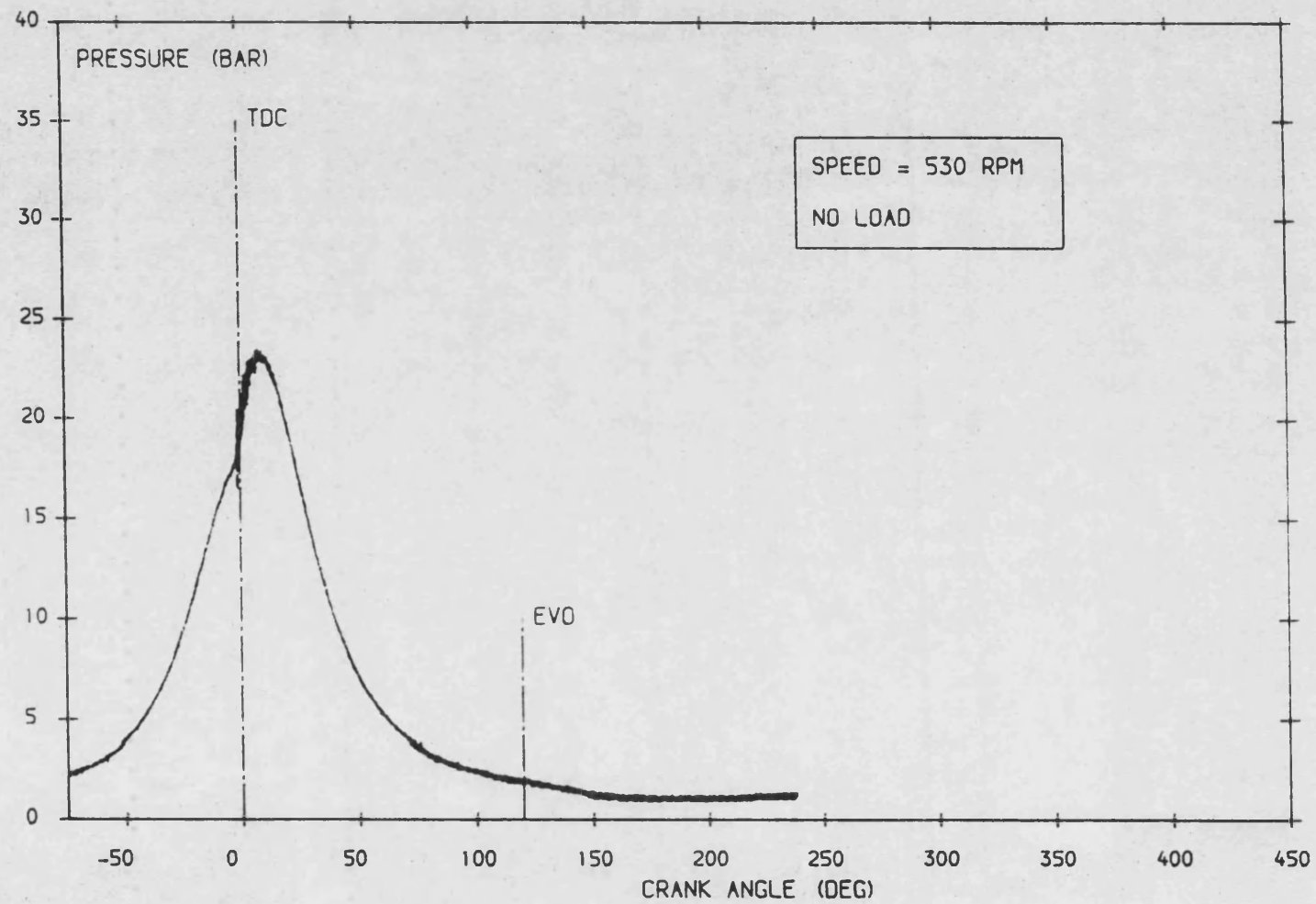


Figure 8.1 Experimental Cylinder Pressure Measurement  
at 530 RPM under No-Load Conditions

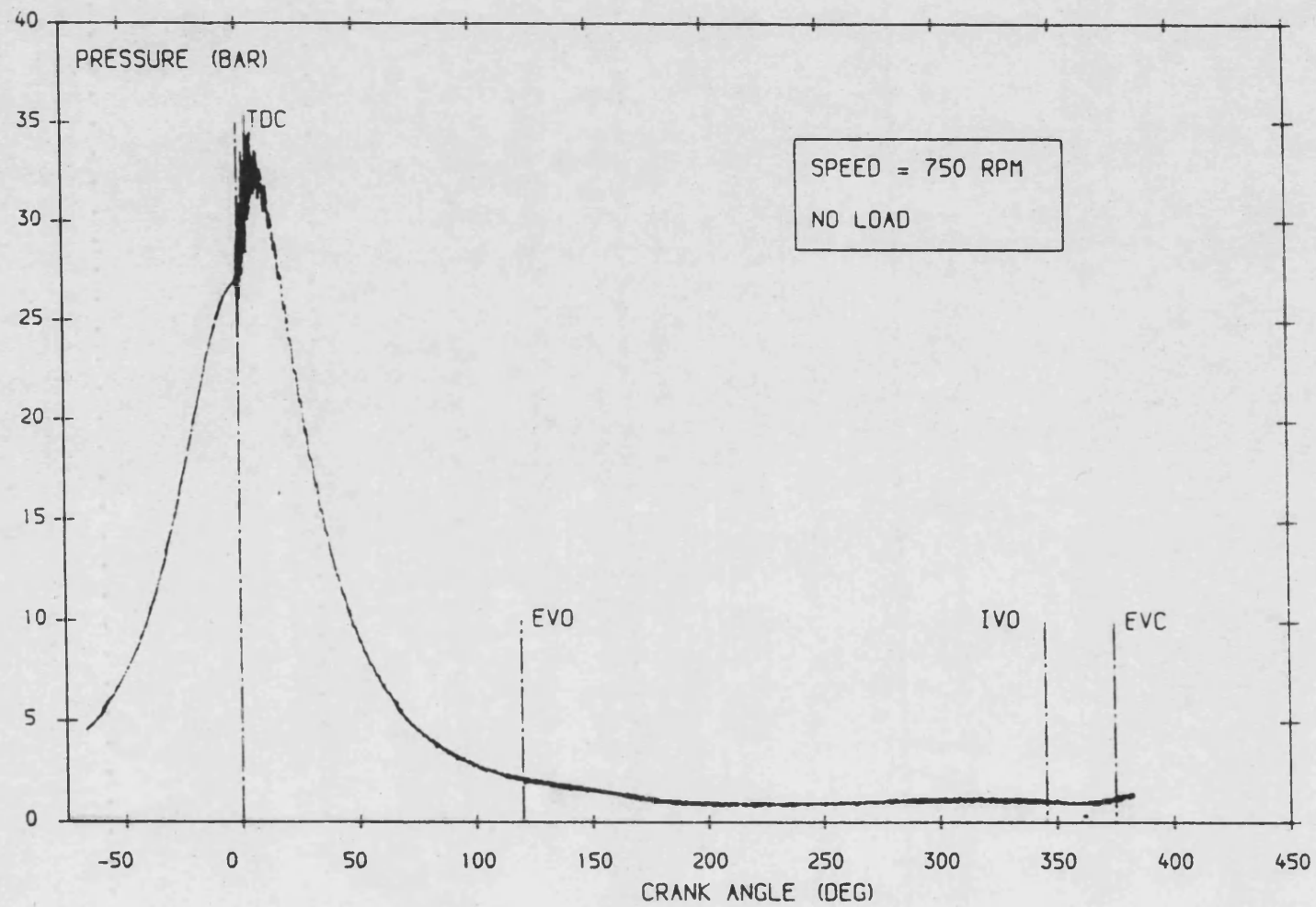


Figure 8.2 Experimental Cylinder Pressure Measurement  
at 750 RPM under No-Load Conditions

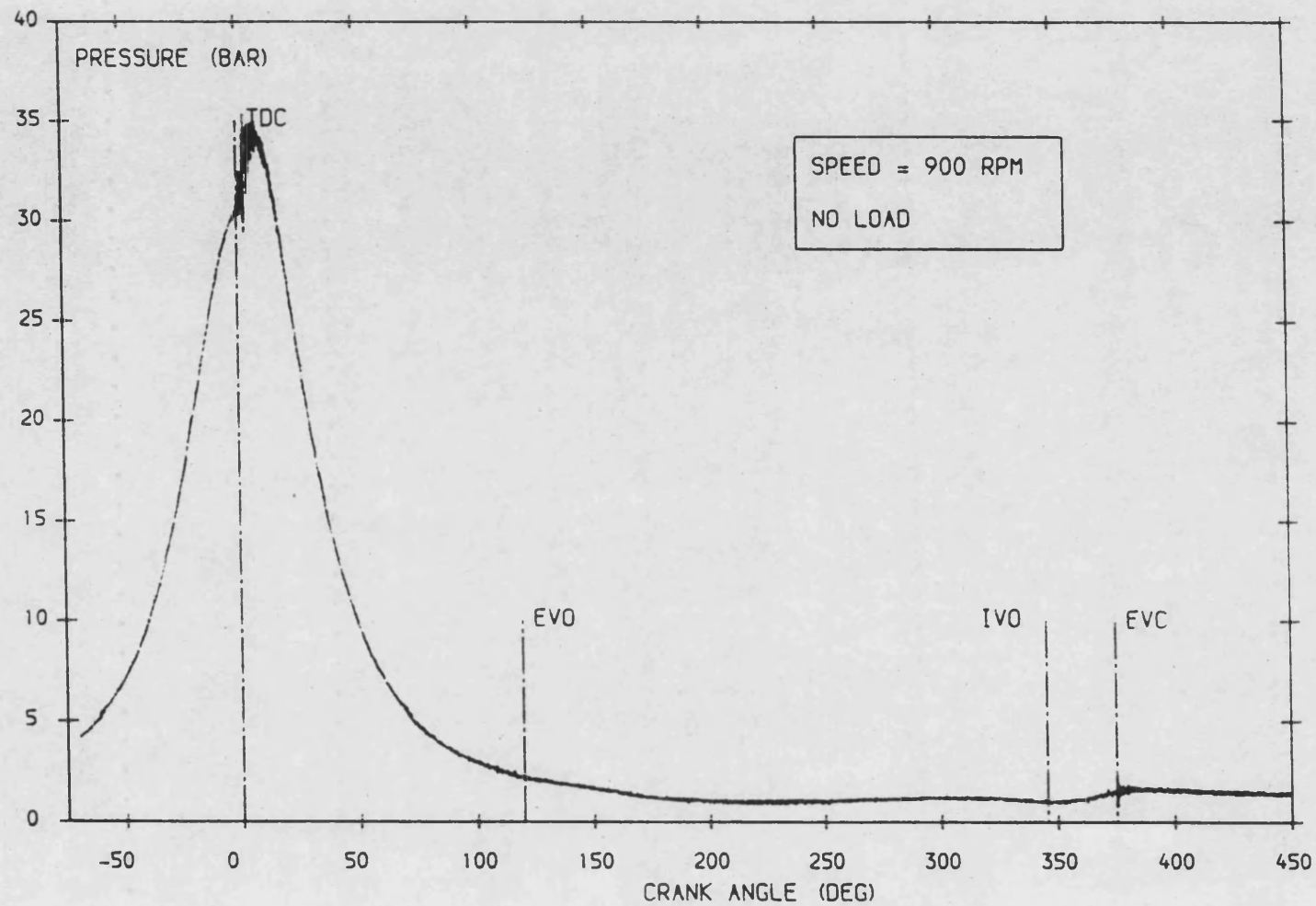


Figure 8.3 Experimental Cylinder Pressure Measurement  
at 900 RPM under No-Load Conditions

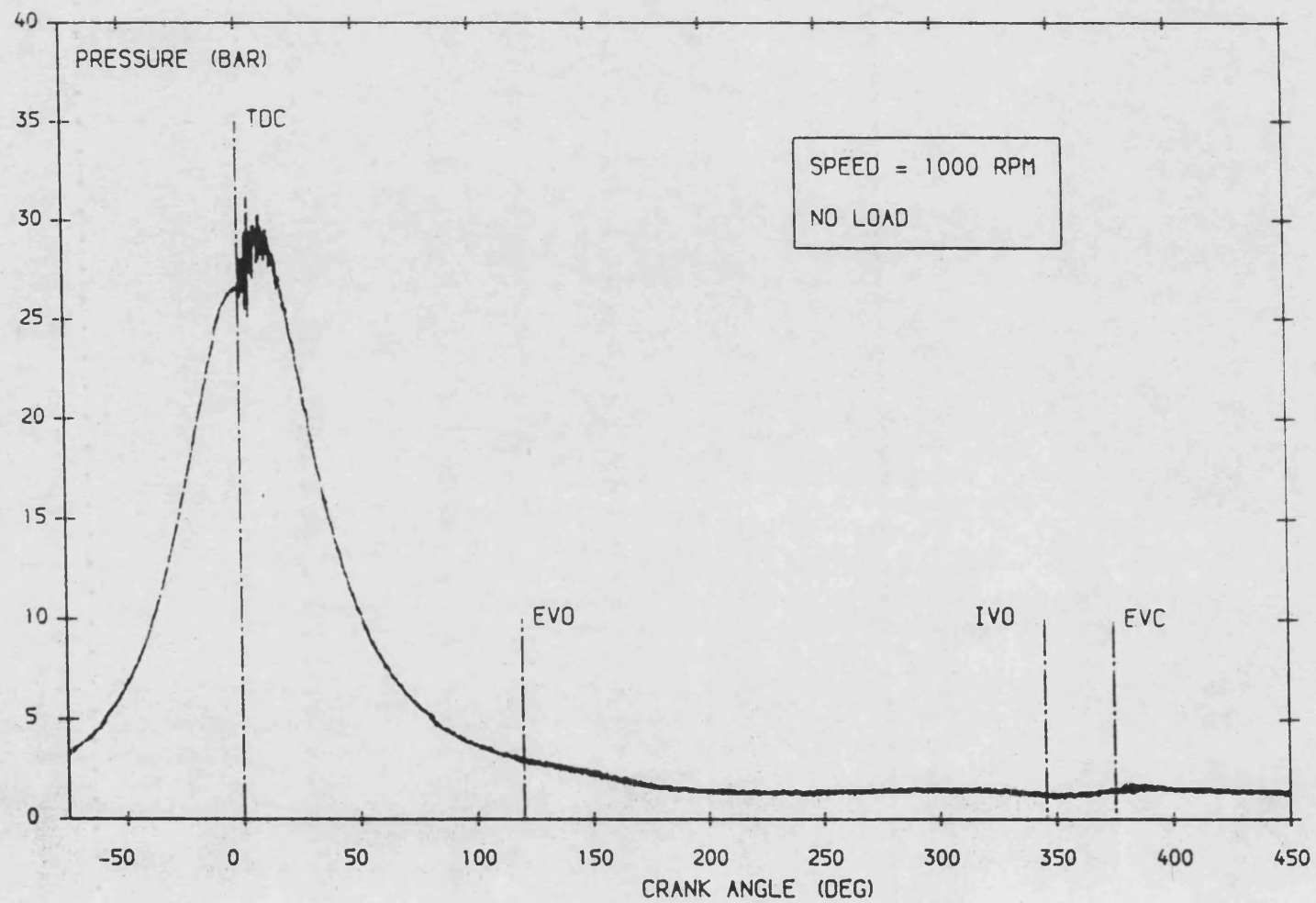


Figure 8.4 Experimental Cylinder Pressure Measurement  
at 1000 RPM under No-Load Conditions

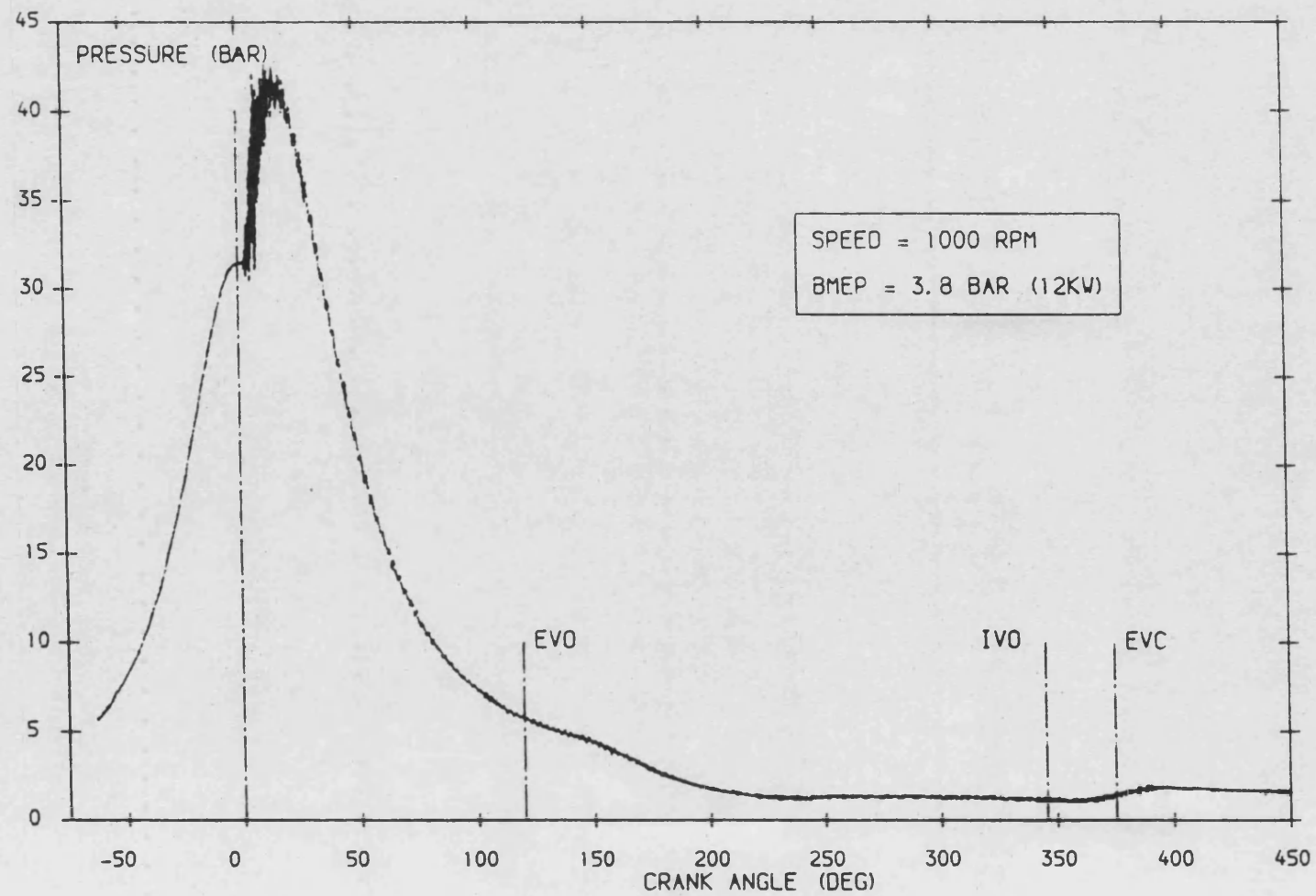


Figure 8.5 Experimental Cylinder Pressure Measurement  
at 1000 RPM under Load (BMEP = 3.8bar)



# CHAPTER 9

## **9. Discussion and Conclusions**

Three years after the commencement of the project the design and manufacture of two single cylinder research engines has been completed. At the time of writing early installation work on the natural gas version of the engine at the University has just finished. A diesel version, refer to figure 9.1, is currently being installed on the Dorman development test-beds at Stafford. Commissioning of the two engines is still to take place. This final chapter reviews the progress made in the three years, and recommends areas for future work. Brief conclusions are presented at the end.

### **9.1 Discussion**

The discussion is broken into three areas: the CASE Project, under which the single cylinder engine was designed; the MEDUSA system which has been used extensively during the design; and the CFD code PHOENICS.

#### **9.1.1 CASE Project**

The initial brief of the CASE project centred on the design and manufacture of a single cylinder research engine. This objective has been met and so the project can be concluded a success. Unfortunately, other goals have only been partially achieved. It had been hoped to undertake a full experimental test program; instead, only a few running hours have been logged. It might be suggested that this was inevitable. Initial estimates set aside 12-15 months for the design. This was an educated guess: it being difficult to foresee likely problems that might arise.

Design work on the engine did not start in earnest until January 1985, though the majority of the time prior to this was spent assessing the most appropriate balancing solution for the single cylinder engine. By July 1985 the need arose for the engine to run

as a gas engine, due to Dorman's decision to develop a lean burn natural gas version of the 6SE engine. (The initial design brief had suggested only a diesel version, which would be used for investigation of high BMEP operation). This came as the overall design for the engine, in diesel form, was nearing completion, although there was still much detailed component work to be done. The requirement for the gas engine, though not necessitating any major re-working of the design, did result in more design work. To a certain extent the arrival of the gas option was beneficial in that it caused a re-assessment of the design and has ensured the design of a flexible research tool - an engine which may be readily adapted to run either in diesel or gas form. As a result the design work took longer than expected.

Initial fears that the physical distance between the company and the University might lead to problems in communication proved unfounded. The atmosphere during the visits to the company was informal and friendly. Access to the required technical information was excellent and the visits always proved very productive. (Undoubtedly, this was largely due to Dr. S.J. Charlton (project supervisor) being a past employee of the company and so contacts were already well established). Their helpfulness, it could be argued, was to be expected: they commissioned the design of the engine and so it was in their interests. This, however, tends to overlook the role of the people involved in running the company on a day to day basis.

This was important because, in some ways, design of the 1SE did not fit easily into the company control structure. This is largely due to the engine not being completely designed in-house. This meant that there was little formal checking of drawings before release. Also, with the need to ensure fairly rapid manufacture of the engine, to try to allow some useful research work to be done within the three year period, supervision of major components fell to one or two key personnel within the company, who were closely involved with the design work from the start. This allowed decisions to be taken quickly, when necessary, and so to a certain extent by-passed the formal production control system.

This did not mean, however, that there was no control of the engine's manufacture within the company. In fact, a fair degree of time was spent drawing up the engine build list - complete listings of all components for the engine, right down to the nuts and bolts. Also once a drawing had been issued, alterations thereafter had to follow the company control procedure; alteration notification, drawing issue change and then issue of the updated drawing. In some cases, assembly drawings had to be altered because in their original form they could not be entered into the production control system.

#### **9.1.2 MEDUSA CAD System**

After development, at a drawing board, of initial layouts and design sketches, all subsequent component drawing and detailing was carried out using the MEDUSA CAD system. In retrospect, it is tempting to suggest that the design for the single cylinder engine would have been too large an undertaking, in the time-scale envisaged, without the use of MEDUSA. Towards the end of the project the sheer number of component drawings required would have severely diluted the challenge and interest that the design offered. Perhaps more significantly was the way the designs were evolved. Neat and accurate drawings were required if the designs were to be assessed properly by the design and production staff at Dorman. Their comments were important, especially as the company would be manufacturing the engine. Any alterations were marked on the drawings to be updated later using MEDUSA. Time consuming alterations and complete re-draws were thus avoided. The use of symbols to transfer drawing information from one sheet to another sheet - for example, hole positions on mating parts - also helps to avoid errors that can arise when components are re-constructed manually, in what might be termed the 'old-fashioned' paper and pencil method.

Beyond the presentation of neat and accurate drawings the other major benefit of the system was as a design tool. The advantages of being able to determine the geometric properties of the balancer shafts and

crankshaft assembly using the integrated solid modelling facility are obvious. Whilst the MEDUSA models of the balancers served merely as a check for the balancer weight designs - their shapes being easily defined geometrically - the model of the crankshaft was fundamental to the design of the crankshaft balancer weights and the achievement of full rotational balancer. Its success was demonstrated when the crankshaft and balance weights were assembled and dynamically balanced.

In general, few problems were encountered with the system. With little experience of MEDUSA within the School at the start of the design work, the initial learning process was slow. The two problems that did arise were fairly minor: an untidiness when using a particular dimensioning style; and having to store each drawing sheet under an unique name. This last point only arises when a complicated component is detailed on more than one sheet. Commonly, in such cases, each sheet would have the same drawing number, but be referred to individually by its sheet number, e.g. sheet 1 of 3. The solution, within MEDUSA, was to add a simple suffix to the drawing number, so that whilst stored separately the drawings could be recognised as belonging together.

In common with all CAD workstations, MEDUSA offers automatic dimensioning; the user only needs to specify where the dimensions are to appear in relation to the component and then pick the points to be dimensioned. A variety of dimensioning styles are available. The accuracy of the dimensions displayed is controlled by fixing the number of decimal places, though is ultimately governed by the input data. To exploit the automatic dimensioning it is usual to put all features to scale. This can lead to a lack of clarity in drawings; radii and chamfers can be difficult to see. In such circumstances on a drawing-board, a certain amount of draughtsman's licence would apply; the features being drawn enlarged to ensure they are clear.

These fairly minor problems apart the MEDUSA system has proved itself to be a very useful draughting tool and design aid. The advantages of its use were perhaps demonstrated by the general ease with which

the single cylinder engine could be assembled, though much of the credit for this, of course, is due to the guidance and supervision of the design and production staff.

### 9.1.3 The PHOENICS CFD code

On conclusion of the design work, i.e. during the time the engine was being manufactured, a theoretical investigation, using the PHOENICS code, was undertaken into the pre-chamber mixing process. In all, the study lasted six months. Initial reactions to using the code were unfavourable. Access to the program was via two main-frame computers which not only required learning two operating systems but also resulted in slow turn around times when submitting jobs. Also from an engineer's viewpoint, when using the PHOENICS code, the user is presented with too much FORTRAN coding. Rather than being able to use interactive pre-processing, as found on the latest finite element packages, the user is required to enter coding directly into the program to define the geometry and boundary conditions of the problem - refer to chapter 5. In fairness it should be said that the version installed at Bath is PHOENICS-81. The latest version (PHOENICS-84) has made advances to address this problem, but generally the CFD user still does not have the pre- and post-processing facilities of his finite element counterpart. Much of the problem can be attributed to the solution method and that the application of these codes is not so widespread.

The development of various models and the results obtained have been discussed in chapter 6. Whilst, at this time, the findings remain unsubstantiated, they did highlight the need for a gas/air mixture to be fed to the pre-chamber, enabling provision for this to be made on the rig, and have led to improved understanding of the mixing process. It would have been interesting to have been able to validate the model and thus assess the code as a design tool: perhaps by modelling different pre-chamber designs, though from the experiences so far this would not be easy.

## 9.2 Recommendations for Future Work

With the 1SE gas engine recently installed and less than four hours running achieved, the major requirement, in the next phase, is for a broad development program, to include commissioning of the engine and instrumentation. If the engine is to be used effectively in the development of the 6SE gas engine then it is important that the operating parameters are clearly defined. There is a particular requirement to map the performance of the induction and exhaust systems and to determine the frictional characteristics of the engine, if a sound basis for comparison with the 6SE is to be established.

The frictional overhead on a single cylinder engine, especially where primary and secondary balancers are employed, is large. Thus comparison of the performance of the 1SE with the six cylinder engine should be based on IMEP (or corrected BMEP), as opposed to actual BMEP which may be misleading. Investigation of the induction and exhaust systems is necessary if turbocharged conditions are to be properly scheduled in terms of temperature and pressure. An extended study of the transient conditions in the exhaust manifold could explore the effect of different orifice plate diameters and gate-valve settings. The mean pressure level and shape of the exhaust pulse play an important part during scavenging. By using a pressure transducer, capable of withstanding the unfavourable conditions in the exhaust manifold, and a high-speed data acquisition system it may be possible to match exactly exhaust conditions on the single to those of the 6SE.

An experimental parametric study, guided by the PHOENICS work, into the mixing process within the pre-chamber would provide Dorman with useful feedback. Initially data would be limited to gross performance parameters, such as fuel consumption, air consumption,  $\text{NO}_x$  levels and power. To be able to validate the predictions of the PHOENICS model, then access inside the pre-chamber is required. One method would be to link the pre-chamber (and cylinder) to a gas sampling valve, to allow distinct mixture samples to be taken over a

few degrees of crank angle. By linking the valve to a hydrocarbon analyser it should be possible to determine the gas concentrations in the two chambers prior to combustion. However, gaining access to the pre-chamber could prove to be an obstacle, and it would be difficult to ensure that samples obtained were global rather than localised values close to the sampling region. If met with success, the results could be used to improve the existing PHOENICS model. From here it might be possible to develop the model to incorporate combustion in the pre-chamber and cylinder, and thus use it to predict emission levels, particularly  $\text{NO}_x$ . With the present version of PHOENICS this might prove to be too ambitious.

A further route to obtaining in-cylinder data would be to design an "optical" head. Used in conjunction with a high speed camera, a suitable design could offer valuable insight; providing, at least, a qualitative appreciation of both the transfer of the flame from the pre-chamber and the flame propagation through the lean mixture. One possible solution to the layout of the optical head would be to exploit the design of the production head which has two exhaust and two inlet valves. Removal of an exhaust valve would have little effect on the mixture prior to combustion, and the space created could be used to house a quartz window, mounted flush with the cylinder head. Any proposed solution would have to address the problems of sooting and durability, and enable the light generated by the flame to be directed back to the camera.



### 9.3 Conclusions

- A single cylinder engine based on the Dorman 6SE engine range has been successfully designed. Two versions (gas and diesel) have been built.
- Early running experiences of the lean burn natural gas version at the University have been encouraging, and suggest the engine will be an invaluable research tool. (The diesel version is still being installed at Dorman Diesels Ltd).
- The use of the MEDUSA CAD system during the design was invaluable; saving time and proving an effective design tool.
- A pre-chamber mixing model has been developed using the CFD code PHOENICS. Results from the model suggest that the pilot supply to the pre-chamber needs to be a gas/air mixture, rather than the current pure gas supply used by the company, if the initiation of combustion is to be reliable and stable.
- The CASE award has been both challenging and rewarding, with liaison between the company and University being excellent.

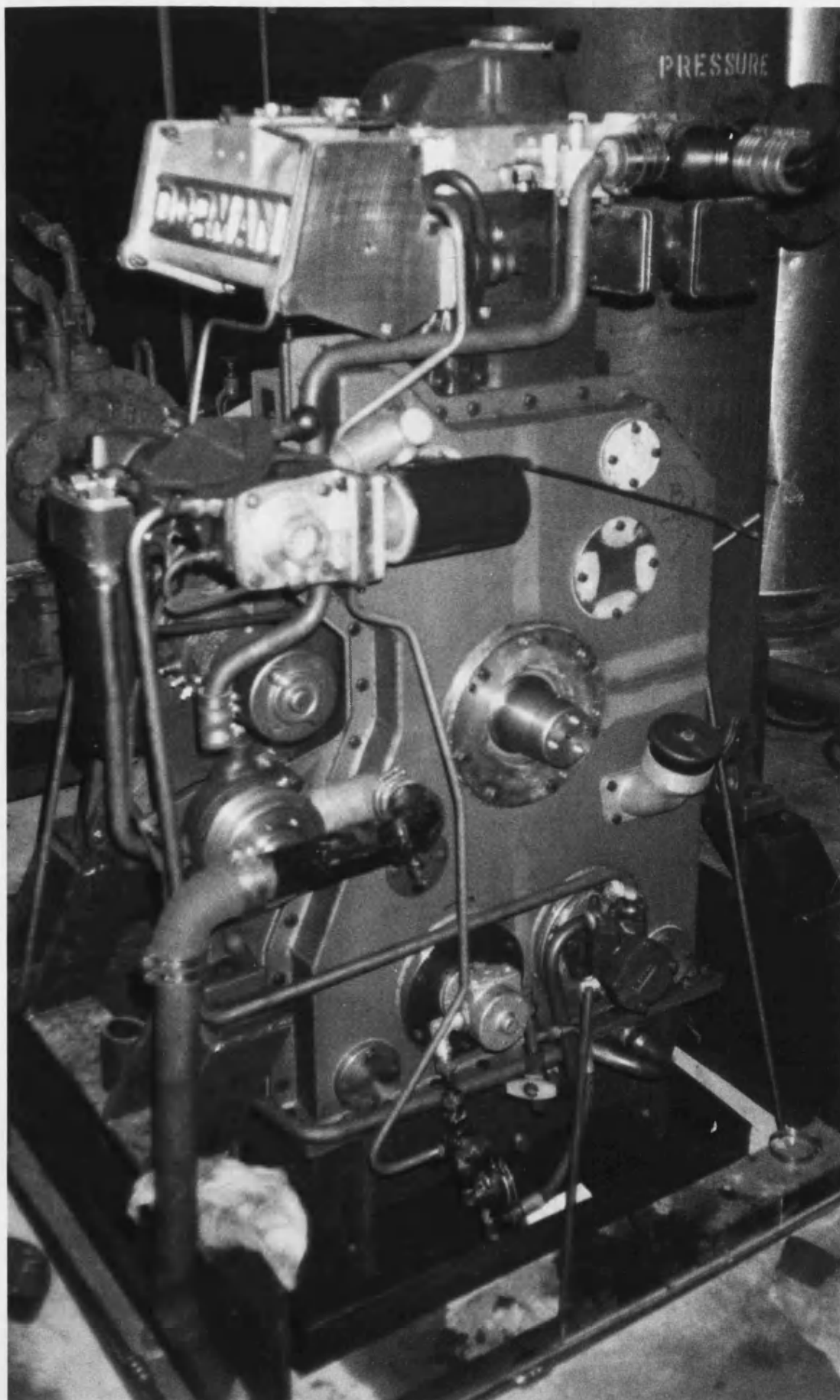


Figure 9.1 Diesel Version of 1SE Engine at Dorman Diesels Ltd.

# REFERENCES

## References

- (1) PACHERNEGG S.J.  
*"Experimente am Einzylinder-Motor zur Entwicklung von Dieselmotoren mit hoher Aufladung und hoher Drehzahl"*  
MTZ 32 (1971) 10
- (2) McKENZIE E.M.J. and DEXTER S.G.  
*"The Use of a Single Cylinder Test Engine for Research and Development of Medium Speed Diesels"*  
Ricardo DP 82/1667 UNRESTRICTED
- (3) HARKNESS J.R.  
*"Methods of Balancing Single Cylinder Engines"*  
SAE 680571
- (4) FRENCH C.C.J., TAYLOR D.H. and MUNDAY C.F.  
*"A New Research Engine for High BMEP Running"*  
International Symposium on Marine Engines, Tokyo, Japan  
Technical Paper, 1973 Session 11 pp. 15-26
- (5) GRIFFIN J.R. and WITTEK H.L.  
*"Versatile Single-Cylinder Diesel Test Engine for Lubricant, Emissions and Fuel Research"*  
SAE 730831
- (6) FRENCH C.C.J.  
*"A Universal Test Engine for Combustion Research"*  
SAE 830453
- (7) CHEN S.K and FLYNN P.F.  
*"Development of a Single Cylinder Compression Ignition Research Engine"*  
SAE 650733

- (8) ROCA J., BELOTTO J.M. and SUNE M.  
*"Design of a Single Cylinder Engine with 350 mm Piston Diameter for the Improvement of an Existing 8-Cylinder Engine In-line"*  
International Congress on Combustion Engines  
11th Proceedings, 1975 Vol. 2 pp. 911-940
- (9) MARSEE F.J. and OLREE R.M.  
*"Distribution Factors that Influence Emissions and Operation of Lean Burn Engines"*  
IMechE 1979 C99/79
- (10) QUADER A.A.  
*"What Limits Lean Burn in S.I. Engines - Flame Initiation or Propagation?"*  
SAE 760760
- (11) MAY M.G.  
*"The High Compression Lean Burn Spark Ignited 4-Stroke Engine"*  
IMechE 1979 C97/79
- (12) MATTAVI J.N., GROFF E.G. and MATEKUNAS F.A.  
*"Turbulence, Flame Motion and Combustion Chamber Geometry - Their Interactions in a Lean Combustion Engine"*  
IMechE 1979 C100/79
- (13) GRUDEN D. and HAHN R.  
*"Performance, Exhaust Emissions and Fuel Consumption of an I.C. Engine operating with Lean Mixtures"*  
IMechE 1979 C111/79
- (14) YAGI S., FUJII I., AJIKI Y. and TSUDA T.  
*"The Antiknock Quality in the Stratified Charge Engine with Auxiliary Combustion Chamber"*  
IMechE 1980 C395/80

- (15) NAGAO A. and TANAKA K.  
*"The Effect of Swirl Control on Combustion Improvement of Spark Ignition Engines"*  
 IMechE 1983 C54/83
- (16) HUGELMANN R.D.  
*"Recent Developments in Swirl Induced Turbulent Mixing for 4-Stroke Cycle Engines"*  
 SAE 820150
- (17) PISCHINGER F. and ADAMS W.  
*"Influence of Intake Swirl on the Characteristics of a Stratified Charge Engine with Pre-chamber Injection"*  
 IMechE 1980 C391/80
- (18) WHITELOW J.H. and VAFIDIS C.  
*"Intake Valve and In-cylinder Flow Development in a Reciprocating Model Engine"*  
 Proc Instn Mech Engrs Vol 200 No C2 41/86
- (19) GERMANE G.J., WOOD C.G. and HESS C.C.  
*"Lean Burn Combustion in Spark Ignited Internal Combustion Engines - A Review"*  
 SAE 831694
- (20) DAGLISH A.G., HORSLER A.G. and ROBB F.F.  
*"Horse Power from Natural Gas - A New Market for a New Fuel"*  
 IHVE Conf Guide 1969
- (21) WHITEHOUSE N.D.  
*"Advances in British Dual Fuel and Gas Engines"*  
 Diesel, Dual Fuel, Gas Engine and Gas Turbine 1972 publ. 353
- (22) McJONES R.W. and CORBEIL R.J.  
*"Natural Gas Fuelled Engines have Lower Exhaust Emissions"*  
 SAE Journal June 1970 Vol 78 No 6

- (23) TESAREK H.  
*"Investigation Concerning the Employment Possibilities of the Diesel-Gas Process for Reducing Exhaust Emissions, especially Soot (Particulate Matters)"*  
SAE 750158
- (24) ADAMS T.G.  
*"The Development of Ford's Natural Gas Powered Ranger"*  
SAE 852277
- (25) DING X. and HILL P.G.  
*"Emissions and Fuel Economy of a Prechamber Diesel Engine with Natural Gas Dual Fuelling"*  
SAE 860069
- (26) RAINE R.R. et al  
*"A Study of the Effects of Natural Gas Composition on Engine Performance, Emissions and Efficiency"*  
Int. Conf.: Gaseous Fuels for Transportation  
Vancouver, Canada August 1986
- (27) STEPHENSON J. et al  
*"Effects of Varying Fuel and Air Supply Condition on the Efficiency of Dual Fuelled Automotive Engines"*  
Inst. of Professional Eng'rs New Zealand  
Annual Conf Feb 1986
- (28) RAINE R.R., ELDER S.T. and STEPHENSON J.  
*"Efficiency, Emissions and Combustion Characteristics of Automotive Diesel Engines in Dual-Fuel Operation"*  
The Soc. of Automotive Eng'rs - Australasia  
Int. Conf. "Fossil Fuels - The End of an Era"
- (29) SHAIR F.H. and RUPE J.H.  
*"Nitric Oxide Emission Studies of Internal Combustion Engines"*  
JPL Quarterly Technical Review, Vol 1, No 2, July 1971

- (30) SERVE J. V.  
*"NO<sub>x</sub> Reduction on Large Bore Turbocharged SI Engines"*  
 ASME 82-DGP-16
- (31) NAGALINGAM B., DUEBEL F. and SCHMILLEN K.  
*"Performance Study Using Natural Gas, Hydrogen-supplemented Natural Gas and Hydrogen in AVL Research Engine"*  
 Int Journal Hydrogen Energy, Vol 8 No 9, pp. 715-720, 1983
- (32) WILSON (Jr) R.P., FOWLE A.A., RAYMOND W.J. and McLEAN W.J.  
*"Model for Nitric Oxide Formation in a Large-bore Spark Gas Engine"*  
 SAE 790293
- (33) KARIM G.A. and ALI I.A.  
*"Combustion, Knock and Emission Characteristics of a Natural Gas Fuelled Spark Ignition Engine with Particular Reference to Low Intake Temperature Conditions"*  
 Proc Instn Mech Engrs Vol 189, 24/75
- (34) WAUKESKA-DRESSER  
*"Update on Emissions"*  
 Product Bulletin January 1982
- (35) WILSON R.  
*"Cat Begin Introduction of Broad Gas Engine Line"*  
 Diesel and Gas Turbine World May 1986
- (36) Anon.  
*"Waukesha's Lean Combustion Gas Engine Moves to Market"*  
 Diesel and Gas Turbine World May 1986
- (37) Anon.  
*"New Gas Engine Combustion System for Delaval Enterprise"*  
 Diesel and Gas Turbine World March 1986



- (38) RHODES N.  
*"Streamlined Solutions to Fluid Flow Problems"*  
CME April 1986
- (39) KOJIMA M. and TAKATA H.  
*"Numerical Analysis of Flows in Reciprocating Engines"*  
JSME Vol 29 No 253 July 1986
- (40) SINDIR M.M.  
*"A Guide to the Computer Code LAST-STEP"*  
UMIST
- (41) LESCHZINER M.A.  
*"An Introduction and Guide to the Computer Code PASSABLE"*  
UMIST March 1982
- (42) SPALDING D.B. (CHAM Ltd.)  
*"A General-Purpose Computer Program for Multi-dimensional One and Two Phase Flow"*  
MACS North Holland Publ Vol XXIII pp 267-276 (1981)
- (43) CAFE (Computer Aided Flow Evaluation)  
Atkins Research and Development, Epsom
- (44) MOSS J.B.  
*"Modelling Combustion Chemistry for Practical Fuels in Engine Flowfield Computations"*  
IMechE 1987 C02/87
- (45) GOSMAN A.D. and JOHNS R.J.R.  
*"Computer Analysis of Fuel Air Mixing in Direct Injection Engines"*  
SAE 800091

- (46) GOSMAN A.D. and HARVEY P.S.  
*"Computer Analysis of Fuel-Air Mixing and Combustion in an Axi-Symmetric D.I. Engine"*  
 SAE 820036
- (47) GOSMAN A.D., WATKINS A.P. and AHMADI-BEFRUI B.  
*"Predictions of In-cylinder Flow and Turbulence with Three Versions of K- $\epsilon$  Turbulence Model and Comparison with Data"*  
 Proc ASME Winter Meeting 1984
- (48) ARCOUMANIS C. and WHITELOW J.H.  
*"Fluid Mechanics of Internal Combustion Engines - A Review"*  
 Proc Instn Mech Engrs Vol 201 No C1
- (49) GOSMAN A.D.  
*"Multi-dimensional Modelling of Cold Flows and Turbulence in Reciprocating Engines"*  
 SAE 850344
- (50) MATSUOKA S. et al  
*"LDA Measurement and a Theoretical Analysis of the In-cylinder Air Motion of a D.I. Diesel Engine"*  
 SAE 850106
- (51) IKEGAMI M., HORIBE K. and KOMATSU G.  
*"Numerical Solution of Flows in an Engine Cylinder (2<sup>nd</sup> Report, Flow in a Deep-bowl Combustion Chamber)"*  
 JSME Vol 29 No 248 Feb. 1986
- (52) BRANDSTAETTER W., JOHNS R.J.R. and WIGLEY G.  
*"The Effect of Inlet Port Geometry on In-cylinder Flow Structure"*  
 SAE 850499
- (53) SHAHED S.M., CHUI W.S. and LYN W.T.  
*"A Mathematical Model of Diesel Combustion"*  
 IMechE 1975 C94/75

- (54) SHAHED S.M., CHUI W.S. and LYN W.T.  
*"A Transient Spray Mixing Model for Diesel Combustion"*  
SAE 760128
- (55) WATKINS A.P. and KHALEGHI H.  
*"Three-dimensional Diesel Engine Spray Modelling"*  
IMechE 1987 C12/87
- (56) SHIRAKAWA S., OHSAWA K. and AOYAMA T.  
*"Simulation of Spray Combustion in an Axisymmetric Small Direct Injection Diesel Engine"*  
IMechE 1987 C01/87
- (57) MAKATOS N.C. and MUKERJEE T.  
*"3-dimensional Computer Analysis of Flow and Combustion in Automotive Internal Combustion Engines"*  
MACS XXIII(1981) pp. 354-366
- (58) BRASSOLI C., BODRITTI G. and CORNETTI G.M.  
*"Optimum Air Momentum and Spray Formation for D.I. Diesels"*  
SAE 850501
- (59) SORENSON S.C. and PAN S.S.  
*"A One-Dimensional Combustion Model for a Dual Chamber Stratified Charge Spark Ignition Engine"*  
SAE 790355
- (60) BENJAMIN S.F. and WEAVING J.H. (in assoc. with CHAM Ltd.)  
*"Development of a Mathematical Model of Flow, Heat Transfer and Combustion in a Stratified Charge Engine"*  
IMechE 1980 C403/80
- (61) KER WILSON W.  
*"Torsional Vibration Problems"*  
Chapman and Hall 1963

- (62) SENIOR G.S.  
*"GEC Dorman Diesels/University of Bath - Single Cylinder SE Diesel Engine 1500 rev/min"*  
Report Glacier Metal Company Ltd. Nov. 1985
- (63) LILLY L.R.C.  
*"Diesel Engine Reference Book"*  
Butterworths 1984
- (64) KER WILSON W.  
*"Vibration Engineering"*  
Chapman and Hall 1959
- (65) CURTIL R. and MAGNET J.L.  
*"Exhaust Pipe Systems for High Pressure Charging"*  
IMechE 1978 C50/78
- (66) CHARLTON S.J.  
*"SPICE (Simulation Program for Internal Combustion Engines) User Manual"*  
School of Mechanical Engineering, Bath, April 1986
- (67) KINGSTON-JONES M.G., MURRAY G.E. and THOMAS J.R.  
*"Dorman 6SE Engine Performance Predictions and Design Feasibility Studies"*  
Ricardo DP 85/1061 RESTRICTED
- (68) MAKATOS N.C., MUKERJEE T. and ROSTEN H.I.  
*"Calculation of the Air Flow in the Combustion Cavity of a Diesel Engine"*  
April 1982 PDR/CHAM/6
- (69) ALDHAM C.  
*"The PHOENICS Implementation of Boundary Conditions"*  
PHOENICS User Club Newsletter Issue No3 July 84

- (70) MASSEY B.S.  
*"Mechanics of Fluids - 4th Edition"*  
Van Nostrand Reinhold Company, Chapter 3, p 88
- (71) MASSEY B.S.  
*"Mechanics of Fluids - 4th Edition"*  
Van Nostrand Reinhold Company, Chapter 12, p 406
- (72) STEWART J.  
*"Torsional Vibration Calculations for Dynamometer Set"*  
Twiflex Ltd., September 1986

# APPENDICES

# APPENDIX 1

## Appendix 1: Connecting Rod Small and Big End Masses

In the balancing of an engine the contribution due to the connecting rod must be taken into account. However, whilst the piston follows a simple reciprocal motion, the locus described by the centroid of the connecting rod is far more complicated. It is therefore convenient, for calculation purposes, to consider the rod as having its mass concentrated at the small and big ends, such that the position of the centre of gravity remains the same.

Referring to figures A1.1 and A1.2 it is evident that by taking moments:

$$M_c a = (a + b) M_{se}$$

and  $M_c b = (a + b) M_{be}$

$$\therefore M_{se} = M_c \frac{a}{(a + b)}$$

$$\therefore M_{be} = M_c \frac{b}{(a + b)}$$

where  $M_c$  = mass of the connecting rod (kg)

$M_{be}$  = connecting rod mass attributable to the big end (kg)

$M_{se}$  = connecting rod mass attributable to the small end (kg)

$a$  = distance from centre of big end to the centroid (m)

$b$  = distance from centre of small end to the centroid (m)

Thus on determining the position of the centroid and knowing the mass of the connecting rod, the mass attributable to each end may be calculated.



# APPENDIX 2

## Appendix 2: Rotating Forces in a Single Cylinder Engine

If a single concentrated mass, attached by a thin arm such that it maintains a fixed radius, is rotated, a centripetal acceleration is imposed on the mass. The corresponding equal and opposite force, the centrifugal force, can be shown to be:

$$F = ma = mv^2/r = m\omega^2r \quad \dots A2.1$$

where  $F$  = centrifugal force (N)  
 $a$  = acceleration ( $m/s^2$ )  
 $v$  = tangential velocity of mass ( $m/s$ )  
 $r$  = radius of rotation (m)  
 $\omega$  = angular velocity (rad/s)

This is the force carried by the bearings due to the out-of-balance of the crank and big end. Thus for balance, a balancing mass  $M_B$ , at a radius  $r_B$  is required, placed opposite to the out-of-balance, such that:

$$\omega^2 M_B r_B = \omega^2 mr \quad \text{with } \omega^2 \text{ common this reduces to:}$$
$$M_B r_B = mr$$

From this it is evident that it is the product of mass and radius that is important not the individual values. In an engine it is not possible to place the balancing mass directly opposite the crankpin and so two masses are used; each equal and symmetrically displaced about the cylinder axis to avoid introducing an unwanted couple.

For a single cylinder engine the balancing moment  $M_B r_B$  is the sum of the products of the individual components which make up the total out-of-balance moment.

$$M_B r_B = M_{BE} r_{BE} + M_{PIN} r_{PIN} + M_{WEBS} r_{WEBS}$$

where  $M_{BE}$  = mass of big end (kg)

$r_{BE}$  = eccentricity of big end from the c'shaft journal (m)

$M_{PIN}$  = mass of the crankpin (kg)

$r_{PIN}$  = eccentricity of the crankpin (m)

$M_{WEBS}$  = mass of the webs (kg)

$r_{WEBS}$  = eccentricity of the webs (m)

Thus the out-of-balance moment of each single cylinder balance weight is  $0.5M_{BE}r_B$ .

# APPENDIX 3

### Appendix 3: Derivation of Engine Reciprocating Forces

Referring to figure A3.1, suppose the total reciprocating mass is  $M_{\text{RECIP}}$ ,  $L$  is the centre-to-centre distance of the connecting rod,  $R$  the crankthrow radius,  $y$  the displacement of the piston from top dead centre,  $\theta$  the angular movement of the crank from TDC, and  $\phi$  the connecting rod obliquity, then:

$$y = R + L - (R\cos\theta + L\cos\phi)$$

$$\text{but } R\sin\theta = L\sin\phi$$

$$\text{or } \sin\phi = (R/L)\sin\theta$$

$$\text{making } \cos\phi = \sqrt{1 - ((R/L)\sin\theta)^2}$$

$$\therefore y = R + L - R\cos\theta - L\sqrt{1 - ((R/L)\sin\theta)^2} \quad \dots A3.1$$

Expanding the expression equal to  $\cos\phi$  as a polynomial,

$$\cos\phi = 1 - \frac{1}{2}(R/L)^2\sin^2\theta - \frac{1}{8}(R/L)^4\sin^4\theta - \frac{1}{16}(R/L)^6\sin^6\theta - \dots$$

For most engines  $R/L \approx 0.3$ , and so

$$\cos\phi = 1 - 0.045\sin^2\theta - 0.00648\sin^4\theta - 0.000045\sin^6\theta - \dots$$

As can be seen after the second term the values become very small and so can be ignored.

$$\therefore \cos\phi \approx 1 - \frac{1}{2}(R/L)^2\sin^2\theta$$

Substituting into equation A3.1

$$\begin{aligned} y &\approx R + L - R\cos\theta - L[1 - \frac{1}{2}(R/L)^2\sin^2\theta] \\ &\approx R + L - R\cos\theta - \frac{1}{2}L(R/L)^2\sin^2\theta \end{aligned}$$

$$\text{Substituting } \sin^2\theta = \frac{1}{2}(1 - \cos 2\theta)$$

$$y \approx R - R\cos\theta + \frac{1}{4}(R/L)^2L - \frac{1}{4}(R/L)^2L\cos 2\theta \quad \dots A3.2$$

The force due to the reciprocating mass  $M_{\text{RECIP}}$  is:

$$F_{\text{RECIP}} = M_{\text{RECIP}}\ddot{y}$$

Now  $\dot{y} = \frac{dy}{dt} = \frac{dy}{d\theta} \cdot \frac{d\theta}{dt} = \frac{dy}{d\theta} \cdot \omega$        $\omega = \text{angular velocity (rad/s)}$

$$\begin{aligned} \frac{dy}{d\theta} &\approx R\sin\theta + 2 \cdot \frac{1}{2} (R/L)^2 L \sin 2\theta && \text{from A3.2} \\ &= R(\sin\theta + \frac{1}{2} (R/L) \sin 2\theta) \end{aligned}$$

$$\therefore \dot{y} \approx \omega R(\sin\theta + \frac{1}{2} (R/L) \sin 2\theta)$$

Similarly

$$\frac{d\dot{y}}{dt} = \ddot{y} = \frac{d\dot{y}}{d\theta} \cdot \frac{d\theta}{dt} = \frac{d\dot{y}}{d\theta} \cdot \omega$$

$$\therefore \ddot{y} = \omega^2 R(\cos\theta + (R/L)\cos 2\theta)$$

Thus the force due to a reciprocating mass is:

$$F_{\text{RECIP}} = M_{\text{RECIP}} \omega^2 R(\cos\theta + (R/L)\cos 2\theta) \quad \dots \text{A3.3}$$

# APPENDIX 4

## Appendix 4: Vibration due to Unbalanced Forces

To evaluate the effect of the out-of-balance reciprocating forces, the engine on its mountings may be represented as a simple mass-spring-damper system. Referring to fig. A4.1, the differential equation for the system is:

$$M\ddot{x} + c\dot{x} + kx = F \quad \dots A4.1$$

where  $M$  = engine mass  
 $k$  = spring stiffness (linear spring)  
 $c$  = damping constant (velocity proportional)  
 $F$  = disturbing force

Knowing the form of the disturbing force,

$$F = M_{\text{RECIP}}\omega^2 R \cos \Omega t + M_{\text{RECIP}}\omega^2 R(R/L) \cos 2\Omega t, \Omega t = \theta$$

a solution of the form given below is assumed

$$x = A \cos \Omega t + B \sin \Omega t + C \cos 2\Omega t + D \sin 2\Omega t \quad \dots A4.2$$

Thus

$$\dot{x} = -A\Omega \sin \Omega t + B\Omega \cos \Omega t - C2\Omega \sin 2\Omega t + D2\Omega \cos 2\Omega t$$

and

$$\ddot{x} = -A\Omega^2 \cos \Omega t - B\Omega^2 \sin \Omega t - C(2\Omega)^2 \cos 2\Omega t - D(2\Omega)^2 \sin 2\Omega t$$

Substituting in equation A4.1

$$\begin{aligned} \Rightarrow & - (MA\Omega^2 \cos \Omega t - MB\Omega^2 \sin \Omega t - MC(2\Omega)^2 \cos 2\Omega t - MD(2\Omega)^2 \sin 2\Omega t \\ & - cA\Omega \sin \Omega t + cB\Omega \cos \Omega t - cC2\Omega \sin 2\Omega t + cD2\Omega \cos 2\Omega t \\ & + kA \cos \Omega t + kB \sin \Omega t + kC \cos 2\Omega t + kD \sin 2\Omega t) \\ & = M_{\text{RECIP}}\omega^2 R \cos \Omega t + M_{\text{RECIP}}\omega^2 R(R/L) \cos 2\Omega t \quad \dots A4.3 \end{aligned}$$

Comparing coefficients in eqn. A4.3

$$\begin{aligned} - & MA\Omega^2 + cB\Omega + kA = M_{\text{RECIP}}\Omega^2 R \\ - & MB\Omega^2 - cA\Omega + kB = 0 \\ - & 4MC\Omega^2 + cD2\Omega + kC = M_{\text{RECIP}}\Omega^2 R(R/L) \\ - & 4MD\Omega^2 - cC2\Omega + kD = 0 \end{aligned}$$



Re-arranging:

$$(k-M\Omega^2)A + c\Omega B = M_{\text{RECIP}}\Omega^2 R \quad \dots A4.4$$

$$(k-M\Omega^2)B - c\Omega A = 0 \quad \dots A4.5$$

$$(k-4M\Omega^2)C + 2c\Omega D = M_{\text{RECIP}}\Omega^2 R(R/L) \quad \dots A4.6$$

$$(k-4M\Omega^2)D - 2c\Omega C = 0 \quad \dots A4.7$$

From A4.5

$$B = \frac{c\Omega}{(k-M\Omega^2)} A$$

Substituting in A4.4

$$(k-M\Omega^2)A + \frac{c\Omega \cdot c\Omega}{(k-M\Omega^2)} A = M_{\text{RECIP}}\Omega^2 R$$

$$\therefore A = M_{\text{RECIP}}\Omega^2 R \cdot \frac{k-M\Omega^2}{(k-M\Omega^2)^2 + (c\Omega)^2}$$

$$\text{and, } B = M_{\text{RECIP}}\Omega^2 R \cdot \frac{c\Omega}{(k-M\Omega^2)^2 + (c\Omega)^2}$$

Similarly for eqtns. A4.6 and A4.7

$$C = M_{\text{RECIP}}\Omega^2 R(R/L) \cdot \frac{k-4M\Omega^2}{(k-4M\Omega^2)^2 + (2c\Omega)^2}$$

$$D = M_{\text{RECIP}}\Omega^2 R(R/L) \cdot \frac{2c\Omega}{(k-4M\Omega^2)^2 + (2c\Omega)^2}$$

Substituting these values of A, B, C and D into eqtn. A4.2

$$x = \frac{M_{\text{RECIP}}\Omega^2 R}{(k-M\Omega^2)^2 + (c\Omega)^2} \cdot [(k-M\Omega^2)\cos\Omega t + c\Omega\sin\Omega t] + \frac{M_{\text{RECIP}}\Omega^2 R(R/L)}{(k-4M\Omega^2)^2 + (2c\Omega)^2} \cdot [(k-4M\Omega^2)\cos 2\Omega t + 2c\Omega\sin 2\Omega t] \quad \dots A4.8$$

Now a function of the form:

$$x = V\cos\Omega t + W\sin\Omega t, \quad \text{may be re-written as}$$

$$x = R\cos(\Omega t - \psi) \quad \text{where } R = (V^2 + W^2)^{1/2}$$

$$\text{and } \tan\psi = W/V$$

Thus eqtn. A4.8 becomes

$$x = \frac{M_{\text{RECIP}} \Omega^2 R \cdot \cos(\Omega t - \psi_1)}{\sqrt{[(k - M\Omega^2)^2 + (c\Omega)^2]}} + \frac{M_{\text{RECIP}} \Omega^2 R(R/L) \cdot \cos(2\Omega t - \psi_2)}{\sqrt{[(k - 4M\Omega^2)^2 + (2c\Omega)^2]}}$$

where  $\tan\psi_1 = B/A$  and  $\tan\psi_2 = D/C$

Using the following substitutions:

$$\begin{aligned}\omega_0 &= \text{natural frequency} = k/M \\ \delta &= \text{damping factor} = c/2M \\ v &= \text{damping coefficient} = \delta/\omega_0 \\ \eta &= \text{frequency ratio} = \Omega/\omega_0\end{aligned}$$

and then re-arranging, the above becomes

$$x = \frac{(M_{\text{RECIP}} R/M) \eta^2 \cdot \cos(\Omega t - \psi_1)}{\sqrt{[(1 - \eta^2)^2 + (2v\eta)^2]}} + \frac{(M_{\text{RECIP}} R(R/L)/M) \eta^2 \cdot \cos(2\Omega t - \psi_2)}{\sqrt{[(1 - 4\eta^2)^2 + (4v\eta)^2]}}$$

where  $\tan\psi_1 = \frac{2v\eta}{1 - \eta^2}$ , and  $\tan\psi_2 = \frac{4v\eta}{1 - 4\eta^2}$  ...A4.9

For a system having only a single forcing frequency i.e.  $F = F_{\text{RECIP}} \cos \Omega t$ , and by plotting  $x/(M_{\text{RECIP}} R/M)$  against  $\eta$  a series of curves is obtained as illustrated in fig. A4.2. It will be noticed that as the frequency ratio  $\eta$  is increased the damping coefficient  $v$  has little effect on the final value of the vibration amplitude.

When mounting an engine it is normally arranged that  $\eta > 3$  - by careful selection of the flexible mountings. Therefore eqtn. A4.9 can be greatly simplified by setting  $v = 0$ , without introducing large inaccuracies.

Thus eqtn. A4.9 becomes:

$$x = \frac{M_{\text{RECIP}} R}{M} \left\{ \frac{\eta^2 \cos \Omega t}{\sqrt{(1 - \eta^2)^2}} + \frac{(R/L) \eta^2 \cos 2\Omega t}{\sqrt{(1 - 4\eta^2)^2}} \right\}$$

Note. The squaring and square root in the denominator are left to ensure values obtained are positive.

Hence the maximum amplitude of vibration is given when the two rotating vectors are superimposed directly upon one another, then:

$$x_{max} = \left| \frac{M_{RECIP} R \eta^2}{M(1-\eta^2)} \right| + \left| \frac{M_{RECIP} R(R/L) \eta^2}{M(1-4\eta^2)} \right|$$

$[x_1]$ 
 $[x_2]$

# APPENDIX 5

## Appendix 5: PHOENICS Skeleton Satellite

```
C$DIRECTIVE**SATLIT
  PROGRAM SATLIT
C   *FILE NAME: MODSTL.FTN
C   *ABSTRACT: SATELLITE MODEL MAIN PROGRAM.
C   *DOCUMENTATION: PHOENICS INSTRUCTION MANUAL (SPRING 1983).

C   *AUXILIARY SUBROUTINES (TAPES, ETC.) ARE IN SATELLITE LIBRARY

C   SERVICEU, WHICH MUST BE INCLUDED IN LINK EDIT TO RUN.
CXXXXXXXXXXXXXXXXXXXXXXXXXXXXXXXXXXXXXXXXXXXXXXXXXXXX STANDARD SECTION 1 STARTS:
C-----

CHAPTER 1  COMMON BLOCKS AND USER'S DATA.
C-----

*** READ(CMNGUS)
*** READ(GUSSEQ)
*** READ(CMNGRF)
    COMMON/CPI/IPWRIT,IDUM(243)
    DIMENSION GDTAPE(3),DFAULT(4)
    DIMENSION ARRAY1(309),ARRAY2(194),ARRAY3(421)
    LOGICAL ARRAY1,LSPDA,WRT,RD,NAMLST
    INTEGER ARRAY2,XPLANE,YPLANE,ZPLANE
    INTEGER P1,PP,U1,U2,V1,V2,W1,W2,R1,R2,RS,EP,H1,H2,H3,C1,C2.

&C3,C4
    REAL NORTH,LOW
    EQUIVALENCE (ARRAY1(1),CARTES),(ARRAY2(1),NX)
    EQUIVALENCE (ARRAY3(1),SPARE1(1)),(M1,R1),(M2,R2)
    EQUIVALENCE (LSTRUN,INTGR(12)),(NAMLST,LOGIC(88))
CXXXXXXXXXXXXXXXXXXXXXXXXXXXXXXXXXXXXXXXXXXXXXXXXXXXX STANDARD SECTION 1 ENDS.

CXXXXXXXXXXXXXXXXXXXXXXXXXXXXXXXXXXXXXXXXXXXXXXXXXXXX USER SECTION 1 STARTS:

C   GRAFFIC ARRAYS DIMENSIONED AS NEEDED...
C   COMMON/GRAF1/PHI1(1) /GRAF2/PHI2(1)
C   POROSITY & SPECIAL DATA ARRAYS DIMENSIONED AS NEEDED...
    DIMENSION PE(1,1,1),PN(1,1,1),PH(1,1,1),PC(1,1,1)
    DIMENSION LSPDA(1),ISPDA(1),RSPDA(1)
C   USER PLACES HIS VARIABLES, ARRAYS, EQUIVALENCES ETC. HERE.

    DATA NLSP,NISP,NRSP/1,1,1/
C   USER PLACES HIS DATA STATEMENTS HERE.
CXXXXXXXXXXXXXXXXXXXXXXXXXXXXXXXXXXXXXXXXXXXXXXXXXXXX USER SECTION 1 ENDS.
CXXXXXXXXXXXXXXXXXXXXXXXXXXXXXXXXXXXXXXXXXXXXXXXXXXXX STANDARD SECTION 2 STARTS:
C-----

CHAPTER 2  SET CONSTANTS, AND ARRANGE FILE MANIPULATIONS.
C-----

C   PLEASE DO NOT ALTER, OR RE-SET, ANY OF THE REMAINING
C   STATEMENTS OF THIS CHAPTER.
    DATA CELL,EAST,WEST,NORTH,SOUTH,HIGH,LOW,VOLUME/
& 0.,1.,2.,3.,4.,5.,6.,7. /
    DATA P1,PP,U1,U2,V1,V2,W1,W2,R1,R2,RS,KE,EP,H1,H2,H3,C1,C2.
```

```
DATA FIXFLU, FIXVAL, ONLYMS, WALL/1, E-10, 1, E10, 0, 0, -10, 0/  
DATA IPLANE, XPLANE, YPLANE, ZPLANE/0, 1, 2, 3/  
DATA WRT, RD, DFAULT/, TRUE, . . FALSE, . 4HDEFA, 4HULT, . 4HDTA/, 1HG/
```

C-----READ DEFAULT FILE IF BLOCKDATA ABSENT

**C**-----

**C** \_\_\_\_\_

**CXXXXXXXXXXXXXXXXXXXXXXXXXXXXXXXXX USER SECTION 2 STARTS:**

C

```
410 RUN(II)=.TRUE.
```

**CXXXXXXXXXXXXXXXXXXXXXXXXXXXXX STANDARD SECTION 3 STARTS:**

CXXXXXXXXXXXXXXXXXXXXXXXXXXXXXXXXXXXXX STANDARD SECTION 3 ENDS.

C--- ALL INTEGER VARIABLES ARE DEFAULTED TO 0, AND REAL VARIABLES

C E.G. BY VARIABLE<10>, OR <10.0> AS APPROPRIATE.

C INDICATED. E. G. VARIABLE<.T.>. OR VARIABLE<.F.>

C--- RUN 1

C-----

C PARAB&lt;. F.&gt;, CARTES&lt;. T.&gt;, ONEPHS&lt;. T.&gt;&gt;

```

C-----
C--- GROUP 2. TRANSIENCE :
C    STEADY<.T.>, ATIME, LSTEP<1>, FSTEP<1>
C    TLAST<1.E10>, TFRAC(1-30) <30*1.>
C    SERVICE SUBROUTINE FOR 'NT' POWER-LAW TIME STEPS:
C    CALL GRDPWR(0, NT, TLAST, POWER)
C-----
C--- GROUP 3. X-DIRECTION :
C    NX<1>, XULAST<1.0>, XFRAC(1-30)
C    SERVICE SUBROUTINE FOR POWER-LAW GRID:
C    CALL GRDPWR(1, NX, XULAST, POWER)
C-----
C--- GROUP 4. Y-DIRECTION :
C    NY<1>, YVLAST<1.0>, YFRAC(1-30), RINNER, SNALFA
C    SERVICE SUBROUTINE FOR POWER-LAW GRID:
C    CALL GRDPWR(2, NY, YVLAST, POWER)
C-----
C--- GROUP 5. Z-DIRECTION :
C    NZ<1>, ZWLAST<1.0>, ZFRAC(1-30)
C    SERVICE SUBROUTINE FOR POWER-LAW GRID:
C    CALL GRDPWR(3, NZ, ZWLAST, POWER)
C-----
C--- GROUP 6. MOVING GRID :
C    MGRID, IZW1, IZW2, AZW2, BZW2, CZW2, PINT, ZW2M1T
C-----
C--- GROUP 7. BLOCKAGE: BLOCK<.F.>, IPLANE, IPWRIT
C    *SET CONSTANT POROSITIES OVER SUB-DOMAINS USING:
C    CALL CONPOR(IR, TYPE, VALUE, IXF, IXL, IYF, IYL, IZF, IZL), WHERE:
C
C    IR=RUN SECTION NUMBER, E.G. 1 FOR RUN1 SECTION: 'TYPE'= EAST,
C    WEST, NORTH, SOUTH, HIGH, LOW & CELL. 'VALUE'=WANTED POROSITY
C
C    OVER REGION IXF,... IZL.
C    *DIMENSION ARRAYS PE(NX, NY, NZ), PN(NX, NY, NZ), PH(NX, NY, NZ), &
C    PC(NX, NY, NZ) ABOVE.
C    *FOR FULLY-BLOCKED CELLS (IE. 'VALUE'= 0.0) USER NEED SET ONLY
C
C    THE 'CELL' POROSITY (TO ZERO), AS CELL-FACE AREAS ARE THEN
C
C    AUTOMATICALLY ZEROED.
C    *FOR SATELLITE PRINTOUT OF ALL POROSITIES IN DOMAIN, 'IPLANE'=
C
C    XPLANE YPLANE OR ZPLANE, FOR DESIRED CROSS-SECTION DIRECTION.
C
C    *FOR EACH 'TYPE' A MAXIMUM OF 10 CALLS TO CONPOR IS ALLOWED,
C
C    BUT IF REQUIREMENTS EXCEED THIS PROVISION SET BLOCK=.T. &
C
C    IPWRIT=-1, AND SET POROSITY ARRAYS EXPLICITLY HERE AS WANTED.
C
C    IN THIS CASE, THE USER M U S T   S E T   A L L   ELEMENTS OF
C
C    ARRAYS PE, PN, PH, PC (MANY MAY BE 0.0 OR 1.0). HE MAY USE:
C
C    CALL CR(PARRAY, VALUE, IXF, IXL, IYF, IYL, IZF, IZL, NX, NY, NZ)
C    ANY NUMBER OF TIMES, TO SET 'PARRAY' (= PE, ETC.) TO

```

```

C      'VALUE' OVER RANGE IXF TO IXL, IYF TO IYL, IZF TO IZL.
C      *CONPOR M U S T N O T BE USED IN CONJUNCTION WITH EXPLICIT

C      SETTINGS OF THE ARRAYS (INCLUDING SETTINGS VIA CR).
C-----
C--- GROUP 8. DEPENDENT VARIABLES TO BE SOLVED FOR OR STORED :
C      SOLVAR(1-25) <25*. F.>, STOVAR(1-25) <25*. F.>, CONC1(1-4) <4*. T.>

C      USE FOLLOWING NAMED INTEGERS FOR ARRAY ELEMENTS 1-20:
C      P1, PP, U1, U2, V1, V2, W1, W2, M1, M2, RS, KE, EP, H1, H2, H3, C1, C2, C3, C4.

C-----
C--- GROUP 9. VARIABLE LABELS :
C      TITLE(1-25) <2HP1, 2HPP, 2HU1, 2HU2, 2HV1, 2HV2, 2HW1, 2HW2, 2HR1,
C      2HR2, 2HRS, 2HKE, 2HEP, 2HH1, 2HH2, 2HH3, 2HC1, 2HC2,
C      2HC3, 2HC4, 2HRX, 2HRY, 2HRZ, 2*4H****>

C-----
C--- GROUP 10 PROPERTIES:
C      IRHO1<1>, IRHO2<1>, RHO1<1. 0>, RHO2<1. 0>,
C      ARHO1<1. 0>, BRHO1<1. 0>, CRHO1<1. 0>
C      IEMU1<1>, EMU1<1. 0>, EMULAM<1. E-10>
C      IHSAT, H1SAT, H2SAT, PSATEX<1. 0>
C      SIGMA(1-25) <1. 0, 2. 0, 1. . 1. E10, 1. . 1. E10, 1. . 1. E10,
C      4*1. 0, 1. 314, 1. 0, 1. E10, 10*1. 0>

C-----
C--- GROUP 11 INTER-PHASE TRANSFER PROCESSES :
C      ICFIP, CFIPS, IMDOT, CMDOT, CA1I<1. E6>, CA2I<1. E6>

C-----
C--- GROUP 12 SPECIAL SOURCES :
C      ISPCSO(1-25), AGRAVX, AGRAVY, AGRAVZ, ABUOY, HREF

C-----
C--- GROUP 13 INITIAL FIELDS :
C      FIINIT(1-25) <25*1. E-10>

C-----
C--- GROUP 14 BOUNDARY/INTERNAL CONDITIONS :
C      ILOOP1, ILOOPN, XCYLE<. F.>, PBAR, REGION(1-10) <10*. T.>
C      *N.B. ALL 10 REGIONS ARE DEFAULTED .TRUE.. THE USER SHOULD

C      SET REGION(I)=.FALSE. FOR UNUSED REGIONS 'I'.
C      DO 20 I=1, 10
C      REGION(I)=.FALSE.
C 20 CONTINUE

C-----
C--- GROUP 15 TO 24: REGIONS 1 TO 10
C--- ONLY THOSE REGIONS ARE ACTIVE WHICH ARE SPECIFIED BY THE
C      USER. PREFERABLY BY WAY OF:-
C      CALL PLACE(IREGN, TYPE, IXF, IXL, IYF, IYL, IZF, IZL) &
C      CALL COVAL(IREGN, VARBLE, COEFF, VALUE)

C-----
C--- GROUP 25 GROUND STATION :
C      GROSTA<. F.>, NAMLST<. F.>
C      *NAMLST ACTIVATES NAMELIST IN GROUND.

C-----
C--- GROUP 26 SOLUTION TYPE AND RELATED PARAMETERS :
C      WHOLEP<. F.>, SUBPST<. F.>, DONACC<. F.>

C-----
C--- GROUP 27 SWEEP AND ITERATION NUMBERS :

```



```

C   FSWEED<1>,LSWEED<1>,LITHYD<1>,LITC<1>,LITKE<1>,LITH<1>,
C   LITER(1-25)<9*1,-1,15*1>
C   IVELF<1>,NVEL<1>,IVELL<10000>,
C   IKEF<1>,NKE<1>,IKEL<10000>,
C   IENTF<1>,NENT<1>,IENTL<10000>,
C   ICNCF<1>,NCNC<1>,ICNCL<10000>,
C   IRHO1F<1>,NRHO1<1>,IRHO1L<10000>,
C   IRHO2F<1>,NRHO2<1>,IRHO2L<10000>
C-----
C--- GROUP 28 TERMINATION CRITERIA :
C   ENDIT(1-25)<9*1.E-10,0.5,15*1.E-10>
C-----
C--- GROUP 29 RELAXATION :
C   RLXP<1.>,RLXPXY<1.>,RLXPZ<1.>,RLXRHO<1.>,RLXMDT<1.>,
C   DTFALS(3-25)<23*1.E10>
C-----
C--- GROUP 30 LIMITS :
C   VELMAX<1.E10>,VELMIN<-1.E10>,RHOMAX<1.E10>,RHOMIN<1.E-10>,
C   TKEMAX<1.E10>,TKEMIN<1.E-10>,EMUMAX<1.E10>,EMUMIN<1.E-10>,
C   EPSMAX<1.E10>,EPSMIN<1.E-10>,AMDTMX<1.E10>,AMDTMN<-1.E10>
C-----
C--- GROUP 31 SLOWING DEVICES : SLORHO<1.>,SLOEMU<1.>
C-----
C--- GROUP 32 PRINT-OUT OF VARIABLES :
C   PRINT(1-25)<.T...F.,23*.T.>,SUBWGR<.F.>
C-----
C--- GROUP 33 MONITOR PRINT-OUT :
C   IXMON<1>,IYMON<1>,IZMON<1>,NPRMON<1>,NPRMNT<1>
C-----
C--- GROUP 34 FIELD PRINT-OUT CONTROL :
C   NPRINT<100>,NTPRIN<100>,NXPRIN<1>,NYPRIN<1>,NZPRIN<1>,
C   IZPRF<1>,ISTPRF<1>,IZPRL<10000>,ISTPRL<10000>
C   NUMCLS<10>,KOUTPT
C-----
C--- GROUP 35 TABLE CONTROL :
C   TABLE<.F.>,NTABLE,NTABVR,LINTAB,NPRTAB,NMON,
C   ITAB(1-8),MTABVR(1-8)
C-----
C   GROUP 36-38 ARE NOT DOCUMENTED IN THE INSTRUCTION
C   MANUAL AND ARE INTENDED FOR MAINTENANCE PURPOSES ONLY
C--- GROUP 36 DEBUG PRINT-OUT SLAB AND TIME-STEP :
C   IZPR1<1>,IZPR2<1>,ISTPR1<1>,ISTPR2<1>
C-----
C--- GROUP 37 DEBUG SWEEP AND SUBROUTINES :
C   KEMU,KMAIN,KINDEX,KGEOM,KINPUT,KSODAT,KCOMPF,KSORCE,
C   KSOLV1,KSOLV2,KSOLV3,KCOMPP,KADJST,KFLUX,KSHIFT,KDIF,
C   KCOMPU,KCOMPV,KCOMPW,KCOMPR,KWALL,KDBRHO<-1>,KDBEXP,KDBMDT
C   KDBGEN
C-----
C--- GROUP 38 MONITOR,TEST,AND FLAG :
C   MONITR<.F.>,FLAG<.F.>,TEST<.T.>,KFLAG<1>
C   END OF MAINTENANCE-ONLY SECTION
C-----
C--- GROUP 39 ERROR AND RESIDUAL PRINT-OUT :

```

```

C      IERRP<1000>,RESREF(1,3-24)<25*1.>,RESMAP<.F.>,
C      RESID(1-25)<2*.F.,23*.T.>,KOUTPT
C-----
C---  GROUP 40 SPECIAL DATA : LOGIC(1..10),INTGR(1..10),RE(21..30),
C
C      NLSP<1>,NISP<1>,NRSP<1>,SPDATA<.F.>,LSPDA(1),ISPDA(1),RSPDA(1)
C
C      USE FIRST 10 ELEMENTS OF ARRAYS LOGIC & INTGR AND 21ST
C      TO 30TH OF ARRAY RE FOR TRANSFERRING SPECIAL DATA FROM
C      SATELLITE TO GROUND, BUT IF REQUIREMENTS EXCEED THIS
C      PROVISION SET SPDATA = .T., AND DIMENSION ARRAYS LSPDA,
C      ISPDA, RSPDA ABOVE AND IN GROUND AS NEEDED, AND SET HERE
C      NLSP, NISP, NRSP TO DIMENSION VALUES.
C-----
C---  GROUP 42 RESTARTS AND DUMPS : SAVEM<.F.>,RESTRT<.F.>,KINPUT
C-----
C---  GROUP 43 GRAFFIC :
C      GRAPHS<.F.>,ORTHOG<.T.>,ANTSYM,NPRT<1>,ITITL<5*4H****>
C---  FOR A GRAFFIC RUN, DIMENSION PHI1 & PHI2 AS FOLLOWS:
C      PHI1(NX*NY*NZ*NM)
C      PHI2((NX+2)*(NY+2)*(NZ+2)*(NM+IBLK)) , WHERE
C      NM=NO. OF VARIABLES STORED + DENSITY(-IES)
C      IBLK=0 IF BLOCK=.FALSE.,=4 IF A 3D RUN,
C      =3 IF A 2D.YZ RUN.
C-----
C      IF(IRUN.EQ.1) GO TO 900
C---  RUN2
C      IF(IRUN.EQ.2) GO TO 900
C---  RUN3
C      IF(IRUN.EQ.3) GO TO 900
C---  RUN4
C      IF(IRUN.EQ.4) GO TO 900
C---  RUN5
C      IF(IRUN.EQ.5) GO TO 900
C---  RUN6
C      IF(IRUN.EQ.6) GO TO 900
C---  RUN7
C      IF(IRUN.EQ.7) GO TO 900
C---  RUN8
C      IF(IRUN.EQ.8) GO TO 900
C---  RUN9
C      IF(IRUN.EQ.9) GO TO 900
C---  RUN10
C      IF(IRUN.EQ.10) GO TO 900
C---  RUN11
C      IF(IRUN.EQ.11) GO TO 900
C---  RUN12
C      IF(IRUN.EQ.12) GO TO 900
C---  RUN13
C      IF(IRUN.EQ.13) GO TO 900
C---  RUN14
C      IF(IRUN.EQ.14) GO TO 900
C---  RUN15
C      IF(IRUN.EQ.15) GO TO 900
C---  RUN16
C      IF(IRUN.EQ.16) GO TO 900
C---  RUN17

```

```

      IF(IRUN.EQ.17) GO TO 900
C--- RUN18
      IF(IRUN.EQ.18) GO TO 900
C--- RUN19
      IF(IRUN.EQ.19) GO TO 900
C--- RUN20
      IF(IRUN.EQ.20) GO TO 900
C--- RUN21
      IF(IRUN.EQ.21) GO TO 900
C--- RUN22
      IF(IRUN.EQ.22) GO TO 900
C--- RUN23
      IF(IRUN.EQ.23) GO TO 900
C--- RUN24
      IF(IRUN.EQ.24) GO TO 900
C--- RUN25
      IF(IRUN.EQ.25) GO TO 900
C--- RUN26
      IF(IRUN.EQ.26) GO TO 900
C--- RUN27
      IF(IRUN.EQ.27) GO TO 900
C--- RUN28
      IF(IRUN.EQ.28) GO TO 900
C--- RUN29
      IF(IRUN.EQ.29) GO TO 900
C--- RUN30
      IF(IRUN.EQ.30) GO TO 900
900 CONTINUE
C--- ALL RUNS
CXXXXXXXXXXXXXXXXXXXXXXXXXXXXXXXXXXXXXXXXX USER SECTION 3 ENDS.
CXXXXXXXXXXXXXXXXXXXXXXXXXXXXXXXXXXXXXXXXX STANDARD SECTION 4 STARTS:
C-----
C WRITE GENERAL DATA ON TO THE GUSIE1.DTA TAPE. ETC...
      IF(SPDATA) CALL WRTSPC(LSPDA,NLSP,ISPDA,NISP,RSPDA,NRSP)

      IF(BLOCK) CALL WRTPOR(PE,PN,PH,PC,NX,NY,NZ,IPLANE)
C OLD PRACTICES RETAINED FOR REFERENCE:
C IF(SPDATA) CALL SPCDAT(IRUN)
C IF(BLOCK) CALL PORDAT(IRUN)
      GRAPHS=.FALSE.
      IF(GRAPHS) CALL SORT(IRUN)
      IF(RESTRT) GO TO 902
      DO 901 INDVAR=1,25
      IF(IFIX(FIINIT(INDVAR)+0.1).NE.10101) GO TO 901
      CALL FLDDAT(IRUN)
      GO TO 902
901 CONTINUE
902 CALL DATAIO(WRT,10)
      IF(MONITR) CALL DATAIO(WRT,-6)
999 CONTINUE
STOP
END

```

## Appendix 6: PHOENICS Skeleton Ground-station

```

C$DIRECTIVE**MAIN
  PROGRAM MAIN
C  *FILE NAME: MODGRD.FTN
C  *INCLUDED SUBROUTINES: THE MODELS OF MAIN, GROUND & STRIDE.
C  *DOCUMENTATION: PHOENICS INSTRUCTION MANUAL (SPRING 1983).
C  *SATELLITE FILE NAME: MODSTL.FTN
  COMMON/ISHIFT/III(57),NFMAX
C SET F-ARRAY DIMENSION AS NEEDED. & SET NFMAX ACCORDINGLY.
  COMMON F(15000)
  NFMAX=15000
  CALL MAIN1
  STOP
  END

C$DIRECTIVE**GROUND
  SUBROUTINE GROUND(IRN,ICHAP,ISTP,ISWP,IZED,INDVAR)
*** READ(CMNGUS)
*** READ(GUSSEQ)
C  INCLUDE 'NMLIST'
CXXXXXXXXXXXXXXXXXXXXXXXXXXXXXXXXXXXXXXXXX STANDARD SECTION 1 STARTS:
C-----
C+++++MEANING OF SUBROUTINE ARGUMENTS:
C  IRN=RUN NUMBER; ICHAP=CHAPTER CALLED; ISTP=TIME STEP;
C  ISWP=SOLUTION SWEEP; IZED=Z-SLAB; INDVAR: SEE CHAPTERS BELOW.
C+++++USER-INTRODUCED VARIABLES & ARRAYS:
C  TO AVOID CONFLICT WITH VARIABLE NAMES USED IN COMMON, ALL
C  VARIABLES INTRODUCED BY THE USER SHOULD HAVE NAMES STARTING
C  WITH 'G' IF REAL, 'J' IF INTEGER, AND 'G' OR 'J' IF LOGICAL.
C  THUS GDZ(IZ) MIGHT BE A Z-INTERVAL ARRAY;
C  GW1(IY,IX) A 2-D ARRAY FOR AXIAL VELOCITY; ETC.
C  USER-GENERATED SUBROUTINES SHOULD BE NAMED CORRESPONDINGLY,EG

C  SUBROUTINE GVISC(GTEMP,GCNC,GVSC), FOR COMPUTING VISCOSITY
C  FROM CONCENTRATION & TEMPERATURE.
C+++++GROUND-TO-EARTH CONNECTING SUBROUTINES:
C  *USE GET(NAME,GARRAY,NY,NX) TO PUT VALUES OF VARIABLE NAMED
C  'NAME' INTO ARRAY 'GARRAY' DIMENSIONED GARRAY(NY,NX).
C  *USE SET(NAME,IXF,IXL,IYF,IYL,GARRAY,NY,NX) TO SET VARIABLE
C  'NAME' TO GARRAY(IY,IX) OVER THE REGION: IXF-IXL & IYF-IYL.
C  *USE PRNSLB(NAME) TO PRINT VARIABLE 'NAME' OVER X-Y PLANE.
C  *USE ADD(NAME,IXF,IXL,IYF,IYL,TYPE,CM,VM,CVAR,VVAR,NY,NX)
C  TO ADD SOURCE TO VARIABLE NAMED 'NAME' (SEE CHAPTER 5).
C  *USE READIZ(IZED) IN CHAPTERS 1, 2, 8, & 9 TO ACCESS P1,...DM
C  & VOL,...AHDZ. (SEE FOOTNOTE TO LEGALITY TABLE)
C  *USE GET1D(NAME,GARRAY,NDIM) TO PUT VARIABLE NAMED 'NAME' IN
C  ONE-D ARRAY 'GARRAY' DIMENSIONED NDIM, THUS:
C  CALL GET1D(NAME,GNX,NX) FOR XG,...DXG & DIMENSION GNX(NX);
C  CALL GET1D(NAME,GNY,NY) FOR YG,...RV & DIMENSION GNY(NY);
C  CALL GET1D(NAME,GNZ,NZ) FOR ZG,...WGRID & DIMENSION GNZ(NZ).
C+++++LEGALITY TABLE FOR USE OF EARTH-CONNECTING SUBROUTINES:
C  ENTRIES IN TABLE GIVE CHAPTERS IN WHICH SUBROUTINES CAN BE
C  USED FOR VARIABLES IN LEFT-HAND COLUMN. (SUBROUTINE
C  STRIDE IS REGARDED AS BEING IN CHAPTER 3)
C
C  -----
C  : VARIABLE:: GET & : SET : ADD : READIZ : GET1D :
C  :           : PRNSLB :           :           :           :
C  -----
C  : P1 - RZ :: ALL : 6 & 7 : 5 : 1,2,8,9: NONE :

```

# APPENDIX 6

```

C      :P10 - RZH::3-7, 10-16:    3 :  NONE :  NONE :  NONE :
C      :VOL -AHDZ::    ALL :    3 :  NONE : 1,2,8,9:  NONE :
C      :D1DP      ::    NONE :   10 :  NONE :  NONE :  NONE :
C      :D2DP      ::    NONE :   11 :  NONE :  NONE :  NONE :
C      :MU1,MU1H :: 5,13-16 :   12 :  NONE :  NONE :  NONE :
C      :EXCO(L,H)::    NONE :   13 :  NONE :  NONE :  NONE :
C      :CFP       ::     5 :   14 :  NONE :  NONE :  NONE :
C      :MDT       ::     5 :   15 :  NONE :  NONE :  NONE :
C      :HST1,HST2:: 5 & 15 :   16 :  NONE :  NONE :  NONE :
C      :XG -WGRID::    NONE :    NONE :  NONE :  NONE :  ALL :

```

# NOTES ON ABOVE TABLE:

\*IN CHAPTERS 1, 2, 8, & 9 VARIABLES P1...DM & GEOMETRY  
VOL...AHDZ CAN BE ACCESSED BUT ONLY IN CONJUNCTION WITH  
USE OF READIZ. THUS:

DO 1 IZED=1,NZ

CALL READIZ(IZED)

1 CALL GET(... AS REQUIRED...)

\*GEOMETRY ACCESSED BY READIZ IS THAT AT INITIAL TIME.

\*D1DP & D2DP ONLY ACCESSIBLE IN UNSTEADY FLOWS.

## C++++GROUND SERVICE SUBROUTINES:

\*USE CONTUR(NAME,IPLANE,ILOC,NINT,I1,I2,J1,J2,GARRAY,NDIM) FOR  
LINE-PRINTER PLOTS OF CONTOURS. 'NAME' = U1....C4:

'IPLANE'= XPLANE, YPLANE, OR ZPLANE; ILOC SETS IX, IY, OR

IZ LOCATION OF IPLANE; I1, I2, J1, & J2 SET FIRST & LAST

CELLS IN HORIZ. & VERT. ON PLOT; GARRAY IS 1-D WORKING ARRAY

OF DIMENSION NX\*NY, NX\*NZ, OR NY\*NZ DICTATED BY IPLANE; &

NDIM SETS VALUE OF DIMENSION OF GARRAY.

\*USE FLD2DA(TITLE,GARRAY,NY,NX) TO PRINT ANY ARRAY DIMENSIONED  
GARRAY(NY,NX); SET 'TITLE' TO REQUIRED NAME ( 4 HOLLERITH  
CHARACTERS ONLY).

\*USE FLD3DA(TITLE,GARRAY,NX,NY,NZ,IPLANE,ILOC) TO PRINT ANY  
ARRAY DIMENSIONED GARRAY(NX,NY,NZ) IN PLANE SPECIFIED BY

'IPLANE' & 'ILOC' AS FOR CONTUR ABOVE; SET 'TITLE' AS FOR

FLD2DA.

VARIABLE NAMES FOR USE IN GROUND:

COMMON/TYPE/CELL,EAST,WEST,NORTH,SOUTH,HIGH,LOW,VOLUME,WALL

COMMON/VAR/P1,PP,U1,U2,V1,V2,W1,W2,R1,R2,RS.

&KE,EP,H1,H2,H3,C1,C2,C3,C4,RX,RY,RZ,S1,S2

COMMON/VAROLD/P10,PPO,U10,U20,V10,V20,W10,W20,R10,R20,RSO.

&KEO,EPO,H10,H20,H30,C10,C20,C30,C40,RXO,RYO,RZO,S10,S20

COMMON/VARLOW/P1L,PPL,U1L,U2L,V1L,V2L,W1L,W2L,R1L,R2L,RSL.

&KEL,EPL,H1L,H2L,H3L,C1L,C2L,C3L,C4L,RXL,RYL,RZL,S1L,S2L

COMMON/VARHI/P1H,PPH,U1H,U2H,V1H,V2H,W1H,W2H,R1H,R2H,RSH.

&KEH,EPH,H1H,H2H,H3H,C1H,C2H,C3H,C4H,RXH,RYH,RZH,S1H,S2H

COMMON/GMTRY/VOL,VOLO,AEAST,ANORTH,AHIGH,AEDX,ANDY,AHDZ

COMMON/PROP/D1,D2,D1DP,D2DP,MU1,MU1LAM,EXCO,CFP,MDT,HST1,HST2

COMMON/PRPOLD/D10,D20

COMMON/PRPLOW/D1L,D2L,EXCOL

COMMON/PRPHI/D1H,D2H,MU1H,EXCOH

COMMON/VARNX/XG,XU,DXU,DXG

COMMON/VARNY/YG,YV,DYV,DYG,R,RV

COMMON/VARNZ/ZG,ZW1,DZW,DZG,WGRID

COMMON/GDMSCI/XPLANE,YPLANE,ZPLANE,ITNO

COMMON/GDMSC/LSLAB,MSLAB,HSLAB,LAMMU



```

C      'ATIME + DT' GIVES THE END TIME OF THE CURRENT TIME STEP.
C      NOT ACCESSED IF STEADY, OR PARABOLIC.
C-----
100  CONTINUE
    RETURN
C-----
C      CHAPTER 2: CALLED AT THE START OF EACH SWEEP.
C-----
200  CONTINUE
    RETURN
C-----
C      CHAPTER 3: CALLED AT THE START OF EACH SLAB;
C      NOT ACCESSED IF PARABOLIC, BUT 'STRIDE' IS.
C-----
300  CONTINUE
    RETURN
C-----
C      CHAPTER 4: CALLED AT THE START OF EACH RE-CALCULATION OF
C      VARIABLES P1,...,C4 AT CURRENT SLAB. ITNO= ITERATION NUMBER.
C-----
400  CONTINUE
    RETURN
C-----
C      CHAPTER 5: GROUND CALLED WHEN SOURCE TERM IS COMPUTED.
C      INDVAR GIVES DEPENDENT VARIABLE IN QUESTION IE. U1,...,C4.
C      TO ADD SOURCE TO DEPENDENT VARIABLE C1(SAY) FOR IX=IXF,IXL
C      AND IY=IYF,IYL INSERT STATEMENT:
C      IF(INDVAR.EQ.C1)
C      &CALL ADD(INDVAR,IXF,IXL,IYF,IYL,TYPE,CM,VM,CVAR,VVAR,NY,NX)
C      NOTES ON 'ADD':
C      *SOURCE= (CVAR(IY,IX)+AMAX1(0.0,MASFLO))*(VVAR(IY,IX)-PHI),
C      WHERE 'PHI' IS IN-CELL VALUE OF VARIABLE IN QUESTION.
C      *'MASFLO'= CM(IY,IX)*(VM(IY,IX)-P),
C      WHERE 'P' IS THE IN-CELL PRESSURE.
C      *FOR INDVAR= M1, OR =M2, SOURCE ADDED IS 'MASFLO' ONLY,
C      EXCEPT FOR ONEPHS=.F. & MASFLO < 0.0 (IE. OUTFLOW) WHEN
C      CM(IY,IX) IS MULTIPLIED BY R1*D1 (FOR M1) & R2*D2 (FOR M2).
C      *BOTH 'CVAR' & 'CM' ARE MULTIPLIED BY CELL-GEOMETRY QUANTITY
C      DICTATED BY SETTING OF 'TYPE' (=CELL, EAST AREA,...VOLUME).
C      *TYPE-SPECIFIED AREAS ARE CALCULATED AS IF BLOCKAGE ABSENT,
C      BUT 'VOLUME' WITH ACCOUNT FOR ITS PRESENCE.
C      *FOR ALL SOLVED VARIABLES, INCLUDING M1 ( & M2 WHEN ONEPHS=F),
C      IF 'CM' > 0.0 CALL 'ADD'; FOR M1 & M2 ALTHOUGH 'CVAR' & 'VVAR'
C      HAVE NO SIGNIFICANCE THEY MUST BE ENTERED AS ARGUMENTS.
C      *'CVAR', 'VVAR', 'CM' & 'VM' MUST BE DIMENSIONED NY,NX.
C-----
500  CONTINUE
    RETURN
C-----
C      CHAPTER 6: CALLED AT THE END OF EACH VARIABLE-RECALCULATION
C      CYCLE COMMENCED AT CHAPTER 4. ITNO = ITERATION NUMBER.
C-----
600  CONTINUE
    RETURN
C-----
C      CHAPTER 7: CALLED AT END OF EACH SLAB-WISE CALCULATION.
C-----
700  CONTINUE

```



RETURN

CHAPTER 8: CALLED AT THE END OF EACH SWEEP;  
NOT ACCESSED IF PARABOLIC.

800 CONTINUE  
RETURN

CHAPTER 9: CALLED AT THE END OF EACH TIME STEP;  
NOT ACCESSED IF PARABOLIC.

900 CONTINUE  
RETURN

CHAPTER 10: SET PHASE 1 DENSITY HERE WHEN IRHO1=-1 IN DATA.  
SET CURRENT-Z 'SLAB' DENSITY, D1, IF MSLAB=.T.,  
EG. IF(MSLAB) CALL SET(D1,1,NX,1,NY,GD1,NY,NX).  
SET NEXT LARGER-Z 'SLAB' DENSITY, D1H, IF HSLAB=.T. & PARAB=F  
EG. IF(HSLAB) CALL SET(D1H,1,NX,1,NY,GD1H,NY,NX).  
SET D(LN(D1))/DP (IE. D1DP) FOR UNSTEADY FLOW.  
EG. IF(MSLAB) CALL SET(D1DP,1,NX,1,NY,GD1DP,NY,NX).

1000 CONTINUE  
RETURN

CHAPTER 11: SET PHASE 2 DENSITY HERE WHEN IRHO2=-1 IN DATA.  
SET CURRENT-Z 'SLAB' DENSITY, D2, IF MSLAB=.T.,  
EG. IF(MSLAB) CALL SET(D2,1,NX,1,NY,GD2,NY,NX).  
SET NEXT LARGER-Z 'SLAB' DENSITY, D2H, IF HSLAB=.T. & PARAB=F  
EG. IF(HSLAB) CALL SET(D2H,1,NX,1,NY,GD2H,NY,NX).  
SET D(LN(D2))/DP FOR UNSTEADY FLOW.  
EG. IF(MSLAB) CALL SET(D2DP,1,NX,1,NY,GD2DP,NY,NX).

1100 CONTINUE  
RETURN

CHAPTER 12: SET PHASE 1 VISCOSITY HERE WHEN IEMU1=-1 IN DATA.  
SET CURRENT-Z 'SLAB' VISCOSITY (MU1), IF MSLAB=.T.,  
EG. IF(MSLAB) CALL SET(MU1,1,NX,1,NY,GVISC,NY,NX).  
SET NEXT LARGER-Z 'SLAB' VISC. (MU1H), IF HSLAB=.T. & PARAB=F  
EG. IF(HSLAB) CALL SET(MU1H,1,NX,1,NY,GVSCH,NY,NX).

CHAPTER ALSO ACCESSED WHEN EMULAM=-1.0 IN DATA, SO THAT THE  
LAMINAR VISCOSITY WHICH APPEARS IN WALL FUNCTIONS & IN THE  
KE-EP TURBULENCE MODEL (IEMU1=2) MAY BE SET NON-CONSTANT.  
SET CURRENT-Z 'SLAB' VALUE (MU1LAM) WHEN LAMMU=.T.,  
EG. IF(LAMMU) CALL SET(MU1LAM,1,NX,1,NY,GVSCL,NY,NX).

1200 CONTINUE  
RETURN

CHAPTER 13: SET EXCHANGE COEFFICIENT (E.C.) FOR VARIABLE  
INDVAR WHEN SIGMA(INDVAR)=-1.0 IN DATA.  
SET CURRENT-Z 'SLAB' E.C. (EXCO) IF MSLAB=.T.,  
EG. IF(MSLAB) CALL SET(EXCO,1,NX,1,NY,GEXCO,NY,NX).  
SET NEXT SMALLER-Z 'SLAB' E.C. (EXCOL) IF LSLAB=.T.,  
EG. IF(LSLAB) CALL SET(EXCOL,1,NX,1,NY,GEXCOL,NY,NX).  
SET NEXT LARGER-Z 'SLAB' E.C. (EXCOH) IF HSLAB=.T.,

```

C      EG.  IF(HSLAB) CALL SET(EXCOH,1,NX,1,NY,GEXCOH,NY,NX).
C      NOTE: FOR MSLAB, INDVAR=U1...C4; FOR LSLAB, INDVAR=U1L...C4L
C      & FOR HSLAB, INDVAR=U1H...C4H. IF PARAB=.T. SET MSLAB ONLY.
C-----
1300 CONTINUE
      RETURN
C-----
C      CHAPTER 14: SET INTER-PHASE FRICTION COEFFICIENT (CFP) HERE
C      WHEN ICFIP = -1 IN DATA; ITS UNITS = FORCE / (CELL * RELATIVE
C      SPEED OF PHASES).
C-----
1400 CONTINUE
      RETURN
C-----
C      CHAPTER 15: SET INTER-PHASE MASS-TRANSFER RATE PER CELL (MDT)
C      HERE WHEN IMDOT = -1 IN DATA.
C-----
1500 CONTINUE
      RETURN
C-----
C      CHAPTER 16: SET HERE PHASE 1 & 2 SATURATION ENTHALPIES
C      ( HST1 & HST2) WHEN IHSAT = -1 IN DATA.
C-----
1600 CONTINUE
      RETURN
      END
C$DIRECTIVE**STRIDE
      SUBROUTINE STRIDE(IZSTEP,IGOTO,IRN)
C-----
C      USE THIS SUBROUTINE TO SPECIFY THE GEOMETRY
C      OF THE FORWARD STEP IN PARABOLIC CALCULATIONS.
C      IZSTEP IS THE CURRENT FORWARD STEP, & NZSTP IS THE LAST
C      FORWARD STEP (FOR PARAB=.T. EARTH SETS NZ=1 ).
C      THE COMMON VARIABLE 'ZWL' GIVES THE DISTANCE OF THE
C      PREVIOUS STEP FROM THE ORIGIN.
C-----
*** READ(CMNGUS)
*** READ(GUSSEQ)
CXXXXXXXXXXXXXXXXXXXXXXXXXXXXXXXXXXXXXXXXX STANDARD SECTION 1 STARTS:
C      SATLIT-EQUIVALENT IRUN:
C      EQUIVALENCE (IRUN,INTGR(11))
CXXXXXXXXXXXXXXXXXXXXXXXXXXXXXXXXXXXXXXXXX STANDARD SECTION 1 ENDS.
CXXXXXXXXXXXXXXXXXXXXXXXXXXXXXXXXXXXXXXXXX USER SECTION 1 STARTS:
C      USER PLACES HIS VARIABLES, ARRAYS, EQUIVALENCES ETC. HERE.
C      USER PLACES HIS DATA STATEMENTS HERE.
CXXXXXXXXXXXXXXXXXXXXXXXXXXXXXXXXXXXXXXXXX USER SECTION 1 ENDS.
CXXXXXXXXXXXXXXXXXXXXXXXXXXXXXXXXXXXXXXXXX STANDARD SECTION 2 STARTS:
C      GO TO (10,20,30,40,50,60).IGOTO
CXXXXXXXXXXXXXXXXXXXXXXXXXXXXXXXXXXXXXXXXX STANDARD SECTION 2 ENDS.
CXXXXXXXXXXXXXXXXXXXXXXXXXXXXXXXXXXXXXXXXX USER SECTION 2 STARTS:
C-----
C      SECTION 1: SET FORWARD STEP SIZE DZ FOR IZSTEP>1 WHEN
C      ZWLAST < 0. IN DATA.
C      AT IZSTEP=1 EARTH SETS DZ = ABS(ZWDIST(1)*ZWLAST)
C-----
10 CONTINUE
C*****USER SETS DZ HERE...
      RETURN

```

```

C-----
C   SECTION 2: SET X-WIDTH (XULAST) OF GRID FOR IZSTEP > 1
C   WHEN XULAST < 0. IN DATA.
C   AT IZSTEP=1 EARTH SETS XULAST = ABS(XULAST)
C-----
      20 CONTINUE
C*****USER SETS XULAST HERE...
      RETURN
C-----
C   SECTION 3: SET Y-WIDTH (YVLAST) OF GRID FOR IZSTEP > 1
C   WHEN YVLAST < 0 IN DATA.
C   AT IZSTEP=1 EARTH SETS YVLAST = ABS(YVLAST)
C-----
      30 CONTINUE
C*****USER SETS YVLAST HERE...
      RETURN
C-----
C   SECTION 4: SET INNER RADIUS (RINNER) OF GRID FOR IZSTEP > 1
C   WHEN RINNER < 0 IN DATA.
C   AT IZSTEP=1 EARTH SETS RINNER = ABS(RINNER)
C-----
      40 CONTINUE
C*****USER SETS RINNER HERE...
      RETURN
C-----
C   SECTION 5: SET SLOPE (SNALFA) OF INNER EDGE OF GRID FOR
C   IZSTEP > 1 WHEN SNALFA > 1. & CARTES = .FALSE.
C   AT IZSTEP=1 EARTH SETS SNALFA = SNALFA-2.
C-----
      50 CONTINUE
C*****USER SETS SNALFA HERE...
      RETURN
C-----
C   SECTION 6: SET MEAN PRESSURE (PBAR) AT NEXT FORWARD STEP
C   WHEN PBAR < 0. IN DATA.
C   FOR UNCONFINED FLOWS WITH IMPRESSED NON-ZERO
C   PRESSURE GRADIENTS SET PBAR HERE: FOR CONFINED
C   FLOWS EARTH AUTOMATICALLY COMPUTES PRESSURE REQUIRED.
C-----
      60 CONTINUE
C*****USER SETS PBAR HERE...
      RETURN
      END

```

# APPENDIX 7

# Appendix 7: Pre-chamber Satellite - PRESAT

```

C♦DIRECTIVE**SATLIT
  PROGRAM SATLIT
C
C-----FILENAME: PRESAT
C-----
C
C-----DESCRIPTION: MODEL FOR MIXTURE FORMATION IN THE PRECHAMBER
C                      OF A NATURAL GAS ENGINE
C
C-----DATE:          JUNE 1987
C
C-----AUTHORS:       M. WILSON AND D.S. MOORE
C                      UNIVERSITY OF BATH
C-----
CHAPTER 1  COMMON BLOCKS AND USER'S DATA.
C-----
*** READ(CMNGUS)
*** READ(GUSSEQ)
*** READ(CMNGRF)
C   PARAMETER NXSAT=1,NYSAT=12,NZSAT=21
C   PARAMETER NDIM=1008
COMMON/DTRAN/ANGLE,NOZY
COMMON/CPI/IPWRIT,IDUM(243)
DIMENSION GDTAPE(3),DFAULT(4)
DIMENSION ARRAY1(309),ARRAY2(194),ARRAY3(421)
LOGICAL ARRAY1,LSPDA,WRT,RD
LOGICAL PRE
INTEGER ARRAY2,XPLANE,YPLANE,ZPLANE
INTEGER P1,PP,U1,U2,V1,V2,W1,W2,R1,R2,RS,EP,H1,H2,H3,C1,C2,
&C3,C4
REAL NORTH,LOW
EQUIVALENCE (ARRAY1(1),CARTES),(ARRAY2(1),NX)
EQUIVALENCE (ARRAY3(1),SPARE1(1)),(M1,R1),(M2,R2)
EQUIVALENCE (LSTRUN,INTGR(12))
CXXXXXXXXXXXXXXXXXXXXXXXXXXXXXXXXXXXXXXXXXXXXXXXXX STANDARD SECTION 1 ENDS.
CXXXXXXXXXXXXXXXXXXXXXXXXXXXXXXXXXXXXXXXXXXXXXXXXX USER SECTION 1 STARTS:
C   GRAFFIC ARRAYS DIMENSIONED AS NEEDED...
C   COMMON/GRAF1/PHI1(1) /GRAF2/PHI2(1)
C   POROSITY & SPECIAL DATA ARRAYS DIMENSIONED AS NEEDED...
DIMENSION PE(9,10,18),PN(9,10,18)
DIMENSION PH(9,10,18),PC(9,10,18)
DIMENSION XGRID(50),YGRID(50),ZGRID(50)
DIMENSION YLOC(11,10),XLOC(11,10)
DIMENSION GU(11,10),GV(11,10)
DIMENSION LSPDA(1),ISPDA(1),RSPDA(1)
C   USER PLACES HIS VARIABLES, ARRAYS, EQUIVALENCES ETC. HERE.
DIMENSION PORE(12),PORHC(12)
DIMENSION NVECT(10)
DATA NLSP,NISP,NRSP/1,1,1/
C   USER PLACES HIS DATA STATEMENTS HERE.
DATA PORE/0.0,0.235,0.470,0.735,0.941,1.0,0.941,0.735,0.470,
&0.235,0.0,0.0/
DATA PORHC/0.0,0.122,0.338,0.488,0.818,0.9898,0.9898,0.818,
& 0.488,0.338,0.122,0.0/
DATA PE,PN,PH,PC/6480*1.0/
CXXXXXXXXXXXXXXXXXXXXXXXXXXXXXXXXXXXXXXXXXXXXXXXXX USER SECTION 1 ENDS.
CXXXXXXXXXXXXXXXXXXXXXXXXXXXXXXXXXXXXXXXXXXXXXXXXX STANDARD SECTION 2 STARTS:

```

```

C-----
CHAPTER 2  SET CONSTANTS, AND ARRANGE FILE MANIPULATIONS.
C-----
C    PLEASE DO NOT ALTER, OR RE-SET, ANY OF THE REMAINING
C    STATEMENTS OF THIS CHAPTER.
    DATA CELL,EAST,WEST,NORTH,SOUTH,HIGH,LOW,VOLUME/
& 0.,1.,2.,3.,4.,5.,6.,7. /
    DATA P1,PP,U1,U2,V1,V2,W1,W2,R1,R2,RS,KE,EP,H1,H2,H3,C1,C2,
&C3,C4/1,2,3,4,5,6,7,8,9,10,11,12,13,14,15,16,17,18,19,20/
    DATA FIXFLU, FIXVAL, ONLYMS, WALL/1, E-10, 1, E10, 0.0, -10.0/
    DATA IPLANE, XPLANE, YPLANE, ZPLANE/0, 1, 2, 3/
    DATA WRT, RD, DFAULT/, TRUE... FALSE... 4HDEFA, 4HULT... 4HDTA/, 1HG/
    DATA GDTAPE/4HGUSI, 4HE1, D, 2HTA/
    DATA NLDATA, NIDATA, NRDATA/309, 194, 421/
    DATA NLCREG, NTCVRG/60, 350/
    CALL TAPES(10, GDTAPE, 3, 1, 4*NRDATA)
C-----READ DEFAULT FILE IF BLOCKDATA ABSENT
    IF(INTGR1(29).NE.10) GO TO 2
    CALL WRIT40(40HDATA ESTABLISHED IN BLOCK DATA.      )
    GO TO 3
2 CALL TAPES(1, DFAULT, 4, 2, 4*NRDATA)
    CALL DATAIO(RD, 1)
    CALL WRIT40(40HDATA TAKEN FROM DEFAULT, DTA ON GROUP A/C)
3 CALL WRIT40(40HFILE MODSTL,FTN IS THE SATLIT USED.      )
C-----
CHAPTER 3  DEFINE DATA FOR NRUN RUNS.
C-----
CXXXXXXXXXXXXXXXXXXXXXXXXXXXXXXXXXXXXXXXXXXXXXXXXXXXX STANDARD SECTION 2 ENDS.
CXXXXXXXXXXXXXXXXXXXXXXXXXXXXXXXXXXXXXXXXXXXXXXXXXXXX USER SECTION 2 STARTS:
C--- GROUP 41 MULTI-RUNS : RUN(1-30)<.T.,29*.F.>
C
    DO 410 II=1,1
    410 RUN(II)=.TRUE.
CXXXXXXXXXXXXXXXXXXXXXXXXXXXXXXXXXXXXXXXXXXXXXXXXXXXX USER SECTION 2 ENDS.
CXXXXXXXXXXXXXXXXXXXXXXXXXXXXXXXXXXXXXXXXXXXXXXXXXXXX STANDARD SECTION 3 STARTS:
    DO 10 IRUN=1,30
    IF(.NOT.RUN(IRUN)) GO TO 10
    NRUN=NRUN+1
    LSTRUN=IRUN
10 CONTINUE
C    DO 999 IRUN=1,LSTRUN
C    IF(.NOT.RUN(IRUN)) GO TO 999
    IRUN=1
    INTGR(11) = IRUN
CXXXXXXXXXXXXXXXXXXXXXXXXXXXXXXXXXXXXXXXXXXXXXXXXXXXX STANDARD SECTION 3 ENDS.
CXXXXXXXXXXXXXXXXXXXXXXXXXXXXXXXXXXXXXXXXXXXXXXXXXXXX USER SECTION 3 STARTS:
C--- ALL INTEGER VARIABLES ARE DEFAULTED TO 0, AND REAL VARIABLES
C    TO 0.0, UNLESS OTHERWISE INDICATED.
C    E.G. BY VARIABLE<10>, OR <10.0> AS APPROPRIATE.
C    THE DEFAULT SETTINGS OF ALL LOGICAL VARIABLES ARE ALWAYS
C    INDICATED, E.G. VARIABLE<.T.>, OR VARIABLE<.F.>.
C
C--- RUN1
C-----
C--- SPECIAL DATA INPUT/OUTPUT
C-----
C
C--- INPUT FILE FOR LSTEP      AND GROUND DATA

```

```

C      FIINIT(P1)
C      FIINIT(H1)
C      LSWEEP
C
C      OPEN(UNIT=65, FILE='PREDAT', STATUS='OLD')
C      READ(65, 6510) FP1, FH1
C      READ(65, 6520) LSWEEP, LSTEP, ATIME, TLAST
C      READ(65, 6522) IFRAC
C      READ(65, 6524) (TFRAC(I), I=1, IFRAC)
C      READ(65, 6510) ZHIGHT, ZWLAST
C
C----- FILE DTRAN FOR DATA TRANSFER TO PREGRD
C
C      OPEN(UNIT=66, FILE='DTRAN', STATUS='NEW')
C
C-----
C-----
C----- GROUP 1. FLOW TYPE :
C      PARAB<. F.>, CARTES<. T.>, ONEPHS<. T.>
C      CARTES=. FALSE.
C-----
C----- GROUP 2. TRANSIENCE :
C      STEADY<. T.>, ATIME, LSTEP<1>, FSTEP<1>
C      TLAST<1. E10>, TFRAC(1-30) <30*1.>
C      SERVICE SUBROUTINE FOR 'NT' POWER-LAW TIME STEPS:
C      CALL GRDPWR(0, NT, TLAST, POWER)
C      STEADY=. FALSE.
C LOCAL VARIABLE RPS DENOTES REVS. PER SEC....
C      RPS=25.0
C      ATIME=ATIME/(360.0*RPS)
C      TLAST=TLAST/(360.0*RPS)
C      TIME INTERVALS FOR AXI-SYMMETRIC BOWL CASE...
C      ANGLE=(TLAST-ATIME)*360.0*RPS
C      TFRAC(1)=-TFRAC(1)
C      DO 210 I=2, IFRAC, 2
C      TFRAC(I)=TFRAC(I)/ANGLE
210 CONTINUE
C
C-----
C-----
C----- GROUP 3. X-DIRECTION :
C      NX<1>, XULAST<1. 0>, XFRAC(1-30)
C      SERVICE SUBROUTINE FOR POWER-LAW GRID:
C      CALL GRDPWR(1, NX, XULAST, POWER)
C      NX=9
C      XULAST=2.0*3.14159
C      XFRAC(1)=0.04
C      XFRAC(2)=0.078
C      XFRAC(3)=0.25
C      XFRAC(4)=0.328
C      XFRAC(5)=0.5
C      XFRAC(6)=0.578
C      XFRAC(7)=0.75
C      XFRAC(8)=0.828
C      XFRAC(9)=1.0
C-----
C----- GROUP 4. Y-DIRECTION :
C      NY<1>, YVLAST<1. 0>, YFRAC(1-30), RINNER, SNALFA
C      SERVICE SUBROUTINE FOR POWER-LAW GRID:
C      CALL GRDPWR(2, NY, YVLAST, POWER)

```

```

NY=10
YVLAST=12.7E-3
YFRAC(1)=0.0709
YFRAC(2)=0.1417
YFRAC(3)=0.2126
YFRAC(4)=0.3150
YFRAC(5)=0.4409
YFRAC(6)=0.5669
YFRAC(7)=0.6614
YFRAC(8)=0.7874
YFRAC(9)=0.9134
YFRAC(10)=1.0
NOZY=3

```

```

C-----
C--- GROUP 5. Z-DIRECTION :
C   NZ<1>,ZWLAST<1.0>,ZFRAC(1-30)
C   SERVICE SUBROUTINE FOR POWER-LAW GRID:
C   CALL GRDPWR(3,NZ,ZWLAST,POWER)
C   NZ=18
C   NSLOPE=7
C   NOZZ=13
C   GRID SPECIFIED AT BDC...
C
C----- (NSLOPE-1) CELLS TO START OF SLOPE. EVENLY SPACED
C
C   NSM1=NSLOPE-1
C   ZFRAC(1)=ZHIGHT/FLOAT(NSM1)
C   DO 510 I=2,NSM1
C     ZFRAC(I)=ZFRAC(I-1)+ZHIGHT/FLOAT(NSM1)
C 510 CONTINUE
C
C----- FIXED GRID FOR NSLOPE - NZ
C----- NOTE: FRACTIONS HERE ARE GIVEN IN TERMS OF
C           (ZWLAST-ZHIGHT) WHICH IS ASSUMED
C           CONSTANT. PRECHAMBER VOLUME MAY BE
C           CHANGED BY SETTING ZHIGHT IN INPUT DATA
C
C   ZFRAC(7)=0.0352
C   ZFRAC(8)=0.0856
C   ZFRAC(9)=0.1720
C   ZFRAC(10)=0.2331
C   ZFRAC(11)=0.3248
C   ZFRAC(12)=0.4140
C   ZFRAC(13)=0.4776
C   ZFRAC(14)=0.6183
C   ZFRAC(15)=0.7610
C   ZFRAC(16)=0.9019
C   ZFRAC(17)=0.9465
C   ZFRAC(18)=1.0
C
C----- CONVERT TO FRACTIONS OF ZWLAST
C
C   DO 520 I=1,NSM1
C     ZFRAC(I)=ZFRAC(I)/ZWLAST
C 520 CONTINUE
C
C   DO 530 I=NSLOPE,NZ
C     ZFRAC(I)=(ZFRAC(I)*(ZWLAST-ZHIGHT)+ZHIGHT)/ZWLAST

```



530 CONTINUE

```
C-----
C--- GROUP 6. MOVING GRID :
C   MGRID, IZW1, IZW2, AZW2, BZW2, CZW2, PINT, ZW2M1T
C-----
C--- GROUP 7. BLOCKAGE: BLOCK<.F.>, IPLANE, IPWRIT
C *SET CONSTANT POROSITIES OVER REGIONS USING:
C   CALL CONPOR(IR, FACE, VALUE, IXF, IXL, IYF, IYL, IZF, IZL). WHERE:
C   IR=RUN SECTION NUMBER, E.G. 1 FOR RUN1 SECTION: 'FACE'= EAST,
C   WEST, NORTH, SOUTH, HIGH, LOW & CELL. 'VALUE'=WANTED POROSITY
C   OVER REGION IXF,...,IZL.
C *DIMENSION ARRAYS PE(NX,NY,NZ), PN(NX,NY,NZ), PH(NX,NY,NZ), &
C   PC(NX,NY,NZ) ABOVE.
C *FOR FULLY-BLOCKED CELLS (IE. 'VALUE'= 0.0) USER NEED SET ONLY
C   THE 'CELL' POROSITY (TO ZERO), AS CELL-FACE AREAS ARE THEN
C   AUTOMATICALLY ZEROED.
C *FOR SATELLITE PRINTOUT OF POROSITIES 'IPLANE'= XPLANE,
C   YPLANE, OR ZPLANE AS DESIRED.
C *FOR EACH 'FACE' A MAXIMUM OF 10 CALLS TO CONPOR IS ALLOWED.
C   BUT IF REQUIREMENTS EXCEED THIS PROVISION SET BLOCK=.T. &
C   IPWRIT=-1, AND SET POROSITY ARRAYS EXPLICITLY HERE AS WANTED.
C   IN THIS CASE, THE USER M U S T   S E T   A L L   ELEMENTS OF
C   ARRAYS PE, PN, PH, PC (MANY MAY BE 0.0 OR 1.0). HE MAY USE:
C   CALL CR(PARRAY, VALUE, IXF, IXL, IYF, IYL, IZF, IZL, NX, NY, NZ)
C   ANY NUMBER OF TIMES, TO SET 'PARRAY' (= PE, ETC.) TO
C   'VALUE' OVER RANGE IXF TO IXL, IYF TO IYL, IZF TO IZL.
C *CONPOR M U S T   N O T   BE USED IN CONJUNCTION WITH EXPLICIT
C   SETTINGS OF THE ARRAYS (INCLUDING SETTINGS VIA CR).
C
C   BLOCK=.TRUE.
C   IPWRIT=-1
C       DO 77 IZ=1, NZ
C       DO 77 IX=1, NX
C       DO 77 IY=1, NY
```

```
C
C-----POROSITIES FOR DORMAN GEOMETRY
```

```
C
C-----BLOCK CELLS ABOVE PRECHAMBER
C   IF(IZ.GT.18) GO TO 77
C   IF(IZ.EQ.7.AND.IY.EQ.10) GO TO 79
C   IF(IZ.EQ.8.AND.IY.EQ.9) GO TO 79
C   IF(IZ.EQ.9.AND.IY.EQ.8) GO TO 79
C   IF(IZ.EQ.10.AND.IY.EQ.7) GO TO 79
C   IF(IZ.EQ.11.AND.IY.EQ.6) GO TO 79
C   IF(IZ.EQ.12.AND.IY.EQ.5) GO TO 79
C   IF(IZ.EQ.13.AND.IY.EQ.4) GO TO 79
```

```
C
C   IF(IZ.GT.7.AND.IY.EQ.10) GO TO 82
C   IF(IZ.GT.8.AND.IY.EQ.9) GO TO 82
C   IF(IZ.GT.9.AND.IY.EQ.8) GO TO 82
C   IF(IZ.GT.10.AND.IY.EQ.7) GO TO 82
C   IF(IZ.GT.11.AND.IY.EQ.6) GO TO 82
C   IF(IZ.GT.12.AND.IY.EQ.5) GO TO 82
C   IF(IZ.GT.13.AND.IY.EQ.4) GO TO 82
```

```
C
C   IF(IZ.EQ.NZ.AND.IY.LE.3) PC(IX,IY,IZ)=0.98
C   GO TO 77
```

```
C-----PARTIALLY BLOCKED CELLS
```

```

79  PN(IX,IY,IZ)=0.
    PH(IX,IY,IZ)=0.
    PC(IX,IY,IZ)=0.5
    GO TO 77

```

```

C-----FULLY BLOCKED CELLS

```

```

82  CONTINUE
    PC(IX,IY,IZ)=0.
77  CONTINUE

```

```

C

```

```

C-----

```

```

C---  GROUP 8. DEPENDENT VARIABLES TO BE SOLVED FOR OR STORED :
C      SOLVAR(1-25) <25*.F.>, STOVAR(1-25) <25*.F.>, CONC1(1-4) <4*.T.>
C      USE FOLLOWING NAMED INTEGERS FOR ARRAY ELEMENTS 1-20:
C      P1, PP, U1, U2, V1, V2, W1, W2, M1, M2, RS, KE, EP, H1, H2, H3, C1, C2, C3, C4.
      SOLVAR(P1)=.TRUE.
      SOLVAR(PP)=.TRUE.
      SOLVAR(U1)=.TRUE.
      SOLVAR(V1)=.TRUE.
      SOLVAR(W1)=.TRUE.
      SOLVAR(KE)=.TRUE.
      SOLVAR(EP)=.TRUE.
      SOLVAR(H1)=.TRUE.
      SOLVAR(C1)=.TRUE.
      SOLVAR(C2)=.TRUE.

```

```

C-----

```

```

C---  GROUP 10 PROPERTIES:
C      IRHO1<1>, IRHO2<1>, RHO1<1.0>, RHO2<1.0>,
C      ARHO1<1.0>, BRHO1<1.0>, CRHO1<1.0>
C      IEMU1<1>, EMU1<1.0>, EMULAM<1.E-10>
C      IHSAT, H1SAT, H2SAT, PSATEX<1.0>
C      SIGMA(1-25) <1.0, 2.0, 1., 1.E10, 1., 1.E10, 1., 1.E10,
C      4*1.0, 1.314, 1.0, 1.E10, 10*1.0>
      IROH1=-1
      EMULAM= 1.0E-5
      IEMU1=2

```

```

C-----

```

```

C---  GROUP 13 INITIAL FIELDS :
C      FIINIT(1-25) <25*1.E-10>
      FIINIT(P1)=FP1
      FIINIT(U1)=2.7*BZW2
      FIINIT(KE)=(0.25*RPS/0.816)**2
      FIINIT(EP)=0.09*FIINIT(KE)**1.5/0.014
      FIINIT(H1)=FH1
      FIINIT(C1)=1.E-10
      FIINIT(C2)=1.0-FIINIT(C1)

```

```

C-----

```

```

C---  GROUP 14 BOUNDARY/INTERNAL CONDITIONS :
C      ILOOP1, ILOOPN, XCYLE<.F.>, PBAR, REGION(1-10) <10*.T.>
C      *N.B. ALL 10 REGIONS ARE DEFAULTED .TRUE.. THE USER SHOULD
C      SET REGION(I)=.FALSE. FOR UNUSED REGIONS 'I'.
      DO 140 IREG=4, 10
      REGION(IREG)=.FALSE.
140  CONTINUE

```

```

C-----

```

```

C---  GROUP 15 TO 24: REGIONS 1 TO 10
C---  ONLY THOSE REGIONS ARE ACTIVE WHICH ARE SPECIFIED BY THE
C      USER, PREFERABLY BY WAY OF:-
C      CALL PLACE(REGION INDEX, TYPE, IXF, IXL, IYF, IYL, IZF, IZL) &

```

```

C      CALL COVAL(REGION INDEX,VARIABLE,COEFFICIENT,VALUE)
C-----
C
C----- PRE-CHAMBER TOP -----
      CALL PLACE(1,HIGH,1,NX,1,NY,1,1)
      CALL COVAL(1,U1,WALL,0.0)
      CALL COVAL(1,V1,WALL,0.0)
      CALL COVAL(1,KE,WALL,0.0)
      CALL COVAL(1,EP,WALL,0.0)
C----- PRE-CHAMBER WALL -----
      CALL PLACE(2,NORTH,1,NX,NY,NY,1,NSLOPE-1)
      CALL COVAL(2,U1,WALL,0.0)
      CALL COVAL(2,W1,WALL,0.0)
      CALL COVAL(2,KE,WALL,0.0)
      CALL COVAL(2,EP,WALL,0.0)
C----- NOZZLE -----
      CALL PLACE(3,NORTH,1,NX,NOZY,NOZY,NOZZ+1,NZ)
      CALL COVAL(3,U1,WALL,0.0)
      CALL COVAL(3,W1,WALL,0.0)
      CALL COVAL(3,KE,WALL,0.0)
      CALL COVAL(3,EP,WALL,0.0)

C
C-----
C---  GROUP 25 GROUND STATION :
C      GROSTA<.F.>
      GROSTA=.TRUE.
C-----
C---  GROUP 26 SOLUTION TYPE AND RELATED PARAMETERS :
C      WHOLEP<.F.> , SUBPST<.F.> , DONACC<.F.>
      260 WHOLEP=.TRUE.
C-----
C---  GROUP 27 SWEEP AND ITERATION NUMBERS :
C      FSWEPT<1> , LSWEPT<1> , LITHYD<1> , LITC<1> , LITKE<1> , LITH<1> ,
C      LITER(1-25)<9*1,-1,15*1>
C      IVELF<1> , NVEL<1> , IVELL<10000> ,
C      IKEF<1> , NKE<1> , IKEL<10000> ,
C      IENTF<1> , NENT<1> , IENTL<10000> ,
C      ICNCF<1> , NCNC<1> , ICNCL<10000> ,
C      IRHO1F<1> , NRHO1<1> , IRHO1L<10000> ,
C      IRHO2F<1> , NRHO2<1> , IRHO2L<10000>
      LITER(PP)=10
C-----
C---  GROUP 28 TERMINATION CRITERIA :
C      ENDIT(1-25)<9*1,E-10,0.5,15*1,E-10>
      ENDIT(P1)=1.0E-5*0.5*XULAST*YVLAST**2*(ZWLAST-2.0*AZW2)
      & *360.0*RPS
      ENDIT(PP)=1.0E-3
      ENDIT(W1)=2.0E-3
      ENDIT(V1)=2.0E-3
      ENDIT(U1)=5.0E-2
      ENDIT(KE)=1.0E-3
      ENDIT(EP)=1.0E-3
      ENDIT(H1)=1.0E-3
      ENDIT(C1)=1.0E-3
      ENDIT(C2)=1.0E-3
C-----
C---  GROUP 32 PRINT-OUT OF VARIABLES :
C      PRINT(1-25)<.T...F.,23*.T.> , SUBWGR<.F.>

```

```

C-----
C    GROUP 33 MONITOR PRINT-OUT :
C    IXMON<1>, IYMON<1>, IZMON<1>, NPRMON<1>, NPRMNT<1>
C    NPRMON=6
C    NPRMNT=10
C    IYMON=2
C    IZMON=15
C-----
C    GROUP 34 FIELD PRINT-OUT CONTROL :
C    NPRINT<100>, NTPRIN<100>, NXPRIN<1>, NYPRIN<1>, NZPRIN<1>,
C    IZPRF<1>, ISTRPF<1>, IZPRL<10000>, ISTRPL<10000>
C    NUMCLS<10>, KOUTPT
C    NPRINT=LSWEEP
C    NZPRIN=1
C    NTPRIN=LSTEP
C-----
C    IF(IRUN.EQ. 1) GO TO 900
C---  RUN2
C    IF(IRUN.EQ. 2) GO TO 900
C    900 CONTINUE
C---  ALL RUNS
CXXXXXXXXXXXXXXXXXXXXXXXXXXXXXXXXXXXXXXXXXXXXXXXXXXXXX USER SECTION 3 ENDS.
CXXXXXXXXXXXXXXXXXXXXXXXXXXXXXXXXXXXXXXXXXXXXXXXXXXXXX STANDARD SECTION 4 STARTS:
C-----
C
C---  DATA TRANSFER TO GROUND
C
C    READ(65, 6530) PSUP, TFUEL, GASIN, CFTIN, PSCALE
C    READ(65, 6540) (NVECT(I), I=1, 10)
C    WRITE(66, 6610) RPS, NOZY
C    WRITE(66, 6530) PSUP, TFUEL, GASIN, CFTIN, PSCALE
C    WRITE(66, 6540) (NVECT(I), I=1, 10)
C---  CLOSE SPECIAL FILES
C    CLOSE(UNIT=65)
C    CLOSE(UNIT=66)
C
C---  FORMATS
C
C    6510 FORMAT(2(1X, E11. 4))
C    6520 FORMAT(2(1X, I3), 2(1X, F5. 1))
C    6522 FORMAT(1X, I3)
C    6524 FORMAT(10(1X, F4. 1))
C    6530 FORMAT(5(1X, E11. 4))
C    6540 FORMAT(10(1X, I3))
C    6610 FORMAT(1X, E11. 4, 1X, I2)
C
C-----GRID INSPECTION
C
C    CALL FDGRID(XFRAC, XULAST, XGRID, NX)
C    CALL FDGRID(YFRAC, YVLAST, YGRID, NY)
C    CALL FDGRID(ZFRAC, ZWLAST, ZGRID, NZ)
C
C-----MAP POLAR X-Y PLANE ONTO CARTESIAN GRID
C
C    CALL CARPOL(YGRID, NY+1, XGRID, NX+1, YLOC, XLOC, GU, GV, 0)
C

```

```

OPEN(UNIT=65, FILE='XYPREM', STATUS='NEW')
OPEN(UNIT=66, FILE='YZPREM', STATUS='NEW')

C
IXP=1
DUM1=0.

C
DO 715 IX=1, NX+1
DO 715 IY=1, NY+1
IF(IY. LE. NY. AND. IX. LE. NX) PBLOK=PC(IX, IY, 1)
WRITE(65, *) XLOC(IY, IX), YLOC(IY, IX), PBLOK, DUM1, DUM1
715 CONTINUE

C
DO 716 IZ=1, NZ+1
DO 716 IY=1, NY+1
IF(IY. LE. NY. AND. IZ. LE. NZ) PBLOK=PC(IXP, IY, IZ)
WRITE(66, *) ZGRID(IZ), YGRID(IY), PBLOK, DUM1, DUM1
716 CONTINUE

C
CLOSE(UNIT=65)
CLOSE(UNIT=66)

C
C
C WRITE GENERAL DATA ON TO THE GUSIE1.DTA TAPE...
IF(SPDATA) CALL WRTSPC(LSPDA, NLSP, ISPDA, NISP, RSPDA, NRSP)
IF(BLOCK) CALL WRTPOR(PE, PN, PH, PC, NX, NY, NZ, IPLANE)
C OLD PRACTICES RETAINED FOR REFERENCE:
C IF(SPDATA) CALL SPCDAT(IRUN)
C IF(BLOCK) CALL PORDAT(IRUN)
GRAPHS=.FALSE.
IF(GRAPHS) CALL SORT(IRUN)
IF(RESTRT) GO TO 902
DO 901 INDVAR=1, 25
IF(IFIX(FIINIT(INDVAR)+0.1). NE. 10101) GO TO 901
CALL FLDDAT(IRUN)
GO TO 902
901 CONTINUE
902 CALL DATAIO(WRT, 10)
IF(MONITR) CALL DATAIO(WRT, -6)
STOP
END

```

# APPENDIX 8

# Appendix 8: Pre-chamber Ground-station - PREGRD

```

C$DIRECTIVE**GROUND
  PROGRAM MAIN
C   *FILE NAME: PREGRD.FTN
C   *INCLUDED SUBROUTINES: MAIN & GROUND.
C   *SATELLITE FILE NAME: PRESAT.FTN
  COMMON/ISHIFT/III(57),NFMAX
C SET F-ARRAY DIMENSION AS NEEDED. & SET NFMAX ACCORDINGLY.
  COMMON F(100000)
  EXTERNAL AMEND
  EXTERNAL BDATA
  EXTERNAL GROUND
  NFMAX=100000
  CALL MAIN1
  STOP
  END
  SUBROUTINE GROUND(IRN,ICHAP,ISTP,ISWP,IZED,INDVAR)
*** READ(CMNGUS)
*** READ(GUSSEQ)
C   INCLUDE 'NMLIST'
CXXXXXXXXXXXXXXXXXXXXXXXXXXXXXXXXXXXXXXXXXXXXXXXXXXXX STANDARD SECTION 1 STARTS:
C   PARAMETER NXG=1,NYG=12,NZG=21
  COMMON/TYPE/CELL,EAST,WEST,NORTH,SOUTH,HIGH,LOW,VOLUME,WALL
  COMMON/VAR/P1,PP,U1,U2,V1,V2,W1,W2,R1,R2,RS,
&KE,EP,H1,H2,H3,C1,C2,C3,C4,RX,RY,RZ,S1,S2
  COMMON/VAROLD/P1O,PPO,U1O,U2O,V1O,V2O,W1O,W2O,R1O,R2O,RSO,
&KEO,EPO,H1O,H2O,H3O,C1O,C2O,C3O,C4O,RXO,RYO,RZO,S1O,S2O
  COMMON/VARLOW/P1L,PPL,U1L,U2L,V1L,V2L,W1L,W2L,R1L,R2L,RSL,
&KEL,EPL,H1L,H2L,H3L,C1L,C2L,C3L,C4L,RXL,RYL,RZL,S1L,S2L
  COMMON/VARHI/P1H,PPH,U1H,U2H,V1H,V2H,W1H,W2H,R1H,R2H,RSH,
&KEH,EPH,H1H,H2H,H3H,C1H,C2H,C3H,C4H,RXH,RYH,RZH,S1H,S2H
  COMMON/GMTRY/VOL,VOLO,AEAST,ANORTH,AHIGH,AEDX,ANDY,AHDZ
  COMMON/PROP/D1,D2,D1DP,D2DP,MU1,MU1LAM,EXCO,CFP,MDT,HST1,HST2
  COMMON/PRPOLD/D1O,D2O
  COMMON/PRPLOW/D1L,D2L,EXCOL
  COMMON/PRPHI/D1H,D2H,MU1H,EXCOH
  COMMON/VARNX/XG,XU,DXU,DXG
  COMMON/VARNY/YG,YV,DYV,DYG,R,RV
  COMMON/VARNZ/ZG,ZW1,DZW,DZG,WGRID
  COMMON/GDMSCI/XPLANE,YPLANE,ZPLANE,ITNO
  COMMON/GDMSC/LSLAB,MSLAB,HSLAB,LAMMU
  REAL NORTH,LOW
  INTEGER P1,PP,U1,U2,V1,V2,W1,W2,R1,R2,RS,
&KE,EP,H1,H2,H3,C1,C2,C3,C4,RX,RY,RZ,S1,S2
  INTEGER P1O,PPO,U1O,U2O,V1O,V2O,W1O,W2O,R1O,R2O,RSO,
&KEO,EPO,H1O,H2O,H3O,C1O,C2O,C3O,C4O,RXO,RYO,RZO,S1O,S2O
  INTEGER P1L,PPL,U1L,U2L,V1L,V2L,W1L,W2L,R1L,R2L,RSL,
&KEL,EPL,H1L,H2L,H3L,C1L,C2L,C3L,C4L,RXL,RYL,RZL,S1L,S2L
  INTEGER P1H,PPH,U1H,U2H,V1H,V2H,W1H,W2H,R1H,R2H,RSH,
&KEH,EPH,H1H,H2H,H3H,C1H,C2H,C3H,C4H,RXH,RYH,RZH,S1H,S2H
  INTEGER VOL,VOLO,AEAST,ANORTH,AHIGH,AEDX,ANDY,AHDZ
  INTEGER D1,D1DP,D2,D2DP,EXCO,CFP,MDT,HST1,HST2
  INTEGER D1O,D2O,D1L,D2L,EXCOL,D1H,D2H,EXCOH
  INTEGER XG,XU,DXU,DXG,YG,YV,DYV,DYG,R,RV,ZG,ZW1,DZW,
&DZG,WGRID
  INTEGER XPLANE,YPLANE,ZPLANE
  LOGICAL LSLAB,MSLAB,HSLAB,LAMMU,LSPDA

```

```

EQUIVALENCE (M1,R1),(M2,R2)
C   SATLIT-EQUIVALENT IRUN:
EQUIVALENCE (IRUN,INTGR(11))
CXXXXXXXXXXXXXXXXXXXXXXXXXXXXXXXXXXXXXXXXXXXXXXXXXXXX STANDARD SECTION 1 ENDS.
CXXXXXXXXXXXXXXXXXXXXXXXXXXXXXXXXXXXXXXXXXXXXXXXXXXXX USER SECTION 1 STARTS:
C   ARRAYS ( DIMENSIONED NY,NX ) FOR USE WITH 'ADD':
DIMENSION CVAR(10,9),VVAR(10,9),CM(10,9),VM(10,9),ZERO(10,9)
C   SPECIAL-DATA ARRAYS DIMENSIONED & DIMENSION VALUES SET HERE:
DIMENSION LSPDA(1),ISPDA(1),RSPDA(1)
C   USER PLACES HIS VARIABLES, ARRAYS, EQUIVALENCES ETC. HERE.
C
C-----ARRAYS FOR VARIABLE STORAGE IN A Z-SLAB
C
DIMENSION GPRES(10,9),GENTH(10,9),GRHO(10,9)
DIMENSION GCONC(10,9),GRES(10,9)
DIMENSION GDDP(10,9)
DIMENSION GVOL(10,9),GAREA(10,9)
C
C-----STORAGE FOR Y-Z PLANE CO-ORDS. W, V AND CONC. FIELDS
C
DIMENSION GRIDY(10),GRIDZ(18),GWVEL(10,9),GVVEL(10,9)
DIMENSION GTSTOR(9,10,18)
DIMENSION GCSTOR(10,18),GARSTOR(10,18)
DIMENSION GZSTOR(10,18),GYSTOR(10,18)
DIMENSION GWSTOR(10,18),GVSTOR(10,18)
DIMENSION GW1STR(10,18),GV1STR(10,18)
DIMENSION GA1STR(10,18)
COMMON/DTRAN/GRPS,NOZY
COMMON/HOLD/GMGTOT,GMATOT,GPVOL,TMFUEL
COMMON/PV/PREPRES,CYLPRES
COMMON/BOUC/PEXT
COMMON/GSTORE/CPMIX,ROF,GVLIN,GPDIF,DMF
COMMON/GINPT/PSUP,TFUEL,GASIN,CFTIN,PSCALE
COMMON/INPT/NVECT(10)
COMMON/GOPEN/FOPN
LOGICAL FOPN
LOGICAL PRE
DATA PRE/,TRUE./
DATA LRES,LPLLOT/25,22/
C
C-----CP VS TEMP. DATA FOR INTERPOLATION OF GAS PROP'S
C
DATA GFMW,GRMW,GAMW,GRO/15.85,29.18,28.96,8314/
DATA CPF1,CPF2,CPA1,CPA2/2226,4814,1005,1167/
DATA CPR1,CPR2/1113,1355/
DATA TMP1,TMP2/300,1150/
C
DATA NLSP,NISP,NRSP/1,1,1/
DATA CVAR,VVAR,CM,VM,ZERO/450*0.0/
C   USER PLACES HIS DATA STATEMENTS HERE.
CXXXXXXXXXXXXXXXXXXXXXXXXXXXXXXXXXXXXXXXXXXXXXXXXXXXX USER SECTION 1 ENDS.
CXXXXXXXXXXXXXXXXXXXXXXXXXXXXXXXXXXXXXXXXXXXXXXXXXXXX STANDARD SECTION 2 STARTS:
      IF(SPDATA)
&CALL RDSPC(IRN,INTGR(12),LSPDA,NLSP,ISPDA,NISP,RSPDA,NRSP)
      CALL GRDUTY(IRN,ICHAP,IZED,INDVAR)
      IF(ICHAP.EQ.-5) GO TO 10
      IF(ICHAP.LE.0.OR.ICHAP.GT.16) RETURN
      GO TO (100,200,300,400,500,600,700,800,900,1000,1100,1200,

```



## RETURN

CXXXXXXXXXXXXXXXXXXXXXXXXXXXXXXXXXXXXX USER SECTION 2 STARTS:

## RETURN

**C**-----

C  
C-----DATA INPUT

**CLOSE(UNIT=65)**

C  
ENDIF

C  
C-----FALSE TIME-STEPS (PDR/6)

500 CONTINUE

### C C-----INJECTOR BOUNDARY CONDITIONS

**C**  
**C-----PRECHAMBER CONDITIONS**

C

```

C-----INJECTION CONDITION
C
    GVLIN=0.
    PCHA=GPRES(8,1)
    IF(PCHA.GE.PSUP) RETURN
C
C-----FIXED VALUES FOR PSUP,TKF,EPF,ROF,H1F
C
    TKF=60.
    GMMW=(1.0-GASIN)*GAMW+GASIN*GFMW
    EPF=2900.
    ROF=PCHA*GMMW/(GRO*TFUEL)
    H1F=CPF1+(TFUEL-TMP1)*(CPF2-CPF1)/(TMP2-TMP1)
    H1F=H1F*TFUEL
C
C-----INJECTION VELOCITY
C
    GPDIF=ABS(PSUP-PCHA)
    GPDF2=GPDIF+GPDIF
    GVLIN=SQRT(GPDF2/ROF)
    GALPHA=5.0*3.14159/180.
    W1F=GVLIN*COS(GALPHA)
    V1F=GVLIN*SIN(GALPHA)
    V1F=-V1F
C
C-----BOUNDARY CONDITIONS INCLUDING DISCHARGE COEFF.
C
    GCD=1.0/0.65
C
    DO 510 IX=1,NX
    DO 510 IY=1,NY
    CM(IY,IX)=ABS(GCD*ROF*GVLIN*1000./PSUP)
    VM(IY,IX)=PSUP
    CVAR(IY,IX)=0.
    VVAR(IY,IX)=0.
    IF(INDVAR.EQ.W1) VVAR(IY,IX)=W1F
    IF(INDVAR.EQ.V1) VVAR(IY,IX)=V1F
    IF(INDVAR.EQ.KE) VVAR(IY,IX)=TKF
    IF(INDVAR.EQ.EP) VVAR(IY,IX)=EPF
    IF(INDVAR.EQ.H1) VVAR(IY,IX)=H1F
    IF(INDVAR.EQ.C1) VVAR(IY,IX)=GASIN
510 CONTINUE
C
C-----ADD BOUNDARY CONDITIONS AS SOURCES
C
    CALL ADD(INDVAR,1,1,8,9,LOW,CM,VM,CVAR,VVAR,
    1NY,NX)
C
    ENDIF
C
C-----NOZZLE BOUNDARY CONDITIONS
C
    IF(IZED.EQ.NZ-1) THEN
C
C-----COMPUTE NOZZLE ENTRY VARIABLES
C
        CALL GET(D1,GRHO,NY,NX)
        CALL GET(P1,GPRES,NY,NX)

```

```

C
CALL INTPOL(P1, ATIME, PEXT)
PEXT=PEXT*PSCALE*1. E5
PNODE=GPRES(2, 1)
DNODE=GRHO(2, 1)

C
GPDIF=PEXT-PNODE
SIGN=1
IF(GPDIF. LT. 0. ) SIGN=-1
WFT=0.
GPDF2=GPDIF+GPDIF
IF(ABS(GPDIF). NE. 0. ) WFT=-SIGN*SQRT(ABS(GPDF2)/DNODE)
FLW=DNODE*WFT
FLW=-FLW

C
C-----VELOCITY COMPONENTS FOR HOLES
C
GBETA=60. *3. 142/180.
VFT=WFT*SIN(GBETA)
WFT=WFT*COS(GBETA)

C
C-----FLOW PROPERTIES AT ENTRY
C
CALL INTPOL(KE, ATIME, TKT)
CALL INTPOL(EP, ATIME, EFT)
CALL INTPOL(H1, ATIME, HFT)
CFT=0.
IF(GPDIF. GT. 0. ) CFT=CFTIN

C
C-----BOUNDARY CONDITIONS
C
GCD=1. 0/0. 65

C
DO 520 IX=1, NX
DO 520 IY=1, NY
CM(IY, IX)=ABS(GCD*FLW*1000. /PEXT)
VM(IY, IX)=PEXT
CVAR(IY, IX)=0.
VVAR(IY, IX)=0.
IF(INDVAR. EQ. W1) VVAR(IY, IX)=WFT
IF(INDVAR. EQ. V1) VVAR(IY, IX)=VFT
IF(INDVAR. EQ. KE) VVAR(IY, IX)=TKT
IF(INDVAR. EQ. EP) VVAR(IY, IX)=EFT
IF(INDVAR. EQ. H1) VVAR(IY, IX)=HFT
IF(INDVAR. EQ. C1) VVAR(IY, IX)=CFT
520 CONTINUE

C
C-----ADD BOUNDARY CONDITIONS AS SOURCES
C
CALL ADD(INDVAR, 1, 2, NOZY, NOZY, NORTH, CM, VM, CVAR, VVAR,
1NY, NX)
CALL ADD(INDVAR, 4, 4, NOZY, NOZY, NORTH, CM, VM, CVAR, VVAR,
1NY, NX)
CALL ADD(INDVAR, 6, 6, NOZY, NOZY, NORTH, CM, VM, CVAR, VVAR,
1NY, NX)
CALL ADD(INDVAR, 8, 8, NOZY, NOZY, NORTH, CM, VM, CVAR, VVAR,
1NY, NX)
ENDIF

```

```

        RETURN
600  CONTINUE
        RETURN
700  CONTINUE
C
C-----CO-ORDS AND VELOCITIES AT A SLAB
C
        CALL GET1D(YG,GRIDY,NY)
        CALL GET1D(ZG,GRIDZ,NZ)
        CALL GET(V1,GVVEL,NY,NX)
        CALL GET(W1,GWVEL,NY,NX)
        CALL GET(C1,GCONC,NY,NX)
        CALL GET(C2,GRES,NY,NX)
C
        DO 710 IY=1,NY
            GWSTOR(IY,IZED)=GWVEL(IY,1)
            GVSTOR(IY,IZED)=GVVEL(IY,1)
            GCSTOR(IY,IZED)=GCONC(IY,1)
710  CONTINUE
C
C-----STORE RESULTS IN IX=6 FOR FULL Y-Z PLANE DISPLAY
C
        IXP=6
        DO 711 IY=1,NY
            GW1STR(IY,IZED)=GWVEL(IY,IXP)
            GV1STR(IY,IZED)=-GVVEL(IY,IXP)
711  CONTINUE
C
C-----COMPUTE PRECHAMBER MASSES FOR SLAB
C
        CALL GET(D1,GRHO,NY,NX)
        CALL GET(VOL,GVOL,NY,NX)
C
        IF(IZED.EQ.1) THEN
            GMGTOT=0.
            GMRTOT=0.
            GMATOT=0.
            GPVOL=0.
            ENDIF
            GMGSUM=0.
            GMRSUM=0.
            GMASUM=0.
            GPVSUM=0.
C
            DO 720 IY=1,NY
                DO 720 IX=1,NX
                    IF(IZED.GE.18) GO TO 720
                    IF(GVOL(IY,IX).EQ.0.0) GO TO 720
                    GMT=GRHO(IY,IX)*GVOL(IY,IX)
                    GMG=GCONC(IY,IX)*GMT
                    GMR=GMT*GRES(IY,IX)
                    GMA=GMT*(1.0-GCONC(IY,IX)-GRES(IY,IX))
                    IF(IX.EQ.1) THEN
                        GARSTOR(IY,IZED)=1.E4
                        IF(GMG.NE.0.0) GARSTOR(IY,IZED)=GMA/GMG
                    ENDIF
                    IF(IX.EQ.IXP) THEN
                        GA1STR(IY,IZED)=1.E4

```

```

      GA1STR(IY, IZED)=GMA/GMG
ENDIF
      GMASUM=GMASUM+GMA
      GMRSUM=GMRSUM+GMR
      GMGSUM=GMGSUM+GMG
      GPVSUM=GPVSUM+GVOL(IY, IX)
720 CONTINUE
C
      GMATOT=GMATOT+GMASUM
      GMRTOT=GMRTOT+GMRSUM
      GMGTOT=GMGTOT+GMGSUM
      GPVOL=GPVOL+GPVSUM
C
C-----MASS OF FUEL INJECTED
C
      IF(IZED.EQ. 1) THEN
      IF(ISTP.EQ. 1.AND. ISWP.EQ. 1) TMFUEL=0.
      CALL GET(AHIGH, GAREA, NY, NX)
      DMF=GASIN*GPDIF*(ROF*GVLIN*1000./PSUP)*(GAREA(8, 1)+GAREA(9, 1))
      DMF=DMF*DT
      ENDIF
C
C-----MONITOR CYLINDER AND PRECHAMBER PRESSURE
C
      IF(IZED.EQ. 5) THEN
      CALL GET(P1, GPRES, NY, NX)
      PREPRES=GPRES(3, 1)
      ENDIF
C
      IF(IZED.EQ. 14) THEN
      CALL GET(P1, GPRES, NY, NX)
      CYLPRES=GPRES(3, 1)
      ENDIF
      RETURN
C
800 CONTINUE
      RETURN
900 CONTINUE
C
C-----ARRANGE INPUT-OUTPUT
C
      IF(ISTP.EQ. 1) THEN
      OPEN(UNIT=LPLOT, FILE='PLOT', STATUS='NEW')
      OPEN(UNIT=LRES, FILE='CARES', STATUS='NEW')
      WRITE(LRES, 9010)
      WRITE(LRES, 9020) FIINIT(P1), FIINIT(H1), LSWEEP, LSTEP
      WRITE(LRES, 9030)
      WRITE(LRES, 9040) PSUP, TFUEL, GASIN, CFTIN, GPVOL
      WRITE(LRES, 9050)
9010 FORMAT(13H PRESAT DATA: .8X, 2HP1, 9X, 2HH1, 7X, 6HLSWEEP,
16X, 5HLSTEP)
9020 FORMAT(17X, 2(E10. 3, 1X), 3X, 2(I3, 9X))
9030 FORMAT(13H PREGRD DATA: .7X, 4HPSUP, 7X, 5HTFUEL, 5X,
16HGAS IN, 6X, 5HCFTIN, 6X, 6HPREVOL)
9040 FORMAT(17X, 5(E10. 3, 1X))
9050 FORMAT(2H P, 4H STP, 4X, 2HCA, 3X, 4HPEXT, 3X,
14HPPRE, 3X, 4HTEMP, 6X, 3HMFT, 6X, 5HMFPRE, 6X,
15HMRPRE, 5X, 3HAFR, 4X, 2HR%)

```

```

C      ENDIF
C-----Y-Z PLANE FIELDS FOR PLOTTING
C      NVECTR=0
C      DO 910 IVEC=1,10
C      IF(NVECT(IVEC).EQ.ISTP) NVECTR=1
910 CONTINUE
C-----OUTPUT COMPLETE Y-Z PLANE (2*NY*NZ POINTS)
C      FROM -YMAX TO +YMAX IN EACH Z SLAB
C      IF(NVECTR.EQ.1) THEN
C      DO 925 IWZ=1,NZ
C      IXP=6
C      DO 919 IWY=1,NY
C      IWY1=NY+1-IWY
C      WRITE(LPLOT,9060) GRIDZ(IWZ),-GRIDY(IWY1),
C      1GW1STR(IWY1,IWZ),GV1STR(IWY1,IWZ),GA1STR(IWY1,IWZ)
919 CONTINUE
C      DO 920 IWY=1,NY
C      WRITE(LPLOT,9060) GRIDZ(IWZ),GRIDY(IWY),
C      1GWSTOR(IWY,IWZ),GVSTOR(IWY,IWZ),GARSTOR(IWY,IWZ)
9060 FORMAT(1X,5(E11.4,1X))
920 CONTINUE
C      925 CONTINUE
C      ENDIF
C-----OUTPUT CRANK ANGLE PRESSURES AND AIR/FUEL RATIO
C      TMFUEL=TMFUEL+DMF
C-----GLOBAL AIR-FUEL RATIO AND RESIDUAL-FUEL RATIO
C      GAFR=GMATOT/GMGTTOT
C      IF(GAFR.LT.0.0) GAFR=0.0
C      RPERC=GMRTOT/(GMGTOT+GMATOT+GMRTOT)
C      IF(TM FUEL.EQ.0.0) THEN
C      GAFR=999.9
C      ENDIF
C      RPERC=RPERC*100.0
C      GCA=ATIME*360.*25.
C      GTMON=0.0
C      DO 930 IZ=1,NZ
C      DO 930 IY=1,NY
C      DO 930 IX=1,NX
C      GTMON=GTMON+GTSTOR(IX,IY,IZ)
930 CONTINUE
C      GTMON=GTMON/1116.0
C-----OUTPUT PRESSURES IN BAR
C

```

```

PEXT=PEXT/1.E5
PREPRES=PREPRES/1.E5
C
WRITE(LRES,9070) NVECTR,ISTP,GCA,PEXT,
1PREPRES,GTMON,TMFUEL,GMGTOT,GMRTOT,GAFR,RPERC
9070 FORMAT(1X,I1,1X,I3,3(1X,F6.2),1X,F6.1,
13(E11.4),2(1X,F5.1))
C
C-----CLOSE FILES AT LAST STEP
C
IF(ISTP.EQ.LSTEP) THEN
CLOSE(UNIT=LPLOT)
CLOSE(UNIT=LRES)
ENDIF
C
RETURN
1000 CONTINUE
C
C-----CHAPTER 10 FOR MIXTURE DENSITY
C
IF(MSLAB) GO TO 1010
JD1=D1H
JP1=P1H
JH1=H1H
JC1=C1H
JC2=C2H
JVL=VOL
GO TO 1020
1010 JP1=P1
JH1=H1
JC1=C1
JC2=C2
JD1=D1
JVL=VOL
C
1020 CALL GET(JP1,GPRES,NY,NX)
CALL GET(JH1,GENTH,NY,NX)
CALL GET(JC1,GCONC,NY,NX)
CALL GET(JC2,GRES,NY,NX)
CALL GET(JD1,GRHO,NY,NX)
CALL GET(JVL,GVOL,NY,NX)
C
C-----TEMPERATURE ITERATION OVER A SLAB
C
IF(ISTP.EQ.0.OR.ISTP.EQ.1) CPMIX=CPR1
C
DO 1030 IY=1,NY
DO 1030 IX=1,NX
IF(MSLAB) GTSTOR(IX,IY,IZED)=0.0
ICOUNT=1
1050 IF(ICOUNT.GT.10) GO TO 1040
CPLAST=CPMIX
GTEMP=GENTH(IY,IX)/CPMIX
IF(GTEMP.EQ.0.) GO TO 1030
CPF=CPF1+(GTEMP-TMP1)*(CPF2-CPF1)/(TMP2-TMP1)
CPA=CPA1+(GTEMP-TMP1)*(CPA2-CPA1)/(TMP2-TMP1)
CPR=CPR1+(GTEMP-TMP1)*(CPR2-CPR1)/(TMP2-TMP1)
GC1=GCONC(IY,IX)

```

```

GC2=GRES(IY,IX)
CPMIX=CPF*GC1+CPR*GC2+CPA*(1.0-GC1-GC2)
ICOUNT=ICOUNT+1
IF(ABS(CPMIX-CPLAST).GT.3.) GO TO 1050
1040 GRHO(IY,IX)=(1.0-GC1-GC2)/GAMW+GC1/GFMW+GC2/GRMW
GRHO(IY,IX)=GPRES(IY,IX)/(GRO*GTEMP*GRHO(IY,IX))
C
C-----CELL TEMPERATURE FIELD
C
IF(MSLAB) THEN
GTSTOR(IX,IY,IZED)=GTEMP
NTCOUN=NTCOUN+1
ENDIF
C
1030 CONTINUE
C
CALL SET(JD1,1,NX,1,NY,GRHO,NY,NX)
C
C-----SET ALSO D[LOG(RHO)]/DT AT MSLAB
C
IF(MSLAB) THEN
DO 1060 IY=1,NY
DO 1060 IX=1,NX
GDDP(IY,IX)=0.
IF(GPRES(IY,IX).EQ.0.0) GO TO 1060
GDDP(IY,IX)=1./GPRES(IY,IX)
1060 CONTINUE
CALL SET(D1DP,1,NX,1,NY,GDDP,NY,NX)
ENDIF
C
RETURN
1100 CONTINUE
RETURN
1200 CONTINUE
RETURN
1300 CONTINUE
RETURN
1400 CONTINUE
RETURN
1500 CONTINUE
RETURN
1600 CONTINUE
RETURN
END

```



Appendix

The appendix

due to the

provisional

condition

transformation

that is

the

the

the

the

## APPENDIX 9

## Appendix 9: Analysis of the Pre-chamber Mixing Process

The analysis considers the mixing that takes place in the pre-chamber due to the rise of the piston on the compression stroke. At BDC the pre-chamber and cylinder contain mixtures of gas and air at different constituencies. After compression - i.e. at TDC - mass has been transferred from the cylinder to the pre-chamber. The amount of mass that is transferred and its constituency determines the final air/fuel ratio in the pre-chamber.

Compression Ratio:

$$CR = (V_s + V_c)/V_c \quad \Rightarrow \quad V_c = V_s/(CR-1) \quad A5.1$$

where: CR = compression ratio

$V_c$  = clearance volume (includes pre-chamber)

$V_s$  = swept volume of cylinder

Mixture Gas Constant:

$$R_{MIX} = (m_{GAS}R_{GAS} + m_{AIR}R_{AIR})/m_{MIX} \quad A5.2$$

where:  $m_{GAS}$  = mass of natural gas =  $f_{MIX}m_{AIR}$

$m_{AIR}$  = mass of air =  $m_{GAS}/f_{MIX}$

$R_{GAS}$  = specific gas constant for natural gas

$R_{AIR}$  = specific gas constant for air

$m_{MIX} = m_{GAS} + m_{AIR}$

$f_{MIX}$  = fuel/air ratio in cylinder

From the above expressions:

$$m_{AIR} = m_{MIX}/(f_{MIX}+1) \quad \text{and} \quad m_{GAS} = m_{MIX}f_{MIX}/(f_{MIX}+1)$$

and replacing:

$$R_{GAS} = R_0/M_{GAS} \quad \text{and} \quad R_{AIR} = R_0/M_{AIR}$$

where:  $R_0$  = Universal Gas Constant

$M_{GAS}$  = molecular mass of natural gas ( $CH_4$ )

$M_{AIR}$  = molecular mass of air

Then by substituting in A5.2:

$$R_{MIX} = \frac{R_O}{(f_{MIX}+1)} \left\{ \frac{f_{MIX}}{M_{GAS}} + \frac{1}{M_{AIR}} \right\} \quad A5.3$$

At BDC (1), mass in cylinder:

$$m_{C1} = p_1 V_{C1} / (R_{MIX} T_1) \quad V_1 = \text{total cylinder volume}$$

$$V_P = \text{pre-chamber volume}$$

$$\text{i.e. } V_{C1} = V_1 - V_P$$

For purposes of calculation assume:  $pV^\gamma = \text{constant}$

$$\text{i.e. } p_2 = p_1 CR^\gamma \quad \text{and} \quad T_2 = T_1 CR^{\gamma-1}$$

At TDC (2), mass in cylinder - assuming AFR remains constant:

$$m_{C2} = p_2 V_{C2} / (R_{MIX} T_2) = p_1 V_{C2} CR / (R_{MIX} T_1)$$

$$V_{C2} = V_2 - V_P$$

Mass transfer to pre-chamber,  $m_T = m_{C1} - m_{C2}$

Substituting in the expressions given above:

$$m_T = \frac{p_1}{R_{MIX} T_1} (V_P [CR-1])$$

Hence,

$$\text{mass of air transferred: } m_{TAIR} = m_T / (1+f_{MIX}) \quad A5.4$$

$$\text{mass of gas transferred: } m_{Tgas} = m_T f_{MIX} / (1+f_{MIX}) \quad A5.5$$

mass of mixture in pre-chamber at BDC:

$$m_{P1} = p_1 V_P / (R_{P1} T_1) \quad \begin{array}{l} \text{assumes pressures and temperatures} \\ \text{are equal in pre-chamber and cylinder} \\ R_{P1} = \text{gas constant for residuals} \end{array}$$

Hence at BDC, as above:

$$\text{mass of air: } m_{P1AIR} = m_{P1} / (1+f_{P1}) \quad A5.6$$

$$\text{mass of gas: } m_{P1gas} = m_{P1} f_{P1} / (1+f_{P1}) \quad A5.7$$

$$f_{P1} = \text{fuel/air ratio in pre-chamber at BDC}$$

The fuel/air ratio at TDC in the pre-chamber is given by:

$$f_{P2} = \frac{m_{P1GAS} + m_{TGAS}}{m_{P1AIR} + m_{TAIR}} \quad A5.8$$

By substituting the expressions A5.3 to A5.7 and setting:

$$R_{P1} = \frac{R_0}{(f_{P1} + 1)} \left\{ \frac{f_{P1}}{M_{GAS}} + \frac{1}{M_{AIR}} \right\}$$

Then by further re-arranging, equation A5.8 may be written:

$$f_{P2} = \frac{M_{GAS} + CR f_{MIX} M_{AIR} + (f_{MIX}/f_{P1}) M_{GAS} (CR-1)}{M_{AIR} (CR-1) + (f_{MIX}/f_{P1}) M_{AIR} + (1/f_{P1}) CR M_{GAS}}$$

where:  $M_{GAS}$  = mol. mass of Methane (16) = natural gas

$M_{AIR}$  = mol. mass of air (29)

CR = compression ratio (10:1)

$f_{MIX}$  = 1/AFR of mixture in the cylinder

$f_{P1}$  = 1/AFR of mixture in the pre-chamber at BDC

$f_{P2}$  = 1/AFR of mixture in the pre-chamber at TDC

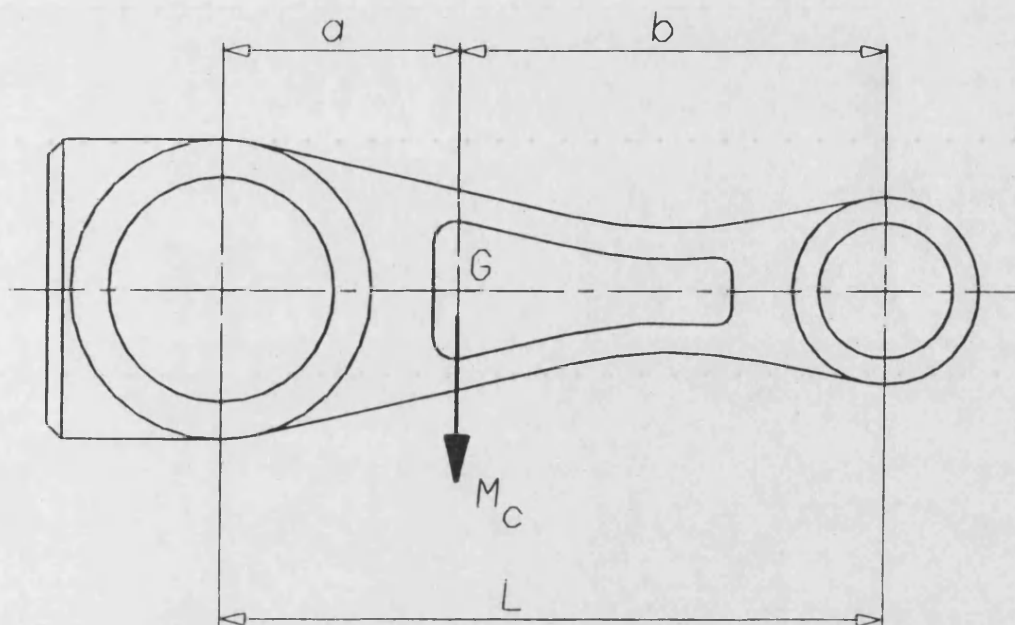
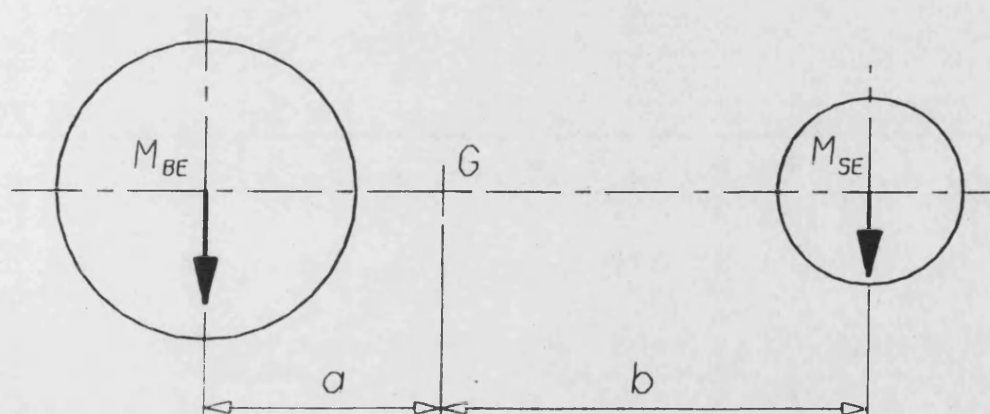


Figure A1.1 Connecting Rod



$$M_C = M_{BE} + M_{SE}$$

Figure A1.2 Representation of Connecting Rod

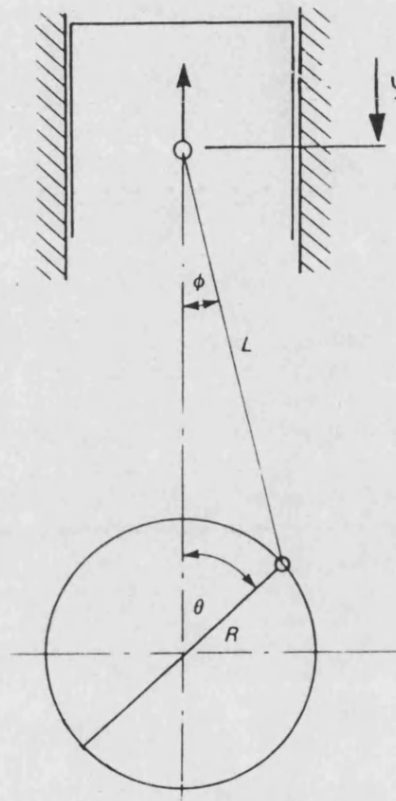
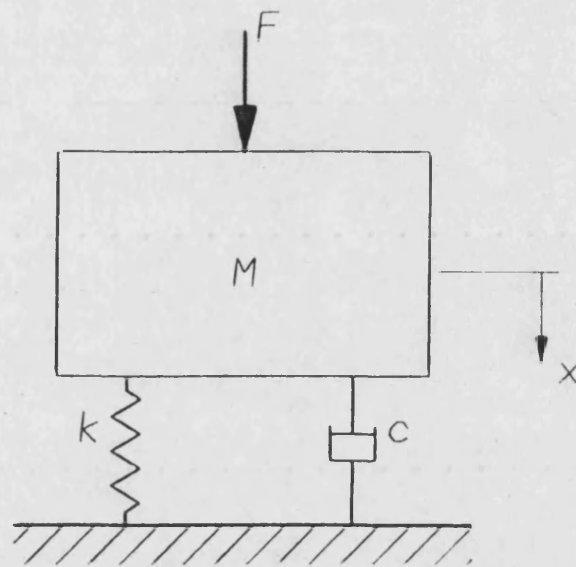
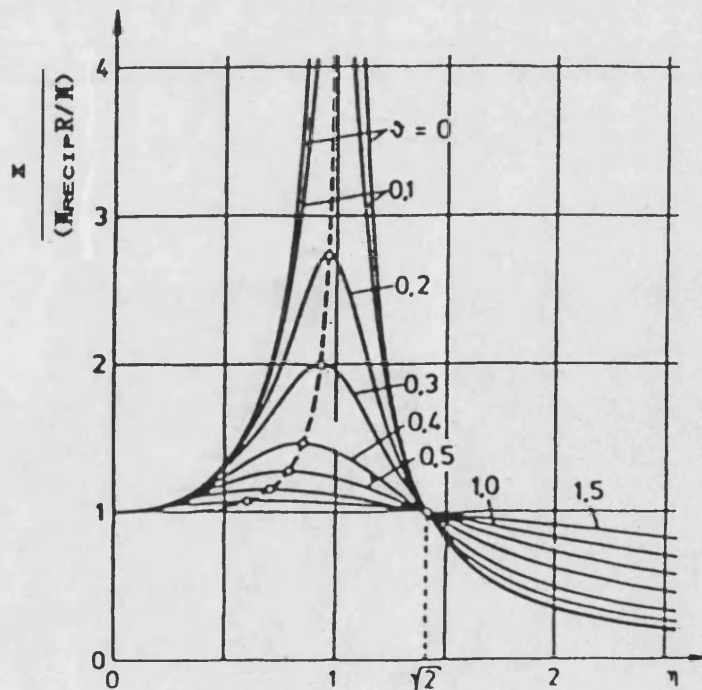


Figure A3.1 Single Throw Crank Arrangement



$M$  = Mass of engine (kg)  
 $k$  = Spring stiffness (N/m)  
 $c$  = Damping constant (kg/s)  
 $x$  = Displacement from equilibrium position (m)  
 $F$  = Unbalanced reciprocating force (N)

**Figure A4.1 Mass-Spring-Damper System representing Engine Installation**



**Figure A4.2 Amplitude of Vibration Curves for a Single Forcing Frequency**